Columbia River Salmon Passage Model

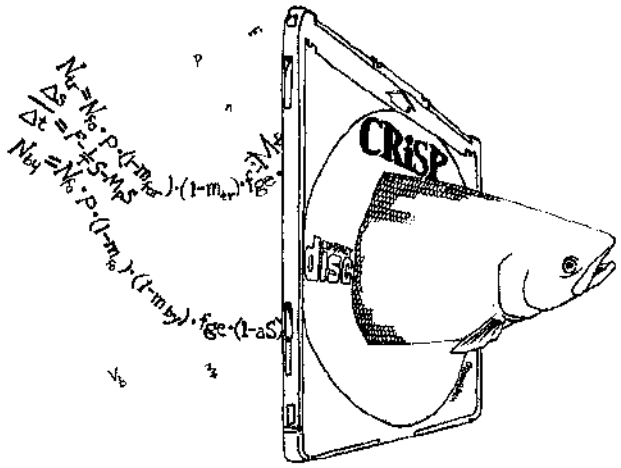

CRiSP.1.5

Theory, Calibration and Validation

May 22, 1998

Developed by Columbia Basin Research

School of Fisheries

University of Washington

Contributors

This model was developed as a team effort involving scientists, managers and computer programmers.

Authors

James Anderson - Principal Investigator, University of Washington
Joshua Hayes - Research Associate, University of Washington
Pamela Shaw - Research Associate, University of Washington
Richard Zabel - Research Associate, University of Washington

Acknowledgments

We wish to thank the following people for their support and suggestions in the development of this model.

David Askren - Bonneville Power Administration
James Geiselman - Bonneville Power Administration
Albert E. Giorgi - Don Chapman and Associates

Funding

Model development was funded by the Bonneville Power Administration under contract:

Contract Number: DE-BI79-89BP02347
Project Number: 89-108

Table of Contents

List of Tables

List of Figures

I. Introduction

This document describes theory, calibration and validation of the Columbia River Salmon Passage model (CRiSP.1). The model tracks the downstream migration and survival of migratory fish through the tributaries and dams of the Columbia and Snake Rivers to the estuary.

CRiSP.1 describes in detail the movement and survival of individual stocks of natural and hatchery-spawned juvenile salmonids through hundreds of miles of river and up to nine dams. Constructed from basic principles of fish ecology and river operation, CRiSP.1 provides a synthesis of current knowledge on how the major hydroelectric system in the country interacts with one of its major fisheries. Biologists, managers and others interested in the river system can use this interactive tool to evaluate the effects of river operations on smolt survival.

There are two modes that CRiSP.1 can use: a Scenario Mode that illustrates the interactions of model variables, and a Monte Carlo Mode, which is stochastic, providing measures of variability and uncertainty in predicted passage survival. Between any two points in the river system, estimates of probability distributions for survival and travel time can be determined for any stock.

CRiSP.1 has advanced programming features including:

- *graphical interface* to access and change model variables and equations
- *flexible data structure* that allows expansion of the model while assuring backwards compatibility with earlier versions
- *reconfigurability* to a different river without reprogramming
- *on-line help* tool.

The model runs on Windows95/NT operating systems and on Sun SPARCstations under the Solaris2 and X Windows graphical interfaces.

CRiSP.1 was developed at the University of Washington's School of Fisheries under a contract from the Bonneville Power Administration's (BPA) Fish and Wildlife Division.

I.1 - General Description

CRiSP.1 models passage and survival of multiple salmon substocks through the Snake and Columbia rivers and their tributaries and the Columbia River Estuary (Fig. 1). The model recognizes and accounts for the following aspects of the life-cycles of migratory fish and their interaction with the river system in which they live.

Fish survival through reservoirs depends on:

- predator density and activity
- nitrogen supersaturation levels dependent on spill
- travel time through a reservoir.

Fish migration rate depends on:

- fish behavior and age

- water velocity which in turn depends on flow, cross-sectional area of a reach, and reservoir elevation.

Fish passage through dams (Fig. 2) depends on:

- water spilled over the lip of the dam
- turbine operations
- bypass screens at turbine entrances and fish guidance sluiceways
- fish diel behavior.

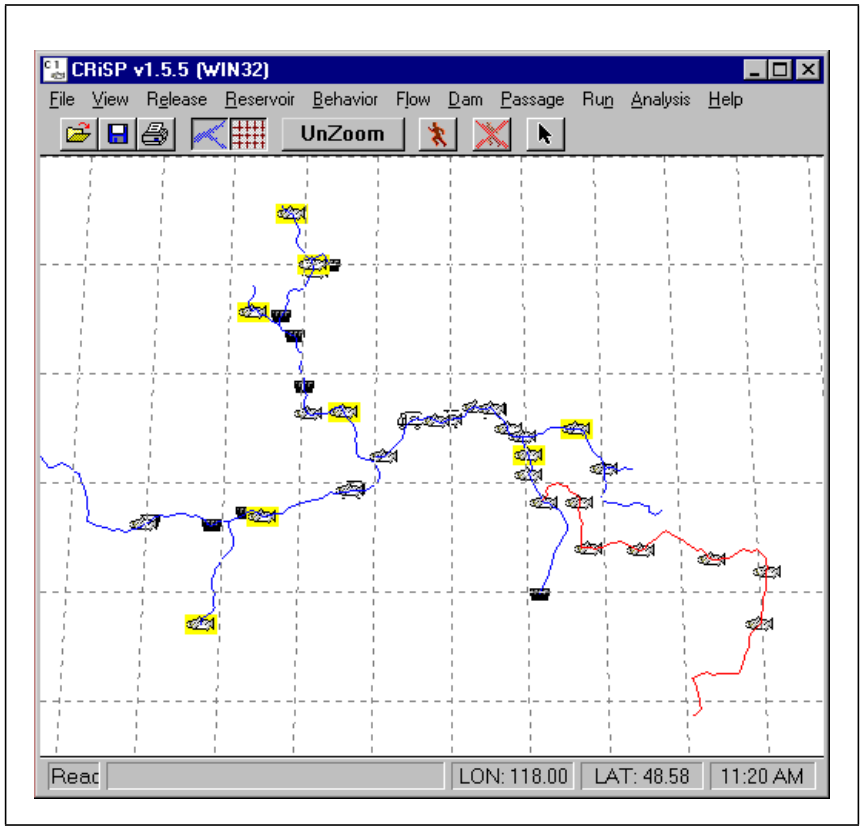

Fig. 1 Map of river with dams and fish hatcheries

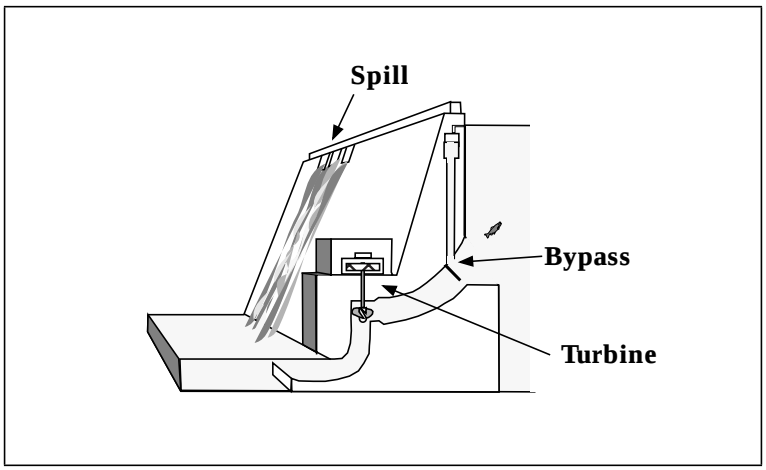

Fig. 2 Dam showing fish passage routes. Fish collected in bypass systems are returned to the tailrace or, in some situations, transported downstream.

I.1.1 -CRiSP.1 in the Decision Making Process

The CRiSP.1 model provides one tool for decision makers. In the Monte Carlo Mode, model parameters are varied and a probability distribution of survival is calculated for a particular management action. Taken on their own, model runs provide compelling evidence for selecting management action.

The question arises: Can the results of a model be trusted? Answering this question is difficult and involves good judgement which must also include societal, economic and political considerations. To proceed, decision makers need to know if a model is in agreement with the existing data, with other models and with the general qualitative understanding of how the system works. The CRiSP.1 model has tools to address these needs.

- Qualitative understanding: users are provided with several tools to develop a qualitative intuition of how the model works
  - Runs of the model done in **Scenario Mode** allow a decision maker to study how each model element affects fish migration and survival
  - The theory manual (available both printed and on-line) provides information on how CRiSP.1 is formulated.
- Comparison with data: to provide users information on how CRiSP.1 fits data, the calibration manual is available (both printed and on-line).
- Predictive understanding: users can obtained quantitative probability based predictions of survival and travel time using the **Monte Carlo Mode** of CRiSP.1. Results can be compared to the quantitative results of other models such as those mentioned above.

I.1.2 -CRiSP.1 Submodels

CRiSP.1 integrates a number of submodels that describe interactions of isolated components. Together they represent the complete model. These elements include submodels for: fish travel time, reservoir mortality, dam passage, nitrogen supersaturation, and flow / velocity relationship. The structure of CRiSP.1 allows the user to select different formulations of these submodels at run time. In this sense, CRiSP.1 can be configured to simple interactions or it can be set up to consider many ecological interactions. CRiSP.1, as it is presently calibrated, has an intermediate level of complexity: age dependent travel time is implemented, but other age dependent factors are switched off. A brief description of submodels follows.

Travel Time

The smolt migration submodel, which moves and spreads releases of fish down river, incorporates flow, river geometry, fish age and date of release. The arrival of fish at a given point in the river is expressed through a probability distribution. All travel time factors can be applied or they can be switched off individually, resulting in a simplified migration model.

The underlying fish migration theory was developed from ecological principles. Each fish stock travels at an intrinsic velocity as well as a particular velocity relative to the water velocity. The velocities can be set to vary with fish age. In addition, within a single release, fish spread as they move down the river.

Predation Rate

The predation rate submodel distinguishes mortality in the reservoir, and the forebay and tailrace of dams. The rate of predation can depend on temperature, diel distribution of light, smolt age, predator density, and reservoir elevation.

Gas Bubble Disease

A separate component of mortality from gas bubble disease produced by nitrogen supersaturation is incorporated into CRiSP.1. The mortality rate is species specific and is adjusted to reflect the effect of fish length and population depth distribution.

Dam Passage

Timing of fish passage at dams is developed in terms of a species dependent distribution factor and the distribution of fish in the forebay, which can change with daily and seasonal light levels. Fish guidance efficiency can be held constant over a season or it can vary with fish age and reservoir level.

Transportation Passage

Transportation of fish at collection dams is in accordance with the methods implemented by the U.S Army Corps of Engineers. The start and termination of transportation and separation of fish according to species can be determined for any dam under the same rules used to manage the transportation program. Time in transportation and transportation mortality can also be set.

Nitrogen Supersaturation

Nitrogen supersaturation, resulting from spill at dams, can be described with a mechanistic submodel that includes information of the geometry of the spill bay and physics of gas entrainment. Alternatively, supersaturation can be described by empirical models.

Flow

Flow is modeled in two ways: it can be specified at dams using results of system hydro-models or it can be described in terms of daily flows at system headwaters. When flow is described in headwater streams, the flow submodel generates a random set of seasonal flows that have statistical properties in accordance with the available water over a year. In this fashion, the model statistically reproduces flow for wet, average and dry years. The user controls the mainstem river flows by adjusting the outflow of the storage reservoirs within their volume constraints.

Water Velocity

Water velocity is used in CRiSP.1 as one of the elements defining fish migration. Velocity is determined from flow, reservoir geometry and reservoir elevation.

Reservoir Drawdown

Reservoir elevation is set on a daily basis from elevation information in the system hydro-models or from user specified files. As water levels drop, part of the reservoir may become a free-flowing stream.

Stochastic Processes

CRiSP.1 can be run in a Monte Carlo Mode in which flows and model parameters vary within prescribed limits. In this mode, survival to any point in the river can be determined as a probability distribution.

Geographical Extent

CRiSP.1 can describe a river to any desired level of detail by changing a single file containing the latitude and longitude of river segments, dams and release sites. In its present configuration, two river-description files are available. One file contains an abbreviated river map with the major tributaries. It contains three representative release sites, although more can be added easily. A second river descriptions file defines a more extensive river and tributary system and has upwards of 100 hatchery release sites.

II. Theory and Calibration

II.1 - Model Computation Diagram

The CRiSP.1 model calculates changes in fish numbers as fish move through tributaries, reservoirs, and dams. This can be diagrammed in terms of a computational tree (Fig. 3). Shaded boxes represent fish entering the system and passing dams and reservoirs on a daily basis. Unshaded square boxes represent calculations for travel time and survival of fish through the system. Rounded boxes represent input data to the calculation modules.

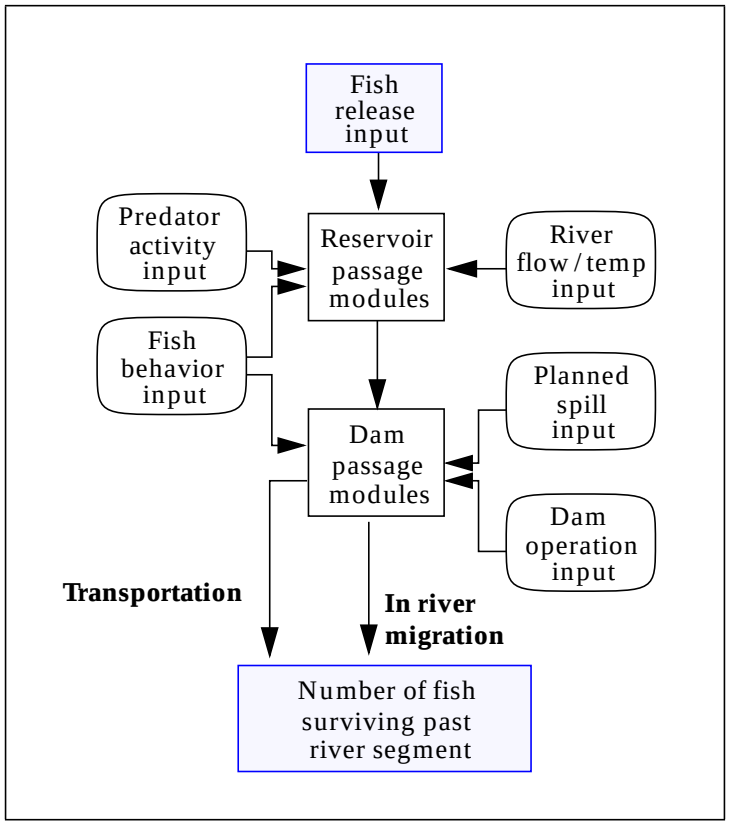

Fig. 3 Diagram of model elements

II.2 - Calibration Overview

CRiSP.1 is a composite of individual, integrated, process submodels or equations that jointly determine smolt migration and survival in detail.

Some equations are mechanistic and are derived from some underlying theory. In these equations the parameters have ecological or physical meanings. The equation relating water flow to velocity, for example, is based on principles of hydrology. A second type of equation is empirical and has no underlying ecological or physical meaning. These are used because they fit the data and are amenable to statistical fitting techniques. The parameters of these types of equations (submodels) seldom have ecological interpretations. For example, in the nitrogen supersaturation submodel four

alternative equations are available to relate nitrogen supersaturation to spill. The first two alternatives are empirical. A third type of equation uses a mixture of empirical and mechanistic based equations. The predator mortality equation is such an equation.

The calibration of these equation types points up their advantages and drawbacks. The advantage of the empirical equations is their simplicity which makes it relatively easy to fit them to data. Their drawback is they can only be fit with data specific to the given situation. Mechanistic equations are advantageous in that their parameters have ecological meanings. In these cases the possible ranges or values of the parameters often can be determined from data sets from other unrelated studies and systems. The disadvantage of mechanistic equations is that fitting them to data is often more difficult and often involves nonlinear fitting algorithms.

The model has a significant number of parameters that must be estimated through a calibration and validation process. Because of this complexity, a variety of data from both field and laboratory studies are used in the calibration. The end result is that through the calibration process diverse theories and data sets are synthesized into a consistent picture of the process of fish migration and survival through the river system. The calibration involves determining the set of parameters that yield the observed passage observations for a given set of river conditions. The relationship between environmental conditions, passage observations and ecological variables is illustrated in Fig. 5.

Environmental variables describe the observable state of the environment in which fish live. These variables are monitored in the system and include weather-related factors such as temperature, and system operating factors such as flow, spill and fish transportation. These variables are accessed in the model with the **Headwater**, **Reach** and **Dam** menus.These variables have been determined from historical records dating back to 1970 for all variables and back to 1937 for a subset of variables. Future values of these variables are assessed from runs of hydromodels and management-derived scenarios of river operations.

Fish passage observations involve a variety of data, extending back several decades, on the passage timing and survival of fish through various segments of the river and hydrosystem. This ranges from relatively small-scale information on the passage of individual groups of fish at individual dams to system-wide estimates of passage and survival of species over specific years plus a number of observations at levels of detail between the smallest and largest scales. Observations include brand release studies conducted from 1970's and 80's and PIT tag studies conducted beginning in the late 80's. These data sets yield two levels of information. The direct observations provide passage numbers and timing at individual dams as well as returns of adults to dams and collection points. These raw numbers can be further reduced to estimates of migration rates and fish survival between points in the river and in some cases collection efficiencies at dams. The model can use both raw information and statistically analyzed data. The model runs on data expressed as initial release numbers and numbers of fish passing any point or bypass route in the river system. Release information is accessed through the **Release** menu. Passage information is accessed through the **Passage** menu of the model. This provides detailed information of passage at any level from passage of a specific dam route to passage through the entire system.

Ecological variables are developed from first principles of how the environmental variables interact with fish behavioral and physiological factors to determine fish passage. These variables, for the most part, characterize the rates of fish passage and

survival, which through equations, generate predicted passage for a set of environmental variables. Model calibration requires estimating these variables. Model validation requires assessing how close our assessments are to actual values. In the model these variables are contained under **Behavior**, **Dam** and **Reservoir** menus.

Our understanding of the ecological interactions of fish is incomplete and several levels of complexity of interactions can be envisioned. The CRiSP.1 model contains a number of different theoretical constructs that can be selected at run time. Any calibration of the model is only specific to a particular choice of theoretical constructs. The selection of which construct to use depends on the available information, the effect of the feature on the calibration, and its ecological soundness.

II.2.1 -Calibration techniques

Ecological variables are estimated from both field observations and laboratory studies. Estimates made from field observations (such as fish passage timing or mortality rates) are used with the corresponding environmental variables (Fig. 4). Estimates made from laboratory experiments are analyzed assuming the corresponding laboratory conditions and are used to infer the relevant ecological variables. For example, the estimation of mortality from gas bubble disease is made based upon laboratory experiments.

The calibration involves mixing results from laboratory experiments, isolated field studies on aspects of migration, and system-wide studies of survival and timing. The calibration proceeds in a hierarchy of steps where calibration of the first steps are required to calibrate the lower ones. The sequence which is reflected in the chapter organization is: River and Environmental Description, Flow Processes, Passage Processes, Dam Processes and finally Reservoir Mortality. The final two steps are in part connected depending on the data set and parameters being calibrated.

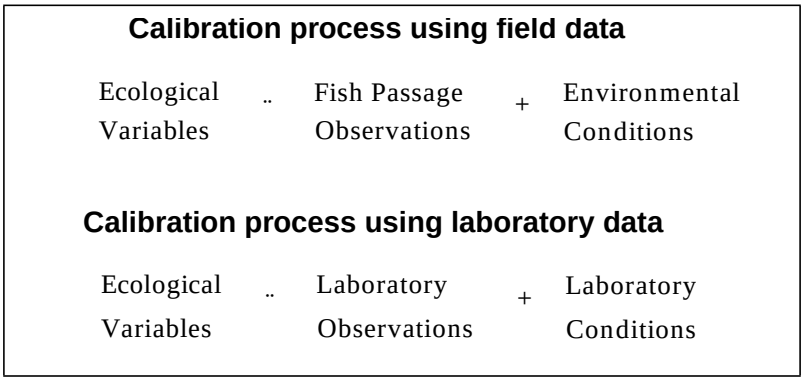

Fig. 4 Calibration process involves using passage and environmental data to estimate the model ecological variables

Goodness-of-fit

In calibration, the variables are adjusted so an equation prediction best fits the observations according to statistical criteria within ecological constraints. A variety of goodness-of-fit measures are applied in the calibrations. The choice of method depends on the type and quantity of data and the dimensions of the data being fit. Where possible graphical examples are given along with statistical measures of the

goodness-of-fit. The following approaches are used.

- Least Squares, 2 dimensional regressions (Numerical Recipes, Press et al. 1988) used for
  - nitrogen mortality rates vs. time
  - size vs. mortality rate
  - spill efficiency equations
- Nonlinear regression using the Gauss-Newton algorithm to minimize sums of squares (SPLUS 1991) used for
  - nitrogen mortality rate vs. nitrogen level
  - prediction of migration rate parameters vs. flow and fish age
- Hyperbolic “amoeba routine” (Numerical Recipes, Press et al. 1988) used for
  - nitrogen mortality rate vs. nitrogen level
- Fourier series analysis (SPLUS 1991) used for
  - determining scenario mode flow modulators
- Maximum likelihood estimators (Zabel 1994) used for
  - determining migration rate parameters

In some cases, with limited data statistical techniques do not converge on a unique solution in that an equation can fit the data equally well with different model parameters. In these cases the parameter set is fit by selecting one of the parameters, either arbitrarily or justified on its range inferred from ecological constraints.

II.2.2 -Calibration status

The calibration process involves fitting the submodels to data using goodness-of-fit measures. First environmental condition variables are ascribed and ecological parameters are calibrated in a hierarchy that can be organized according to categories of similarity and interdependency.

Calibration status by variable type

Variables are listed below along with a description of the state of their calibration.

- Environmental conditions (define river condition)
  - River description parameters relating geometry of river and dams. These parameters are fairly well described and no further improvements of these parameters are expected at this time.
  - Headwater parameters define the river environment flow and temperatures. Flow data exist for years from 1960 through 1995. Temperature in headwaters exists from 1966 through 1995. These parameters are fairly well described and no improvements are expected at this time.
  - Predator density in each reservoir is up to date as of 1994. As additional indices are obtained they will be included.
- Passage observations (define movement and survival of fish)

- Release parameters include the number of fish released at each site at each day, the beginning and end of smoltiticaion onset
- survival and passage timing: information on passage timing and survival of fish through the hydrosystem are adjusted according to model run specifics.

❍ Ecological parameters (characterize ecological interactions)

- Nitrogen supersaturation parameters relate the buildup of gas as function of spill, flow, and temperature. These have been calibrated with data current through 1994.
- Age at smoltification initiation (smolt_onset) and completion (smolt_finish) which are release-specific and also may depend on release date itself. Release information along with the predicted passage information at dams and reaches comprises the passage data in the model. These parameters are critical to survival estimates and are under further study.
- Dam parameters describing passage mortality at dams and fish guidance efficiency have been derived from two decades of studies including results obtained from recent PIT tag studies.
- Migration rate parameters have been calibrated for spring/summer and fall chinook and steelhead.
- Predator activity has been calibrated with squawfish consumption information from John Day reservoir for spring and fall chinook and steelhead.
- Transportation mortality calibration depends on the transport benefit ratio and in-river survival estimates. Although initial estimates have been obtained, both of these factors are under further analysis.

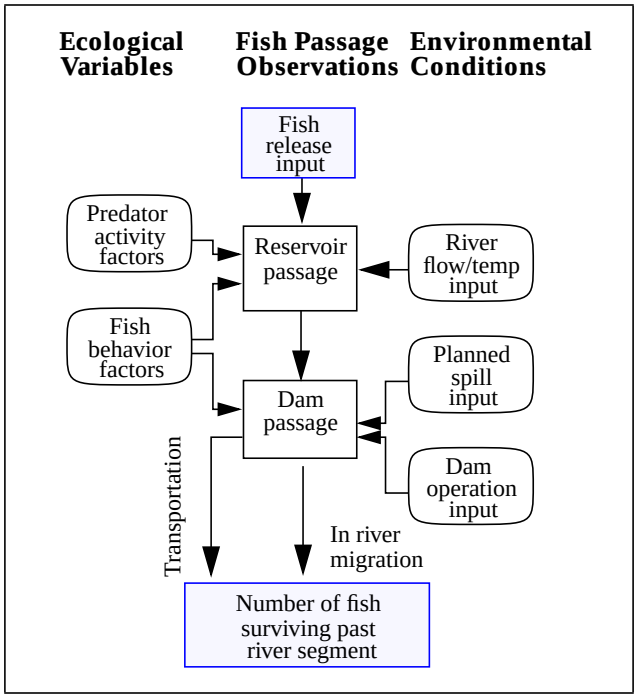

Fig. 5 Model relating environmental variables, fish passage and model ecological variables.

Calibration status by submodel

The CRiSP.1 submodels were individually calibrated. Thus CRiSP.1 was not directly calibrated from mark-recapture survival studies. Instead, such studies provided a check on the calibrations of the individual mechanisms of the model. Notes of the submodel calibrations are detailed below.

Travel Time

The travel time submodel was calibrated for fall chinook, spring chinook, and steelhead using tagging data from the entire river system and over the entire migration season. Two separate calibrations steps were applied: one to measure the spread of fish as they moved through the reservoir, and the other to measure the change in relative migration velocity with fish age. The first used marked, individual stock releases over a short period of time, and the second used marked and recaptured fish over entire seasons.

Predation Rate

Predator-prey interactions in CRiSP.1 were calibrated with information from predation studies in John Day Reservoir and information on the predation index for each of the major reservoirs.

Gas Bubble Disease

The rate of mortality was calibrated from dose-response studies conducted in both field and laboratory conditions.

Dam Passage

Diel passage elements of CRiSP.1 were calibrated from hydroacoustic and radio-tagging studies at dams. Fish guidance efficiency and spill efficiency were calibrated from a number of studies at a variety of dams. Fish guidance efficiency can be set to change with fish age and reservoir level or it can be set constant over the year. Mortalities in dam passage were determined from mark-recapture studies at dams.

Transportation Passage

Separation of large and small fish in transportation was applied from general information on the efficiency of the separators in the transportation facilities at dams. A transportation mortality was estimated for each species. In addition, time to transport fish through the river system was specified.

Nitrogen Supersaturation

Nitrogen supersaturation models were calibrated with data from the Army Corps and includes new information collected in the 1992 drawdown study in Lower Granite Reservoir and Little Goose Reservoirs and from total dissolved measurements in 1994.

Flow

Headwater flows in the Scenario Mode were calibrated from information on stream flows provided by the USGS. In Monte Carlo Mode, modulators of the period

average hydro-model flows were calibrated with daily flow records at dams.

Water Velocity

Water velocity requires information on reservoir and geometry. The relationship between geometry and elevation and free stream velocities were determined from Lower Granite Reservoir drawdown studies.

Stochastic Processes

The ranges for variables used in the Monte Carlo Mode have been calibrated to available data in the above mentioned studies.

II.3 - Flows

II.3.1 -Overview of Flow Computation

This section defines the theory for calculation of flows in CRiSP.1. Flow information is treated differently for the Monte Carlo and Scenario Modes. In the Monte Carlo Mode, average flows over defined periods at the dams are read as input from flow archive files. The period average flows are then *modulated* to give simulated daily flows at the dams. Using this information, flows in the headwaters are calculated with an *upstream propagation* algorithm. Finally, flows through river segments are calculated from the headwaters with the *downstream propagation* algorithm. In the Scenario Mode, flows can be specified at headwaters using modulators based on historical flows or drawn in using the mouse. Outflows from storage reservoirs are specified according to the volume constraints of the reservoirs. Finally, river flows are produced using the *downstream propagation* algorithm which combines storage reservoir flows and unregulated headwater flows.

II.3.2 -Monte Carlo Flow Calculation

When running CRiSP.1 in the Monte Carlo Mode, flow information is specified at dams from flow archive files generated by one of several hydroregulation models. CRiSP.1 uses a step-wise process to calculate daily headwater flows. These steps are as follows:

1. Read period-averaged flows at dams from the flow archive file
2. Modulate period-averaged dam flows to give daily dam flows
3. Modulate losses in reservoirs
4. Propagate upstream flows to determine daily headwater flows as well as gains and losses from river segments
5. Propagate downstream flows through all river segments using the headwater flows and the segments' gains and losses.

Calculation of river flows in the Monte Carlo Mode begins with flows at the dams and distributes upstream flows to achieve a mass balance. The procedure uses water conservation equations for losses / gains in river segments and flows at unregulated streams and from storage reservoirs. Definitions for flow calculations (Fig. 6) are listed below.

- Regulated headwater segment has a dam, a storage reservoir, and a river source.
- Unregulated headwater segment has a confluence at its downstream end and a river source at its upstream end.
- Loss is a withdrawal (+) or deposit (-) of water to a river segment from an unspecified source. Losses are used to represent irrigation removals and ground water returns to river segments.
- Dams are points that regulate flow, but only dams specified in the flow archive file are considered to be regulation points.
- Confluences are points where two flows upstream of the confluence combine to create the flow downstream of the point.

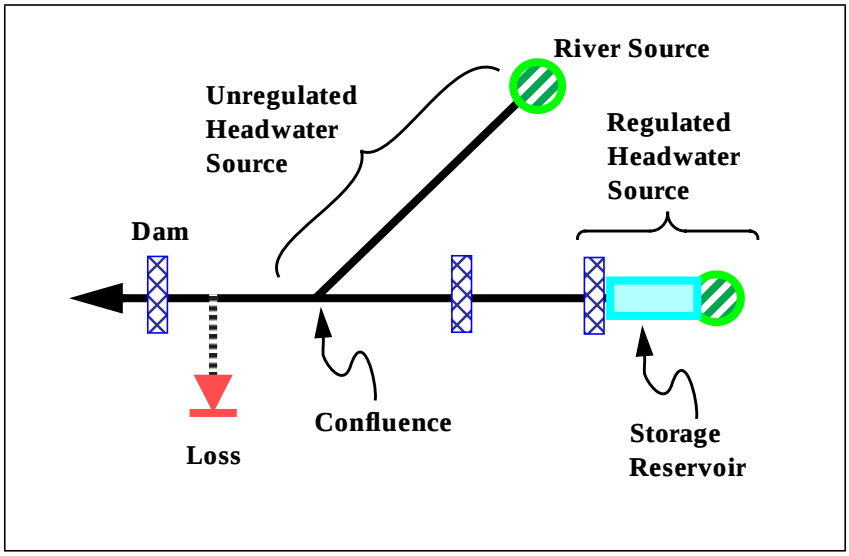

Fig. 6 Main objects for the Flow submodel

Hydroregulation Models

Flow files for the Monte Carlo runs are obtained from *Flow Archive* files that are generated from runs of hydroregulation models maintained by two agencies:

- HYDROSIM is run by the Bonneville Power Administration
- HYSSR is run by the U.S. Army Corps of Engineers

The models provide flow on a monthly or bimonthly basis over the entire Columbia Basin hydrosystem and are themselves complex models with many variables and special conditions. As a result, these models are not available to be run directly, although outputs of model runs are available for use in CRiSP.1.

The models use information on natural runoff, regional electrical demand and storage capacity of the reservoirs to model the stream flow on a period averaged basis. Models use historical flow records for natural runoff and generate river flows that meet power generation demand in monthly periods. The exceptions to the monthly periods are April and August which are each divided into two periods. In addition, the HYDROSIM model provides elevations of all reservoirs.

Flow Modulation

Flow inputs in the Monte Carlo Mode runs consist of predicted daily flow averaged over monthly or bimonthly intervals at each dam used in CRiSP.1. This input generated from HYDROSIM, or HYSSR flow archive files typically looks like Fig. 7 below. While this record retains most of the annual and seasonal flow variations, actual historic river flows (Fig. 8) exhibit considerable weekly and daily variations that are not replicated by the hydroregulation models used as flow data for CRiSP.1.

The purpose of the modulator is to more accurately simulate real flow patterns encountered by adding variations at finer time-scales consistent with historic flows. These variations include both random and deterministic components.

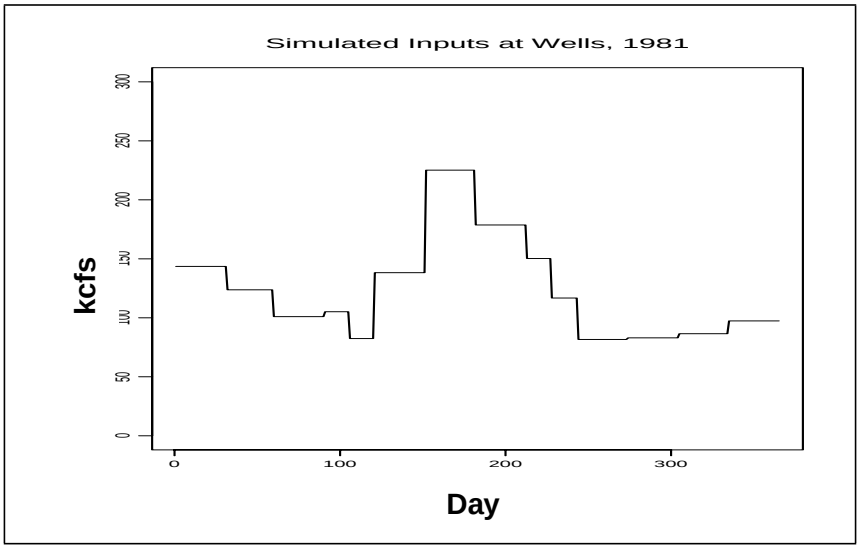

Fig. 7 Hydroregulation model simulated input - Wells, 1981

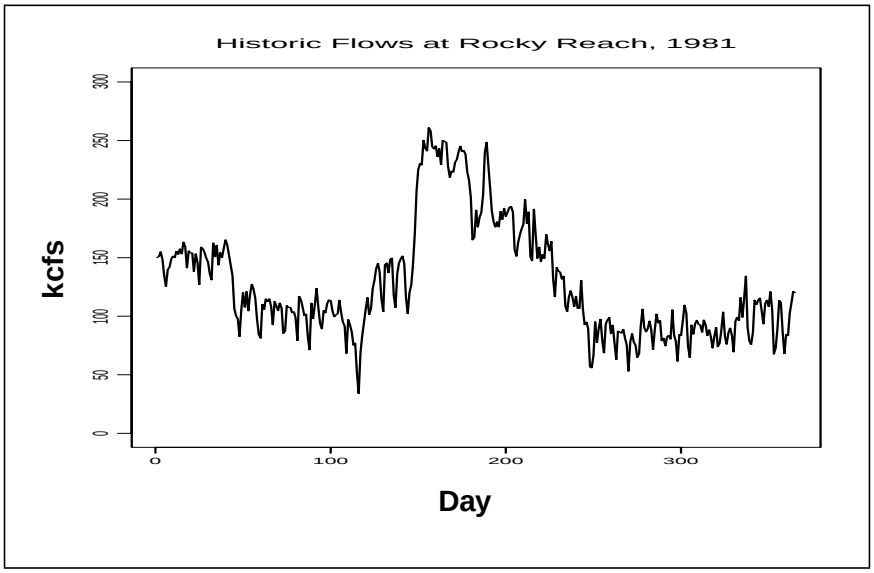

Fig. 8 Historic flows at Rocky Reach, 1981

Spectral Analysis of Flow

The CRiSP.1 modulators were developed from the following analysis of flows in the Columbia River system. The goal was to develop a modulator that represented daily and weekly variations in flow and had the same spectral qualities as the flows in the river system as it is now operated.

A spectral analysis of an eleven-year time series (1979-1989) of flows revealed the general trend is a decline in spectral power that is qualitatively similar to a pink noise spectrum[1]. In addition, the spectrum has distinct peaks at frequencies of 1/7, 2/7, 3/7 etc., indicating a seven day cycle (Fig. 9).

This spectrum suggest several distinct processes. The weekly component is the result of flow decreasing on weekends when electric power consumptions is less. The pink noise element of the spectrum is probably the result of seasonal and short term correlations in weather patterns that alter the power consumption and unregulated runoff directly.

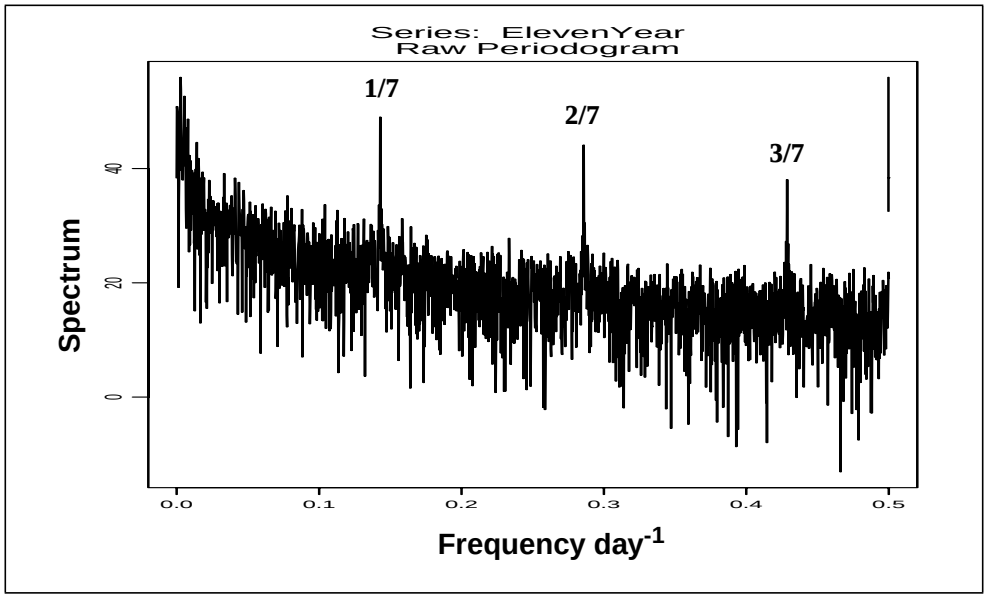

Fig. 9 Spectrogram: eleven year time series

Modulator Applications

The strategy for using period averaged archive flows to simulate flows with the spectral qualities of the actual ones involves adding flow variations at several points in the system (Fig. 6). These variations are produced by modulators. Since flows start in the headwaters and are summed downstream, flow variation can be added sequentially according to the manner by which they are produced. First, the archive flows are prescribed at all dams. Next, three modulations are applied. *Weekly* and *daily* modulations are added at the regulated headwaters to reproduce variations that occur between dams from additions and subtractions of water in the river segments and a *loss* modulation is added at downstream dams. After modulation, an upstream propagation process is applied to calculate the flows in unregulated headwaters. This forces the total modulation into the unregulated streams. In the case of the weekly

1. Pink noise is random pattern that exhibits some correlation for short time scales

modulation this is an artifact since it is induced by hydrosystem operation. The error is not significant though, since the weekly modulation is a small fraction of the total variation.

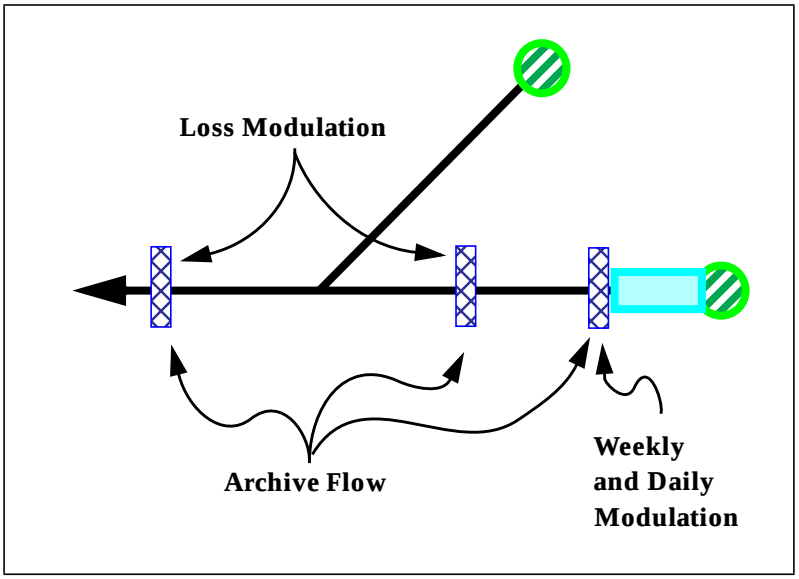

Fig. 10 Points of flow modulation in system.

Weekly Modulators

The weekly modulation, applied in the regulated headwaters, simulates hydrosystem power generations patterns in which electrical demand decreases on weekends. The modulators, producing lower flows on weekends and higher flows midweek (Fig. 11), are approximated with a three-term Fourier series with fixed amplitude. The equation is

$$F(t)_{\text{week(j)}} = -G \sum_{n=1}^{3} a_n \cos(b_n(t+\delta)) \qquad (1)$$

where

- $F(t)_{\text{week (j)}}$ = weekly variation in flow for headwater dam j
- G = flow scaling factor in kcfs

  This is set to 12.0 to reproduce the observed weekly variation in flow at Wells Dam for the years 1979 to 1989 excluding 1983 for which flows are missing.
- a_n, b_n = Fourier coefficients

  $a_1 = 1, a_2 = 2/3, a_3 = 1/3$

  $b_1 = 6\pi/7, b_2 = 4\pi/7, b_3 = 2\pi/7$
- t = day of the year
- δ = offset for day of week alignment.

The offset is calculated so that for any year from 1900 to 2100 the minimum value of W occurs on Sunday.

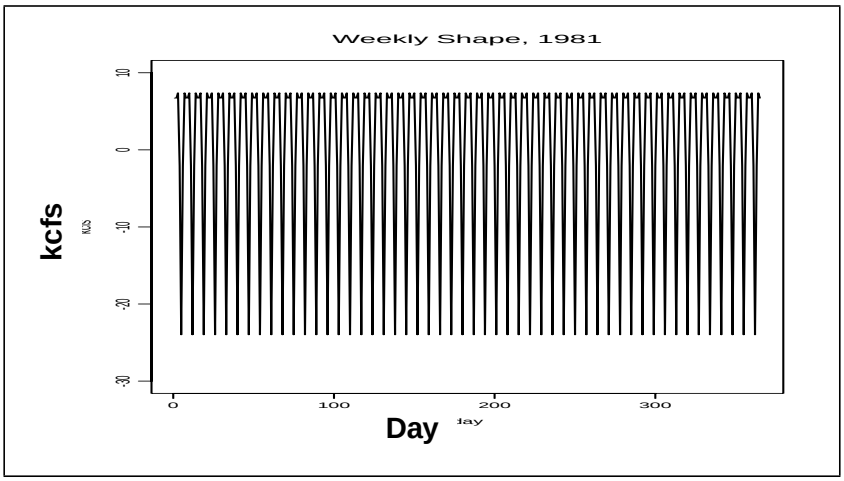

Fig. 11 Weekly shape pattern

Daily Modulators

Daily modulation simulates all variations not associated with the weekly and seasonal variations. A discrete realization of an Ornstein-Uhlenbeck (OU) process (Gardiner 1985) was used to generate the daily variation. The process has two important characteristics: variations are slightly correlated from one day to the next and variances stabilize over time. This is a correlated random walk in which autocorrelation decays in time. The stochastic differential equation for an O-U process is

$$\frac{dF_{\text{day}}}{dt} = -r \cdot F_{\text{day}} + \sigma \cdot w(t) \tag{2}$$

where

- F_{day} = daily variation in flow in kcfs at headwater dam
- r = deterministic rate of change of flow per unit of flow (the range is confined such that $0 < r < 1$)
- σ = intensity on the random variations in flow
- $w(t)$ = Gaussian white noise process describing the temporal aspects of the flow variation.

An O-U process has a conditional probability density function (Goel and Richter-Dyn 1974)

$$P(x|y, t) = \frac{\exp\left[-\frac{1}{2}\left(\frac{x - m(t)}{V(t)}\right)^2\right]}{\sqrt{2\pi V^2(t)}} \tag{3}$$

where the mean and variance of the process are defined

$$m(t) = y \cdot \exp(-rt) \tag{4}$$

$$V^2(t) = \frac{\sigma^2}{2r}(1 - e^{-2rt}) \tag{5}$$

When rt is large enough that exp (-2rt) is negligible, m and V^2 tend to be constant values and the time series is stationary.

Changing the continuous differential equation into a discrete one with $\Delta t = 1$ reservoir time step, and rearranging gives

$$F(t+1)_{\text{day(j)}} = (1 - r_j) \cdot F(t)_{\text{day(j)}} + \sigma_j \cdot w(t) \tag{6}$$

r = 0 gives an unbiased random walk, r = 1 gives a series of uncorrelated normal variates.

For the modulators, a system in stochastic equilibrium is sought such that m = 0. Taking $X_0 = y = 0$ gives m = 0, and discarding the first 35 iterations yields stable variance for any value of r useful in this context. Modulator parameters selected for the different portions of the system are given in Table 1 and are based on daily flow data for the years 1979 to 1989 at Wells and Lower Granite Dams.

Table 1 Daily modulator parameters for river

River	σ_j	r_j
Upper Columbia	13	0.5
Lower Columbia	13	0.5
Snake	7	0.5

Random daily variation is added by a numerical form of an Ornstein-Uhlenbeck (O-U) random process created for each run (Fig. 12).

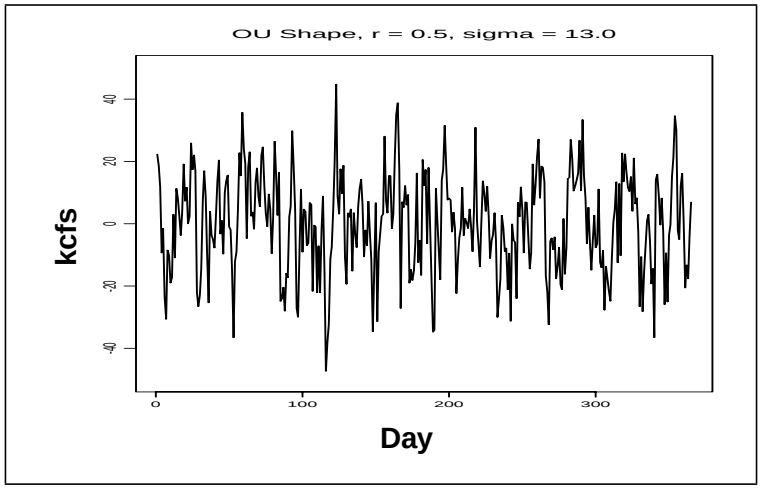

Fig. 12 O-U shape; r = 0.5, sigma = 13

Monte Carlo Flow Modulator Validation

Using daily flow records for Ice Harbor, Priest Rapids and John Day dams during 1981, monthly and bimonthly (April and August) average daily flows were computed and appended to a CRiSP.1 flow archive from which CRiSP.1 generated modulated flows for these dams. Graphs of observed and model-produced flows for the first 300 days of the year at John Day Dam appear in Fig. 13. The model appears to produce realistic patterns of flow variation that mimic natural flows very well.

At a finer scale, however, note that CRiSP-modulated flows generally exhibit less variability than do observed flows, e.g. compare January and July (Fig. 14). In general, modulated flows are about as variable as observed flows in January, but clearly less variable than observed flows in July. This is also reflected in the variance around the mean flow, given in Table 2. This phenomenon is probably due at least partially to "step-like changes" of flows in July that do not occur in January. There is some variation around the mean due solely to that trend, and this will not be captured in a purely random modulation scheme.

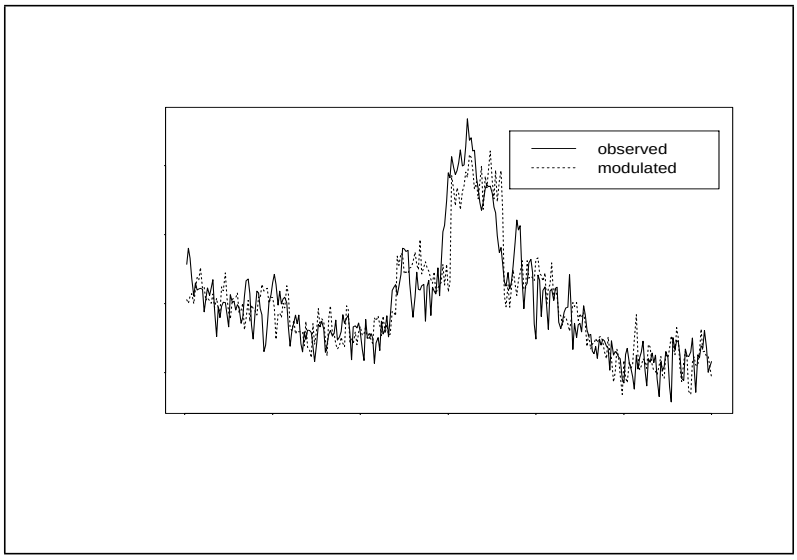

Fig. 13 Flows at John Day Dam, 1981

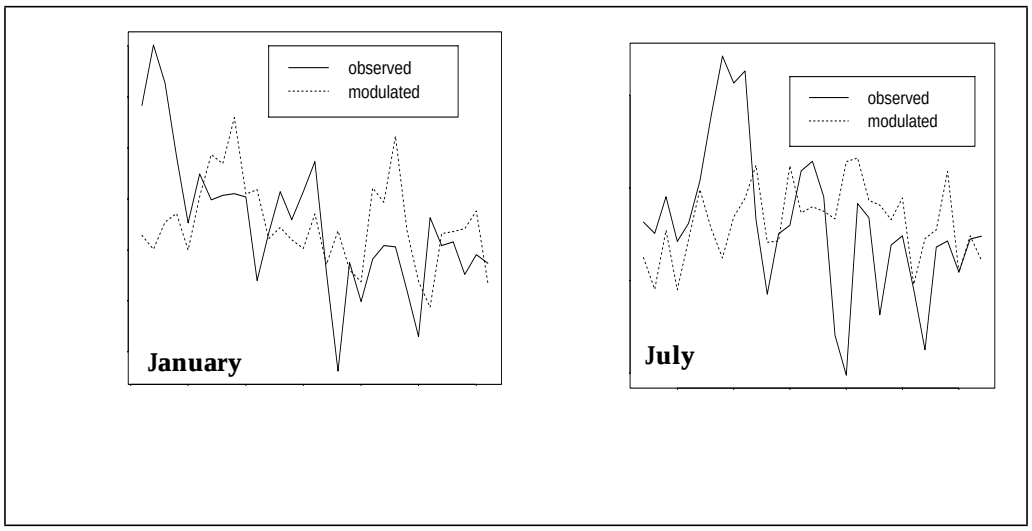

Fig. 14 January and July flows at John Day Dam, 1981

Table 2 Variance about mean flow for observed and modulated flows at three dams in 1981

Dam	Month	Variance about monthly mean flow	
		Observed	Modeled
John Day	January	728.38	287.54
	July	1620.08	401.74
Priest Rapids	January	67.34	160.29
	July	512.97	170.42
Ice Harbor	January	247.65	156.96
	July	149.83	61.83

Flow Loss

The term 'loss' represents withdrawals from the system, mainly for irrigation. These withdrawals are positive in CRiSP.1. Negative losses are return flows through ground water.

The loss data in a segment represents the change in flow that occurs between the flow input (calculated from the flow of upstream segments) and the flow output (stored as data in the segment). Where not specified, flow loss is set to zero.

During the upstream propagation operation, new flow loss values are computed for reaches that lie between two dams. A dam is said to have no component of unregulated flow if no unregulated headwater flows into the dam without first flowing through some regulation point.

For each reach *r* enclosed between a dam and upstream regulation points (Fig. 6), a new flow loss $F_{L(r)}$ is set by distributing any mass imbalance over all reaches between the dam and/or regulated inflow points in proportion to each reach's maximum allowable flow:

$$F_{L(r)} = \left[\sum_{j=1}^{n} F_{R(j)} - F_{D(r)} \right] \frac{F_{M(r)}}{\sum_{i=1}^{p} F_{M(i)}} \qquad (7)$$

where

- $F_{D(r)}$ = flow output at dam immediately below reach *r*
- $F_{L(r)}$ = new flow loss at reach *r*, as adjusted for mass imbalance
- $F_{M(r)}$ = flow maximum at reach *r*
- $F_{M(i)}$ = flow maximum at reach *i*
- $F_{R(j)}$ = flow at regulation point *j*
- *n* = number of upstream regulated points
- *p* = number of reaches between dam *r* and all regulation point

Note: maximum allowable flows are set in the **`columbia.desc`** file using the keyword **`flow_max`**.

Flow loss is not modified by the upstream propagation in any reach not fully enclosed by regulated headwaters or dams. After appropriate loss values are set, flow loss in every segment is used as input data for unregulated headwater calculations.

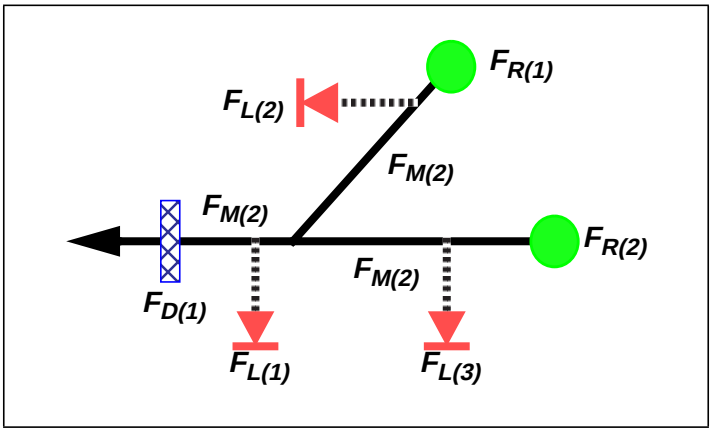

Fig. 15 Diagram of reach structure for loss calculation

Reservoir Loss Modulation

At downstream dams, variations in flow from losses due to irrigation and evaporation and additions from surface and subsurface groundwater flows are accounted for with *loss* modulators. The intensity of this variation is based on the

differences in flows observed at adjacent dams as indicated in period averaged hydro-model flows (Fig. 16).

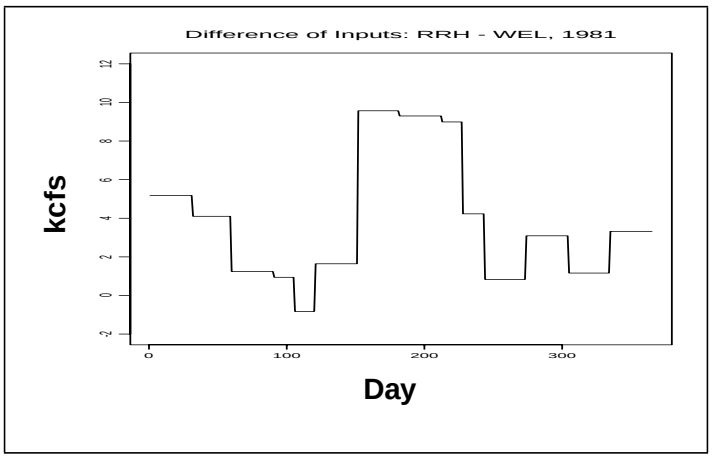

Fig. 16 Inputs at Rocky Reach minus inputs at Wells, 1981

The loss modulation is simulated with a white noise process (Fig. 17). A normal variate random factor is added to modulated flow of all run of the river dam. The equation is

$$F_{loss(i)} = \sigma_i \cdot \mathrm{Norm}(0, 1) \tag{8}$$

where

- $F_{\text{loss (i)}}$ = modulated flow loss at downstream dam *i*
- σ_i = the standard deviation of the difference in flows (kcfs) at dam *i* and *i* +1 as computed by daily observed flows at all dams over the years 1979-1981.

Table 3 Flow loss modulator parameter for eq (8)

Dam	σ_i (kcfs)	Dam	σ_i (kcfs)
Bonneville	11.0	Little Goose	5.4
The Dalles	4.1	Priest Rapids	4.0
John Day	17.0	Wanapum	5.0
McNary	12.75	Rock Island	2.65
Ice Harbor	2.75	Rocky Reach	3.0
Lower Monumental	2.4	Wells	6.5

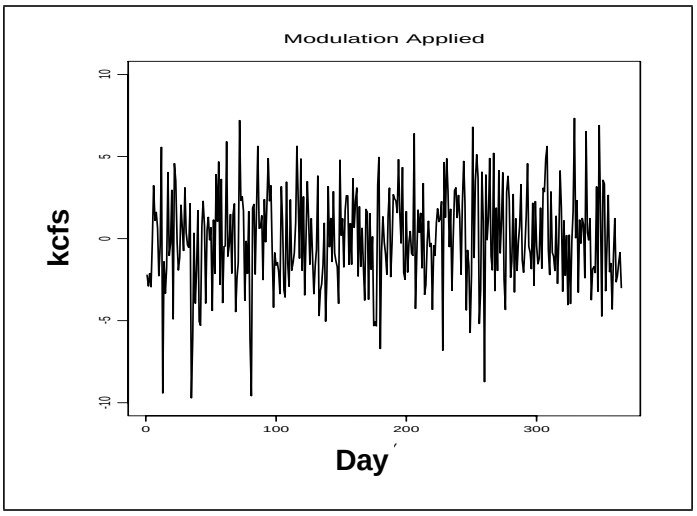

Fig. 17 Random factor modulation at Rocky Reach, 1981

Headwater Computation

Once flows are modulated at dams and the losses and gains are calculated, the headwater flows can be calculated with the algorithms described below.

Regulated Headwater

Regulated headwaters are storage reservoir outflows for the Monte Carlo Mode. No losses are considered for storage reservoir flows other than the dam outflow.

Unregulated Headwaters

Each unregulated headwater is examined. If the flow for a given headwater has not yet been computed, then flow for that and all adjacent unregulated headwaters is calculated.

The *region* of computation for a segment is defined as all segments within the river map subgraph with endpoints consisting of the nearest downstream dam, and the nearest regulation points or headwaters upstream from the dam. An example of a region with several unregulated headwaters is given in Fig. 18.

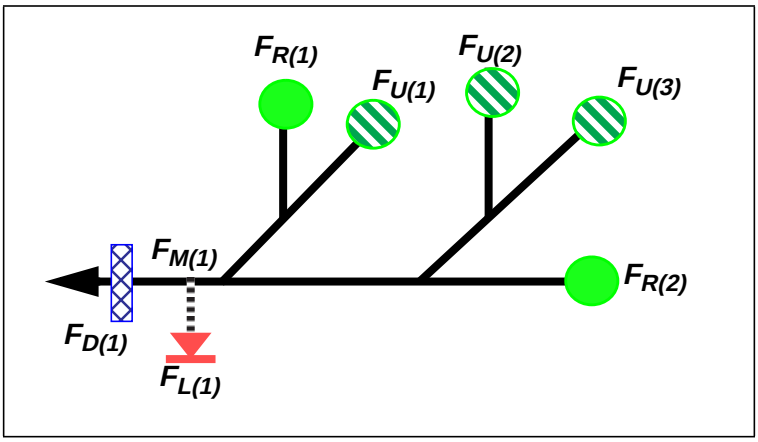

Fig. 18 Region of regulated F_R and unregulated F_U rivers

To calculate the unregulated headwater flows, first the total unregulated flow input to dam *r* (*D*(1) in Fig. 18) is computed by subtracting the total regulated flow from flow at dam *r*. The equation is

$$F_{TU(r)} = F_{D(r)} - \sum_{j=1}^{p} F_{R(j)} \tag{9}$$

where

- $F_{TU(r)}$ = total unregulated flow input to dam *r*
- *p* = number of regulated flows in region
- $F_{D(r)}$ = flow output at dam *r*
- $F_{R(j)}$ = flow output at regulation point *j*

The total unregulated flow is then distributed over all unregulated tributaries upstream of dam *r* in proportion to each tributary's maximum flow, as specified in **`columbia.desc`** by the keyword flow_max. The flow coefficient *K* at each unregulated headwater *i* is the percentage of total unregulated flow contributed by that headwater and is defined

$$K_i = F_{Umax(i)} \Big/ \left(\sum_{j=1}^{q} F_{Umax(j)} \right) \tag{10}$$

where

- K_i = flow coefficient at unregulated headwater *i*
- *q* = number of adjacent unregulated headwaters in region
- $F_{U\,max\,(i)}$ = maximum flow at unregulated headwater *i or j*

Finally, the flow at each unregulated headwater in the region of the dam, $F_{U(i)}$, is defined

$$F_{U(i)} = K_i \cdot F_{TU} \tag{11}$$

The logic for the unregulated flow calculation is complete except when flow at any unregulated headwater falls below the minimum set in **`columbia.desc`** for that headwater, which can be zero. In this case

$$\begin{aligned} &\text{if} \quad F_{U(i)} < F_{U(i)min} \\ &\text{then} \quad F_{U(i)} = F_{U(i)min} \end{aligned} \tag{12}$$

and then for each reach *r* enclosed by dams the new loss $F_{L(r)}$ is

$$F_{L(r)} = \left[\sum_{j=1}^{n} F_{R(j)} - F_{D(r)} + \sum_{i=1}^{m} F_{U(i)} \right] \frac{F_{M(r)}}{\sum_{i=1}^{p} F_{M(i)}} \tag{13}$$

where

- $F_{D(r)}$ = flow output at dam immediately below reach *r*
- $F_{L(r)}$ = new flow loss at reach *r,* as adjusted for mass imbalance
- $F_{M(r)}$ = flow maximum at reach *r or i*
- $F_{R(j)}$ = flow at regulation point *j*
- $F_{U(i)}$ = flow at unregulated headwater *i*
- *m* = number of unregulated headwaters above **r** (*m* = 3 in Fig. 18)
- *n* = number of regulated points adjacent to nearest upstream regulation point (*n* = 2 in Fig. 18)
- *p* = number of reaches between dam *r* and all upstream regulation points (*p* = 9 in Fig. 18).

Downstream Propagation

Downstream propagation of flow in the Monte Carlo Mode is computed after modulation, flow loss and unregulated headwater flows are computed. Starting at a headwater, flow is propagated by traversing the downstream segments, subtracting loss at each to determine new flow values, and adding flows together at confluences. Thus, flows are assigned at each segment in a downstream recursive descent traversal. The flow for each day is

$$F_i(t) = \sum_{i+1} F_i(t) - F_{L(i)} \tag{14}$$

where

- $F_i(t)$ = flow regulation point *i* at reservoir time increment *t*
- $F_{L(i)}$ = flow loss at reach *i*
- $F_j(t)$ = flow at regulation point *j* immediately upstream at reservoir time increment *t*.

Combined Modulated Flow

The modulators are combined with archive flows to give daily flows at the dams according to the equation

$$F(t)_i = F(t)_{\text{arch(i)}} + \sum_j^J \{F(t)_{\text{day(j)}} + F(t)_{\text{week(j)}}\} + \sum_i^I F_{\text{loss(i)}} \qquad (15)$$

$$\text{if} \quad F(t)_i < F_{\text{min(i)}} \quad \text{then} \quad F(t)_i = F_{\text{min(i)}}$$

where

- $F(t)_i$ = modulated flow at dam *i*
- $F(t)_{\text{arch (i)}}$ = archive flow at dam *i*
- $F(t)_{\text{day (i)}}$ = daily modulated flow in regulated headwater *j*
- $F(t)_{\text{week (i)}}$ = weekly modulated flow in regulated headwater *j*
- $F_{\text{loss (i)}}$ = loss modulated flow in river segment upstream of dam *i*
- $F_{\text{min(i)}}$ = minimum allowable flow at dam *i*
- *J* = number of regulated headwaters upstream of dam *i*
- *I* = number of dams upstream of dam *i*, including dam *i*

At each dam, flows are adjusted to conform to minimum values given in Project Data and Operating Limits (Report 49, Revised Book No. 1 and 2, US Army Corps of Engineers, North Pacific Division, July 1989). If the flow drops below the minimum it is set to the minimum flow. Minima are in the **`.dat`** file under the keyword flow_min. Note: flow minima also exist in the **`columbia.desc`** file and are used to set minimum flows in river segments.

Table 4 Flow minimum (kcfs) at dams.

Dam	$F_{\text{min (i)}}$	Dam	$F_{\text{min (i)}}$
Bonneville	80	Dworshak	1
The Dalles	12.5	Hells Canyon	5
John Day	12.5	Priest Rapids	36
McNary	12.5	Wanapum	36
Ice Harbor	7.5	Rock Island	36
Lower Monumental	1	Rocky Reach	36
Little Goose	1	Wells	35
Lower Granite	1	Chief Joseph	35

II.3.3 -Scenario Mode Flow Generation

In the Scenario Mode, seasonal flows for unregulated, i.e. un-dammed, streams are identified on a daily basis. These can be set by the user simply by drawing headwater seasonal flows or they can be generated from modulators that distribute the total

annual headwater runoff according to the historical seasonal patterns.

Unregulated headwater flows connect directly to the river mainstem or to storage reservoirs. For storage reservoirs, the user can set the schedule of outflow according to constraints of the volume of the reservoir and the inflow. System flows are determined by unregulated stream flows and regulated flows from storage reservoir dams.

Headwater Modulation

In the Scenario Mode, flow from unregulated headwaters are modeled by the following equation:

$$Y_t = mp \cdot (F_t + e_t) \tag{16}$$

where

- t = Julian day (t = 1 to 365)
- Y_t = estimated daily flow
- m = mean annual flow computed over a 10 year period
- p = fraction of mean annual for the scenario
- e_t = stochastic error term
- F_t = Fourier term

$$F_t = 1 + \sum_{k=1}^{4} a_k \cdot \cos(k\omega t) + \sum_{k=1}^{4} b_k \cdot \sin(k\omega t) \tag{17}$$

- a_k, b_k = Fourier coefficients estimated for each river
- $\omega = 2\pi / 365$

The equation given for F_t above is a smooth Fourier estimate for the annual stream flow for each river, in units of multiples of the mean. For each scenario, an error term is randomly generated to incorporate the expected fluctuations. There tend to be more pronounced deviations from the modeled curve in the wet season (spring), when the exact fluctuations are more difficult to predict. For this reason, the error component is generated from a low variance normal distribution in the dry season, and a higher variance normal distribution in the wet season. Also, since daily flows tend to be highly correlated, the generated (independent) error estimates (r_t) are artificially correlated according to the following equation:

$$e_t = 0.925 \cdot e_{t-1} + r_t \tag{18}$$

where

- r_t = randomly generated variable from a normal distribution centered on 0 with variance appropriate for dry and wet years as described above. The switch from dry year to wet year variance parameters occurs at p = 0.4.
- $e_0 = 0$.

The user chooses the type of year to be modeled relative to an average year, which is designated by p = 1. CRiSP.1 multiplies this proportion of the appropriate average flow parameter, m times (F_t + e_t), which yields an estimate for daily flow for the Scenario Mode flow.

Reservoir Volume and Flow

The storage reservoirs receive flows from the headwaters which are set by the Scenario Flow Modulators or directly by the user. The flow out of the storage reservoirs can be set by the user under constraints established by the maximum and minimum volume of the storage reservoirs. The equation describing the reservoir usable volume is

$$\frac{dV}{dt} = F_U - F_R \tag{19}$$

where

- dV = change in reservoir volume in acre-ft
- dt = time increment, typically 1 day
- F_U = unregulated natural flow into the reservoir in kcfs
- F_R = regulated flow out of the reservoir, which is controlled by the user under volume constraints in kcfs

The volume for each reservoir is determined a reservoir time step increment from a numerical form of the volume equation

$$V(i+1) = V(i) + c[F_U(i) - F_R(i)]\Delta t \tag{20}$$

where

- $V(i)$ = reservoir volume time step i with units of acre-ft
- Δt = one day increment
- F_U and F_R = unregulated and regulated flows in kcfs
- c = 1983.5 is a conversion factor

acre-ft = (86400 s / d) * (0.023 acre-ft / k ft^3) * (k ft^3 / s) * (d)

V = (86400) * (0.023) *(F) * (Δt)

V = 1983.5 * (F) * (Δt)

The user requests reservoir output F_R with the following constraints: The user is allowed to draw any flow curve for reservoir withdrawal as long as the reservoir is between minimum and maximum operating volumes. If a request requires a volume exceeding the allowable range, CRiSP.1 alters the request to fit within the volume constraints. The algorithm is

$$V_{request}(i+1) = V(i) + c[F_U(i) - F_R(i)] \tag{21}$$

with constraints on reservoir outflow and volume defined by the algorithm

---

if $V_{request}(i+1) > V_{max}$ then

$V_{request}(i+1) = V_{max}$

$F_R(i) = F_U(i) + [V(i) - V_{max}] / c$

else (22)

if $V_{request}(i+1) < V_{min}$ then

$V_{request}(i+1) = V_{min}$

if $F_{request}(i) > F_U$ then

$F_R(i) = F_U(i)$

else

$F_R(i) = F_{request}(i)$

else

$F_R(i) = F_{request}(i)$

---

where

- F_R = outflow from reservoir according to the constraints
- F_U = unregulated inflow to reservoir
- $V_{request}$ = requested outflow from reservoir
- $F_{request}$ = requested outflow from reservoir
- $V(i)$ = reservoir volume in reservoir time step i
- V_{max} = maximum reservoir volume
- V_{min} = minimum reservoir volume

Theory for Parameter Estimation

Average daily flow (designated flow_mean) was computed for all available years. Each daily flow was divided by that year's average. Elements of the resulting series were denoted by X_t, where t = day_of_year. Next, the first nine terms of a Fourier series were computed with a fast Fourier transform. Since the mean of each series was 1, corresponding to the normalized annual mean flow, it follows $a_0 = 1.0$. The remaining Fourier coefficients were estimated according to the equations

$$a_k = \frac{2}{365} \cdot \sum_{t=1}^{365} X_t \cos(k\omega t) \qquad b_k = \frac{2}{365} \cdot \sum_{t=1}^{365} X_t \sin(k\omega t) \tag{23}$$

where

- $\omega = 2\pi / 365$
- k = value between 1 and 4

The residual time series, R_t were computed by the equation

$$R_t = X_t - 1 - \sum_{k=1}^{4} [a_k \cdot \cos(k\omega t) + b_k \cdot \sin(k\omega t)] \tag{24}$$

The residuals were split into high-variance and low-variance parts, and sample standard deviations computed. mod_start_hi_sigma and mod_end_hi_sigma are the Julian day when high flow variance begins and ends. Period average high and low standard deviation are mod_hi_sigma and mod_lo_sigma, respectively.

Data

The daily flow from *Hydrodata*, a CD-ROM database marketed by Hydrosphere, Inc., were obtained for the following locations and dates:

- Clearwater River @ Orifino, Idaho: Oct. 1980 - Sept. 1989
- Salmon River @ Whitebird, Idaho: Oct. 1980 - Sept. 1989
- Grande Ronde River @ Troy, Oregon: Oct. 1980 - Sept. 1989
- Imnaha River @ Imnaha, Oregon: Oct. 1980 - Sept. 1989

Flow modulator parameter estimates derived from flow data listed above were compared to modulator parameters estimated from flows over the previous 10 years at the same location (Oct 1970-Sep 1980). The parameters were slightly different, but graphs of smooth flow curves were nearly identical for Clearwater, Salmon, and Imnaha rivers. The Grande Ronde had a different shape, so for this river the parameters were adjusted to include all data from 1970 to 1989 data.

Table 5 shows parameters estimated for the unregulated headwater modulators. Parameters mod_coeffs_a and mod_coeffs_b correspond to a_k and b_k respectively. Table 6 shows data for regulated headwaters, i.e., Columbia above Grand Coulee Dam, North Fork Clearwater above Dworshak Dam, and Snake River above Brownlee Dam. Daily mean flow observations for each year were obtained from the US Army Corps of Engineers, North Pacific Division and processed as in Table 6. Data were obtained for the following locations and dates:

- North Fork Clearwater RiverOct. 1973 - Sept. 1991
- Grand Coulee Dam Oct. 1971 - Sept. 1991
- Brownlee DamOct. 1981 - Sept. 1991

Table 5 Unregulated headwater flow parameter estimates

	Clearwater	Salmon	G. Ronde	Imnaha
flow_mean (kcfs)	8.790	11.240	3.066	0.514
mod_coeffs_a = a_1	-0.76	-0.84	-0.34	-0.73
mod_coeffs_a = a_2	+0.09	+0.34	-0.18	+0.09
mod_coeffs_a = a_3	+0.10	-0.06	-0.03	+0.03
mod_coeffs_a = a_4	-0.14	-0.09	0.00	-0.04
mod_coeffs_b = b_1	+0.87	+0.50	+0.93	+0.74
mod_coeffs_b = b_2	-0.72	-0.64	-0.32	+0.56
mod_coeffs_b = b_3	-0.35	+0.44	+0.04	+0.20
mod_coeffs_b = b_4	-0.16	-0.25	-0.14	-0.12
mod_lo_sigma	0.06	0.04	0.05	0.06
mod_hi_sigma	0.29	0.20	0.28	0.25
mod_start_hi_sigma	46	86	7	46
mod_end_hi_sigma	196	196	175	196

Table 6 Regulated headwater flow parameter estimates

	Columbia	Snake	Clearwater
flow_mean (kcfs)	110.0	21.50	5.50
mod_coeffs_a = a_1	- 0.238	0.029	- 0.508
mod_coeffs_a = a_2	0.198	0.132	- 0.038
mod_coeffs_a = a_3	0.005	0.008	0.159
mod_coeffs_a = a_4	0.041	0.002	- 0.152
mod_coeffs_b = b_1	0.128	0.348	0.881
mod_coeffs_b = b_2	0.102	0.156	- 0.624
mod_coeffs_b = b_3	0.100	0.045	0.159
mod_coeffs_b = b_4	0.024	0.061	- 0.082
mod_lo_sigma	0.062	0.05	0.230
mod_hi_sigma	0.084	0.10	0.305
mod_start_hi_sigma	96	96	96
mod_end_hi_sigma	196	196	196

Maximum Unregulated Flows

Observed maximum flows in the tributaries were obtained from the peak flow data of *Hydrodata*, a CD-ROM database marketed by Hydrosphere, Inc. The data record length was variable (Table 7).

Table 7 Maximum unregulated flow (kcfs)

Unregulated River	Maximum Flow
Wind	30
Hood	30
West Fork Hood	15
East Fork Hood	15
Klickitat	39
Warm Springs	8
Umatilla	18
Walla Walla	21
Tucannon	5
Clearwater	166
Middle Fork Clearwater	78
Red	10
Salmon	129
Little Salmon	10

Table 7 Maximum unregulated flow (kcfs)

Unregulated River	Maximum Flow
Rapid River	10
South Fork Salmon	19
Pahsimeroi	1
East Fork Salmon	4
Redfish	1
Yakima	64
Wenatchee	31
Entiat	6
Methow	33
Grande Ronde	36
Imnaha	6

Storage Reservoirs Parameter Values

Storage reservoirs volumes are obtained from Project Data and Operating Limits (1989 a and b) and are given in Table 8.

Table 8 Storage reservoirs. Shaded items are used in model.

Reservoir	Max Pool ft	Min Pool ft	Usable Storage in acre-ft	Powerhouse Hydraulic Capacity (kcfs)
Grand Coulee	1290	1208	5,185,500	280
Libby Dam	2459	2287	4,979,599	24.1
Hungry Horse	3565	3336	3,161,000	8.9
Duncan	1897	1794	1,398,600	20
Mica	2478	2320	7,770,000[a]	41.6
Coulee total[b]			22,494,699	
Dworshak	1605	1445	2,015,800	10.5
Brownlee	2080	1976	975,318	34.5

a. estimated
b. In the model all storage reservoirs above Grand Coulee are summed to represent the combined storage capacity of the upper Columbia system.

Desired reservoir elevation levels for flood control, obtained from Project Data and Operating Limits (1989 a and b), are presented in Table 9. This is not used by CRiSP.1 at the present time.

Table 9 Storage reservoirs flood control elevation rule curves

Reservoir	Date (Elevation in ft.)			
Libby Dam	Nov 1	Dec 1	Jan 1	-
	2459	2448	2411	-
Dworshak	Sept. 1	Oct 1	Nov 15	Dec 15
	1600	1586	1579	1558

II.3.4 -Flow-Velocity-Elevation

The river velocity used in fish migration calculations is related to river flow and pool geometry and varies with pool drawdown as a function of the volume. The pool is represented as an idealized channel having sloping sides and longitudinal sloping bottom. As a pool is drawn down, part of it may return to a free flowing stream that merges with a smaller pool at the downstream end of the reservoir. The submodel is illustrated in Fig. 19 and Fig. 20. Important parameters are as follows:

- H_u = full pool depth at the upstream end of the segment
- H_d = full pool depth at the downstream end of the segment
- L = pool length at full pool
- x = pool length at lowered pool
- E = pool elevation drop below full pool elevation
- W = pool width averaged over reach length at full pool
- θ = average slope of the pool side
- F = flow through the pool in kcfs
- U_{free} = velocity of free flowing river.

Other parameters illustrated in Fig. 19 are used to develop the relationships between the parameters listed above and water velocity and pool volume. They are not named explicitly.

Pool Volume

Reservoir volume depends on elevation. Elevation is measured in terms of E, the elevation drop below the full pool level. The volume calculation is based on the assumptions that the width of the pool at the bottom and the pool side slopes are constant over pool length. As a consequence of these two assumptions, the pool width at the surface increases going downstream in proportion to the increasing depth of the pool downstream. When $E > H_u$, the drawn down elevation is below the level of the upstream end and the upper end of the segment becomes a free flowing river section that connects to a pool downstream in the segment. When $E < H_u$, the reservoir extends to the upper end of the segment and for mathematical convenience CRiSP.1 calculates a larger volume and subtracts off the excess. The volume relationship (as a function of elevation drop for E positive measured downward) is developed below.

The total volume is defined

$$V(E) = V_1(E) - V_2(E) \qquad E < H_u \tag{25}$$

First the equation for V_1 is developed. Note that when $E \geq H_u$ the volume V_1 divides into two parts

$$V_1 = 2V' + V'' \tag{26}$$

where V' is a side volume and V'' is the thalweg[1] volume. They are defined

$$V' = \frac{zxy'}{6} \qquad V'' = \frac{zxy''}{2} \tag{27}$$

where

$$x = L\frac{H_d - E}{H_d - H_u} \tag{28}$$

$$z = H_d - E \tag{29}$$

$$y' = z\tan\theta \qquad y'' = W - (H_d + H_u)\tan\theta . \tag{30}$$

Combining these terms, when $E \geq H_u$ it follows pool volume is

$$V_1 = \frac{zxy'}{3} + \frac{zxy''}{2} \tag{31}$$

In terms of the fundamental variables in equations (26) to (31) this is

$$V_1(E) = L\left[\frac{(H_d - E)^2}{H_d - H_u}\right]\left[\frac{W}{2} - \left(\frac{H_d}{6} + \frac{H_u}{2} + \frac{E}{3}\right)\tan\theta\right] \tag{32}$$

for $E \geq H_u$ and $x \leq L$.

1. A thalweg is the longitudinal profile of a canyon.

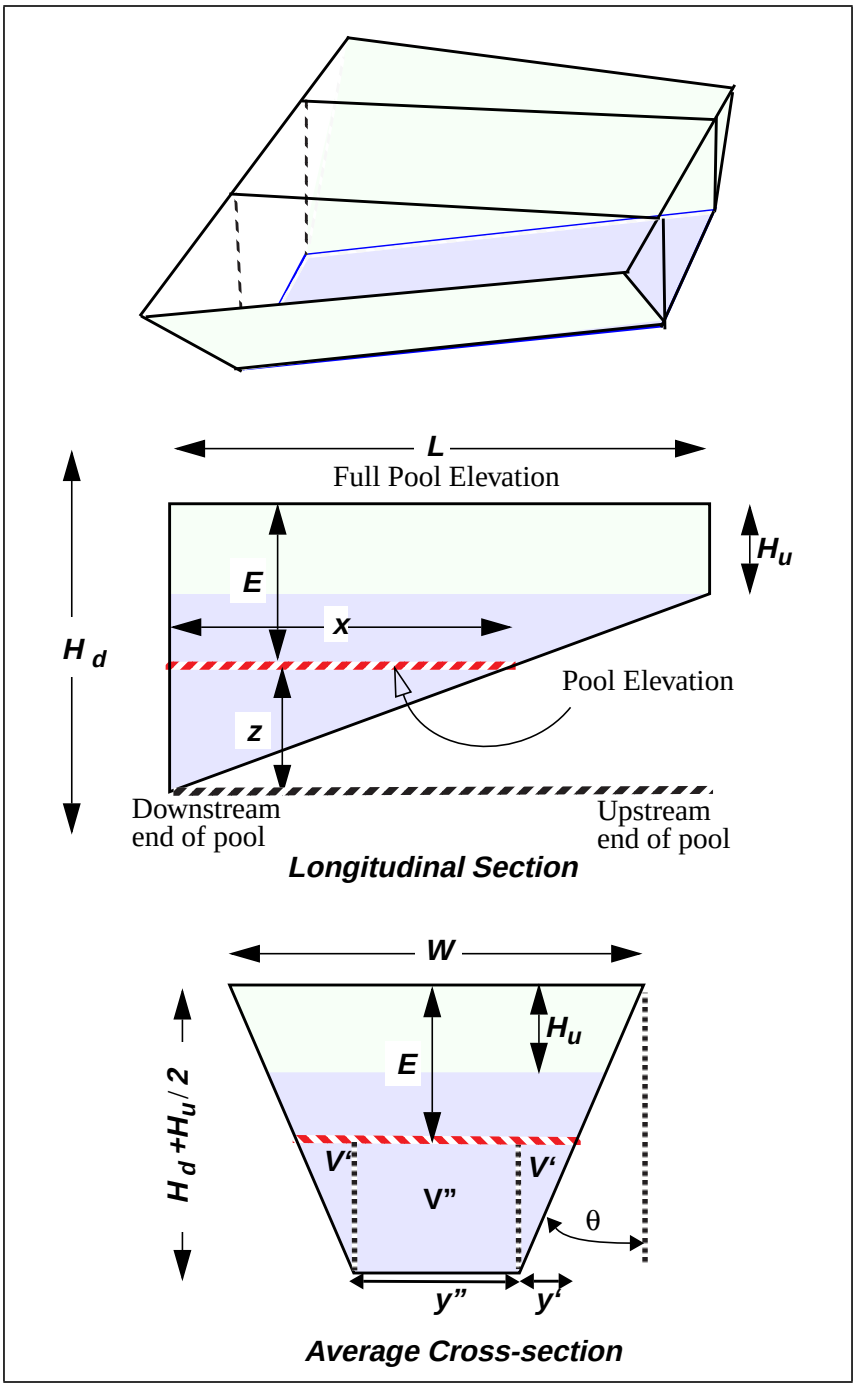

Fig. 19 Pool geometry for volume calculations showing perspective of a pool and cross-sections. The pool bottom with remains constant while the surface widens in the downstream direction

When the pool elevation drop is less than the upper depth (so $E < H_u$ and $x = L$) pool volume is $V(E)$ where

$$V(E) = V_1(E) - V_2(E) \tag{33}$$

The term $V_1(E)$ is the volume of the pool extended longitudinally above the dam, where the depth is H_u, so as to form the same triangular longitudinal cross-section as before. This is done so that the volume can still be expressed by eq (32). The term $V_2(E)$ is the excess volume of the portion of the pool above the dam and can be expressed

$$V_2(E) = L\left[\frac{(H_u - E)^2}{H_d - H_u}\right]\left[\frac{W}{2} - \left(\frac{H_d}{2} + \frac{H_u}{6} + \frac{E}{3}\right)\tan\theta\right] \tag{34}$$

Summarizing, the volume relationship as a function of elevation drop, for E positive measured downward, is

$$\begin{aligned} V(E) &= V_1(E) && E \geq H_u \\ V(E) &= V_1(E) - V_2(E) && E < H_u \end{aligned} \tag{35}$$

where

$$\begin{aligned} V_1(E) &= L\left[\frac{(H_d - E)^2}{H_d - H_u}\right]\left[\frac{W}{2} - \left(\frac{H_d}{6} + \frac{H_u}{2} + \frac{E}{3}\right)\tan\theta\right] \\ V_2(E) &= L\left[\frac{(H_u - E)^2}{H_d - H_u}\right]\left[\frac{W}{2} - \left(\frac{H_d}{2} + \frac{H_u}{6} + \frac{E}{3}\right)\tan\theta\right] \end{aligned} \tag{36}$$

The equation for full pool volume can be expressed

$$V(0) = L\left[W\frac{H_d + H_u}{2} - \frac{\tan\theta}{3}\left(\frac{(H_d + H_u)^2}{2} + H_d H_u\right)\right] \tag{37}$$

When the bottom width is zero the full pool volume becomes

$$V(0) = \frac{LW}{3}\left[\frac{H_d^3 - H_u^3}{H_d^2 - H_u^2}\right] \tag{38}$$

Water Velocity

Water velocity through a reservoir is described in terms of the residence time *T* and the length of the segment *L*. The residence time in a segment depends on the amount of the reservoir that is pooled and free flowing (Fig. 20).

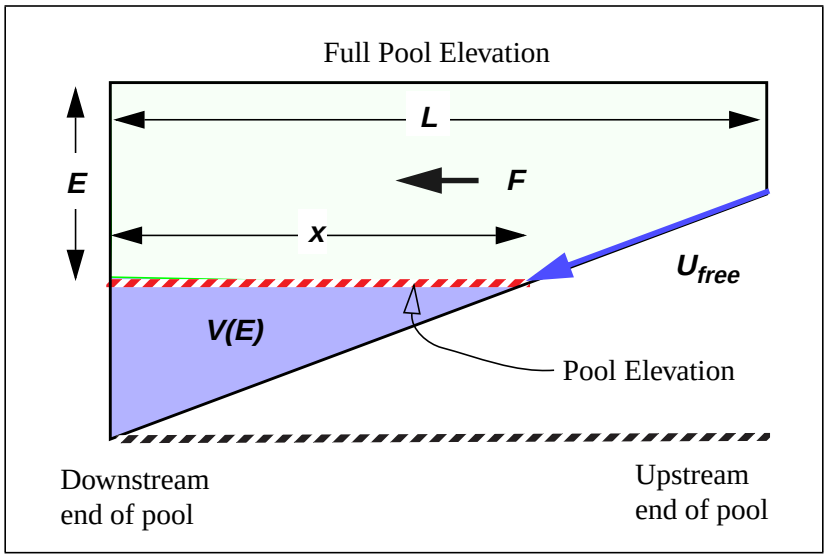

Fig. 20 Reservoir with flowing and pool portions

The equations for residence time are

$$T = \frac{V(E)}{F} + \frac{L - x}{U_{free}} \qquad E \geq H_u$$
$$T = \frac{V(E)}{F} \qquad E < H_u \tag{39}$$

where

- $V(E)$ = pool volume (ft^3) as a function of elevation drop E in feet
- F = flow in 1000 cubic feet per second or kcfs
- L = segment length in feet
- x = pool length defined by eq (28) and with units of feet
- U_{free} = velocity of water in the free stream (kfs) (using the John Day River, the default value is 4.5 ft / s which is 4.5 x 10^{-3} kfs)
- T = residence time in this calculation is in kilo seconds or ks.

The velocity in the segment is

$$U = \frac{L}{T} \tag{40}$$

The velocity with the above units is in thousands of feet per second.

Combining equations eq (36), eq (39) and eq (40) the segment velocities are:

for $E \geq H_u$

$$U = \frac{L}{\frac{V_1(E)}{F} + \frac{L - x}{U_{free}}} \tag{41}$$

and for $E < H_u$

$$U = \frac{LF}{V_1(H_u) + V_2(E)} \tag{42}$$

where

- U = average river velocity in ft/s
- U_{free} = the velocity of a free flowing stream in ft/s
- F = flow in kcfs
- E = elevation drop (positive downward) in ft
- H_u = depth of the upper end of the segment in ft
- V_1 and V_2 = volume elements defined by eq (36)

Flow-Velocity Calibration

The calibration of the volume equation requires determining the average pool slope from the pool volume. The equation is the smaller angle of the two forms

$$\theta = \text{atan}\left(\frac{3W(H_d + H_u) - 6\frac{V(0)}{L}}{(H_d + H_u)^2 + 2H_d H_u}\right) \quad \text{or} \quad \theta = \text{atan}\left(\frac{W}{H_d + H_u}\right) \tag{43}$$

where

- $V(0)$ = pool volume at full pool

This scheme using eq(43) reflects the volume versus pool elevation relationship developed for each reservoir by the U.S. Army Corps of Engineers. Capacity versus elevation curves were obtained from several dams to check the accuracy of our volume model. The figures below show data points from these curves versus CRiSP's volume curve for two dams. Fig. 21 illustrates Lower Granite pool, with model coefficients of H_u = 40 ft., H_d = 118 ft, $\theta = 80.7^o$, L = 53 miles, W = 2000 ft, and Wanapum pool, with

model coefficients H_u = 42ft., H_d = 116 ft, θ = 87.0^o, L = 38 miles, W = 2996.1ft.

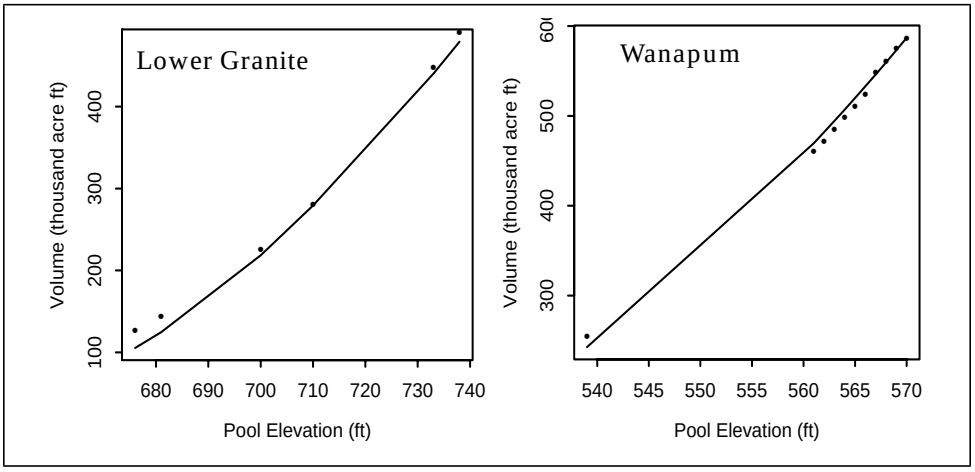

Fig. 21 Pool elevation vs. volume for Lower Granite and Wanapum Pools

Table 10 Geometric data on Columbia River system. Elev is normal full pool elevation, in feet above mean sea level. MOP is minimum operating pool elevation.

Segment	L	Elev	MOP	V	A	W	H_u	H_d	θ
Units	miles	ft MSL	ft MSL	kAf	k ft ^{2}	feet	feet	feet	^{o} of arc
Bonneville	46.2	77.0	70.0	565	101.8	3643	40	72	88.2
The Dalles	23.9	160.0	155.0	332	114.6	3624	25	70	87.9
John Day	76.4	268.0	257.0	2,370	255.9	5399	30	125	88.1
McNary	61	340.0	335.0	1,350	182.6	5153	35	85	88.4
Hanford Reach	44	---	---	131	24.6	3213	28.4	28.4	---
Priest Rapids	18	488.0	465.0	199	91.2	3208	32	72	88.1
Wanapum	38	570.0	539.0	587	127.4	2996	42	116	87.0
Rock Island	21	613.0	609.0	113	44.4	982	27	74	64.4
Rocky Reach	41.8	707.0	703.0	430	84.8	1815	20	120	84.5
Wells	29.2	781.0	767.0	300	84.8	3023	43	58	87.9
Chief Joseph	52	956.0	930.0	516	81.9	3023	70	80	87.1
Ice Harbor	31.9	440.0	437.0	407	105.2	2154	25	100	83.3
L. Monumental	28.7	540.0	537.0	377	108.4	1937	30	112	81.3
Little Goose	37.2	638.0	633.0	365	80.9	2200	25	105	86.6
Lower Granite	53	738.0	733.0	484	75.3	2000	40	118	80.7

The water particle residence time in a segment is given in eq (39). The pool volume velocity / travel time equation was tested against particle travel calculations for Lower Granite Pool as reported by the Army Corps of Engineers in the Lower Granite Drawdown studies report (1993) (Fig. 22.)

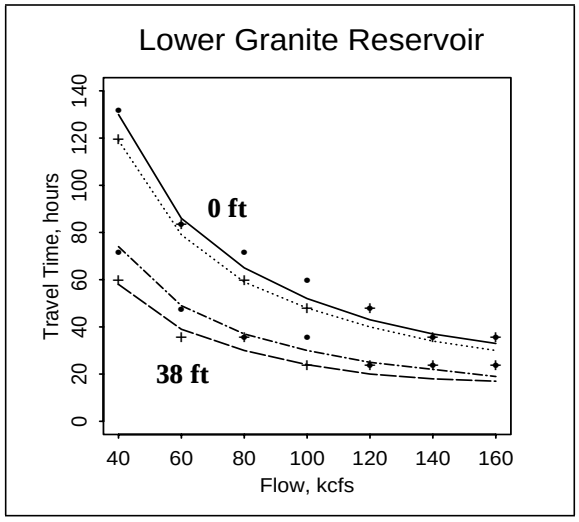

Fig. 22 Water particle travel time vs. flow for CRiSP (points) and Army Corps calculations (lines) at two elevations full pool(0) and 38 ft below full pool for Lower Granite Dam.

II.3.5 -Temperature

River temperature is computed from mixing of headwater temperatures according to the equation

$$\theta(t) = \frac{\sum_i \theta_i(t) F_i(t)}{\sum_i F_i(t)} \tag{44}$$

where

- $F_i(t)$ = flow from headwater *i* through the river segment in question on day *t*
- $\theta_i(t)$ = temperature from headwater *i* on day *t*
- $\theta(t)$ = temperature for selected river segment on day *t*

Headwater temperatures are identified for the Snake River using measured temperatures from Lower Granite Dam as available in the Army Corps of Engineers CROHMS data base. Head water temperatures for the Mid-Columbia are identified from CROHMS and supplemented using data collected by the US Geological Survey (USGS).

II.4 - Reservoir Passage

In CRiSP.1, passage and survival of fish through a reservoir is expressed in terms of the fish travel time through the reservoir, the predation rate in the reservoir and a mortality rate resulting from fish exposure to nitrogen supersaturation, an effect called Gas Bubble Disease. CRiSP.1 formulates these mortality factors individually (Fig. 23).

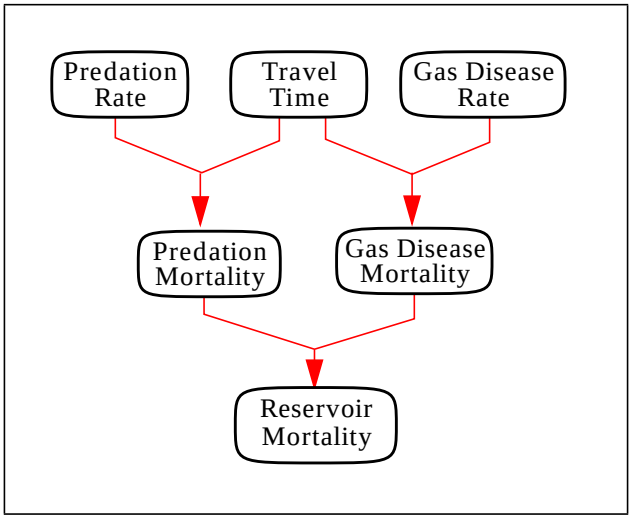

Fig. 23 Reservoir mortality processes

The processes that determine the factors are complex, and not fully understood, while information to characterize them is limited. In light of the observational and theoretical uncertainties, the modeling approach has been to develop alternative submodels of reservoir mortality. In this manner CRiSP.1 users can run a scenario with alternative models and compare the different effects on fish survival.

II.5 - Fish Migration

II.5.1 -Theory

The movement of fish through river segments is described in terms of an average migration velocity and a stochastic velocity that varies from moment to moment. The migration velocity equation for a group of fish is defined by the Wiener stochastic differential equation

$$\frac{dX}{dt} = r + \sigma W(t) \tag{45}$$

where

- X = position of a fish down the axis of the river
- dX/dt = velocity of fish in migration
- r = average velocity of fish in the segment

  This is a combination of water movement and fish behavior.
- σ = spread parameter setting variability in the fish velocity
- $W(t)$ = Gaussian white noise process to represent variation in velocity

Numerical simulation of time vs. distance traveled according to eq (45) is illustrated in Fig. 24.

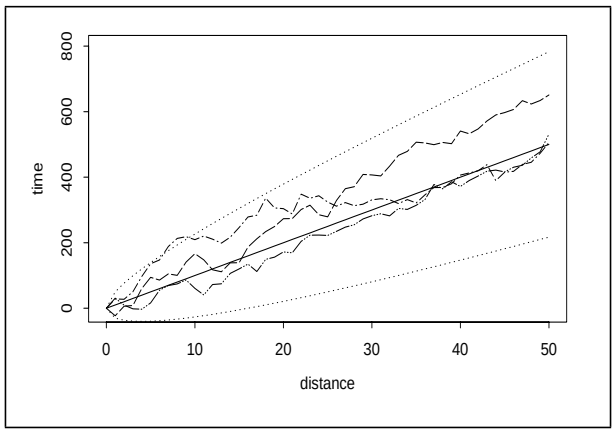

Fig. 24 Movement along axis of segment vs. time. Shown are mean path, three paths, and 95% confidence intervals. For these simulations, r is set at 10, and σ set at 20.

Probability Density Function

The stochastic equation describing fish positions is random so we must define the probability distribution of fish position over time instead of the actual position, which changes from one fish to another. The probability density function (pdf) of the stochastic differential equation (eq (46)) can be defined with a Fokker-Planck (Gardiner 1985) equation

$$\frac{\partial p}{\partial t} = -r\frac{\partial p}{\partial x} + \frac{\sigma^2}{2}\frac{\partial^2 p}{\partial x^2} \tag{46}$$

where $p = p(x, t)$ is the pdf describing the probability density of the fish being at position x at time t given it was at position $x = 0$ at time $t = 0$.

Boundary Conditions

To solve the pdf from eq (46), boundary conditions must be identified. We assume that upon release into a segment a fish can move upstream or downstream in the segment but once it has reached the downstream end of the segment, at $x = L$, it will move into the next segment. The next downstream segment may be a confluence or the forebay of a dam. The boundary conditions are

$$\begin{aligned} p(L, t) &= 0 \\ p(-\infty, t) &= 0 \end{aligned} \tag{47}$$

Solution

The solution to the partial differential equation (eq (46)) describing the probability distribution of fish in a river segment is a probability density function for the fish. This is

$$p(x,t) = \frac{1}{\sqrt{2\pi\sigma^2 t}}\left[\exp\frac{-(x-rt)^2}{2\sigma^2 t} - exp\left(\frac{2Lr}{\sigma^2} - \frac{(x-2L-rt)^2}{2\sigma^2 t}\right)\right] \quad (48)$$

An example of the distribution of p with respect to x for different times is illustrated in Fig. 25. The pdf in the figure can be interpreted as probability where a fish is in the river at any time. It can also be interpreted as the distribution of a group of fish in a river segment if they have experienced no predation. Notice that the group moves down the segment and spreads over time. At the absorbing boundary representing a dam, the fish enter the boundary regions and pass through to the next segment. Note that the equation cannot define the deterministic path of fish with time.

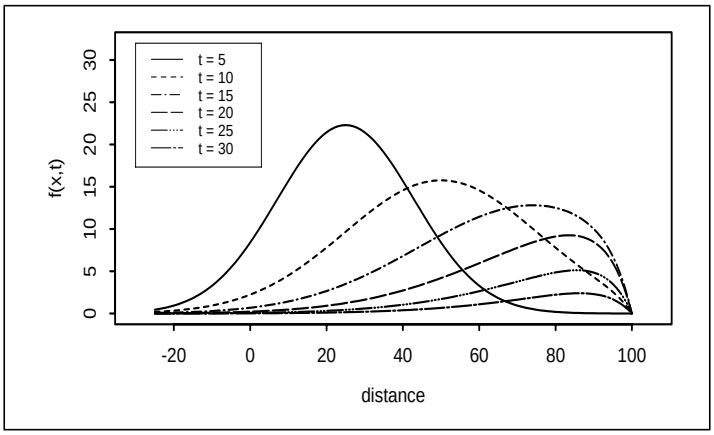

Fig. 25 Plot of eq (48) for various values of t. Parameters r, σ and L are set at 5, 8, and 100 respectively.

Passage Probability

The probability that a fish that entered the river segment at time t_i is still in the river segment at time t_j is obtained by integrating eq (48) over reservoir length. This is expressed

$$P(t_j|t_i) = \int_{-\infty}^{L} p(x, t_j - t_i)dx = \Phi\left(\frac{L - r\cdot(t_j - t_i)}{\sigma\sqrt{t_j - t_i}}\right) - \exp\left(\frac{2Lr}{\sigma^2}\right)\Phi\left(\frac{-L - r\cdot(t_j - t_i)}{\sigma\sqrt{t_j - t_i}}\right) \quad (49)$$

where

- Φ = cumulative distribution of the standard normal distribution
- L = segment length
- r = average migration velocity through the segment (developed on page II.54).

The probability of a fish leaving a segment between time t and $t + \Delta t$ is

$$\Delta P(t_j | t_i) = P(t_j | t_i) - P(t_{j-1} | t_i) \quad (50)$$

This is the arrival time distribution at the point *L*, which is generally a dam or river confluence. The number of fish exiting each river segment is defined by eq (50).

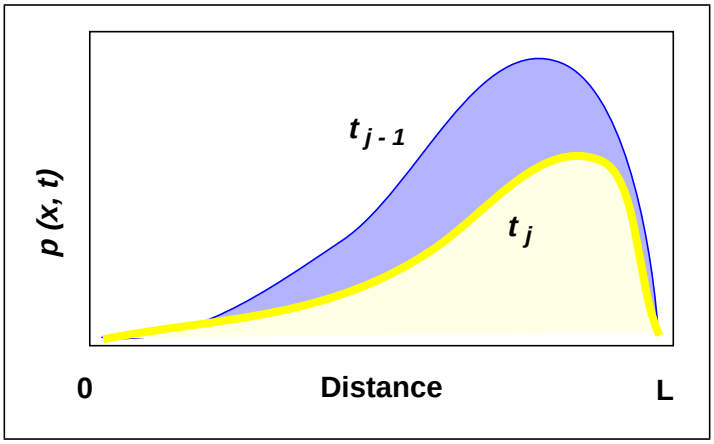

Fig. 26 Fish distribution, $p(x, t)$, at t_j and t_{j-1}. Size of the shaded area represents probability of fish leaving the segment over the interval $t_j - t_{j-1}$

Migration Parameters

Active Migration equation

The goal of the active migration equation is to be flexible enough to capture a variety of migratory behaviors without requiring an excessive number of parameters to fit. The equation has a term that relates migration rate to river velocity and a term that is independent of river velocity. Both terms have temporal components, with migration rate increasing with time of year.

The flow independent migration rate is driven by two parameters, β_{min} and β_{max}. β_{min} is the flow independent migration rate at the time of release (T_{RLS}), and β_{max} is the maximum flow independent migration rate. In the equation below (eq(51)), it is easier to express the equation in terms of β_0 and β_1, with the following relations:

$$\begin{aligned} \beta_{min} &= \beta_0 + \frac{\beta_1}{2} \\ \beta_{max} &= \beta_0 + \beta_1 \end{aligned} \quad (51)$$

With $\beta_{max} > \beta_{min}$, the fish have a tendency to migrate faster the longer they have been in the river. This tendency can be "turned off" by setting $\beta_{max} = \beta_{min}$. Also, flow independent migration can be turned off entirely by setting $\beta_{max} = \beta_{min} = 0$.

The magnitude of the flow dependent term is determined by β_{flow}. This term determines the percentage of the average river velocity that is used by the fish in downstream migration. This term has a seasonal component determined by the

T_{SEASN} term, which is expressed in terms of Julian date. This has the effect of the fish using less of the flow early in the season and more of the flow later in the season. Values of T_{SEASN} that are relatively early in the season mean that the fish mature relatively early. The α parameter determines how quickly the fish mature from early season behavior to later season behavior. Setting α equal to 0 has the effect of "turning off" the flow / season interaction, resulting in a linear relationship between migration rate and river flow.

Migration rate is modeled as:

$$r(t) = \beta_0 + \beta_1\left[\frac{1}{1 + exp(-0.1(t - T_{RLS}))}\right] + \beta_{FLOW}\bar{V}_t\left[\frac{1}{1 + exp(-\alpha(t - T_{SEASN}))}\right] \quad (52)$$

where

- $r(t)$ =migration rate (miles / day)
- t =Julian date
- β's = regression coefficients, described above
- $\bar{V}_t$ = average river velocity during the average migration period
- α = slope parameter
- T_{SEASN} = seasonal inflection point (in Julian Days)
- T_{RLS} = release date (in Julian Days).

Both the flow dependent and flow independent components of eq (52) use the logistic equation (term in brackets). The logistic equation is expressed in general as

$$y = \beta_0 + \beta_1\left[\frac{1}{1 + \exp(-\alpha(t - T_0))}\right] \quad (53)$$

The equation has a minimum value of β_0 and a maximum value of $\beta_0 + \beta_1$. T_0 determines the inflection point, and α determines the slope. Fig. 27 contains example plots of the equation and demonstrates how varying the parameter affects the shape of the curve.

The logistic equation is used instead of a linear equation because upper and lower bounds can be set. This eliminates the problem of unrealistically high or low migration rates that can occur outside observed ranges with linear equations. Also, for suitable parameter values, the logistic equation effectively mimics a linear relationship.

Velocity Variance

The spread parameter σ sets the variability in the migration velocity. This term represents variability from all causes including water velocity and fish behavior. In CRiSP.1, $\sigma^2 = V_{var}$ which is the variance in the velocity. This can vary on a daily basis.

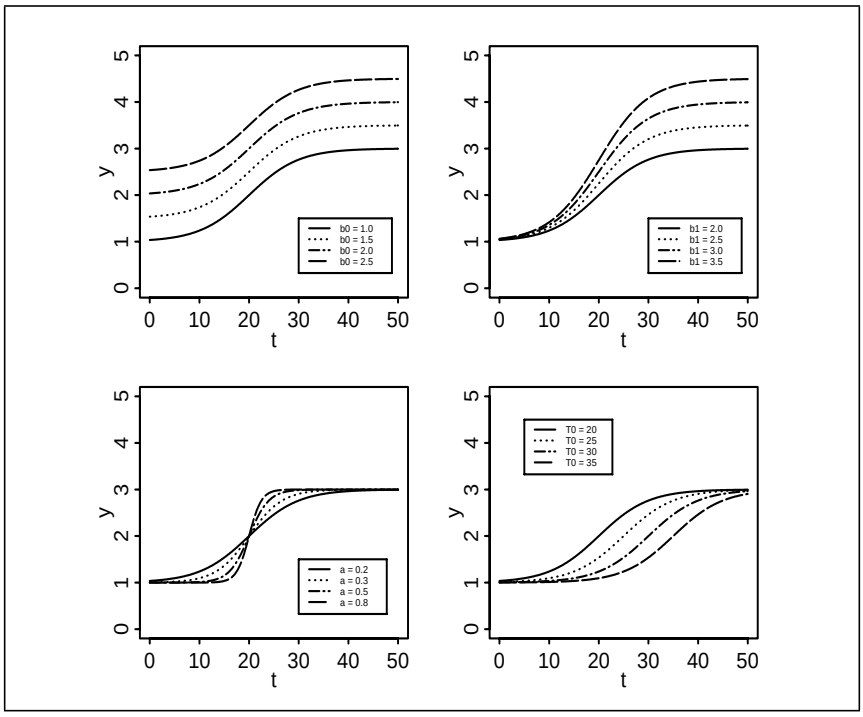

Fig. 27 Examples of the logistic equation (eq (53)) with various parameter values. In all four plots, the parameter values for the solid curves are: $\beta_0 = 1.0$, $\beta_1 = 2.0$, $\alpha = 0.2$, and $T_0 = 20$. In the upper left plot β_0 is varied, and β_1 is varied in the upper right. In the lower left plot, α is varied, and T_0 is varied in the lower right.

Variance in Migration Rate

Variance in the migration rate is applied for each release, thus randomly representing differences in the migration characteristics of each release. Although studies suggest differences in migration can partly be attributed to differences in fish condition and perhaps stock to stock variations, these factors have not been sufficiently identified so their contribution to differences in travel time is randomized. The equation is

$$r_i(t) = r(t) \cdot V(i) \tag{54}$$

where

- $r(t)$ = determined from eq (52)
- $V(i)$ = variance factor that varies *between* releases only.

$V(i)$ is drawn from the broken-stick distribution. The mean value is set at 100%, representing $r(t)$, and the upper and lower values are set with sliders under the migration rate variance item in the **Behavior** menu.

Pre-smolt behavior

In some cases, fish are released into the river before they are ready to initiate migration. This may be the case with hatchery releases or fish that are sampled and

released in their rearing grounds. The probability of moving from the release site is determined by two dates, $smolt_{start}$ and $smolt_{stop}$:

$$p = \begin{cases} 0 & for \quad (t < smolt_{start}) \\ \dfrac{(t - smolt_{start})}{(smolt_{stop} - smolt_{start})} & for \quad (t < smolt_{start} < smolt_{stop}) \\ 1 & for \quad (t > smolt_{stop}) \end{cases} \quad (55)$$

In other words, the probability of initiating migration is 0 before $smolt_{start}$, 1 after $smolt_{stop}$, and linearly increasing with time between the two values. Fish are subjected to predation prior to the onset of smoltification. The predation activity coefficient for pre-smolt mortality uses the activity coefficient for the first day of smoltification $t = 1$.

Implementing the Travel Time Algorithm

The basic unit of the travel time algorithm is a reach of river between two nodes, where a node is a dam, confluence of two rivers, or a release point (Fig. 28). The travel time algorithm passes a group of fish from node to node and determines the distribution of travel times from an upstream node to the next downstream node.

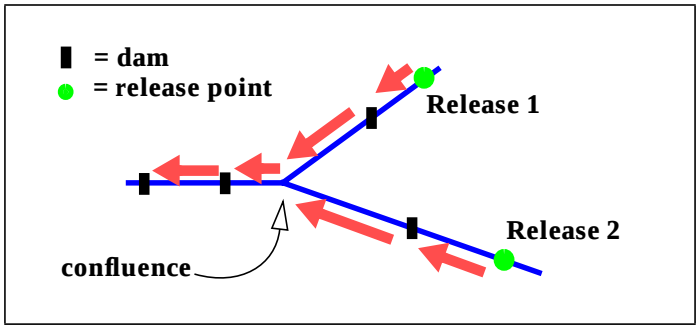

Fig. 28 Schematic diagram of a river system. Arrows represent the migration of release groups 1 and 2 through reaches. At the confluence, groups are combined for counting purposes only, i.e they still exhibit their unique migration characteristics.

CRiSP.1 groups fish according to user preference. The user defines *species* (and *stocks*, if desired) in the **`columbia.desc`** file and associates behavioral characteristics with each species through the user interface or the yearly input data file[1]. For instance, the user may decide that all chinook 1's should be treated identically or that wild and hatchery stocks be treated separately. All releases that are treated similarly are referred to as a release group, except for the random selection of a migration rate variance.

During one iteration of the travel time algorithm, fish from a release group pass through a reach. The input to CRiSP.1 is the number of fish from the release group that are ready to depart a node during the time interval. This input group is passed to the next node downstream with the travel time distributions determined by eq (49) and eq (50). Fig. 29 demonstrates a single iteration of the travel time algorithm.

1. As configured the columbia.desc creates three species: chinook 1 = spring chinook, chinook 0 = autumn chinook, and steelhead.

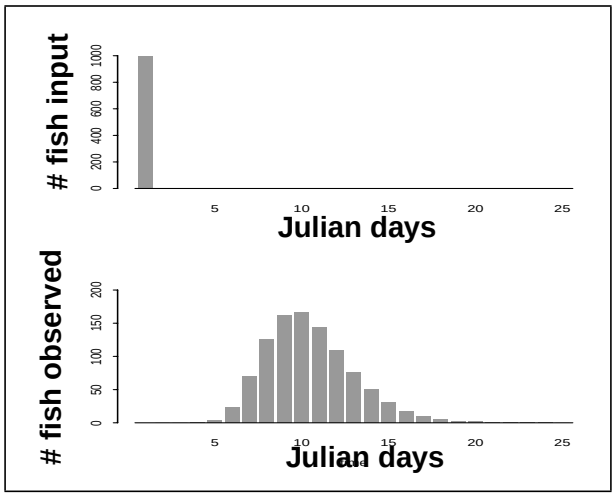

Fig. 29 Plots of a single iteration of the travel time algorithm through a single reach. One thousand fish released at the upstream node are distributed through time at the next downstream node. Parameter: $r = 10$, $\sigma = 8$, $L = 100$.

II.5.2 -Calibration of Fish Travel Time Algorithms

Migration rate is calculated on a reach and time step basis. (See Fish Migration section on page II.51.) At each time step that fish are released at the top of a reach, a unique migration rate is determined for that reach. Migration rate is defined by eq (52). The equation has the following coefficients:

- $r(t)$ = migration rate (miles / day)
- t = Julian date
- β's = regression coefficients
- V_f = average river velocity during the average migration period
- α = slope parameter
- T_{SEASN} = inflection point of flow dependent term (in Julian date)
- T_{RLS} = release date (in Julian date).

The minimum flow independent migration rate (β_{min}) is equal to $\beta_0 + \beta_1/2$, and the maximum flow independent migration rate is equal to $\beta_0 + \beta_1$. The parameters that must be estimated are β_{min}, β_{max}, β_{flow}, α, and $T_{seasn.}$ Note that if $\beta_{min} = \beta_{max}$, there is no increase in the flow independent component with time. Also, flow dependency can be eliminated by setting $\beta_{flow} = 0$.

These parameters are estimated using a calibration program that is, in effect, a stripped-down version of CRiSP that only encompasses the travel time component. The migration rate parameters and river flow information are provided to the program, and it returns average travel times to several points along the river. These model-predicted average travel times are then compared to observed average travel times. Migration rate parameters are selected that give the best model fit to the data.

Several criteria are used to select appropriate data sets. First, because migration rate is related to date in season and date of release, it is essential that the calibration

data sets have fish released over long periods of time so these effects can be measured. Also, it is desirable to have fish released from the same site over multiple years so that a variety of river conditions are encountered. Sufficient numbers of fish must be observed at downstream observation sites, and fish must be observed at multiple sites. Finally, data sets are selected to represent as many stocks of fish and sections of the river as possible.

The procedure is to first organize fish into cohorts, which comprise fish released on the same day or on several consecutive days. Based on these cohorts, the following equation is minimized with respect to the migration rate parameters:

$$SS = \sum_{i=1}^{n} \sum_{j=1}^{k} (\overline{tt_{mod}} - \overline{tt_{obs}})^2 \qquad (56)$$

where n is the total number of cohorts, and k is the total number of observation sites. This equation is fit using a Levenberg-Marquardt routine (Press, et al., 1992), with derivatives calculated numerically using a finite difference method (Seber and Wild, 1989; Gill, Murray, and Wright, 1981).

In the following sections, the estimated migration rate parameters are provided, along with plots that compare the model-predicted average travel times to observed average travel times.

Estimating *Vvar*

Vvar determines the rate of spreading of the cohort of fish and requires more detailed information to estimate than the migration rate parameters, which just require average travel time information. Estimating *Vvar* requires the distribution of travel times for a cohort; thus the unit of information for calibration is the daily counts. Since there is a great deal of variability in the variances associated with the daily counts, generalized least squares (Draper and Smith, 1981) is used to estimate *Vvar*. Zabel (1994) provide the details of this procedure.

Smolt start/stop date

The smolt dates determine when fish initiate migration. Before smolt start date, no migration occurs. After smolt start date and before smolt stop date, a proportion of the release initiate migration on a daily basis. After smolt stop date, all fish in the release have initiated migration. Note that these dates are only relevant if fish are released before they are ready to migrate. If the fish are active migrants, then smolt start and stop dates should be set to dates previous to release dates.

In order to estimate these dates, we require data of fish released before they are ready to migrate. Based on the arrival distribution at the first observation point and the travel time to reach that point, smolt start and stop dates can be estimated.

Travel time data sets

As of the writing of this manual, these are the data sets that have been analyzed for travel time calibration. The number of stocks analyzed is being expanded, and in the next release of the manual, several more stocks will be included.

Snake River spring chinook

These are PIT tagged fish released at the Snake Trap (top of Lower Granite Pool) and observed at Lower Granite, Little Goose, and McNary Dams. The release period is from early April to early May, with separate releases occurring daily. Although these fish are classified as run-of-the-river fish, it is likely that the vast majority of these fish are spring chinook based on the distribution of lengths (most fish longer than 110 millimeters) and the timing of migration (early spring). This is consistent with other treatments of these fish (e.g., Fish Passage Center, 1991). Release cohorts were formed by lumping together releases from up to three consecutive days to achieve sample sizes of at least 80 individuals observed at Lower Granite Dam. Data from the years 1989-1994 were analyzed; 52 cohorts were analyzed over this period.

The migration rate equation was fit to all three of the observation points simultaneously. Plots of the results are contained in Fig. 30, and the parameter estimates are in Table 11. Because these fish are active migrants, smolt start and stop dates are set to day 90, which is the earliest day that fish are observed at Snake Trap.

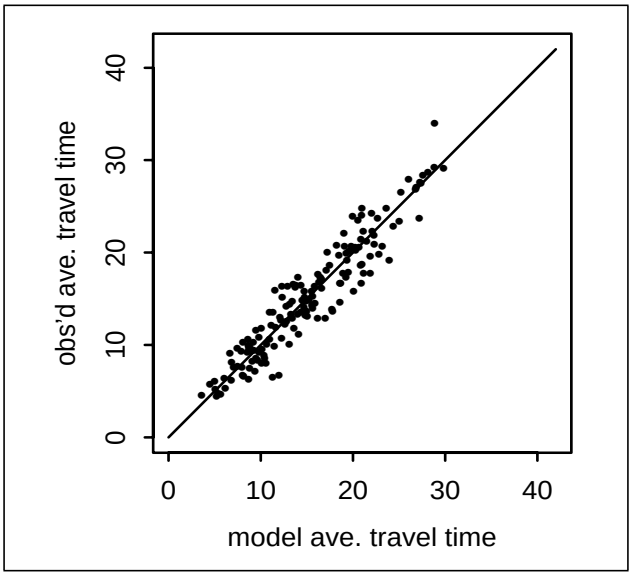

Fig. 30 Spring chinook observed travel time vs. modeled travel time. Data includes travel time to three dams, L. Granite, L. Goose, and McNary.

Mid-Columbia fall chinook

Two groups of mid-Columbia summer / fall chinook were analyzed: Priest Rapids hatchery fish (brand) and run-of-the-river fish collected and released at Rock Island Dam (PIT tag).

The brand release hatchery fish were released at Priest Rapids and observed at McNary and John Day Dams. Five groups were released each year on separate days, and these release groups were the units of the analysis. Data was analyzed from 1988, 1989, 1991, 1992, 1993 (1990 has censored data). The release groups from all the years were analyzed together to estimate migration rate parameters. Also, smolt dates were estimated from these data.

The run-of-the-river PIT tag fish were collected, tagged, and released at Rock

Island Dam. The fish analyzed were identified as summer / fall chinook by Chapman, et al. (1994) for the 1992 and 1993 fish. We used the same criteria to identify the 1994 summer fall chinook. Release groups over 7 consecutive days were lumped together to form cohorts of adequate sample size. This resulted in 3 cohorts for 1992, 8 cohorts in 1993, and 6 cohorts in 1994. These fish are active migrants, so smolt start and stop dates could not be estimated.

There is no evidence that these fish increase their migration rate as they spend more time in the river, so $\beta_{min} = \beta_{max}$. The parameter estimates are contained in Table 11, and plots of the results for both groups are contained in Fig. 31.

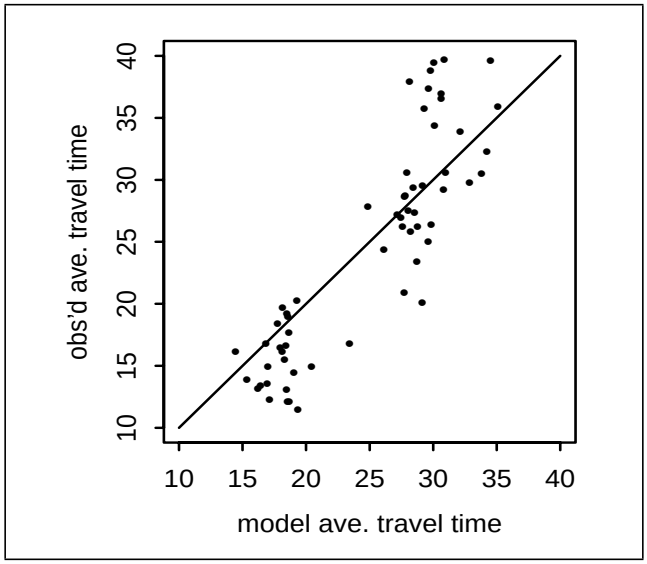

Fig. 31 Fall chinook - Priest Rapids brand releases- 1988-1989, 1991-1993. Observation Points: McNary and John Day.

Table 11 CRiSP migration rate parameters for the data sets described in this section.

release site	β_{min}	β_{max}	β_{flow}	a	T_{seasn}	V_{var}	smolt dates	
							start	stop
yearling chinook								
Snake	1.34	20.2	0.71	0.10	119.8	100.0	90	90
subyearling chinook								
Priest	6.11	6.11	0.12	0.860	176.0	225.0	160	165
R.I.	4.89	4.89	0.12	0.425	205.1	225.0	-	-
steelhead								
Dworshak (hatchery)	0.240	0.246	1.401	0.867	122.2	400.0	90	90
Snake (Wild)	-7.45	23.64	3.136	0.001	121.3	280.0	90	90

Snake River fall chinook

Wild fall chinook were collected (by beach seining) in the Snake River above the confluence of the Clearwater River in the years 1991-1994. The fish were PIT tagged and then detected as they passed Lower Granite and Little Goose Dams. Fish were also detected at McNary Dam but sample sizes there were very low (approximately 5-10 fish per year). Many of the fish sampled were in the premigratory phase (well below 85 mm in length) making travel time calibration more difficult.

To calibrate Snake River fall chinook travel time our approach was to use the travel time parameters obtained for the Rock Island fall chinook (Table 11) and vary smolt start/stop dates on a yearly basis. For consistency, the duration between smolt start and stop dates was kept constant over the four years. The modeled average arrival dates at Lower Granite and Little Goose Dams were fit to the observed average arrival dates to these dams. The results are contained in Fig. 31 and Table 12. In the future, we will relate variability in smolt start/stop date for fall chinook to river temperature.

Table 12 Smolt start and stop dates for the Snake River fall chinook. Dates are based on PIT tag data with observations at Lower Granite and Little Goose.Other migration rate parameters are obtained from Table 11.

year	smolt date	
	start	stop
1991	194	214
1992	166	186
1993	196	216
1994	199	219

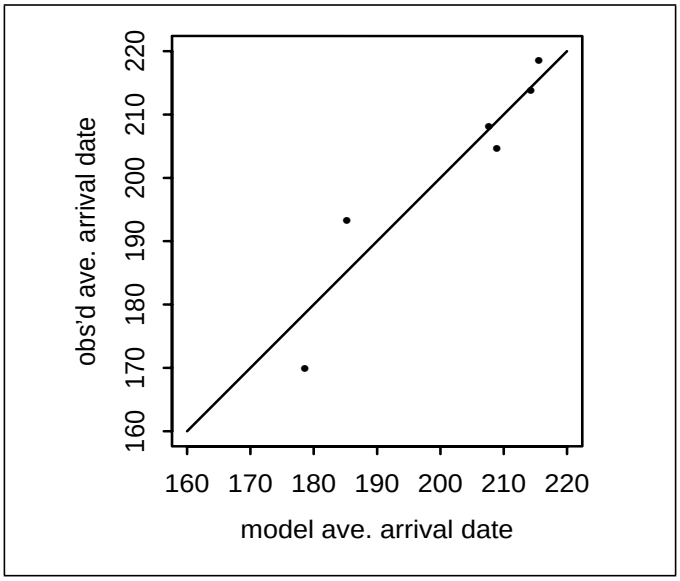

Fig. 32 Fall chinook - Snake River PIT tag releases - 1991-1993. Observation Points: Lower Granite and Little Goose Dams.

Dworshak Hatchery steelhead

Five years of PIT tag data were analyzed to estimate travel time parameters for Dworshak Hatchery steelhead. The fish were released at the hatchery and observed at Lower Granite, Little Goose and McNary Dams. The travel time parameters were estimated by comparing observed average travel times to the 3 collection sites to model predicted values. The results are contained in Table 11 and Fig. 33. These data were also used to estimate *FGE* (see Steelhead FGE section on page II.127).

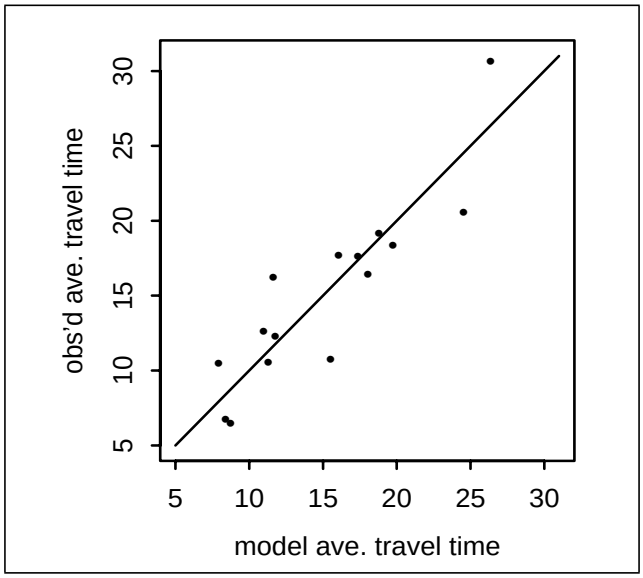

Fig. 33 Observed average travel time versus modeled average travel time for Dworshak Hatchery steelhead. The PIT tagged fish were released at Dworshak and observed at Lower Granite, Little Goose and McNary during the years 1989-1993.

Snake River wild Steelhead

Wild Snake River steelhead were PIT tagged at the Snake River trap and observed at Lower Granite, Little Goose, and McNary dams. These fish were released over the seven year period 1989-1995. Results are given in Table 11.

Variance in migration rate

Variability in plots of observed versus modeled average travel times result from variations among particular releases. To account for this a multiplicative variance is introduced by eq (54) where

- r = determined
- $V(i)$ = variance factor that varies *between* releases only.

$V(i)$ is drawn from the broken-stick distribution. The default values for spring and fall chinook and steelhead are mean = 1 low = 0.7 and high = 1.3

II.6 - Reservoir Survival

Fish mortality in reservoirs depends on a multitude of interactive factors. An important component of this is the predation rate which in turn is dependent on the number and behavior of predators, size of prey, genetic disposition of prey, disease, stress from dam passage, and degree of smoltification. Theory presented here approximates mortality processes in reservoirs while future versions of CRiSP will deal with these interactions. At the current time mortality involves the predation rate and travel time. These factors in turn depend on flow, predator density, and river temperature. An interaction between predator density and reservoir volume is provided as a switchable function to represent the impact of confining predators in a smaller volume when a reservoir is lowered. (Fig. 34).

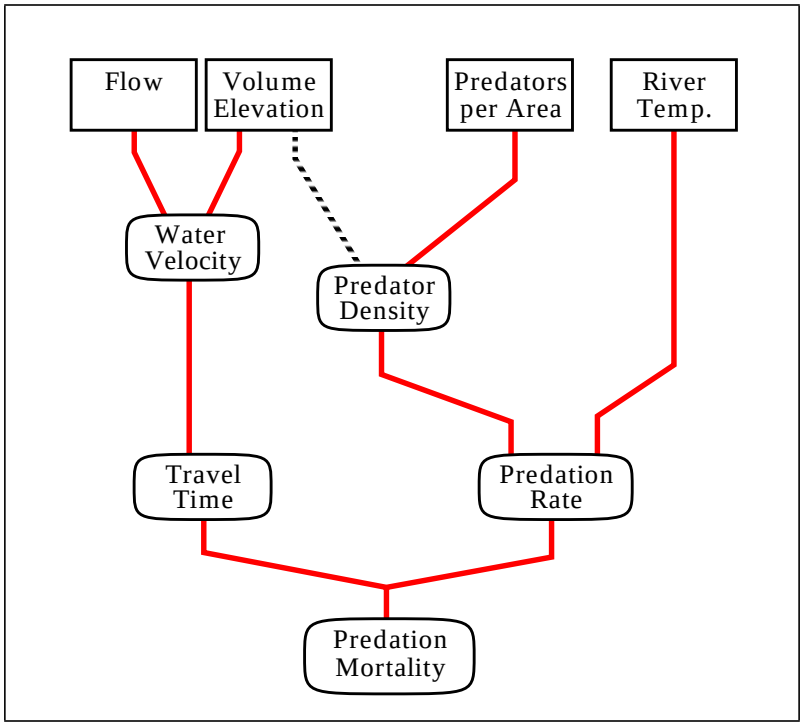

Fig. 34 Elements in reservoir mortality algorithm. Elements used in all model conditions designated by (——). Element selected by the user is designated by (·····)

The theoretical framework for describing reservoir mortality in the current model uses the time fish spend in a river segment and the segment rate of mortality. The basic equation describing the rate of mortality as a function of time is

$$\frac{dS}{dt} = -\varphi S \tag{57}$$

where

- S = measure of smolt density in the river segment and can be taken as the total number in the segment
- φ = mortality rate from all causes.

In the present model two causes of mortality are identified: predation and gas

bubble disease. CRiSP.1 assumes the rates of each are independent and this is expressed by the equation

$$\frac{dS}{dt} = -\varphi S = -(M_p + M_n)S \tag{58}$$

where

- M_p = mortality rate from predation with units of time^{-1}
- M_n = mortality rate from nitrogen supersaturation with units of time^{-1}
- S = number of smolts leaving reservoir per day (smolts reservoir^{-1})
- φ = combined mortality rate as used in eq (62).

Fish enter and leave river segments every day and spend differing amounts of time in a segment as described by the migration equations. Thus, on a given day the group of fish leaving a segment may have entered on different days and thus have different residence time in the segment. To describe the number of fish that survive a river segment on a daily basis CRiSP.1 solves eq (57) for each group, identified by when they entered the segment and when they exited. The solution is

$$S(t_j|t_i) = S_0(t_j|t_i) \cdot exp\left(-\int_{t_i}^{t_j} \varphi(t)dt\right) \tag{59}$$

where

- $S_0(t_j \mid t_i)$ = potential number of fish that enter the segment on day t_i and survive to leave the segment on day t_j
- $S(t_j \mid t_i)$ = actual number of fish that enter the segment on day t_i and leave on day t_j.

Applying an elementary property of integrals the integral is expressed

$$\int_{t_i}^{t_j} \varphi(t)dt = \int_0^{t_j} \varphi(t)dt - \int_0^{t_i} \varphi(t)dt \tag{60}$$

In general, the numerical form of the integral is

$$\int_0^{t_j} \varphi(t)dt = \sum_{k=0}^{j} \varphi(t)(t_k)\Delta t \tag{61}$$

where

- Δt = reservoir computational time increment.

The resulting equation for the number of fish passing through each river segment as a function of when it entered the segment is expressed

$$S(t_j|t_i) = S_0(t_j|t_i) \cdot exp\left(-\sum_{k=0}^{j} \varphi(t_k)\Delta t + \sum_{k=0}^{i} \varphi(t_k)\Delta t\right) \tag{62}$$

The input term $S_0(t_j \mid t_i)$ expressing the potential number that exit on day t_j given then entered the segment on day t_i can be expressed

$$S_0(t_j|t_i) = N(t_i) \cdot \Delta P(t_j|t_i) \tag{63}$$

where

- $N(t_i)$ = number of fish that enter the river segment on day t_i
- $\Delta P(t_j \mid t_i)$ = probability that a fish entering on day t_i survives to exit on day t_j. This probability is defined by eq (50).

II.6.1 -Predation Mortality Theory

The predation rate is assumed to depend on both predator density and activity. The relationship of these elements with other factors is uncertain and several possible mechanisms may alter predator density. In CRiSP.1 two relationships are available.

- Simple predation relationship where reservoir volume has no effect on predation rate.
- Predator density / reservoir volume interaction where changing the reservoir elevation changes effective predator densities. The effect is that lowering reservoir elevation concentrates predators and increases the predation rate.

General Relationship

The general predator mortality rate coefficient M_p is defined

$$M_p = a \cdot P(E) \cdot exp(u\theta) \tag{64}$$

where

- a = Predator Activity Coefficient
- $P(E)$ = Predator Density / Reservoir Volume Coefficient (a function of the elevation of the river segment below full pool)
- θ = temperature in ^oC
- u = Predator Activity Temperature Exponent.

The coefficient u expresses an increase in predator activity as determined from the work of ODF&W[1]. The exponent is assumed to depend on the predators only and thus is independent of prey species. The interaction with reservoir volume is contained in $P(E)$. This factor can be separately applied using the runtime settings of CRiSP.1.

Predation Activity Coefficient

The predation activity coefficient is fixed for a given species but may have additive deterministic ($\bar{a}_0$) and stochastic parts (a'_0) so

$$a_0 = \bar{a}_0 + a'_0 \tag{65}$$

1. Reported in "Predation by Resident Fish on Juvenile Salmonids in John Day Reservoir 1983-1986", Volume 1.

Predator Density / Reservoir Volume

The predator enhancement equation expressing how the effective predator density may change with reservoir elevation change is

$$P(E) = P(0)\frac{V(0)}{V(E)} \tag{66}$$

where

- $V(0)$ = river segment volume at full pool conditions and is fixed for each river segment
- $V(E)$ = river segment volume when elevation is lowered by E as defined in the Flow-Velocity-Elevation section on page II.43; may change with Julian Day
- $P(0)$ = predator density in a river segment per unit area at full pool (predators km^{-2}).

Predator enhancement factors for the tailrace and forebay are also included with this option.

The term a is specific to species and can have deterministic and stochastic parts. Individual terms are identified for the reservoir, tailrace and forebay.

For reservoirs with variable pool level the predator density can be defined by eq(66) where

- E = elevation of the river segment below full pool
- $V(0)$ = river segment volume at full pool conditions
- $V(E)$ = river segment volume when the elevation is lowered by an amount E
- P = predator density at full pool.

For tailraces and forebay with variable pool level:

$$P(E) = \frac{h(0)}{h(E)}P \tag{67}$$

- $h(0)$ = forebay or tailrace depth at full pool conditions
- $h(E)$ = forebay or tailrace depth at elevation E

Predator Density

Predator density is required for calibrating the activity coefficient and for estimating reservoir mortality rate. Calibration of predator density uses data from the predation studies in John Day Reservoir conducted between 1984 and 1986 and from predator indexing between 1990 and 1993. The estimation of predator density has been complicated by an ongoing predator removal program that has been implemented since 1992. These alterations are adjusted for in the model calibration using information on predator exploitation rates.

Predator Density in John Day Reservoir

Total predator density in each region of John Day Reservoir is required to calculate

predator activity coefficient from predation consumption data in the reservoir. Since there are three major predators, squawfish, smallmouth bass and walleye, but the model only considers a generic predator, the effect of all predators was expressed in equivalent densities that reflect each species' rate of smolt consumption. The equivalent measure was adjusted to squawfish over 250 mm in length, this being the minimum fish length that consumes smolts. The adjustment was based on the ratio of consumption rates for smallmouth bass and walleye to squawfish. In addition, the predator population was partitioned into forebay, pool and tailrace regions.

Rieman et al. (1991) indicates that squawfish are distributed in each zone of the reservoir according to the zone's dimension and the catch per unit effort (CPUE) in each zone, while walleye and bass are mostly confined to the reservoir proper.

Expressing densities in squawfish equivalents and applying a CPUE correction, predator densities in each zone are as follows.

The *equivalent squawfish predator density* in the reservoir is

$$P_{\text{re}} = \left[\frac{c_{\text{w}}}{c_{\text{s}}}P_{\text{w}} + \frac{c_{\text{b}}}{c_{\text{s}}}P_{\text{b}}\right]\frac{A_{re}}{A_{re}+A_{fb}} + w\frac{A_{re}}{A_{re}+A_{fb}}P_{\text{s}} \tag{68}$$

where

- P_{re} = equivalent density of predators in the reservoir zone including smallmouth bass, walleye and squawfish
- c_{name} = average salmonid consumption rate of walleye (w), smallmouth bass (b) or squawfish (s) in zones (From Table 23 on page 80)
- P_{name} = total density of walleye (w), smallmouth bass (b) or squawfish (s) (From Table 13)
- A_{name} = area of each zone [tailrace (tr) reservoir (re) and forebay (fb)] (From Table 22 on page 79)
- w = squawfish distribution factor based on CPUE according to the equation (From Table 14). This is the fraction of total predators in the entire reservoir that is in the forebay and reservoir pool

$$w = \frac{(A_{\text{re}}+A_{fb})CPUE_{\text{pool}}}{A_{\text{tr}}CPUE_{\text{tr}} + (A_{\text{re}}+A_{fb})CPUE_{\text{pool}}} \tag{69}$$

where

- $CPUE_{\text{name}}$ = catch per unit effort in the tailrace (tr) or the combined regions of the forebay and reservoir (pool).

The *equivalent squawfish predator density* in the *forebay* is defined

$$P_{\text{fb}} = \left(\frac{c_{\text{w}}}{c_{\text{s}}}P_{\text{w}} + \frac{c_{\text{b}}}{c_{\text{s}}}P_{\text{b}}\right)\frac{A_{\text{fb}}}{A_{re}+A_{fb}} + w\frac{A_{\text{fb}}}{A_{re}+A_{fb}}P_{\text{s}} \tag{70}$$

The *equivalent squawfish predator density* in the *tailrace*, which contains only squawfish due to the high flow speeds, is defined by

$$P_{tr} = (1 - w)P_s \quad (71)$$

where

- w = squawfish distribution factor expressed by eq(69).

The density of each predator in John Day Reservoir over the years 1984-1986 is given in Table 13 (Beamesderfer and Rieman 1991).

Table 13 Estimated number of predators in John Day Reservoir for 1984-1986[a]

Squawfish	Walleye	Bass
85,000	10,000	35,000

a. Average of multiple mark recapture data

CPUE per month of northern squawfish in John Day Reservoir is given in Table 14 (Beamesderfer and Rieman 1991).

Table 14 CPUE in tailrace and pool in John Day Reservoir for 1984 - 1986

Month	Tailrace	Pool
April	6.03	0.35
May	8.81	0.54
June	10.81	0.51
July	8.63	0.43
August	9.94	0.28

The resulting densities using eq(69), eq(70) and eq(71) are given in Table 15.

Table 15 Predator numbers in the tailrace, reservoir and forebay in squawfish equivalents for John Day Reservoir for 1984-1986.

Month	P_{tr}	P_{re}	P_{fb}
April	10518	79413	3394
May	10026	77939	3331
June	12582	91155	3895
July	12008	123556	5280
August	19159	111807	4778

The mean predator density in each region is obtained by averaging each region

over all months. The result is shown in Table 16.

Table 16 Average predator density *P*, in squawfish equivalents, and area of each zone in John Day Reservoir for 1984-1986

Variable (dimension)	Tailrace	Reservoir	Forebay
Density (predators km^{-2})	7104	456	456
Area (km^2)	1.8	211.8	9

Predator Density in System

Predator abundances in Columbia and Snake River reservoirs are estimated from the Predator Index studies conducted by USFWS, ODFW and WDFW between 1990 and 1993 (Table 17). Squawfish density indices are defined as 1 divided by the square root of the proportion of electrofishing runs in which no northern squawfish were caught. Each reservoir is referenced to John Day Reservoir. This involves estimating the reference to the John Day reservoir during the period of the predator studies, 1984-1986. Estimates of the change in density from predator removal can be derived from information on the productivity of the fishery and exploitation rate (Table 19). From this information predator density estimates can be constructed for a number of years.

The predator density in a given reservoir expressed in terms of the John Day reservoir is given by

$$P_i = I_i \cdot P_{\text{ref}} \tag{72}$$

where

- P_i = squawfish density (predators km^{-2}) in a given segment *i*
- I_i = Northern squawfish density index in segment *i*. The predator density index is calculated according to Ward and Peterson Table 5 (in press) as the Index value 1 divided by the square root of the proportion of the zero catch electrofishing runs.
- P_{ref} = reference average squawfish density = 472 (predators km^{-2})

Table 17 Squawfish density index plus (sample #) by year and area.

Reservoir	Forebay	Reservoir[a]	Tailrace	Tailrace	Upper reservoir
1990 sampling year (Reference Ward et al. 1993)					
Bonneville Tailrace	-	1.73 (27)	-	3.46 (27)	-
Bonneville	4.85 (47)	1.96 (50)	1.27 (37)	1.80 (13)	-
The Dalles	1.46 (62)	1.51 (34)	1.68 (45)	3.32 (11)	-
John Day	1.18 (56)	1.12 (61)	1.28 (39)	1.79 (12)	
McNary	1.05 (64)	116 (60)	1.14 (38)	2.16 (14)	1.28 (54)
1991 sampling year (Reference Ward et al. 1993)					
John Day	1.19 (61)	1.12 (58)	1.14 (44)	3.87 (15)	-
Ice Harbor	1.02 (57)	1.09 (59)	1.24 (49)	1.41 (18)	-

Table 17 Squawfish density index plus (sample #) by year and area.

Reservoir	Forebay	Reservoir[a]	Tailrace	Tailrace	Upper reservoir
Low Monumental	1.21 (66)	1.26 (60)	1.42 (40)	2.83 (16)	-
Little Goose	1.20 (61)	1.12 (56)	1.29 (40)	4.12 (17)	-
Lower Granite	1.15 (57)	1.05 (58)	-	-	1.80 (55)
1992 sampling year (Reference Parker et al. 1994)					
John Day	1.24 (68)	1.17 (62)	1.04 (47)	2.38 (17)	-
River km 71-121	1.66 (69)	1.71 (67)	-	-	1.46 (68)
River km 122-177	1.34 (66)	1.44 (71)	-	-	1.65 (65)
River km 178-224	1.71 (64)	1.35 (66)	-	-	1.25 (73)
1993 sampling year (Reference: Loch et al. 1994)					
John Day	1.26 (36)	1.08 (43)	1.22 (37)	1.73 (9)	-
Hanford Reach	-	-	1.47 (54)	1.87 (14)	-
Priest Rapids	1.51 (16)	1.13 (117)	1.30 (47)	2.55 (13)	-
Wanapum	1.41 (20)	1.43 (107)	1.32 (52)	3.74 (14)	-
Rock Island	1.21 (16)	1.46 (102)	1.50 (52)	1.51 (6)	-
Rock Reach	2.24 (15)	1.58 (114)	1.53 (49)	1.47 (13)	-
Wells	1.47 (13)	1.14 (130)	1.33 (59)[b]	1.46 (15)[b]	-

a. Includes forebay outside the BRZ and the mid-reservoir
b. Chief Joseph Tailrace

Reference density is calculated using information on total population number in the reservoir in a given year and the index for that year from each segment. The procedure is as follows. First the average predator index I_{ave} for the reservoir is calculated for each area according to the equation

$$I_{ave} = (\sum I_i \cdot \text{Area}_i)/(\sum \text{Area}_i) = 1.15 \quad (73)$$

where I_i is the index for each reservoir segment and is obtained from year 1991 in Table 17. The reference density, which is the density for which the index is 1, can be calculated from the average index, the total population of squawfish, N, and the total area of the reservoir (Area_{res}). The formula and result for 1991 using a predator population number in Ward et al. (1993 page 390) is

$$P_{ref} = \frac{N}{I_{ave} \cdot \text{Area}_{res}} = \frac{108000}{1.15 \cdot 222.6} = 472 \quad (74)$$

The squawfish predator densities given in Table 18 are calculated using information from eq(72) and indices given in Table 17.

Table 18 Predator density (predators km^{-2}) for year indexed.

River segment	year	Reservoir[a]	Tailrace	Forebay
Estuary	1992	678	-	-
Jones Beach	1992	620	-	-
Columbia Gorge	1992	601	-	-
Bonneville Tailrace	1990	1456	-	-
Bonneville	1990	824	758	2042
The Dalles	1990	635	1398	614
John Day	1990 1991 1992 1993	471 417 492 482	753 1629 1002 728	497 501 522 530
John Day average[b]	1990-93	480	1029	512
McNary (upper reservoir [c])	1990	539		
McNary	1990	489	909	442
Ice Harbor	1991	455	594	429
Low.Monumental	1991	530	1192	509
Little Goose	1991	471	1735	505
Lower Granite	1991	442	1414	484
Lower Granite (upper reservoir)	1990	758	-	-
Hanford Reach	1993	787	619	
Priest Rapids	1993	497	1074	635
Wanapum	1993	788	2115	797
Rock Island	1993	835	848	684
Rock Reach	1993	884	831	1267
Wells	1993	680	825	831

a. Combined data from reservoir and tailrace outside of BRZ
b. Average from years 1990 -1993.
c. Upper reservoir segment

Predator removal adjustments

The above predator density estimates were indexed in specific reservoirs for specific years. These densities must be adjusted for changes in density resulting from predator removal efforts that were initiated during the index studies. This adjustment is problematic since it requires knowledge of population growth and natural mortality as well as the exploitation rate.

The response of predators to exploitation was studied by Rieman and Beamesderfer (1990) using a generalized population model designed for simulating

age-structured populations. The model included age-specific natural mortality, exploitation rates and recruitments described by either a Beverton-Holt or Ricker stock-recruitment function.

Since the population dynamics in CRiSP1 use a combined predator density, age-specific predator population information must be represented as a combined generic predator. The approach was to represent the dynamics of an age-specific predator population model by a continuous logistic curve which is equivalent to the Beverton-Holt stock-recruitment equation. The parameters of the logistic model were then adjusted to provide the same response as the stock recruitment-based model of Rieman and Beamesderfer (1990).

The logistic-based population model incorporates a generalized net growth rate and a death rate term that depends on population size. The equation is

$$\frac{dP}{dt} = gP\left(1 - \frac{P}{K}\right) - fP \tag{75}$$

where

- P = predator population density
- g = intrinsic predator population growth rate: the difference between growth mortality rate elements independent of population size
- f = exploitation rate from the predator removal program
- K = carrying capacity of predators in a reservoir. This is taken as the predator index-based value prior to predator removal.

Solving eq(75) the population size at some future date under a constant exploitation rate over the interval of time is given by

$$P(t + \Delta t) = \frac{K\left(1 - \frac{f}{g}\right)}{1 + \left(\frac{K\left(1 - \frac{f}{g}\right)}{P(t)} - 1\right) e^{-(g - f)\Delta t}} \tag{76}$$

where

- $P(t)$ = predator population density at time t
- $P(t + \Delta t)$ = predator population density at time $t + \Delta t$

To estimate the effect of the predator removal program we require estimates of the carrying capacity K, the intrinsic growth rate g, and the exploitation rate f.

To estimate the carrying capacity assume that prior to exploitation the population was at its carrying capacity. As a first approximation of carrying capacity we take the predator index study which was initiated in the first years of predator removal efforts. The carrying capacities for the reservoirs are thus taken from Table 18.

The predator population growth coefficient was adjusted to fit the population growth suggested in by Reiman and Beamsderfer (1990). In this analysis the suggested range for the Beverton-Holt recruitment factor was 0.5 to 0.98. This gave a population that upon termination of exploitation would return to 90% of carrying capacity in 6 to

30 years. The same response from the logistic equation gave a growth parameter of g = 0.375 yr.$^{-1}$ for the 6 year return time and g = 0.075 yr.$^{-1}$ for the 30 year return time.

The exploitation rate was estimated in the predator index studies. The exploitation rates for the reservoirs is given in Table 19. Exploitation rates for 1990, 1991, 1992 and 1993 were obtained from Ward et al. 1993, Ward et al. 1994, and Ward et al. 1995.

Using the above estimates of the growth rate in eq(76) the predator densities in the reservoirs can be corrected for exploitation.

The choice of a representative population growth rate is bounded by the estimates conforming to the work of Reiman and Beamsderfer (1990). They discussed the possible range of growth and concluded that other studies supported their estimates. The consequences of the different estimates of growth on predator density and the ability of the model to fit the survival studies is discussed in the validation section of the manual. The growth rate choice has a small effect on estimates of predator density and this in turn has a small effect on smolt survival.

In the model the predator density was taken as the average of the densities estimated from the two growth rate. These densities are given in Table 20.

Table 19 Exploitation rates in % of population per year.

	1990[a,b]	1991[c]	1992[d]	1993
Downstream of Bonneville	2.6	9.8	11.8	11-18
Bonneville	~3	3.2	6.8	-
The Dalles	3.2	28.3	7.2	-
John Day	5.7	11.1	14.3	10.5
McNary	2.2	6.4	5.6	-
Ice Harbor	-	19.2	-	-
L. Monumental	-	23.6	7.7	-
Little Goose	-	23.5	18	6.6
Lower Granite	-	-	14.6	-

a. Vigg et al. 1990
b. Ward et al. 1993 page 360
c. Ward et al. 1993 Tables G-4, G-5 and G-6
d. Parker, et al. 1992 page 387 Table 4

Table 20 Averaged predator density.

Dam	1990	1991	1992	1993	1994
Downstream of Bonneville	633	579	529	476	498
Bonneville	824	798	754	766	776
The Dalles	635	492	486	503	521

Table 20 Averaged predator density.

Dam	1990	1991	1992	1993	1994
John Day	480	434	388	366	382
McNary	489	462	443	451	456
Ice Harbor	455	332	394	404	410
L. Monumental	530	428	414	432	445
Little Goose	471	380	335	334	352
Lower Granite	442	442	442	388	396

Activity Coefficient Estimation: Theory

The predation activity coefficient in reservoirs is estimated from data on the rate of consumption of smolts by predators. The general strategy is to construct a simple equation describing the flux of smolts through a reservoir in terms of the smolt migration rate, the predator density, and predation rate. Assuming a steady state smolt distribution on a monthly basis, an equation can be developed describing the consumption rate coefficient in terms of the flux of smolts, the consumption rate of each predator, and the number of predators in the reservoir. The calculation is applied sequentially to the tailrace, reservoir proper, and forebay of John Day reservoir, and yields the activity coefficient for each region. The coefficients are then adjusted for temperature using information on the effect of temperature on squawfish feeding behavior. Since CRiSP.1 only tracks one predator type, the contribution to predation by fish other than squawfish is accounted for by expressing other predator densities in terms of their equivalence in squawfish where the equivalence is related by the rate of smolt consumption for the different predators.

The above calibration approach estimates predator activity coefficients for each region of John Day Reservoir. These coefficients are then applied to other reservoirs throughout the system. The coefficient describing the rate of predation on smolts was estimated using data derived from both experiments and field studies. The analysis uses data from John Day Reservoir because this is the only reservoir in which extensive predation studies were conducted. In order to define an equation describing the rate of change of smolts in a single reservoir, three regions are defined as in Fig. 35.

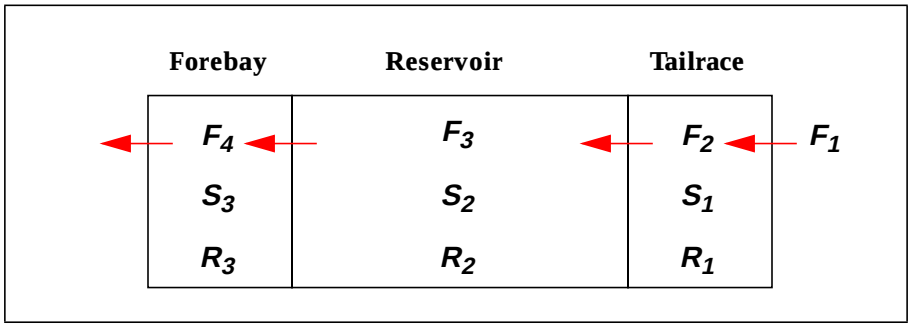

Fig. 35 Regions with fish fluxes F, smolt number S, and rates R

Smolt equation

The equation balances the rate of change in the number of smolts in each region with the flux and the consumption of smolts by predators in the region. The equation is

$$\frac{dS_i}{dt} = F_i - F_{i+1} - R_i \tag{77}$$

where

- dS_i / dt = rate of change of smolts in region i
- F_i = flux of smolts into the region
- F_{i+1} = flux of smolts out of the region
- R_i = consumption rate of smolts by predators in the region.

The consumption rate of smolts is assumed to be dependent on smolt density, predator density and a rate coefficient. The term is expressed

$$R_i = r_i S_i P_i \tag{78}$$

where

- S and P = average numbers of smolts and predators in the region which could also be expressed on a unit area basis
- r_i = consumption rate coefficient.

In this submodel, the actual equation describing changes in smolt density is solved with a finite increment numerical method. Smolt numbers in the river segment are computed on a time increment which is some fraction of a day. The numerical solution of eq(77) is

$$S_i(t + \Delta t) = S_i(t) + \left.\frac{dS_i}{dt}\right|_t \Delta t \tag{79}$$

The calibration strategy is to work with eq(77) to estimate the rate term R, which itself is defined in eq(78). The important parameter is the activity coefficient r_i describing the chance of predation given that predator and prey encounter each other. The densities of prey and predator and the residence time of prey in the river segment determine the number of encounters. The following equations develop this algorithm.

Smolt exit flux

The smolt flux out of a region is assumed to be

$$F_{i+1} = b_i S_i \tag{80}$$

where

- b_i = rate at which smolts exit the region.

The rate at which smolts exit region i, b_i above, can be related to smolt travel time for a given release[1]. Assuming that smolts are initially evenly distributed in the region and loss is a first order process, then the exit rate of a specified group of fish in the region follows the equation

$$\frac{dS}{dt} = -bS \tag{81}$$

Taking the average travel time TT_{ave}, which is the time for 50% of the fish to exit a segment, the coefficient b is

$$b = -\frac{\log(0.5)}{TT_{\text{ave}}} \tag{82}$$

Travel times are measured as medians which differ from the average travel time since the distribution of fish is skewed with increasing time. The relationship between mean and median is dependent on the travel time parameters. This difference can be estimated from the model by following a single release through John Day reservoir.

The average travel time was estimated from the median travel time using a ratio of the two from CRiSP output through John Day Reservoir. The conversion is expressed

$$TT_{\text{ave}} = TT_{\text{median}} \cdot \frac{\text{CRiSP}.TT_{\text{ave}}}{\text{CRiSP}.TT_{\text{median}}} \tag{83}$$

A sensitivity analysis indicated that the transformation of travel time from median to average was a sensitive parameter and could change the results by tens of percentage points.

Steady state

Assuming that local smolt density is at steady state, such that the rate of change of smolts is zero, the calculations are greatly simplified. This assumption does not produce a significant bias in the estimates since the rate parameter is calculated over a period of time in which the smolt concentration first increases and then decreases in the reservoir. The result is that rate estimates with positive and negative biases are averaged so that the net bias is small.

The resulting population balance at steady state using eq(77), eq(78) and eq(80) is,

$$F_i - b_i S_i^* - r_i S_i^* P_i = 0 \tag{84}$$

where

- S_i^* = steady state average smolt density in region i

An estimate of the rate of predation per predator was made based on studies of the stomach contents of predators (Vigg et al. 1991). Using this, the steady state population can be expressed

$$F_i - b_i S_i^* - c_i P_i = 0 \tag{85}$$

1. This non-steady state assumption used for a particular release does not conflict with the steady-state assumptions for total density since as fish leave the downstream end they are replaced with fish at the upstream end of the region.

where c_i is the consumption rate smolts predator^{-1}day^{-1}. Assuming that predator consumption rate coefficient, r_i, does not vary during the migration period of a species it follows that

$$c_i = r_i S_i \tag{86}$$

Rearranging eq(85) the equilibrium smolt density is

$$S_i^* = \frac{F_i - c_i P_i}{b_i} \tag{87}$$

Combining eq(86) and eq(87), the consumption rate coefficient is

$$r_i = \frac{b_i c_i}{F_i - c_i P_i} \tag{88}$$

The flux into the next adjacent region downstream is expressed

$$F_{i+1} = b_i S_i^* = F_i - c_i P_i \tag{89}$$

Temperature factor

The model applies a temperature correction to the rate term in order to express the rate coefficient independent of temperature. Based upon the work of Vigg et al. (1990) the equation is

$$r = a \cdot exp(u\theta) \tag{90}$$

where

- a = predation activity coefficient defined in eq(64).
- u = temperature coefficient for the predation rate. This rate changes with temperature. CRiSP.1 uses u equal to 0.207 $^oC^{-1}$. This value was inferred from a relationship of how squawfish satiation changes with temperature (Vigg & Burley 1991).
- θ = water temperature in ^oC.

Data for Activity Coefficients

The data for estimates of the predator activity coefficient are obtained from the following sources:

Flux estimate

The flux of salmonids into John Day Reservoir is given in Table 21 from data presented in Rieman et al. (1991). The flux estimates were computed from passage indices at McNary Dam and number of hatchery fish released into John Day reservoir on a monthly basis and using the fish guidance efficiency through the counting facilities at McNary Dam. The guidance efficiency estimated for salmon was 40% and for steelhead was 75% (Giorgi and Sims 1987). Fish removed at McNary Dam and transported through the reservoir in barges were accounted for in the estimates.

Travel time

Travel times (Table 21) in April and May were estimated from studies by Stevenson and Olson (1990). Travel times during June, July and August were obtained from reports by Giorgi et al. (1990). Temperatures in Table 21 represent monthly average temperatures for John Day reservoir as generated from CRiSP data files. The model was calibrated to these temperatures since model runs use temperatures generated from headwaters.

Table 21 John Day reservoir properties. F_1 = smolts month^{-1} entering reservoir. Median TT is travel time in days.

Month	F_1 salmon	F_1 steelhead	TT (days)	θ_{cal}[a] (^oC)
April	1567000	129000	5.8	8.09
May	5896000	955000	5.8	10.47
June	4465000	210000	12.9	14.26
July	5246000	3000	18.2	18.03
August	801000	1000	24.6	19.78

a. Monthly average temperatures are computed for John Day Reservoir using temperature generated by CRiSP using data files for 1984-85-86.

Consumption rate estimate

The consumption rates of smolts by squawfish were obtained from Vigg et al. (1991). In that study, stomach contents of adult northern squawfish were analyzed and identified as either salmon or steelhead. The rate of consumption was determined from the number and weight of digested prey and the literature on gut evacuation rates of squawfish. Further detail on how the data were distributed by sampling station and month, were provided by J. Peterson (personal communication) (Table 22). The John Day study also measured consumption rates of secondary predators: walleye and smallmouth bass. The results of these studies on a whole-reservoir basis are given in Table 23 along with a reservoir averaged consumption rate for squawfish.

Calculation of activity coefficients from consumption rate data in John Day Reservoir required combining data into three groups representing the regions defined in CRiSP.1.

Table 22 Monthly capture rates *C*, of salmonids by northern squawfish at five location in John Day Reservoir. Rate is measured in salmonids predator^{-1} day^{-1}.

	John Day	Arlington	Irrigon	McNary Tailrace	McNary BRZ[a]
April	0.06	0.07	0.00	0.02	0.14
May	0.33	0.07	0.09	0.38	0.49
June	0.15	0.11	0.00	0.04	0.35

Table 22 Monthly capture rates *C*, of salmonids by northern squawfish at five location in John Day Reservoir. Rate is measured in salmonids predator^{-1} day^{-1}.

	John Day	Arlington	Irrigon	McNary Tailrace	McNary BRZ[a]
July	0.27	0.05	0.00	0.21	1.95
August	0.13	0.04	0.00	0.09	0.35
# of sample	899	448	236	413	2371
km from McNary	118 to 123	75	20	2 to 5	1
Area, A_i km^2	9	128	76	7.2	1.8
index (i)	1	2	3	4	5
Region	John Day Dam Forebay	John Day Reservoir			McNary Dam Tailrace

a. Boat Restricted Zone

Table 23 Mean daily salmonid consumption rate combining forebay and reservoir estimates (salmonids predator^{-1} day^{-1}). From Table 6 in Vigg et al. 1991.

Month	Squawfish	Walleye	Bass
April	0.043	0.021	0.003
May	0.251	0.113	0.009
June	0.086	0.118	0.019
July	0.154	0.447	0.118
August	0.094	0.232	0.070

To obtain a consumption rate for salmon, excluding steelhead, the consumption rates (Table 22) are scaled by the ratio of salmon to all salmonids found in squawfish stomachs (Table 24).

Table 24 Fraction by month of salmon in salmonid samples

Month	G_m
April	0.88
May	0.85
June	0.91
July	1.00
August	1.00

Average salmon consumption rates in the three regions--tailrace, reservoir, and forebay--can be generated from the equation

$$C_{salmonid,\,m} = \left(G_m \sum_{i=j}^{k} C_{i,\,m} A_i \right) \Big/ \left(\sum_{i=j}^{k} A_i \right) \tag{91}$$

where

- G_m = fraction of salmon in the salmonids samples for month *m* as given in Table 24
- $C_{i,\,m}$ = salmonid consumption rate for zone *i* in month *m* as given in Table 22
- A_m = area of zone in as given in Table 22.

The indices for the model regions for eq(91) are as follows:

McNary Dam tailrace:	$j = 1,$	$k = 1$
John Day Reservoir:	$j = 2,$	$k = 4$
John Day Dam forebay:	$j = 5,$	$k = 5.$

Consumption rates of salmon by squawfish as developed in eq(91) are given in Table 25.

The consumption rate for steelhead can be estimated from the same data since the remaining salmonids were steelhead. The steelhead consumption rate can be expressed by the equation

$$C_{steel,\,m} = \left((1 - G_m) \sum_{i=j}^{k} C_{i,\,m} A_i \right) \Big/ \left(\sum_{i=j}^{k} A_i \right) \tag{92}$$

where all terms are analogous to those in eq(91). Steelhead consumption rates are given in Table 26.

Table 25 Rate of salmon consumption by squawfish, $c_{salmon,m}$. Units are salmon squawfish^{-1} day^{-1}

Month	Tailrace	Reservoir	Forebay
April	0.123	0.043	0.053
May	0.416	0.075	0.280
June	0.318	0.062	0.136
July	1.950	0.037	0.270
August	0.350	0.027	0.130

Table 26 Rate of steelhead consumption by squawfish $c_{steel,m}$. Units are steelhead squawfish^{-1} day^{-1}

Month	Tailrace	Reservoir	Forebay
April	0.017	0.006	0.007
May	0.073	0.013	0.049
June	0.031	0.006	0.013
July	< 0.001	<0.001	<0.001
August	< 0.001	<0.001	<0.001

The estimation of fish average travel time from the mean travel time is given in Table 27. The difference was calculated by using 1986 flow levels and the movement of spring and fall chinook through John Day reservoir.

Table 27 Travel time (days) through segments and CRiSP based ratio of average to median travel time through John Day reservoir. April and May for spring chinook and June to August relate to fall chinook.

variable	April	May	June	July	Aug.
CRiSP ave. / median	1.61	1.43	1.31	1.29	1.30
median TT RZ	0.05	0.05	0.10	0.15	0.20
median TT reservoir	5.5	5.5	12.3	17.3	23.4
median TT forebay	0.23	0.23	0.52	0.74	1.00

Activity Coefficient Calibration

Using data from the tables in the section on Data for Activity Coefficients estimates starting on page II.78 the predator activity coefficients on a per month basis in each zone can be calculated for steelhead and salmon. The calculations use eq(88), eq(89) and eq(90) and the coefficient is designated *a.*

The majority of fish in the system in April and May are spring chinook while fall chinook are dominant June through August. Steelhead predominantly pass in May. Thus as a first order approximation, activity coefficients for each species can be estimated by averaging coefficients according to the weights of smolt passage numbers. Weighting coefficients as fractions of the total flux are shown in Table 28.

Table 28 Population weighting coefficients, W_m

Month	spring chinook	fall chinook	steelhead
April	0.21	0	0.10
May	0.79	0	0.74
June	0	0.42	0.16
July	0	0.50	-

Table 28 Population weighting coefficients, W_m

Month	spring chinook	fall chinook	steelhead
August	0	0.08	-

The average activity coefficient for each species in each region is now obtained by averaging the month specific activities using the weighting functions in Table 28. The equation for average predator activity coefficient for a species is

$$a = factor \sum_m W_m a_m \tag{93}$$

where the *factor* is used to convert the measure from an activity coefficient based on predator equivalents to a predator activity coefficient based on squawfish only.

The predator adjustment (*factor*) is based on the following: From Table 16 the equivalent predator density in John Day reservoir for the period 1984-1986 is 456 predators km^{-2}. The average squawfish density in the reservoir is 326 squawfish km^{-2}. The factor converting the activity coefficient from one based on predator equivalents to one based on squawfish is 456 / 326 = 1.39. This coefficient is applied to the reservoir and forebay, these being the two regions where walleye and smallmouth bass are found. Since only squawfish are found in the tailrace the *factor* for the trailrace is 1.

The predator activity coefficients are input in the model under **BEHAVIOR** submenu **pred coef**. They reflect the predator activity in river passage.

Table 29 Base activity coefficients, *a* designated **pred_coef** in CRiSP.1.

Species	Tailrace	Reservoir	Forebay
spring chinook	77.6×10^{-7}	26.7×10^{-7}	63.8×10^{-7}
fall chinook	20.2×10^{-7}	7.4×10^{-7}	11.7×10^{-7}
steelhead	78.3×10^{-7}	36.8×10^{-7}	74.5×10^{-7}

Activity Coefficient Variability

To estimate the range of the activity coefficient, confidence limits in mortality estimated from a Monte Carlo simulation by Rieman et al. (1991) are applied. To equate mortality confidence interval to an upper and lower range of the activity coefficient, we define the survival of smolts while in the reservoir in terms of the equation

$$\frac{dS}{dt} = -rPS \tag{94}$$

This yields the solution

$$S(t) = S(0)e^{-rPt} \tag{95}$$

where

- $S(*)$ = smolt density
- t = representative time in the reservoir
- P = predator density
- r = predation rate.

Under the condition that $S(t)/S(0) \sim 1$ (in actuality, the number is about 0.85 reflecting about a 15% mortality in the reservoir proper) the following approximation can be used

$$\frac{S(t)}{S(0)} \approx 1 - rPt \tag{96}$$

and so the total mortality m within a reservoir can be approximated

$$m = 1 - \frac{S(t)}{S(0)} \approx rPt = ae^{u\theta}Pt \tag{97}$$

A ratio of two activity coefficients is thus related to a ratio of two mortality estimates with all other factors equal. It follows then that the range of estimates in mortality can be related to the range of estimates in the predator activity coefficient. The equation is

$$\frac{m_{\text{low}}}{m_{\text{mean}}} \approx \frac{a_{\text{low}}}{a_{\text{mean}}} \tag{98}$$

The upper and lower limits of the activity coefficient can be estimated from the 95% confidence limits of mortality given by Rieman et al. (1991). They estimated total salmonid mortality in John Day reservoir at 14% with a 95% confidence interval from 9% to 19%. Upper and lower estimates of the activity coefficient are

$$\begin{aligned} a_{\text{low}} &= \frac{m_{\text{low}}}{m_{\text{mean}}} a_{\text{mean}} = \frac{9}{14} a_{\text{mean}} = 0.643 a_{\text{mean}} \\ a_{\text{high}} &= \frac{m_{\text{high}}}{m_{\text{mean}}} a_{\text{mean}} = \frac{19}{14} a_{\text{mean}} = 1.357 a_{\text{mean}} \end{aligned} \tag{99}$$

II.6.2 -Supersaturation Mortality

High levels of total dissolved gas in the river lead to the development of gas bubble disease (GBD) in smolts, as well as other aquatic life. This condition involves the formation of bubbles in the fish's organs, tissues, and vascular system. GBD is also suspected of compromising the fish's vitality by increasing its susceptibility to predators, bacteria and disease (Dissolved Gas Abatement Interim Letter Report,1994). Because of the varied symptoms and effects of total dissolved gas, GBD will be considered an independent force of mortality.

There is uncertainty as to the significance of GBD-induced mortality at low levels of supersaturation (<110%) but it is clear in all studies that as the amount of

supersaturation increases (> 110%) the rate of mortality increases significantly. The transition between low levels of generally sublethal effects to the higher level lethal condition involves a shift in the bubble-related mechanisms that lead to death. Specifically, at levels of supersaturation below the threshold fish are more susceptible to death related to infection and stress while above the threshold fish experience death from large intravascular bubbles (White et al. 1991).

Theory

In CRiSP, the level of total dissolved gas is represented by percent nitrogen saturation. Nitrogen is generated by spill at the dams and then dissipated as the water moves downstream. In the model, the effects of both lethal and sublethal levels of nitrogen are considered as well as the changes in the effective nitrogen concentration resulting from depth and distance downstream.

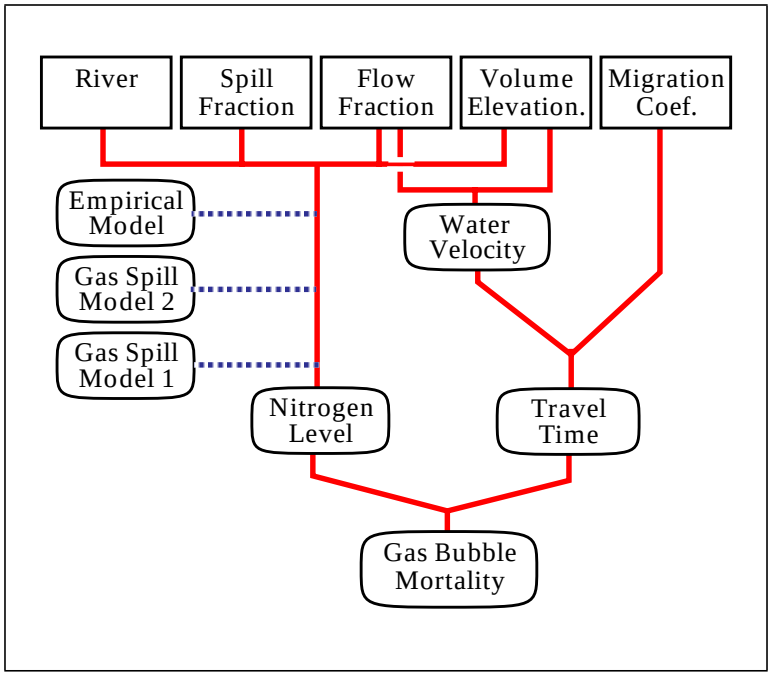

Fig. 36 Factors in gas bubble disease model. Elements used in all model conditions designated by (——). Elements selected by the user are designated by (·····).

The relationship between migration factors and gas bubble disease is illustrated in Fig. 36. Nitrogen supersaturation can be defined with any of three submodels selected from the Nsat equation window opened from the **DAM** menu.

Mortality rate equation

To incorporate both the lethal and sublethal effects of gas bubble disease the model uses a piecewise-linear function that expresses the rate of mortality M_n as a function of N_s, the level of nitrogen above supersaturation (see figure below). This piecewise-linear characteristic is accomplished by using the Heaviside function H() which switches from 0 to 1 as its argument changes from negative to positive. This allows the

model to assume a moderate linear increase in mortality (slope a) at low levels of nitrogen supersaturation. When the lethal threshold of saturation N_c is reached, the Heaviside function turns on and the mortality curve increases linearly but now at a higher rate (slope $a + b$). Using the work of Dawley et al. (1976) the empirical mortality rate equation is

$$M_{\mathrm{n}} = a \cdot N_s + b(N_s - N_c) \cdot H(N_s - N_c) \qquad (100)$$

where

- N_s = percent nitrogen saturation *above* 100% as measured at the surface.
- N_c = threshold above 100% at which the gas bubble disease mortality rate is observed to change more rapidly towards more lethal levels.
- a = species-specific gas mortality rate coefficient with units of N^{-1} day^{-1} determining the initial rate of increase of mortality per %-increase in nitrogen saturation.
- b = species-specific gas mortality rate coefficient with units of N^{-1} day^{-1}, determining the change in mortality rate at N_c.
- H() = Heaviside function, also known as the unit step function; equal to zero when its argument is negative, and equal to one when its argument is positive.

Eq(100) is illustrated in Fig. 37.

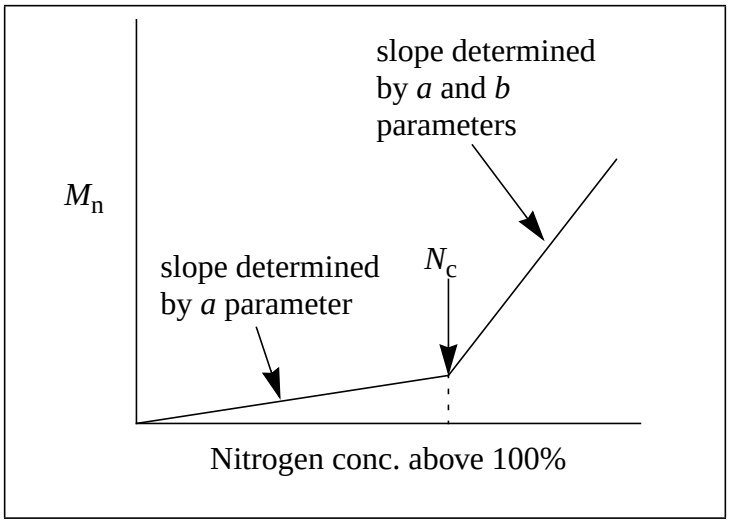

Fig. 37 The Nitrogen mortality equation is a function of three parameters.

Depth dependent critical values

Fidler and Miller (1994) demonstrated that the critical nitrogen supersaturation concentration (N_c) is depth dependent, with N_c increasing as depth increases. They observed a decrease in effective nitrogen supersaturation of about 10% per meter below the surface. In other words, fish at lower depths are less susceptible to nitrogen supersaturation. Based on this work, CRiSP utilizes a linear relationship to relate N_c to fish depth:

$$N_c = m_c \cdot z + n_c \quad (101)$$

where

- z is fish depth,
- m_c is a slope parameter,
- n_c is the critical nitrogen supersaturation concentration at the surface.

Thus to obtain an effective N_c for a stock, eq(101) is multiplied by fish density as a function of depth, and then this term is integrated over the reservoir depth. Calibration for juvenile salmon converted into the model units are n_c = 10.9, the surface critical level with units of %saturation of nitrogen above 100%, and m_c = 2.96, the rate of decrease of N_c with units of %saturation of nitrogen above 100%·ft^{-1}.

Downstream dissipation

As fish move downstream in a reservoir their mortality rate due to nitrogen supersaturation decreases because dissolved gas levels are highest at the upstream end and dissipate as the water moves downstream. The saturation level can be expressed as

$$N_s(t) = N_0 \cdot e^{-k \cdot t} \quad (102)$$

where

- N_0 = is percent supersaturation above 100% at the upstream end of a river segment, which may be a tailrace
- k = dissipation constant defined by eq (129) on page 101.

To express the supersaturation in spatial coordinates the time coordinate is transformed to distance downstream by

$$x = U_{ave} \cdot t \quad (103)$$

where

- U_{ave} = average water velocity through the river segment
- t = time

Transforming time to downstream distance using eq (103) and defining a new parameter

$$l = k / U_{ave} \quad (104)$$

the surface supersaturation above 100% is

$$N_s(x) = N_0 \cdot e^{-l \cdot x} \quad (105)$$

where

- x = distance downstream and $0 \le x \le L$, where L is the pool length (miles).

The rate of mortality as a function of fish depth and distance downstream can be expressed by substituting eq (101) and eq (105) into eq (100) to give

$$M_n = a \cdot N_0 \cdot e^{-lx} + b \cdot (N_0 \cdot e^{-lx} - m_c z - n_c) \cdot H(N_0 \cdot e^{-lx} - m_c z - n_c) \quad (106)$$

Isopleths of constant mortality rate through the reservoir can be generated by setting eq (106) to a constant and solving for *z* as a function of *x*. The resulting isopleths of constant mortality are illustrated in Fig. 38.

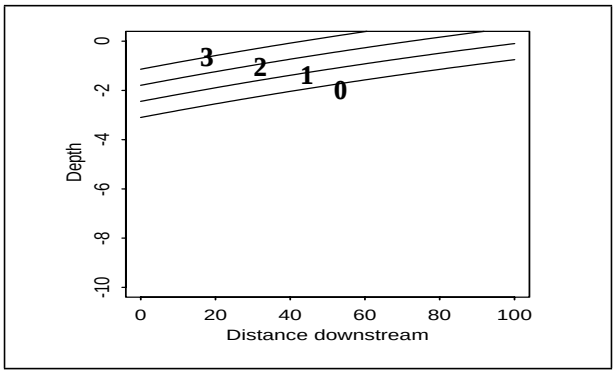

Fig. 38 Gas bubble disease mortality rate as *%loss/ day* through a pool. Depth from surface in *ft*. Distance downstream in *miles*.

Vertical distribution

A population of fish from a given species will spread out vertically. A number of distribution functions have been hypothesized (Zabel, 1994). For simplicity, CRiSP.1 uses an isosceles triangular distribution given by:

$$Dist(z) = H(z_D - z)[m_0 z \cdot H(z) + (m_1 - m_0)(z - z_m)H(z - z_m) - m_1(z - z_b)H(z - z_b)] \quad (107)$$

where

- z_D = depth of the reservoir
- z_b = maximum depth of fish distribution
- z_m = mode of fish distribution
- m_0 = slope of distribution function above mode
- m_1 = slope of distribution function below mode

The fish depth distribution is illustrated in Fig. 39.

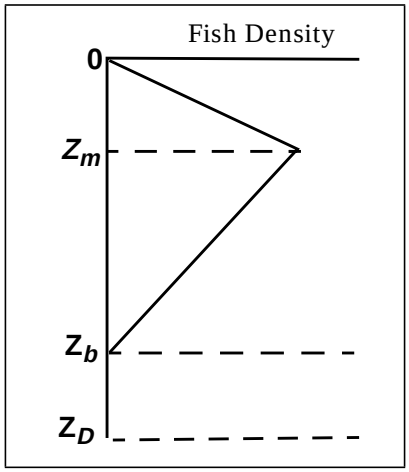

Fig. 39 Vertical distribution of fish

The work of Zabel (1994) shows that fish of a given species tend to seek specific depths that are correlated to level of illumination.

Integrate for average rate through pool.

The average mortality rate for a fish while it is in a pool is given by the equation:

$$\overline{M} = \frac{1}{L}\int_0^{z_D}\int_0^{L} Dist(z)\cdot (aN_0e^{-lx} + b[N_0e^{-lx} - m_c z - n_c]\cdot H[N_0e^{-lx} - m_c z - n_c])dxdz \quad (108)$$

where

- $\overline{M}$ = the mortality rate due to gas bubble disease averaged throughout the length and depth of the pool.

Calibration

The calibration was done in a three step process. First, cumulative mortality curves were fit with the CRiSP nitrogen mortality equation to generate estimates of the mortality rate. Second, these mortality rates for different nitrogen levels were plotted and fit with the CRiSP rate equation expressing rate vs. supersaturation. Third, mortality rates were corrected for fish length where the correction was developed using the first two steps and experiments conducted by Dawley et al. (1976).

Mortality Rates

The first step in the calibration was to fit cumulative mortality curves. The nitrogen mortality equation is given by eq (58) setting the predator mortality to zero. The equation to fit is then

$$\log S = -M_n t \quad (109)$$

where

- S = cumulative survival
- M_n = nitrogen mortality rate at a specific nitrogen supersaturation.

The results of fitting the cumulative mortality for fall chinook and steelhead are illustrated in Fig. 40 and Fig. 41 below. The estimated mortality rates from the regressions are given in Table 30. For steelhead (Fig. 40) the model fit is close for all levels of nitrogen and for all exposure times. For fall chinook (Fig. 41), with low levels of supersaturation, mortality rate is overestimated for short duration exposures and the rate is underestimated for the longer exposures. For higher levels the fit is better.

Table 30 Mortality rates from fitting eq(109).

Nsat (%)	fall chinook M_n	steelhead M_n
105	0.0016	-
110	0.0033	0.305
115	0.0087	0.599
120	0.0153	1.084
124	1.2333	-
127	1.0300	3.895

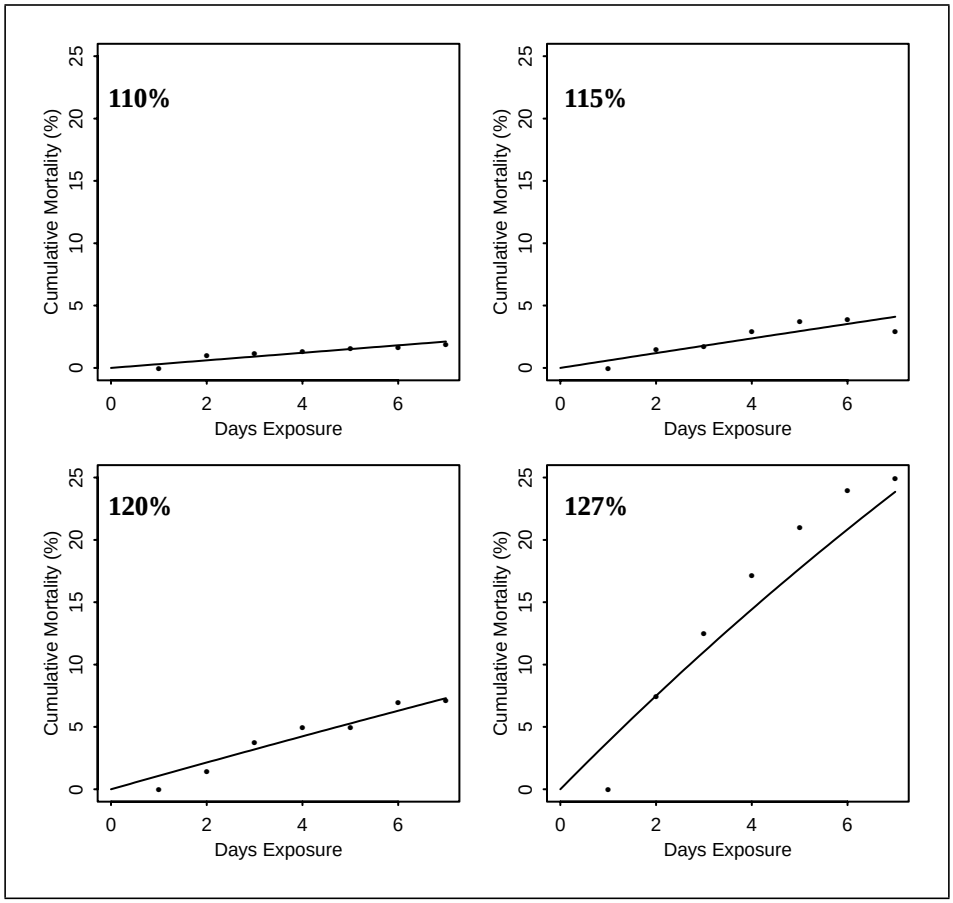

Fig. 40 Juvenile steelhead cumulative mortality from gas bubble disease at different levels of nitrogen supersaturation. Data points from Dawley et al. 1976, curve from fit of eq(109).

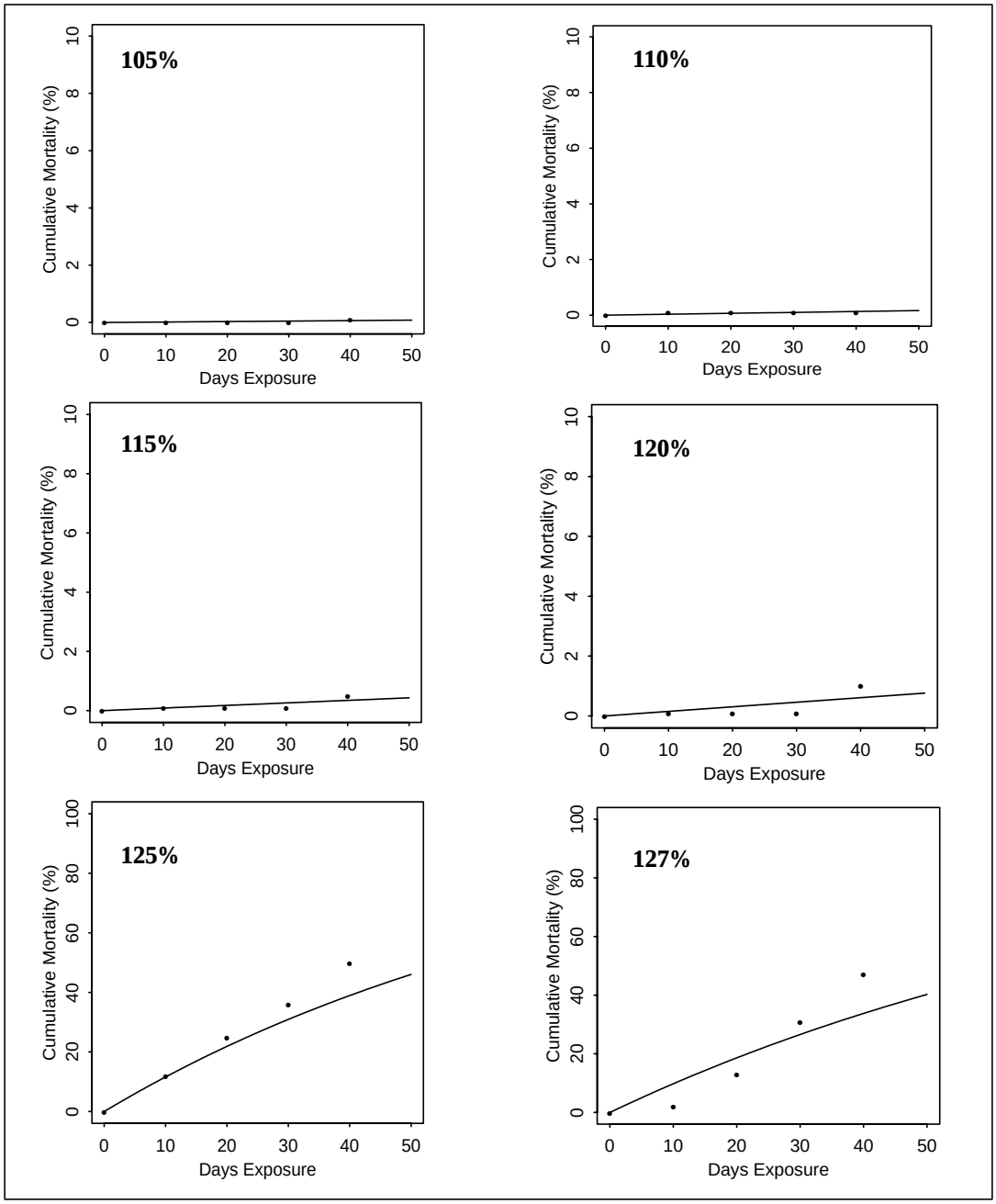

Fig. 41 Juvenile fall chinook cumulative mortality from gas bubble disease at different levels of nitrogen supersaturation. Data points from Dawley et al. 1976, curve from fit of eq(109).

Size Difference

Dawley et al. (1976) demonstrated that large fish have higher levels of mortality. In a shallow tank using fall chinook of different sizes exposed to 112% and 115% supersaturation they determined cumulative mortality curves were significantly different (Fig. 10 in Dawley et al. 1976). These data can be used to infer the effect of fish length on nitrogen mortality in reservoirs since the study also demonstrated that shallow tank mortality curves had the same pattern as deep tank mortalities with higher nitrogen supersaturation levels. The studies indicated that mortality curves in

shallow tanks at 112% saturation were equivalent to mortality curves in a deep tank with 122% supersaturation.

The resulting mortality-length relationship can be used to extrapolate experimental results using one fish length to field conditions where the fish were larger. The first step was to determine an empirical relationship relating nitrogen supersaturation mortality to fish length. With this relationship the results of fall chinook studies in the Dawley experiments are extrapolated to fall and spring chinook in the Lower Granite reservoir using different average fish lengths for each stock (Table 31). The study also determined the mortality rate for steelhead. This value is used to extrapolate to steelhead in the Lower Granite reservoir.

Size-mortality relationship

To determine the relationship between fish size and nitrogen supersaturation mortality the mortality rate is first estimated by fitting eq(109) to cumulative mortality vs. exposure time for different sized fall chinook and steelhead (Fig. 42). The estimated rates are given in Table 31.

Table 31 Nitrogen mortality rates and fish length in shallow tank experiments (Dawley et al. 1976). Plotting symbols refer to Fig. 42.

Species	Plotting Symbols	Length (*mm*)	*Nsat* (%)	M_n (1/day)
fall chinook	•	40	112	0.175
	❑	42	115	0.843
	+	53	112	3.113
	✳	67	112	3.771
steelhead	●	180	115	8.586

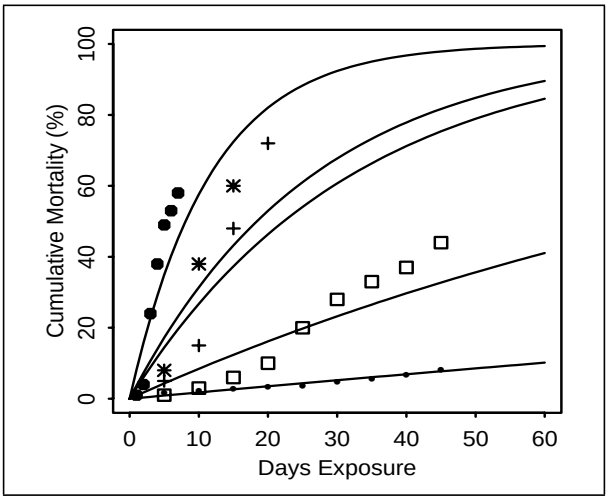

Fig. 42 Cumulative mortality vs. exposure time to nitrogen supersaturation for different fish length. See Table 31 for explanation of symbols.

The resulting mortality rates plotted against fish length are illustrated in (Fig. 43). The graph combines fall chinook ranging from 40 to 67 mm and steelhead 180 mm in length. The line in the figure is a linear fit with a least squares regression constrained to pass through zero.

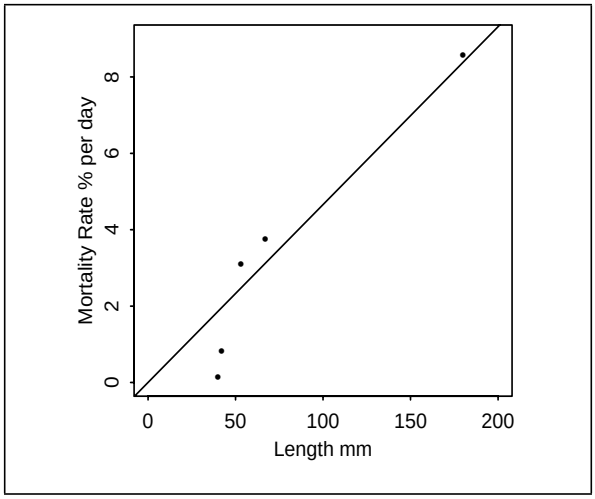

Fig. 43 Mortality rate of fish of different lengths.

Although no mechanism has been developed justifying a linear relationship, qualitatively the ability of a fish to establish gas equilibrium with its environment should be related to its volume to surface area ratio, which is proportional to fish length. Thus on physical principles of gas exchange a length relationship should be involved with nitrogen supersaturation mortality. The regression in Fig. 43 is

$$M_n(L) = aL \tag{110}$$

where

- $M_n(L)$ = nitrogen mortality rate as a function of fish length
- L = fish length in mm
- a = 0.0466 mm^{-1}, length coefficient for nitrogen mortality rate with an r^2 of 0.95.

From eq(110) the nitrogen mortality rate can be corrected for fish length using

$$M_n(L) = M_n(L_e)\frac{L}{L_e} \tag{111}$$

where

- L = length of fish in environment
- L_e = length of fish in nitrogen mortality experiments

Length-corrected nitrogen mortality rates are given in Table 32.

Table 32 Nitrogen mortality rates adjusted for observed fish length (L) above Lower Granite Dam (from Scully et al. 1983). L_e is length of test fish.

% Saturation		Length	fall chinook	spring chinook	steelhead
2.5 m tank	at surface	L_e	40	40	180
		L	112	130	230
105	95		0.005	0.005	-
110	100		0.009	0.011	0.390
115	105		0.024	0.028	0.765
120	109		0.043	0.050	1.385
124	123		3.455	4.008	-
127	115		3.586	3.348	4.977

Relating Mortality Rate to Nitrogen

To relate the length-adjusted mortality rates to nitrogen supersaturation eq (100) on page 86 is applied where

- N = percent nitrogen saturation *above* 100%
- N_{crit} = critical supersaturation level
- a = a species specific gas mortality rate (low slope)
- b = a species specific gas mortality rate (high slope).

It was fit one segment at a time using the Splus lsfit() function. A critical value was selected and lsfit() was used to fit mortalities at supersaturations between 0% and N_{crit}, constraining the line through 0% mortality at 0% supersaturation. The remaining points were fit to a line constrained to meet the first at $N = N_{crit}$. The resulting coefficients for the three species, and χ^2 values for the fit are given in Table 33.

Table 33 Nitrogen mortality rate coefficients

Parameter	fall chinook	spring chinook	steelhead
a	$1.785e^{-3}$	$2.072e^{-3}$	$59.425e^{-3}$
b	.517	0.600	.541
N_{crit}	10%	10%	10%
χ^2	0.747	0.867	0.156

The fits of the rate curves are illustrated in Fig. 44

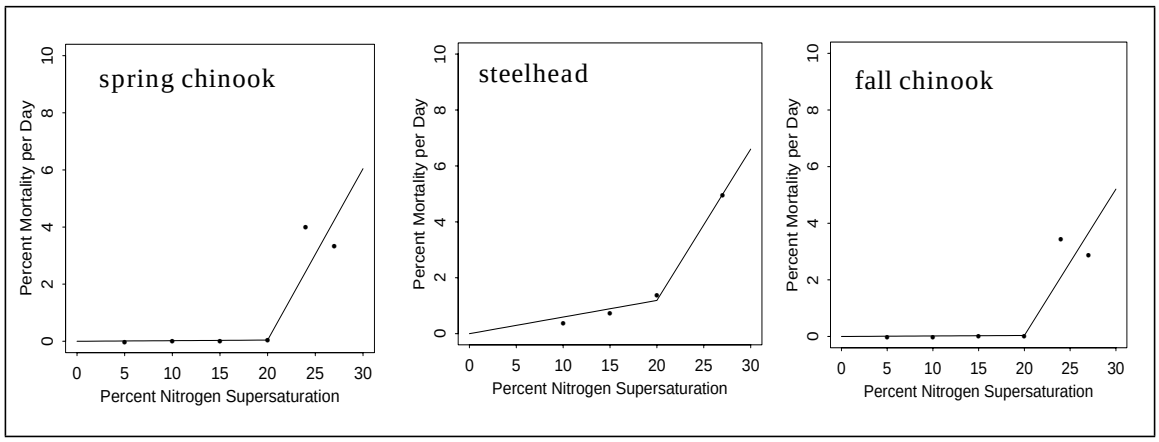

Fig. 44 Percent mortality rate of juvenile spring and autumn chinook and steelhead as a function of nitrogen supersaturation

Fish Depth

The gas bubble disease rate depends on fish depth which is characterized by a mode depth and bottom depth. Fish depths vary continuously over day and night, fish age, and position in the river. For the current model a representative depth is required for each species. These were selected after reviewing the data on fish vertical distributions. The literature and essential elements are given in Table 34.

Table 34 Fish depth information

Species	Location	Time	Mode depth	Reference
spring chinook	Forebay	Day	39 ft 5 ft	Johnson, et al. 1985 Ebel 1973
	Reservoir	Day	12-24 ft 27-36 ft	Smith, 1974 Dauble, et al. 1989
		Night	0-12 ft 27-36 ft	Smith, 1974 Dauble et al. 1989
fall chinook	Forebay	Day	-	-
	Reservoir	Day	12-20 ft	Dauble, et al. 1989
		Night	12-20 ft	Dauble, et al. 1989
steelhead	Forebay	Day	13 ft 4 ft	Johnson et al., 1985 Ebel 1973
		Night	-	-
	Reservoir	Day	0-12 ft	Smith, 1974
		Night	12-24 ft	Smith, 1974

The modal depth is taken to represent most typical fish depth (Table 35).

Table 35 Fish depth in model

Species	Mode depth	Maximum depth
spring chinook	12 ft	24ft
fall chinook	12 ft	36 ft
steelhead	12 ft	36 ft

II.7 - Nitrogen from Spill:

II.7.1 -Theory

Equations for nitrogen supersaturation are of two types. One type constitutes empirical equations with no underlying theory but which provide a general fit to observed supersaturation data as a function of spill. The other type constitutes mechanistic equations which define nitrogen levels in terms of physical processes producing spill. CRiSP.1 contains two empirical models and two mechanistic models. CRiSP.1 is calibrated to all submodels. In general, we recommend using the model called Gas Spill 2. Relevant parameters in the submodels are illustrated in Fig. 45.

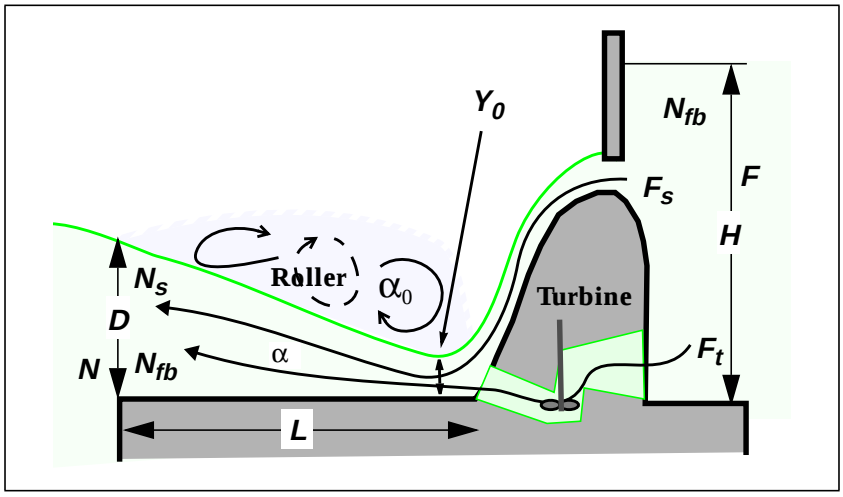

Fig. 45 Representation of spillway and stilling basin.

Exponential Saturation Equation

An empirical nitrogen supersaturation equation based on an exponential relationship between spill flow and supersaturation in the spilled water can be expressed

$$N_s = bF_s + a(1 - exp(-kF_s)) \quad (112)$$

where

- N_s = percent supersaturation above 100%

- F_s = spillway flow volume in kcfs
- a, b and k = coefficients specific to each dam derived from nitrogen rating curves provided by the Corps of Engineers.

The exponential equation was developed first and was used in CRiSP.1 version 3. It is retained in version 4 for backward compatibility of models. The hyperbolic model fits the data better than the exponential model.

Hyperbolic Saturation Equation

The nitrogen supersaturation equation data can also be fit with a hyperbolic relationship between spill flow and supersaturation. The relationship is

$$N_s = bF_s + \frac{aF_s}{h + F_s} \tag{113}$$

where

- N_s = percent supersaturation above 100%
- F_s = spillway flow volume in kcfs
- a, b and h = coefficients specific to each dam and can be derived from nitrogen rating curves available from the Corps of Engineers.

Although this submodel can produce a degree of supersaturation at zero spill flow (when $h = 0$), this does not contribute to supersaturation in the tailrace water since the contribution of spill water to the tailrace is zero with zero spill as is defined in eq (123). This model is the preferred empirical model and should be used in place of the exponential model if an empirical model is selected.

Mechanistic Equation

The theory for nitrogen supersaturation from the physical process of spilling water and dissolving excess nitrogen in the tailrace water is developed below.[1] The mechanistic model begins with an equation for nitrogen concentration as

$$N_s = N_{eq} \cdot \bar{P} - (N_{eq} \cdot \bar{P} - N_{fb}) \cdot \exp\left(-\frac{K_e}{F_s} WL\Delta\right) \tag{114}$$

where

- F = total flow in kcfs
- F_s = spill in kcfs
- N_s = nitrogen concentration in tailrace in mg./l
- N_{fb} = nitrogen concentration in the forebay in mg./l
- N_{eq} = nitrogen equilibrium concentration as a function of temperature in degrees C at one atmospheric pressure

This is approximated by:

$$N_{eq} = 21.1 - 0.3125 \cdot T \tag{115}$$

1. This model was developed by Water Resources Engineers (WRE), Inc. (1971) for the Corps of Engineers and reviewed by Boyer (1974).

- L = length of the stilling basin in feet
- $\bar{P}$ = average hydrostatic pressure in the main flow of the stilling basin in atmospheres

  This is defined

$$\bar{P} = P_0 + \frac{\alpha_0}{2}(D - Y_0) + \frac{\alpha}{4}(D + Y_0) \quad (116)$$

- P_0 = barometric pressure in atmospheres (assume P_0 is 1)
- α = density of water (0.0295 atm / ft)
- α_0 = specific gravity of the roller at the base of the spill

  This depends on the degree of aeration of the roller.
- W = spillway width
- D = water depth at the end of the stilling basin
- Y_0 = thickness of the spill at the stilling basin entrance, where

$$Y_0 = \frac{F_s}{W\sqrt{2gH}} \quad (117)$$

- H = hydraulic head expressing the forebay elevation minus the elevation of the spilling basin floor (H is in ft and gravity constant, g, is 32 ft s^{-2})
- Δ = differential pressure factor defined

$$\Delta = \left(\bar{P} + \frac{\alpha}{4}(D + Y_0)\right)^{1/3} - \left(\bar{P} - \frac{\alpha}{4}(D + Y_0)\right)^{1/3} \quad (118)$$

- K_e = bubble entrainment coefficient with units of ft $s^{-1}atm^{-1/3}$ and is defined

$$K_e = K_{20}(1.028)^{(T-20)} \quad (119)$$

- T = temperature in degrees C
- K_{20} = temperature compensated entrainment coefficient.

  The coefficient are estimated using different relationships depending upon the dam. These are known as Gas Spill 1 and Gas Spill 2 and are detailed as follows.

Gas Spill 1

Gas Spill 1 is a three-parameter *multiplicative* model, used by the Corps of Engineers at Bonneville Dam only. The equation is

$$K_{20} = 10^a \cdot E^b \cdot P^c \quad (120)$$

Gas Spill 2

Gas Spill 2 is a three-parameter *additive* model used at all other dams. It is defined

$$K_{20} = a + b \cdot E + c \cdot P \quad (121)$$

where

- E = energy loss rate expressed as total headloss divided by residence time of water in the stilling basin

$$E = \frac{F_s}{LWD}(H - D) - \left(\frac{F_s}{D}\right)^3 \frac{1}{2gL} \tag{122}$$

- P = forebay percent saturation
- a, b, and c = dam dependent empirical coefficients.

The original WRE model used a two-parameter multiplicative model, which was identical to Gas Spill 1 with $c = 0$.

Nitrogen in the Tailrace

Nitrogen supersaturation in the tailrace results from mixing spill water with water passing through turbines (Fig. 45). The equation is

$$N = N_{fb} + \frac{F_s}{F}(N_s - N_{fb}) \tag{123}$$

where

- F = total flow through the dam in kcfs
- F_s = spill flow in kcfs
- N = tailwater nitrogen supersaturation (in percent)
- N_{fb} = forebay nitrogen supersaturation (in percent)
- N_s = spill water nitrogen in percent saturation as defined by an empirical or mechanistic saturation equation.

Nitrogen at a Confluence

The nitrogen at a confluence is determined by the addition of two flows with different nitrogen levels. The equation is

$$N = \frac{F_1 N_1 + F_2 N_2}{F_1 + F_2} \tag{124}$$

where

- F_i = flow in kcfs in segment i
- N_i = nitrogen in percent supersaturation in segment i of the confluences.

Nitrogen Dissipation

Nitrogen levels above the saturation level are lost from the river as a first order process. This is defined (WRE) by a total flux equation for a segment as

$$\Phi = AK_d(N_{eq} - N) \tag{125}$$

where

- Φ = flux of nitrogen across the air water interface
- N = nitrogen supersaturation concentration in the segment
- N_{eq} = nitrogen equilibrium concentration
- A = surface area of the segment
- K_d = transfer coefficient defined

$$K_d = \left(\frac{D_m U}{D}\right)^{0.5} \tag{126}$$

where

- D_m = molecular diffusion coefficient of nitrogen
- U = hydraulic stream velocity
- D = depth of the segment

To express the loss in terms of concentration we divided eq (125) by AD to give

$$\frac{dN}{dt} = \frac{\Phi}{AD} = (N_{eq} - N)\sqrt{\frac{D_m U}{D^3}} \tag{127}$$

To put the calculation in units of miles and days, note that one mile = 16.0934 x 10^4 cm = 5280 ft, and one day = 8.64 x10^4 seconds. Expressing U in miles / day and D in feet and D_m in cm^2 / s, the diffusion coefficient per unit square mile of river is

$$\frac{dN}{dt} = k(N_{eq} - N) \tag{128}$$

where the coefficient k is expressed

$$k = 700.75\sqrt{\frac{D_m U}{D^3}} \approx 0.085 \text{ /day} \tag{129}$$

assuming:

D_m = order[1] of 2 x 10^{-5} $cm^2 s^{-1}$

U = order of (20 miles / day) 1.2 ft / s. Note this changes on a daily basis and for each reach in the model

D = order of 30 ft. Note this changes on a reach specific basis and is dependent on reservoir elevation.

The constant 700.75 gives the coefficient k in unit of day^{-1}

Nitrogen loss rate due to degassing can be expressed as a function of time since the water entered the tailrace. The equation describing the nitrogen level as a function of residence time in a river segment is

$$N(t) = N_{eq} + [N(0) - N_{eq}]e^{-kt} \tag{130}$$

where

- N_{eq} = nitrogen equilibrium concentration defined by eq (115)

1. F.A. Richards 1965.

- N(0) = tailrace concentration defined by eq (123)
- k = dissipation coefficient defined by eq (129)
- t = time in a river segment

Noting that in the models N is in terms of percent above supersaturation we then set $N_{eq} = 0$.

Adjustments of k

The nitrogen dissipation coefficient depends on the average depth as defined in eq (129). The average depth is variable according to the geometry of the reservoir and the pool elevation. This depth is defined as

$$D = \frac{Volume}{WL} \tag{131}$$

where

- *Volume* = pool volume at a specific elevation
- W = average pool width at full pool
- L = length of pool

II.7.2 -Calibration

Calibration of both the empirical and mechanistic equations is show below.

Empirical Equation

The calibration is applied to the hyperbolic empirical model given by eq (113) where

- N_s = percent supersaturation above 100%
- F_s = spillway flow volume in kcfs
- a, b and h = coefficients specific to each dam, derived from nitrogen rating curves provided by the Corps of Engineers.

Data for fitting these parameters were obtained from rating curves provided by Bolyvong Tanovan of the Army Corps of Engineers North Pacific Division, Portland, OR. The graphs showing observed nitrogen concentrations in supersaturation for spill flows were copies of in-house documents -unreferenced and unpublished. The graphs were identified with the codes NPDEN-WC, DLL/KPA, 8MAR79. The ruling of the rating curves allowed a precision of ± 0.5 kcfs, and ± 0.1 % saturation.

The parameters in Table 36 were obtained by fitting the hyperbolic submodel of eq (113) to the rating curves using a nonlinear “amoeba” routine from *Numerical Recipes* (Press et al. 1988). Constraints on fitted parameters were

$$0 \le a \le 50$$
$$0 \le b \le 0.12$$
$$0 \le h \le 100.$$

Table 36 Values for empirical nitrogen model

Dam	*a*	*b*	*h*	resid[a]
Bonneville	29.92	0.020	6.07	21.
The Dalles	20.21	0.0006	22.32	72.4
John Day	8.43	0.095	0.00	42.63
McNary	16.33	0.000	35.33	2.22
Ice Harbor	17.36	0.117	3.82	44.07
Low. Monumental	25.44	0.000	8.55	4.05
Little Goose	40.78	0.000	37.36	3.52
Lower Granite	24.22	0.000	18.07	6.12
Priest Rapids	22.02	0.038	3.31	49.22
Wanapum	28.03	0.047	10.35	29.17
Rock Island	42.26	0.0003	99.95	48.30
Rocky Reach	23.82	0.020	1.49	19.08
Wells	20.83	0.065	0.20	9.51
Chief Joseph	28.74	0.008	11.68	39.56

a. resid = residual sum of squares / number of data points.

Mechanistic Equation

The mechanistic nitrogen saturation submodel (see Mechanistic Equation section on page II.98) was calibrated using flow / spill / gas saturation data from the rating curve data 1984 to 1990 at most projects. (This data set was supplied by Tom Miller of the Walla Walla District of the U.S. Army Corps of Engineers.) The data originated from the Columbia River Operations Hydrological Monitoring System (CROHMS) data base. At each dam the data consisted of: hourly flow and spill, forebay saturation, forebay elevation, tailrace elevation, and temperature, all measured throughout the summer. Using the same gas dissipation mechanism as was used in earlier versions of CRiSP.1, the tailrace gas saturation was back-calculated from the next dam downstream.

For each point in time the three parameters *a*, *b*, and *c* below were estimated using a multiple linear regression of the equation defining K_{20} in terms of the energy loss rate, the forebay concentration, and the entrainment coefficient. The mechanistic model for GasSpill 2 assumes that these parameters are related as is given by eq (121) where

- K_{20} = entrainment coefficient
- E = energy loss rate
- C_f = forebay concentration
- *a*, *b*, and *c* = coefficients calculated from multiple linear regression of data in Table 37.

For each dam K_{20} is calculated from data using:

$$K_{20} = 1.028^{20-T} \cdot \frac{S}{W \cdot L \cdot \Delta} \cdot \log \frac{P - N_{fb}}{P - N_{sw}} \quad (132)$$

where

- T = water temperature in the forebay in degrees C.
- S = spill in kcfs
- W = spillway width (gates x width / gate)
- L = stilling basin length in feet
- N_{fb} = forebay gas saturation
- N_{sw} = back-calculated spillway gas saturation

$$P = B + (sgr \cdot \alpha \cdot 0.5 \cdot (d - y_0)) + (0.25 \cdot \alpha \cdot (d + y_0))$$

where

- sgr = specific gravity of roller (usually 1)
- α = 0.0295
- d = stilling basin depth in feet
- $y_0 = S/(W \cdot \sqrt{2GH})$
- H = hydraulic head in ft is obtained from information in Table 38
- G = 32.2 (gravitational constant)

and

$$\Delta = \sqrt[3]{P + 0.25\alpha(d + y_0)} - \sqrt[3]{P - 0.25\alpha(d + y_0)}$$

No data were available for Wanapum Dam thus preventing calibration of both Wanapum and Rock Island, the dam immediately upstream. In these cases the initial calibration of Water Resources Engineers Inc. (WRE 1971) was used as the calibration.

The spill program of 1994 presented an opportunity to recalibrate Gasspill parameters using up-to-date data at a variety of spill levels, including some observations at very high levels that had not previously occurred. Daily average gas levels were compared to those estimated using previously calibrated GasSpill parameters, and parameters were adjusted on a dam by dam basis to bring model predictions into closer agreement with observed data. Required changes were quite small, but the improvement of fit was noticeable; current estimates and observed gas levels are shown for several points in the system in Fig. 46. Note that in all four graphs the predicted and observed saturation tracks do not differ significantly (chi-squared goodness-of-fit test, in all cases $p>0.05$).

Table 37 Parameters for Gas spill model equations

Dam	*L*	Basin Floor Elev.	gate wd	# gates	sgr	*a*	*b*	*c*
BON	144.5	-16.0	60	18	1.0	2.469	1.108	-1.103
TDA	170.0	55.0	60	23	0.50	37.00	3.255	-0.394
JDA	185.0	114.0	62	20	1.0	5.200	0.798	-0.050
MCN	270.0	228.0	60	22	1.0	5.700	0.810	-0.050
IHR	178.0	304.0	60	10	1.0	0.524	0.146	0.000
LMN	218.7	392.0	50	8	1.0	-1.900	1.037	0.010
LGS	78.6	466.5	50	8	1.0	4.072	1.247	-0.035
LWG	188.0	580.0	50	8	1.0	-5.150	0.400	0.060
DWR	40.0	954.0	60	2	1.0	3.310	0.460	-0.032
HCY	80.0	1480.0	50	1	1.0	3.310	0.460	-0.032
PRD	75.3	387.0	40	22	1.0	5.000	-0.337	-0.037
WAN	100.0	456.0	50	12	1.0	0.000	0.029	0.051
RIS	100.0	530.0	30	37	0.1	-4.000	-0.137	0.051
RRH	150.0	599.0	50	12	1.0	22.25	-1.14	-0.077
WEL	30.0	670.0	46	11	1.0	28.00	0.804	0.000
CHJ	180.0	743.0	40	19	1.0	-5.05	0.295	-0.070

Table 38 Variables for reservoir geometry, in feet. Dam abbreviations correspond to dams in Table 36.

Dam	Maximum Forebay Elevation	Full Pool Depth at Head	Forebay Depth	Elevation Spillway Crest	Normal Tailwater Elevation
BON	82.5	68	98.5	24	14.5
TDA	182.3	85	127.3	121	72
JDA	276.5	105	162.5	210	160
MCN	357	75	129.0	291	265
IHR	446	100	142.0	391	340
LMN	548.3	100	156.3	483	440
LGS	646.5	98	180.0	581	540
LWG	746.5	100	166.5	681	638
PRD	488	82.5	101.0		------

Table 38 Variables for reservoir geometry, in feet. Dam abbreviations correspond to dams in Table 36.

Dam	Maximum Forebay Elevation	Full Pool Depth at Head	Forebay Depth	Elevation Spillway Crest	Normal Tailwater Elevation
WAN	575	83.5	121.0		485
RIS	619	54	189.0		570
RRH	710	93	111.0		613
WEL	791	72	121.0		705

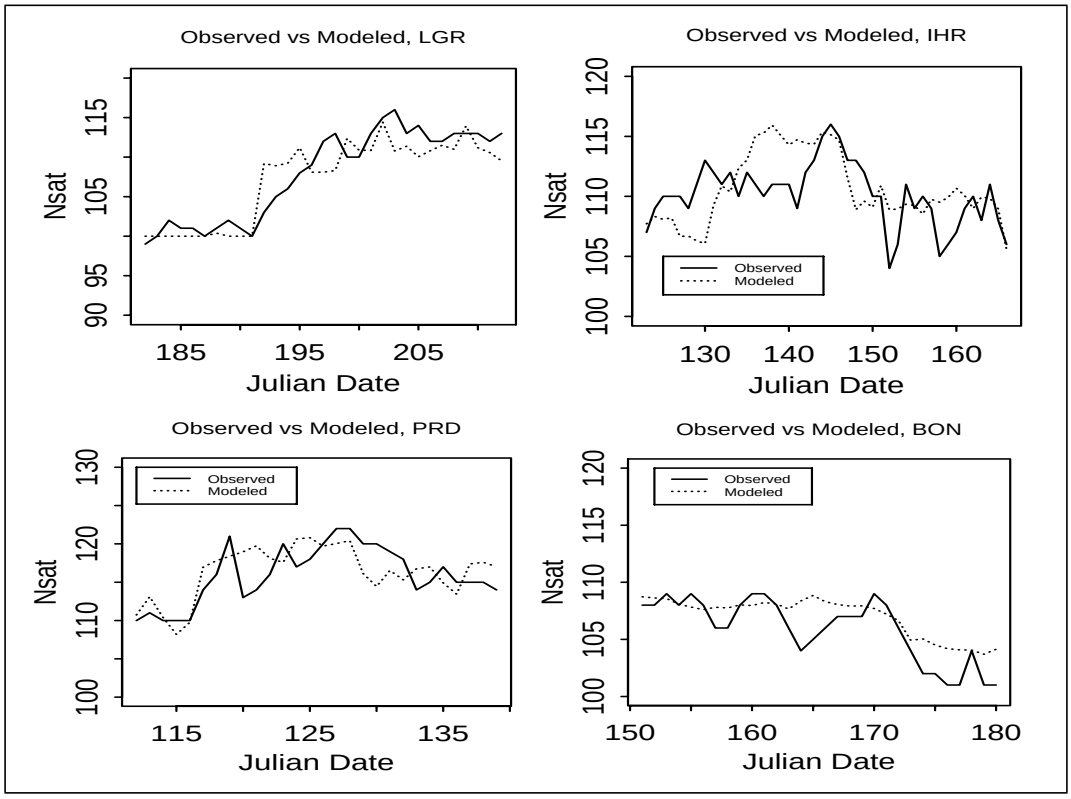

Fig. 46 Comparison of observed and modeled gas supersaturation for 1994 data. Lower Granite Pool Chi-square = 1.88, p>0.05. Ice Harbor Pool Chi-square = 3.38, p>0.05. Priest Rapids Pool Chi-square = 2.01, p>0.05. Bonneville Pool Chi-square = 1.08, p>0.05.

II.8 - Dam Passage

Fish enter the forebay of a dam from the reservoir and experience predation during delays due to diel and flow related processes. They leave the forebay and pass the dam mainly at night through spill, bypass or turbine routes, or are diverted to barges or trucks for transportation. Once they leave the forebay, each route has an associated mortality and fish returning to the river are exposed to predators in the tailrace before they enter the next reservoir. These regions are illustrated and the details of passage through the regions of the dam are illustrated schematically in (Fig. 47).

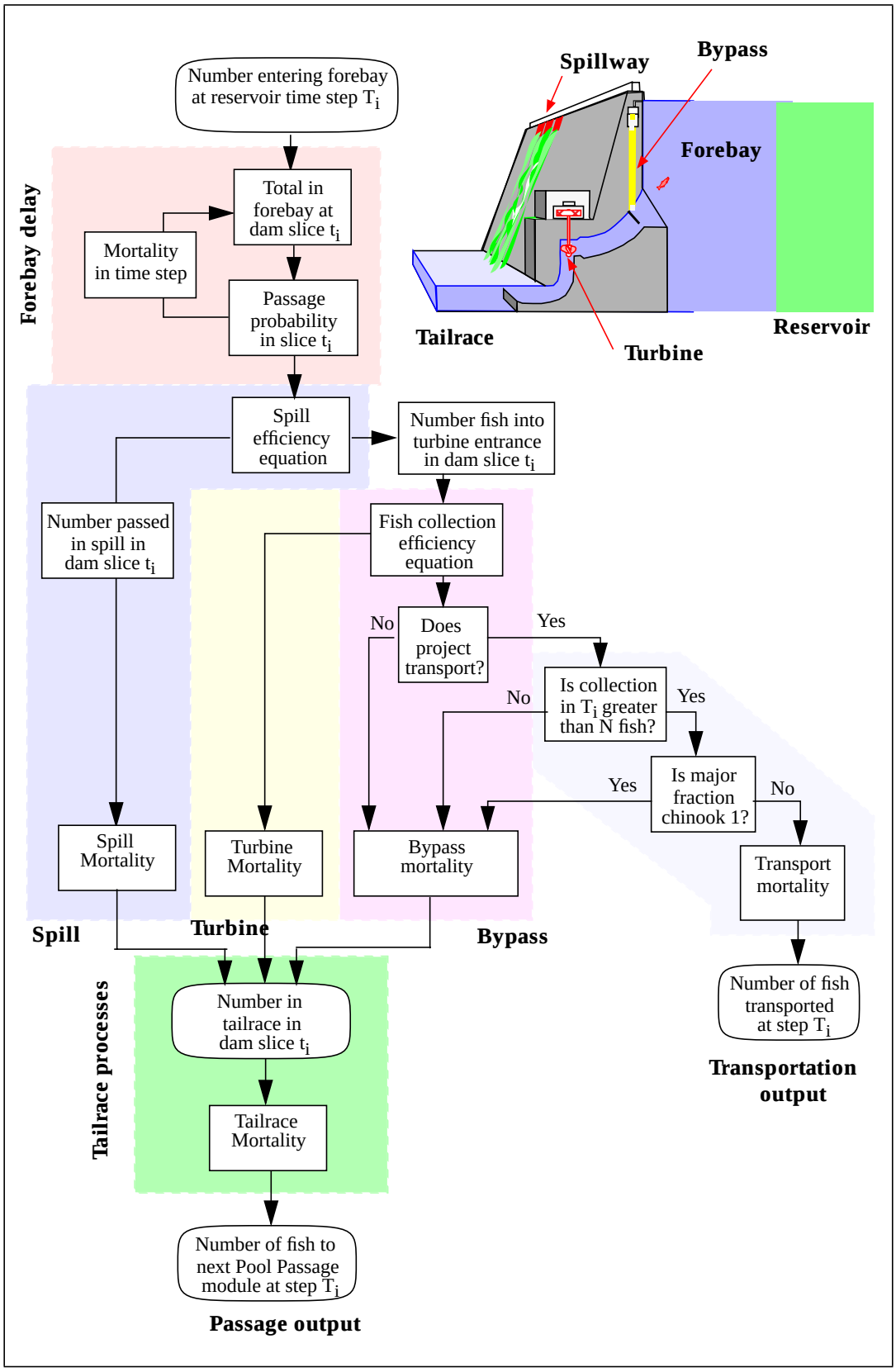

Fig. 47 Dam processes showing passage routes and mortality

The movement and allocation of fish through the forebay is illustrated in Fig. 48. Fish entering from the reservoir are delayed in the forebay before they pass through one of three passage routes. Fish exiting the reservoir in each reservoir time slice, typically two slices per day, are evenly allocated as input to the forebay over the dam time slices, which are shorter than the reservoir time slices. In the forebay fish experience mortality. Output from the forebay in each dam time slice depends on flow and diel illumination. Allocation to the passage routes depends on spill schedules and passage efficiencies through the routes. Calculations are performed in the order: mortality, delay, spill passage, dam passage.

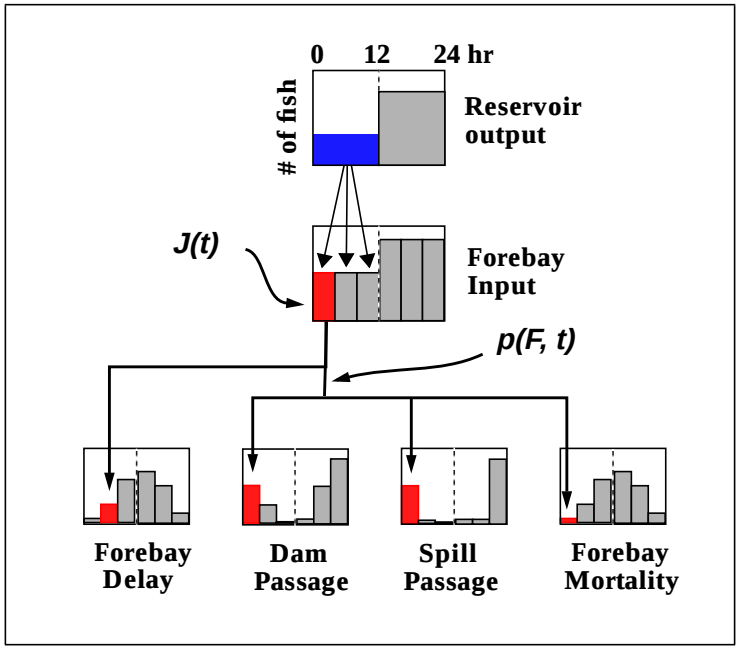

Fig. 48 Transfer of fish from reservoir to forebay to dam. Diagram shows allocation of fish from a reservoir time slice of 12 hours to dam time slices of 2 hours each. Four hour dam slices are indicated for graphical clarity.

II.8.1 -Forebay Delay

Studies of the timing of fish passage at dams indicate that passage occurs mostly at night, with fish delaying passage during daylight hours. This delay process is represented in CRiSP.1 as a simple input-output submodel. Fish enter the forebay at a rate determined by reservoir passage factors. Fish are assumed to be more susceptible to being drawn into turbine intakes or spill at night than during the day, and this susceptibility is represented through the flow and the volume of the forebay area occupied by the fish. CRiSP.1 expands this volume in the day and contracts it at night.

The essential elements of this submodel include a forebay volume defined by the forebay depth *H*, a horizontal length scale *L*, which changes with illumination *I*, and river flow *F* (Fig. 49).

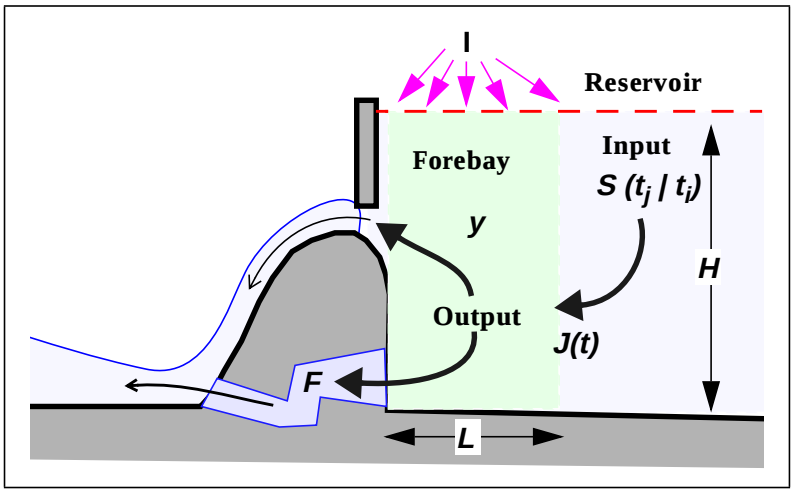

Fig. 49 Variables for dam passage delay model

Forebay Input

The number of fish entering the forebay in each dam time slice is determined by the number leaving the reservoir. Since reservoir time slices are longer than dam time slices, input from a reservoir is evenly distributed across the corresponding dam slices according to the formula

$$J(t) = \sum_{i=1}^{j} S(t_j | t_i) \frac{\Delta t}{\Delta T} \qquad \text{for} \qquad t_j \le t \le t_j + \Delta T \tag{133}$$

where

- $S(t_j \mid t_i)$ = number of fish entering the reservoir on increment t_i and exiting the reservoir at increment t_j as defined in eq (62)
- $J(t)$ = number of fish entering the forebay on dam slice increment t
- Δt = hours in a dam time slice, typically set for 2 hours
- ΔT = hours in a reservoir time slice, typically set for 12 hours

Forebay Passage Dynamics

Forebay passage is defined in terms of the following equation

$$\frac{dy}{dt} = J(t) - p(F,t)y(t) \tag{134}$$

where

- y = fish in forebay
- t = time (resolved to time of day and Julian day)
- $J(t)$ = input to forebay from the reservoir
- $p(F,t)$ = rate at which fish pass from the forebay into the dam
- F = flow through the dam in kcfs.

The corresponding difference equation used in CRiSP.1 is

$$Y_{t+\Delta t} = [1 - p(F, t)\Delta t]Y_t + J(t)\Delta t \quad (135)$$

where

- Δt = duration of a dam time slice, typically 2 hours
- Y_t = number of fish in the forebay in the dam time slice t
- $p(F, t)$ = forebay rate coefficient. This depends on the flow F, and an illumination dependent time t as is developed below.

Forebay Passage Coefficients

To alter passage according to the diel distribution, the rate coefficient depends on time of day / light level. In addition, CRiSP.1 alters passage according to the river flow relative to the hydraulic capacity of the dam. The forebay rate coefficient is defined

$$p(F, t) = k\frac{F(T)}{F_{\max}V_{\text{forebay}}(t)} \quad (136)$$

where

- k = dimensionless constant which is species dependent describing the propensity of the fish to move with the flow
- $F(T)$ = river flow in kcfs which depends on the reservoir time slice
- $F_{\max}$ = hydraulic capacity of a project in kcfs
- $V_{\text{forebay}}(t)$ = effective forebay volume containing fish, which depends on illumination I as a function of time.

The effective volume is assumed to vary with project forebay depth and level of illumination using the equation

$$V_{\text{forebay}}(t) = H_{\text{forebay}}[L_{\text{night}} + (L_{\text{day}} - L_{\text{night}})B(I(t))]^2 \quad (137)$$

where

- H_{forebay} = depth of forebay
- L_{day} = forebay horizontal length scale associated with fish in full daylight
- L_{night} = forebay horizontal length scale associated with fish in the night. Note: $L_{\text{day}} > L_{\text{night}}$
- I = illumination which depends on season and time of day
- $B(I(t))$ = behavioral factor dependent on the illumination.

  This selects the appropriate length scale within a dam time slice. B is zero when the illumination is below a threshold level through the time slice and is one when illumination is above the threshold. For dam time slices in which the illumination crosses the threshold, B is the fraction of time the slice is above the threshold and is a function of the time of day and Julian date. (Fig. 50).

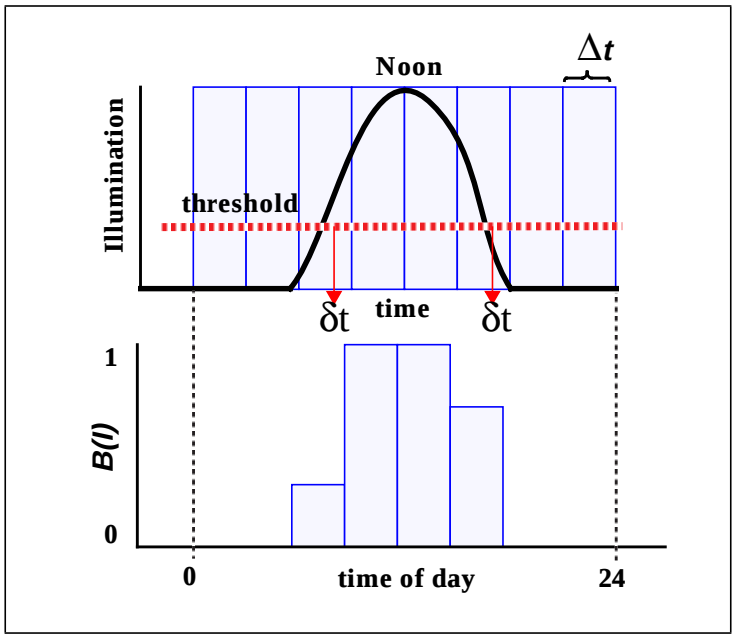

Fig. 50 Relationship between illumination and behavioral factor for dam time slices over a day

The illumination as a function of time of day and Julian date[1] is

$$I(t) = \max\left[0, \cos^3\left(\frac{t - \text{localnoon}}{D(T)}\pi\right)\right] \tag{138}$$

where

- t = hour of day
- local noon = typically 1300 hr with daylight savings time
- $D(T)$ = day length is a function Julian day, T,

  The vernal equinox is day 80 and the mean length of daylight is 14 hr so the equation is

$$D(T) = 14 + \sin\left(2\pi\frac{T - 80}{365}\right) \tag{139}$$

The time before or after local noon when the threshold is crossed is determined by setting illumination equal to the threshold value and solving for δt as

$$\delta t = \frac{D(T)}{\pi} \cdot [\operatorname{acos} I_{\text{threshold}}]^{1/3} \tag{140}$$

where

- δt = time in hours before or after local noon of the threshold crossing
- $I_{\text{threshold}}$ = light threshold at which fish behavior switches.

1. Ikushima, 1967, as cited in Parsons and Takahashi, 1973.

Calibration of Forebay Delay

Variation in any of the dam delay parameters produce families of curves relating delay probability and time of day for a given fish depth, flow, and day of the year (see examples in Fig. 51).

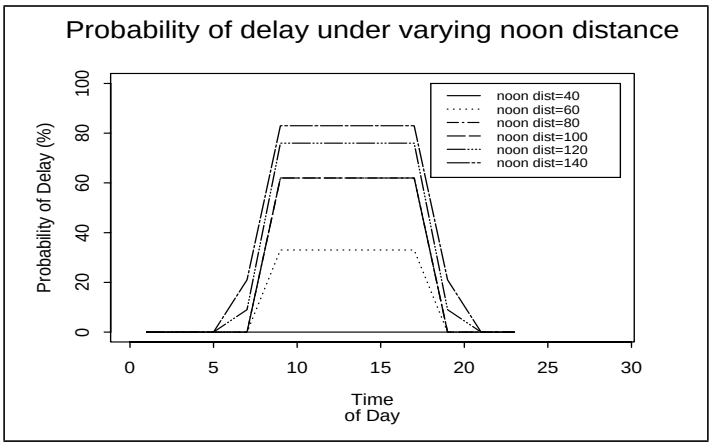

Fig. 51 Family of trajectories for delay versus time of day under varying noon distance values.

Note that probability of delay does not map directly onto passage frequency. Passage will be affected by delay, but also by the arrival frequency of potential migrants and by the rate of predation that delayed smolts incur in the forebay. If smolt arrival is assumed to be uniform during the day (probably not accurate; A. Giorgi personal communication) and we assign an arbitrary predation loss of 10% during a two-hour time period, the delay probabilities shown in Fig. 51 produce diel passage patterns as shown in Fig. 52 A.

As fish forebay residence time increases they suffer an increasing accumulation of mortality due to predation. As noon distance (L_{day}) increases from 40 feet to 140 feet, while holding night distance (L_{night}) constant at 40 feet, mortality increases from 0% to just over 10% during the entire 24-hour cycle (see Fig. 52 B).

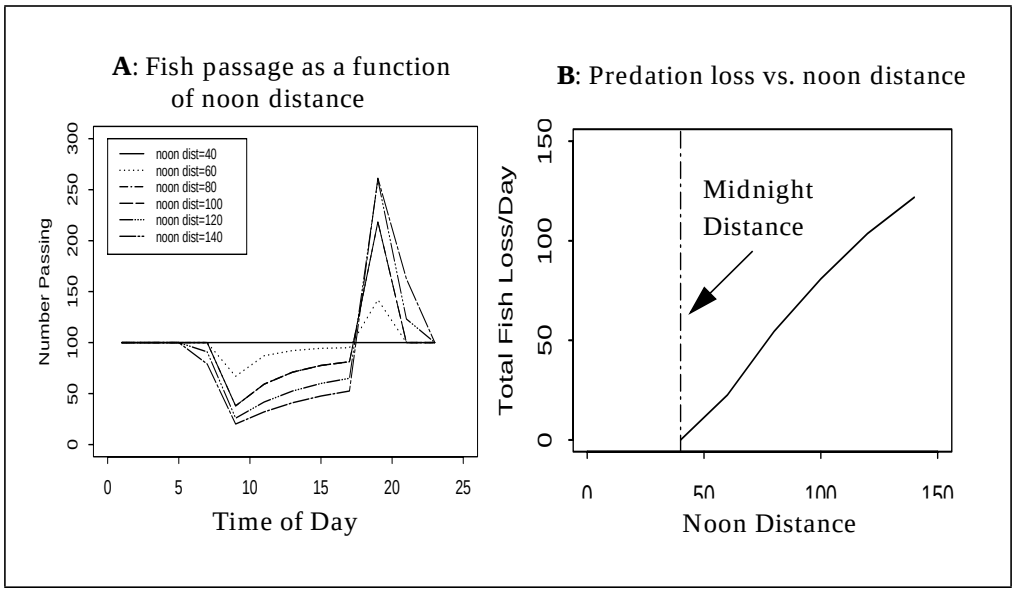

Fig. 52 A. Diel passage patterns from by delay probabilities in Fig. 51. **B.** Mortality experienced by smolts with increasing delay.

Comparison Data

Numerous data sets exist that provide information on diel passage (e.g. Raemhild et al. 1983, Steig and Johnson 1986, Ransom and Sullivan 1989). Very few data sets, however, provide information on the difference between arrival at the dam and actual passage. Diel passage patterns can be summarized simply: more fish pass at night than during the day. Generally peak passage occurs around 2100 hr.

The delay model is calibrated to radio-tag data. Radio tags were inserted into the gut of spring chinook salmon (*Oncorhynchus tshawytscha*), the fish released, and their movement patterns tracked.The comparison data set comes from John Day Dam and its reservoir (Giorgi et al., 1985).

These data include the date and time of arrival in the forebay for each fish, as well as the date and time of passage through the dam. The mode of passage - powerhouse or spillway - is also noted. The difference between these two times is the delay experienced by each fish. Because our model is based on delays induced at the powerhouse, fish that pass the dams via the spillway have been excluded. There is a significant relationship between the delay experienced and the time of day the fish arrive at the dam (Fig. 53; Kendall's tau = -0.297, p = 0.0096). Fish arriving during the day experience longer delays; those arriving at night pass the dam quickly.

The data suggest that fish arriving during the day are delayed 2 hours. Since CRiSP currently uses a 2-hour dam time step, this is equivalent to a delay probability of 50% during daylight, and no delay at night. A particular linear combination of model parameters produces these values: any point taken from this linear collection will achieve the desired effect using the values given in Table 39.

Table 39 Delay equation parameters

Noon Distance	150
Night Distance	80
k (x 10^2)	24
Threshold (x 10^{-3})	50

These values have a good fit to observed of arrival and passage (Fig. 54).

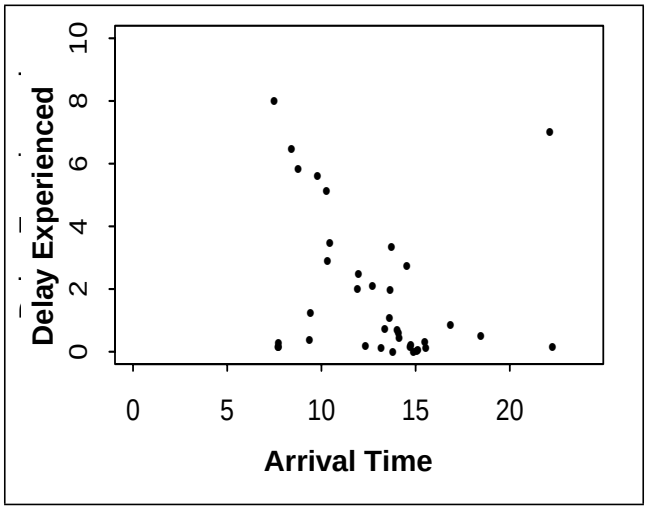

Fig. 53 Delay as a function of time of day of arrival.

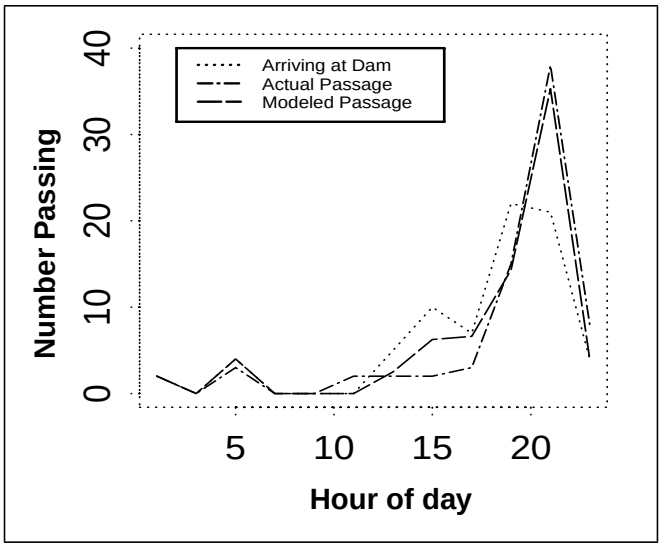

Fig. 54 Arrival and diel passage of spring chinook at John Day Dam, observed and simulated.

II.8.2 -Forebay and Tailrace Mortality

Mortality of fish in the forebay and tailrace of a dam depends on predator density, water temperature, the amount of time in the zones, and the diurnal light distribution. An illustration of the zones is shown in Fig. 55. The full pool depth of the reservoir is *H* and *h* is the depth with a lowered pool elevation.

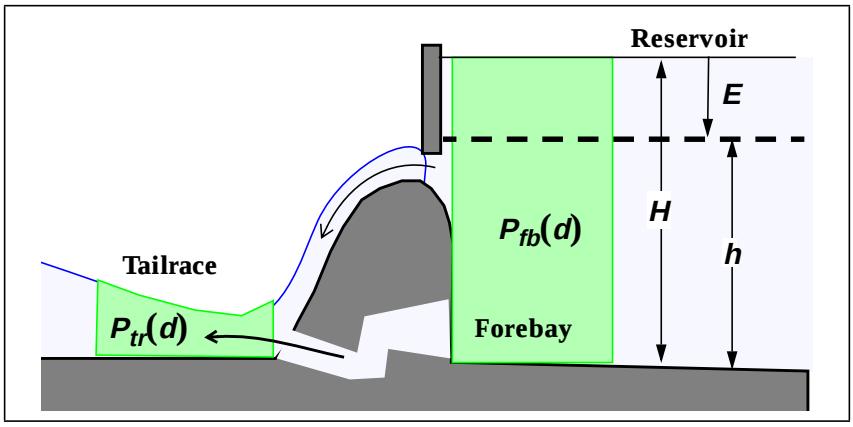

Fig. 55 Tailrace and Forebay geometry for mortality submodel. Line *E* is pool elevation with less than full pool.

Predator Density / Volume Interaction

Predators may be concentrated in the forebay or tailrace when the depth of the regions is decreased by lowering the reservoirs. It is possible that concentrating predators increases the encounter rate between predators and prey and thus effectively increases the mortality rate in the forebay and tailrace.

This mortality increase can be included in CRiSP.1 runs by choosing the appropriate check box in the **settings** window opened from the **RUN** menu. If the **predator density/volume interaction** is selected, predator density is a function of pool elevation for reservoir, forebay and tailrace regions. Predator density adjustments to the forebay and tailrace (Fig. 56) are given by[1]

$$\begin{aligned} P(h) &= P\frac{H}{h} \qquad \text{if} \qquad \frac{h}{H} > 0.05 \\ P(h) &= 20P \qquad \text{if} \qquad \frac{h}{H} \le 0.05 \end{aligned} \tag{141}$$

where

- H = forebay (tailrace) depth at full pool
- h = forebay (tailrace) depth at a lowered pool
- P = predator density at full pool for the forebay (tailrace)

1. The limit $h/H < 0.05$ is arbitrary and required to prevent divide by zero errors. The limit equates to a river depth just over the head of most managers.

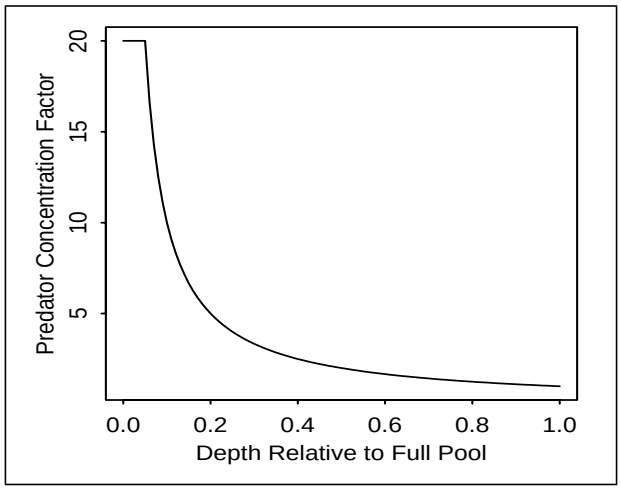

Fig. 56 Predator concentration function at dam

Forebay Mortality

Forebay mortality occurs while fish are delayed in passing the dam. The rate equation has the same form as used in the reservoir although predator densities and predation rate coefficients are different. The rate equation is

$$\frac{dX}{dt} = a\mathrm{e}^{u\theta}P(h)_{fb}b(\mathrm{t})X \tag{142}$$

where

- X = smolt density in the forebay
- $P(h)_{fb}$ = predator density in the forebay as a function of forebay depth h (predators km^{-2}) defined by eq (141)
- θ = temperature in degree centigrade
- a = predator activity parameter depending on prey species (this parameter has deterministic and stochastic parts)
- u = predator activity exponent independent of prey species
- $b(t)$ = diurnal mortality rate factor $0 \leq b \leq 1$ assumed to be constant over a dam time slice.

The fraction f of the forebay population surviving predators in each dam time slice Δt is

$$f(t+\Delta t) = \frac{X(t+\Delta t)}{X(t)} = \exp[a\mathrm{e}^{u\theta}P(E)_{fb}b(\mathrm{t})\Delta t] \tag{143}$$

Tailrace Mortality

Tailrace mortality follows a process similar to those in the reservoir and forebay. The predation coefficient in the tailrace is larger than in the other regions, reflecting a temporary increase in fish susceptibility to predation after they exit the dam. The number of fish surviving the tailrace on each dam time slice is

$$X(t) = X_0(t)\exp[ae^{u\theta}P(E)_{fb}b(t)\delta t] \quad (144)$$

where

- $X_0(t)$ = number of fish entering the tailrace at dam time step t
- $X(t)$ = number of fish exiting the tailrace within dam time step t
- δt = residence time of fish in the tailrace (see eq (145))
- $P(h)_{tr}$ = predator density in the tailrace as a function of tailrace depth h (predators km^{-2}). This is defined by eq (141)
- θ = temperature in degree centigrade
- a = predator activity parameter depending on prey species (this parameter has deterministic and stochastic parts)
- u = predator activity exponent independent of prey species
- $b(t)$ = diurnal mortality rate factor where $0 \leq b \leq 1$ assumed to be constant over a dam time slice.

Tailrace Residence Time

The tailrace residence time of fish, which is used in eq (144), depends on the level of flow and the volume of the tailrace. The equation is

$$\delta t = \frac{1}{F} L \cdot W \cdot H_u \quad (145)$$

where

- L = tailrace length as set by a slider at each dam (default is 1000 ft.)
- W = reservoir width
- H_u = depth of the tailrace, the upper depth of a reservoir at full pool
- F = flow at the project.

The tailrace time scale is not precisely defined and depends on the choice of the length scale L. In general, the length scale expresses the size of the region below a dam where predators are concentrated and the cross channel velocity distribution is influenced by turbine flows. The boat restricted zone of the tailrace is one possible measure of the length scale; BRZs are typically about 1000 feet long.

II.8.3 -Spill

The spill algorithm represents allocations of spill from flow models (HYDROSIM or HYSSR) through Flow Archive Files or the Spill Schedule Tool window.

Flow Archive Spill

When spill is allocated from Flow Archive files, it is identified as a percent of daily averaged flow over multi-day periods. Consequently, for use in CRiSP.1, archive derived spill must be allocated to specific days and hours of the day. Special adjustments to spill allocations in years of low and high water are not implemented at this time. CRiSP.1 considers three types of spill:

Planned Fish Spill is requested by the fisheries agencies. The schedule for this can be obtained from the Flow Archive Files or can be set in the Spill Schedule Window.

Overgeneration Spill occurs when electrical generation demand is less than that available in flow. This is obtained from the Flow Archive File only.

Forced Spill occurs when river flow exceeds powerhouse capacity. This is calculated by CRiSP.1.

CRiSP.1 allocates spill flows in the following order.

➔First, **Planned Fish Spill** is allocated. For each period, planned spill is distributed over scheduled spill days and fish spill hours (within those days) using the following steps.

1. Total modulated flow in the period that occurs in fish spill hours on planned spill days is calculated and designated

   flow_available (in kcfs units).

2. The requested spill in a period is designated

   spill_request (in kcfs units).

3. Percent spill during Fish Hours is calculated as

   spill_daily_percent = spill_request/flow_available.

4. If **spill_daily_percent** > 100%

   then **spill_daily_percent** = 100%

   of the flow available in the request periods and the rest is discarded and a warning message is generated.

➔ Second, **Overgeneration Spill** identified in the flow models for 2 or 4 week periods is evenly distributed over all days in the periods. The following calculations are made on a daily basis.

1. Overgeneration Spill is added to Planned Fish Spill in Fish Hours every day in a period to yield total spill.
2. If Total Spill in Fish Hours is now greater than the total flow over the hours then the excess is distributed over the rest of the day.
3. If Total Spill for the entire day is greater than the total daily modulated flow then the spill is set to the total daily modulated flow.

➔ Third, **Forced Spill** occurs when river flow exceeds powerhouse capacity. Forced Spill is calculated on the dam time slice periods. This is typically a 2 hour interval. CRiSP.1 uses the following logic:

1. Calculate the quantity

   flow - powerhouse capacity/flow = possible forced spill

2. Then, if

   possible forced spill > total fish & overgeneration spill

   assign

   total spill = possible forced spill.

   Otherwise the forced spill is assimilated into fish and overgeneration spills.

Spill from Spill Schedule Tool

Planned Spill can be set by specifying spill information with the Spill Schedule Tool. The following information is entered:

- fraction of flow spilled
- days over which the spill fraction applies
- days in which actual spill occurs, i.e. the planned spill
- hours of planned spill for the indicated days.

Overgeneration Spill is only applied if a Monte Carlo Mode is used. Forced Spill is calculated as described above and is applied in both Scenario and Monte Carlo Modes.

Spill Caps

The maximum allowable planned spill is set by spill caps at each dam. If planned spill exceeds the cap then spill is limited to spill cap. Forced spill can exceed the spill cap. Spill cap is under the **DAM** menu.

Spill Efficiency

The fraction of fish passed with spilled water is defined by one of seven possible empirical equations that can be selected by the user.

Table 40 Equations used in spill efficiency

Equation number	index	Equation form
eq(146)	a	$Y = a + b \cdot X + e$
	b	$Y = a + b \cdot X + X \cdot e$
	c	$Y = b \cdot exp(a \cdot X + e)$
	d	$Y = b \cdot exp(a \cdot X) + X \cdot e$
	e	$Y = b \cdot X^{a+e}$
	f	$Y = b \cdot X^{a} + X \cdot e$
	g	$Y = a + b \cdot lnX + e$

where

- Y = fraction of total fish passed in spill
- X = fraction of water spilled
- a and b = regression coefficients
- e = error term (var) selected from random distribution.

The equations and parameters defining spill efficiency (often called “effectiveness” in the literature) are indicated in Table 41. These values were used

beginning with the SOR screening runs of CRiSP.1.

Table 41 Spill efficiency (% fish passed in spillway / % flow passed in spillway).

Dam	Spill equation	Reference
Wells	zero[a]	Erho et al. 1988, Kudera et al. 1991
Rocky Reach	% pass = 0.65 * (% spill)	Raemhild et al. 1984
Rock Island	% pass = 0.94 * (% spill) + 11.3	Ransom et al. 1988
Wanapum	% pass = 15.42 * ln (% spill)	Dawson et al. 1983
Priest Rapids	% pass = (% spill) ^ 0.82	
L. Monumental	% pass = 1.2 * (% spill)	Johnson et al. 1985. Ransom / Sullivan 1989
The Dalles	% pass = 2 * (% spill)	
all other dams	% pass = (% spill)	-

a. Wells Dam is designed to pass smolts preferentially through the spillway system: about 96% of all smolts pass via the spillway. This is modeled by assigning an FGE value of 96% (range 95-97%) at Wells with a zero spill efficiency for years 1991 on.

II.9 - Fish Guidance Efficiency:

II.9.1 -FGE Theory

Guidance of fish into the bypass systems of dams is achieved by diverting fish into a bypass slot. Individual fge are specified for day and night at each dam and for each species. In addition, CRiSP.1 can treat fge as constant over time or vary fge with the age of the fish relative to the onset of smoltification.

Constant FGE

Fish guidance efficiency is fixed in time and set for day and night from the **fge** window selected from the **DAM** menu. This is activated by switching “off” the **age dependent fge** toggle in **Runtime Settings** from the **RUN** menu (this is the default setting). Note that only the mean remains constant; FGE can still vary in a stochastic fashion if variance suppression is disabled.

Age Dependent FGE

Studies on fish guidance at several dams in the Columbia system indicate that fge varies with seasons from a number of factors including the water quality and the degree of smolt development in the fish, which changes with age. If the age dependent option is selected, fish depth in the forebay varies with age, which in turn alters the fge. The algorithm assumes that fish above some critical depth *z* enter the bypass system and fish below *z* enter the turbine (Fig. 57). Thus, to define age dependent fge, fish depth in the forebay is defined as a function of age. If the surface drops below the level of the bypass orifice fish bypass goes to zero.

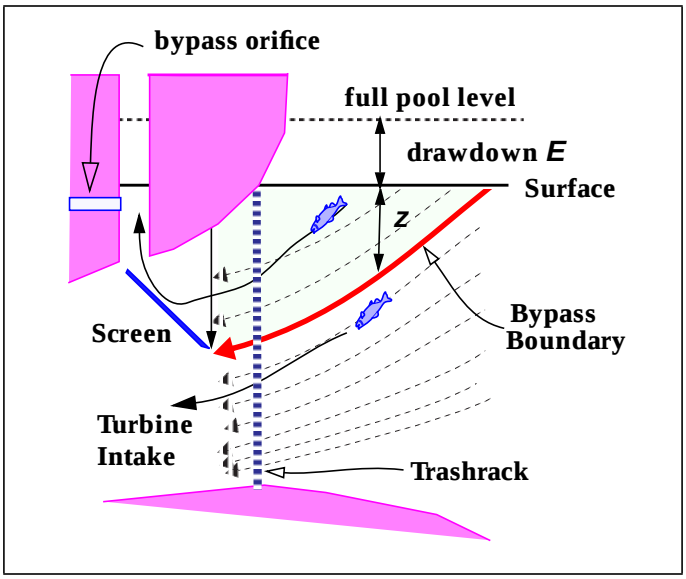

Fig. 57 Critical parameters in fish guidance are fish forebay depth *z*, screen depth *D* and elevation drop *E*. Only fish above *z* are bypassed. Bypass stops when the surface is below the bypass orifice depth.

The fge is based on the fge model of Anderson (1992). Behavioral and hydraulic factors affecting fge are combined into a calibration factor D_c. In addition, the affect of drawdown on fge can be expressed in terms of screen depth relative to the surface. The modified equation is

$$fge = 1 - exp\left(\frac{-0.693}{z}(D - D_c - E)\right) \quad (147)$$

where

- *fge* = fish guidance efficiency
- *z* = median depth of fish in the forebay at a distance from the dam where fish are susceptible to being drawn into the intake.
- *D* = screen depth relative to full pool forebay elevation
- D_c = fge calibration parameter
- *E* = amount the pool is lowered below full pool elevation

Thus, changes in fge result from changes in fish depth and changes in reservoir elevation. The parameter D_c depends on physical and hydraulic properties of a dam, and behavioral properties of fish. As such, the term is specific to both a given species and a given dam. In addition, separate coefficients are defined for day and night dam passage.

Changes in fge with fish age are represented by changes in fish forebay depth which is described by a linear equation

$$\begin{aligned} t < t_0 \qquad & z(t) = z_0 \\ t_0 < t < t_0 + \Delta t \qquad & z(t) = z_0 + (z_1 - z_0)\left(\frac{t - t_0}{\Delta t}\right) \\ t > t_0 + \Delta t \qquad & z(t) = z_1 \end{aligned} \tag{148}$$

To implement the fge equation define the calibration coefficient

$$K = \frac{\log(1 - fge_0)}{-0.693} = \frac{D - D_c}{z_0} \tag{149}$$

Combining eq (147), eq (148) and eq (149) the final fge equation is

$$fge(t) = 1 - exp\left(-\frac{0.693}{z(t)}(z_0 K - E(t))\right) \tag{150}$$

where

- t = fish age since the onset of smoltification, see eq (55) on page 57
- t_0 = onset of change in fge relative to the onset of smoltification set in the release window
- Δt = increment of time over which fge changes
- z_0 = initial mean fish depth (at age t equals 0) in the forebay
- z_1= final mean fish depth (at age t equals $t_0 + \Delta t$) in the forebay
- fge_0 = fge at onset of smoltification
- $E(t)$ = elevation drop.

The resulting fge and depth are illustrated in (Fig. 58).

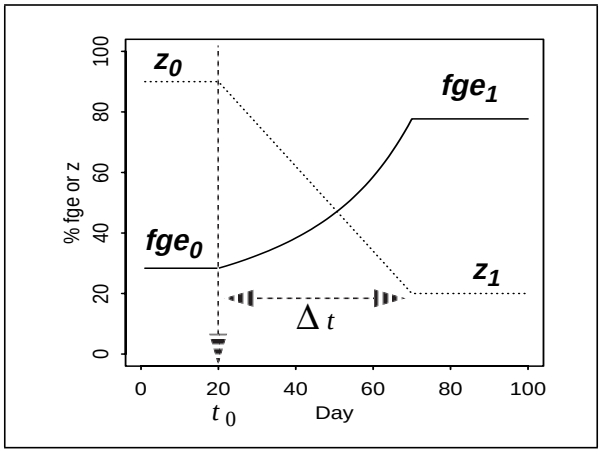

Fig. 58 Fge and fish depth over fish age

II.9.2 -FGE Calibration

Spring and fall chinook fish guidance efficiencies (*FGE*) at Snake River Dams and McNary dam were estimated using CRiSP1.5 and Snake River PIT tags data. For fall chinook the results were calibrated with data from 1993 through 1995. For spring chinook the data extended from 1989 through 1995.

The fit involved a stepwise process in which *FGE* was adjusted sequentially from Lower Granite dam down to McNary dam. In this approach the *FGE* at a specific dam was dependent on the *FGE*'s of the dams upstream. To test the validity of the *FGE* estimation the results were compared to *FGE* measured independently at Lower Granite (LGR), Little Goose (LGO) and McNary (MCN) dams. In this way *FGE* the was only parameter that was adjusted to fit the observed PIT tag recoveries at the dams. All other parameters were fixed.

Spring Chinook

The *FGE*'s were calibrated with data from fish collected and PIT tagged in the Snake River trap and recovered at LGR, LGS, LMO (1993-1995 only), and MCN dams. Data was used from the years 1990 through 1995. The numbers marked and recaptured are given in Table 42. The data was extracted from the PTAGIS data base. All recoveries were used, which means that in 1993-1995 significant numbers of fish were detected more than once due to slide-gate operations for NMFS survival studies.

The *FGE*'s estimated from the fitting process are given in Table 43 and comparisons to *FGE*'s determined by fyke net and PIT tag studies are given in Table 44. The CRiSP-based estimates are within a standard deviation for the PIT tag derived values for Lower Granite an Little Goose dams and for the fyke net derived value for McNary dam. The fyke net derived value for Lower Granite and Little Goose dams are higher than the CRiSP based estimates. This difference suggests that point-estimated fyke net-based FGE values may not be representative of seasonal passage conditions at upriver dams, due to changing fish condition, smoltification, and other factors.

Results for 1993-1995 are complicated by slide-gate operation at some of the projects; while this was included in modeling FGE, it adds a degree of uncertainty to our estimates. Clearly, FGE at McNary Dam was not 100% in 1994 - although a remarkably large fraction of the release was detected there as compared to other years (27% in 1994; average of other years with slide gates = 16.5%). Similarly, detections at Lower Monumental in 1995 were surprisingly high. Moreover, system operations in 1989 allowed many tagged fish to escape collection at Lower Granite Dam, despite entering the bypass system; this would lead us to underestimate FGE at Lower Granite and to overestimate at downstream projects, since more fish were in the system than should have been (G. Matthews, NMFS Seattle, pers. comm.). We consider these numbers anomalous and recommend using mean values that exclude the outliers (see Table 46).

Note that our estimates are consistent with estimates of FGE and collection efficiencies determined during the NMFS survival studies of 1993-1995 (Table 45)(Iwamoto et al. 1994, Muir et al. 1995, 1996). While collection efficiencies represent minimum estimates of FGE due to loss of smolts via spillway passage, they provide another check on CRiSP calibration.

The fyke net estimates may be high because the experiments were only conducted

in early evening and characterize the passage of fish milling in front of the dam prior to sunset. *FGE* is in part determined from the vertical position of the fish when they enter the dam. Fish near the surface yield high *FGE*. The fyke net experiments, being conducted in early evening, measured the *FGE* of the surface oriented fish. Consequently, the estimate of *FGE* was biased high. By comparison, fish passing dams at other times of the day are postulated to be distributed throughout the water column and so the *FGE* would be lower. The PIT tag-based *FGE* represents guidance conditions over a number of days and so they are expected to be a better representation of the average *FGE* (J. Williams NMFS Seattle personal communication).

The *FGE*'s developed using CRiSP are consistent with the observed passage numbers and the more robust estimates based on PIT tag studies. The suggested *FGE* means and ranges for uses in modeling passage conditions for the period 1996-1998 are given in Table 46. The range was derived from the range observed in MCN fyke net studies in 1992 which was from 37 to 91 with a mean of 61.

Note in Table 44 that the fyke net *FGE* estimates are generally greater than the CRiSP-derived estimates. Since this may be from bias in the *FGE* studies we suggest lowering all fyke net *FGE*'s by some amount. The average CRiSP derived *FGE* is about 80% of the fyke net-derived estimates from three dams. We therefore suggest lowering the *FGE* to 80% of the fyke estimates.

Table 42 Snake River Trap PIT tag release and recapture data at dams, extracted from the PIT tag data base.

	1989	1990	1991	1992	1993	1994	1995
Release Start Julian Day	83	99	96	98	99	103	90
Release Numbers	6163	2254	3768	1218	4302	3778	5994
Lower Granite Count	2387	960	1607	435	1898	1241	2676
Little Goose Count	1443	345	689	195	1069	623	1819
Lower Monumental Count	--	--	--	--	831	645	1895
McNary Count	724	201	227	126	535	1003	1259

Table 43 FGE required to fit the Snake Trap PIT tag data for 1989 -1995. Asterisks indicate questionable data, not used in calculating mean FGE.

Dam	1989	1990	1991	1992	1993	1994	1995	mean	S.D.
Lower Granite	45.1	48.4	50.0	42.3	53.9	42.3	56.0	48.8	5.2
Little Goose	59.5	39.6	49.8	38.4	49.3	36.2	59.9	47.0	8.4
Lower Monumental	2	2	2	52.0	54.1	56.5	89.0*	66.5	19.5
Ice Harbor	34.4	34.4	34.4	34.4	54.0	54.0	54.0	--	--
McNary	85.8*	61.3	59.7	57.7	51.8	100.0*	71.6	57.8	9.0

Table 44 Comparisons of observed and calculated spring chinook FGE. Observed FGE provided by J. Williams NMFS Seattle.

Dam	Year	Observed			Calculated FGE
		Method	dates	FGE	
Lower Granite	1993	PIT tag	4/15 - 5/15	49.5	53.9
	1989	Fyke nets	4/11 - 4/30	57	48.7
Little Goose	1993	PIT tag	4/15 - 5/15	56	49.3
	1993	Fyke nets	5/22 - 5/24	74	49.3
McNary	1992	Fyke nets	4/28 - 5/28	61	57.7
	1982+92	Fyke nets	4/28 - 5/28	66	57.7
	1989	PIT tag		63[a]	85.8
	1995	PIT tag		60[b]	71.6

a. Stuehrenberg and Johnson (1990)
b. Cramer, Willis and Witty (1995)

Table 45 Comparison of modeled FGE at Snake River projects versus FGE (1993) and collection efficiency (1994-95) estimates from NMFS survival studies.

			NMFS FGE/collection efficiency	
Year	Project	CRiSP	Mean	Maximum
1993	LGR	53.9	44.2	n/a
	LGS	49.3	50.5	n/a
1994	LGR	42.3	39.7	49.0
	LGS	36.2	23.8	40.6
	LMN	56.5	35.4	54.8
1995	LGR	56.0	43.3	52.4
	LGS	59.9	35.4	40.6
	LMN	89.0	44.8	65.3

Table 46 Suggested FGE for spring chinook modeling over the period 1996-1998.

Dam	Mean (%)	Range (± %)
Lower Granite	45	20
Little Goose	45	20
Lower Monumental	55.3	20
Ice Harbor	57[a]	20
McNary	52.5	20
John Day	58	10
The Dalles	34	11
Bonneville I	30	7
Bonneville II	54	13

a. Based on estimate from coordination process and adjusted downward to account for bias in fyke net studies (provided by D. Askren of BPA)

Fall Chinook FGE

PIT tag data from wild-caught Snake River subyearling chinook were used to estimate actual *FGE* during 1993 through 1995. Previous years' data suffered from small sample sizes and poor collection rates. The approach is to create a release of fish in CRiSP that has the same properties as the actual tagging groups and then to adjust *FGE* at Lower Granite, Little Goose, and McNary dams to obtain good agreement in number of fish collected. The data are given in Table 47 and the resulting *FGE* calibration is given in Table 48 below, along with the NMFS Coordination estimates for mean, low, and high *FGE*'s at the relevant projects. For 1994 a considerable mortality rate must be assumed following tagging given the extremely low rate of recapture; also note that in 1995 slide gate operations resulted in considerable rates of return to the river for PIT-tagged fish during the fall chinook outmigration season. Note that estimates of *FGE* are close to the specified range of coordination FGE values.

Table 47 Fall chinook PIT tag release and recapture information for 1993-1995

Year	Release	LGR	LGO	LMO	MCN
1993	1509	251	52	10	5
1994	2776	201	50	50	33
1995	1652	440	238	198	147

Table 48 NMFS and CRiSP estimates of FGE for subyearling chinook at collection facilities.

Dam	NMFS coordinated FGE	1993	1994	1995
LGR	35% (20-40%)	35%	35%	32%
LGS	35% (20-40%)	30%	18%	24%
LMN	31% (29-35%)	n/a	35%	29%
MCN	47% (10-81%)	40%	65%	42%

Steelhead FGE

A similar approach was taken for juvenile steelhead PIT tagged from the Dworshak hatchery. These fish were detected at Lower Granite, Little Goose, and McNary Dams, and assuming travel time and mortality algorithms were calibrated, estimates of *FGE* could obtained for these projects. *FGE* was estimated using data from 1989-1995 inclusive (Table 49). Because of the variation in year-to-year fits, the average of these years' *FGE* values was used. Note that the PIT tag-calibrated *FGE* value is close to that estimated by NMFS for coordination purposes, but at McNary, for spring chinook, the calibrated value is about 5/6 that of the coordination value in the System Operation Review. This makes sense in the context of the fyke net argument made above. Also note that 1994 and 1995 observations are complicated by the fact that slide gates were in operation at all three upper projects; this led, for example, to an astonishingly high collection rate at Lower Monumental Dam in 1995.

Table 49 CRiSP estimated FGE for steelhead.

Year	LGR	LGO	LMN	MCN
1989	82%	89%	n/a	90%
1990	77%	66%	n/a	27%
1991	89%	99%	n/a	100%
1992	77%	63%	n/a	41%
1993	56%	88%	n/a	54%
1994	72%	58%	73%	50%
1995	81%	67%	100%	54%
average	76.3%	75.7%	86.5%	59.4%
SOR value	79.0%	79.0%	76.0%	75.0%

Historical FGE Values

Nearly all Federal projects on the Columbia and Snake Rivers have undergone considerable change since their initial construction. Most have added bypass systems or other mechanisms to provide improved juvenile passage; consequently, *FGE* has improved over time. We have used current estimates of *FGE* and scaled them for historical patterns of screen addition, gate raises, and other operational changes that alter *FGE*. Estimated historical *FGE* values for CRiSP 1.5 for all species are given in Table 50. A comparison of the CRiSP1.5 FGE values to values used in CRiSP1.4 and in the Previous Coordinations are given in Table 51.

Table 50 Historical FGE values for each dam, by stock used for CRiSP1.5. Note FGE in the early years of transportation are adjusted to generate estimated transport numbers for Snake River dams. See Table 72 on page 170 for relationship of FGE and transport numbers.

Dam	Year	spring chinook	fall chinook	steelhead
Bonneville I	1975-1983	16%	15%	17%
	1984-1992	30%	10%	65%
	1993-1994	30%	15%	65%
Bonneville II	1983-1992	15%	24%	52%
	1993-1994	54%	24%	52%
The Dalles	1975-	34%	43%	36%
John Day	1975-1984	2%	2%	2%
	1985	33%	16%	41%
	1986	44%	20%	55%
	1987-1994	58%	26%	72%
McNary	1975-1977	2%	2%	2%
	1978	4%	5%	4%
	1979	8%	8%	9%
	1980	25%	21%	27%
	1981	52%	40%	62%
	1982-1988	57%	40%	62%
	1989	58%	40%	62%
	1990	61%	40%	62%
	1991	60%	40%	62%
	1992	58%	40%	62%
	1993	52%	40%	62%
	1994	58%	40%	62%
Wells	1991-1994	96%	96%	96%
Ice Harbor	1975-1983	2%	2%	2%
	1984-1992	43%	43%	47%
	1993	57%	31%	77%
	1994	68%	31%	77%
L. Monumental	1975-1991	2%	2%	2%
	1992	52%	31%	63%
	1993	54%	31%	63%
	1994	56%	31%	63%

Table 50 Historical FGE values for each dam, by stock used for CRiSP1.5. Note FGE in the early years of transportation are adjusted to generate estimated transport numbers for Snake River dams. See Table 72 on page 170 for relationship of FGE and transport numbers.

Dam	Year	spring chinook	fall chinook	steelhead
Little Goose	1971	9%		
	1972	18%		
	1973	7%		
	1974	7%		
	1975	12%	24%	38%
	1976	21%	24%	38%
	1977	47%	30%	56%
	1978	37%	30%	56%
	1979	33%	30%	56%
	1980	44%	30%	56%
	1981	29%	30%	56%
	1982	44%	30%	56%
	1983	44%	30%	56%
	1984-1988	44%	30%	56%
	1989	59%	30%	81%
	1990	40%	30%	81%
	1991	50%	30%	81%
	1992	38%	30%	81%
	1993	50%	30%	81%
	1994	36%	30%	81%
Lower Granite	1975	7%	13%	22%
	1976	7%	35%	62%
	1977	47%	35%	62%
	1978	37%	35%	62%
	1979	33%	35%	62%
	1980	34%	35%	62%
	1981	29%	35%	62%
	1982	52%	35%	62%
	1983-1988	46%	35%	62%
	1989	45%	35%	76%
	1990	48%	35%	76%
	1991	50%	35%	76%
	1992	42%	35%	76%
	1993	54%	35%	76%
	1994	42%	35%	76%

Table 51 Spring chinook historical FGE values for CRiSP1.4, CRiSP.1.5, Previous Coordination for the System Operation Review and Field Observations of FGE.

Year	Previous Coordination Max/Avg/Min	Field Observ Max/Avg/Min	Model values Max/Avg/Min		Condition
			CRiSP1.4	CRiSP1.5	
Lower Granite					
2003	90%		86$	86$	Surface Collector as FGE enhancer
1998	83/67/59		53$	53$	Extended STS
1991-97	74/56/36		66/46/26	66/46/26	Raised gate
1995	56		50	56	
1994	56		50	42	
1993	56	49.5	50	54	Survival study 4/15-5/15
1992	56		40	42	
1991	56		46	50	Raised gate

Table 51 Spring chinook historical FGE values for CRiSP1.4, CRiSP.1.5, Previous Coordination for the System Operation Review and Field Observations of FGE.

Year	Previous Coordination Max/Avg/Min	Field Observ Max/Avg/Min	Model values Max/Avg/Min		Condition
			CRiSP1.4	CRiSP1.5	
1990	53		44	48	
1989	53	66/57/43	47	45	Fyke Nets 4/11-4/30
1983-1988	71/53/35		66/46/26*	46	Fully screened
1982				52	
1981				29	
1980				34	
1979				33	
1978				37	
1977				47	
1976	26/19/12		21/15/10*	7	
1975	26/19/12		21/15/10*	7	1 of 3 turbines screened
Little Goose					
2003	93%		86$	86$	Surface Collector as FGE enhancer
1998	80/77/75		53$	53$	Extended SBS
1991-97	74/70/65		67/45/40	67/45/40	Raised gate
1995	70		45	60	
1994	70		45	36	
1993	70	56	49	49	Survival study 4/15-5/15
1993	70	80/74/67			Fyke net 5/22-5/24
1992	70		39	38	
1991	70		47	50	Raised gate
1990	59		38	40	
1989	59		49	59	
1982-1988	74/**59/43**		64/44/24*	44	Fully screened
1981				29	
1980				44	
1979				33	
1978				37	
1977				47	
1976	**51/40/29**		11	21	
1975	**51/40/29**		**41/32/23***	12	2/3 screened
1974				7	2/3 screened
1973				7	
1972				18	2/3 screened
1971				9	2/3 screened
Lower Monumental					
2003	90%		86	86	Surface Collector as FGE enhancer
1998	**80/67/52**		**64/54/42**	**64/54/42**	Gate raise
1995-1997	71/65/57		57/52/46	75/55/35	
1994				76/56/36	
1993				74/54/34	
1992				57/52/46	Bypass, STS, flush gate
1989-91	4/2/0		4/2/0	4/2/0	
1970-91	4/2/0		4/2/0	4/2/0	Sluiceway
Ice Harbor					
2003	93%		89	89	Surface Collector as FGE enhancer
1996-98	85/77/73		68/62/58	68/62/58	Bypass, STS, raised gate
1993-95	**76/68/64**		61/54/51	61/54/51	STS with sluiceway
1989-92	43		34	34	
1984-92	51/43/40		34	34	Sluiceway for fish diversion
1962-83	4/2/0		2	2	Sluiceway
McNary					

Table 51 Spring chinook historical FGE values for CRiSP1.4, CRiSP.1.5, Previous Coordination for the System Operation Review and Field Observations of FGE.

Year	Previous Coordination Max/Avg/Min	Field Observ Max/Avg/Min	Model values Max/Avg/Min		Condition
			CRiSP1.4	CRiSP1.5	
2003	87%		91%	91%	Surface Collector as FGE enhancer
2003	87%		70$	70$	No Surface Collector
1998	90/87/78		**70**	**70**	Gate raise, extended SBS
1981-97	91/70/36		**73/56/29**	**73/56/29**	
1995	70		52	72	
1994	70		52	58	
1993	70		52	52	
1992	70	91/61/37	61	58	Fyke nets 4/28-5/28
1991	70		57	60	
1990	70		58	61	
1989	70		53	58	
1982-88	70		57	57	
1981	70		**73/56/29**	**73/52/29**	Fully screened, flush gate
1980	41/31/15		33/25/12*	33/25/12*	6 screens
1979	16/12/5		13/8/4*	13/8/4*	2 screens
1978	10/7/3		8/4/2*	8/4/2*	1 screen of 14
1957-77	4/2/0		4/2/0*	4/2/0*	Sluiceway
John Day					
2003	72%		87$	87$	Surface Collector as FGE enhancer
2003	72%		58$	58$	No Surface Collector
1987-98	78/72/55		62/58/44	62/58/44	Standard STS, gate removed, bypass
1986	60/55/41		48/44/33	48/44/33	12/16 screens installed
1985	46/41/31		37/33/25	37/33/25	9/16 screens installed
1971-84	4/2/0		4/2/0	4/2/0	Sluiceway
The Dales					
2003	74%		88$	88$	Surface Collector as FGE enhancer
2003	74%		59$	59$	No Surface Collector
1998	87/74/56		70/59/45	70/59/45	Bypass, gate raise, extended SBS
1960-97	51/43/23		41/34/18	41/34/18	Sluiceway as fish passage
Bonneville					
2003	37%		79$	79$	Surface Collector as FGE enhancer
2003	37%		30$	30$	No Surface Collector
1984-98	46/37/29		37/30/23	37/30/23	Flush-stored gates, bypass, STS
1933-83	20/20/20		16/16/16	16/16/16	Sluiceway
Bonneville Second					
2003	44%		81$	81$	Surface Collector as FGE enhancer
2003	44%		35$	35$	No Surface Collector
1993-98	**54/44/34**		**43/35/27**	**43/35/27**	Streamlined trashracks, turbine intake extensions, lowered SBS
1983-92	51/19/6		40/15/4	40/15/4	Flush-stored gates, bypass, STS

* Interpolated FGEs assume a minimum 2% volitional entry

CRiSP FGEs are reduced by factors of 70% at Little Goose and 80% for all other projects to reflect CRiSP calibration to 1989-93 PIT tag observations and available fyke net FGE estimates. Historical FGEs are interpolated from the calibration or reduced FGE, assuming a minimum FGE of 2% for volitional entry into bypass systems.

$ 2003 FGEs for projects having surface collectors compute FGE = (Surface Collector FGE) + (1 - Surface Collector FGE) * (Bypass Screen FGE) assuming Surface Collector FGE=70%

Time Variable *FGE*

The calibration of time varying FGE is not available for CRiSP1.5.

Bypass orifice and FGE

Fish guidance goes to zero when the surface elevation drops below the bypass orifice elevation (Fig. 57). This parameter, designated **bypass_elevation**, is set in the **columbia.desc** file. If **bypass_elevation** is missing or commented out (with #) the bypass elevation is set to the pool **floor_elevation** and bypass will occur for all reservoir elevations. This function applies with or without selection of age dependent fge.

Bypass Elevations

The bypass elevations and forebay elevations in feet above sea level (obtained from the Army Corps of Engineers) are set in the **columbia.desc** file for each dam where a bypass system exists.

Table 52 Bypass and forebay elevations of dams with bypass systems

Dam	Bypass elevation (ft)	forebay elevation (ft)
Bon # 1 and 2	65.5	77
The Dalles	149	160
John Day	250.5	269
McNary	330	340
Wells	716	781
Ice Harbor	431.5	440
L. Monumental	531.5	540
Little Goose	628.9	638
Lower Granite	729	738

II.9.3 -Multiple Powerhouses

Bonneville Dam and Rock Island Dam each have two powerhouses that can be operated independently to optimize survival during the fish passage season since each project has a single spillway. Multiple-powerhouse dams can be represented schematically as shown in Fig. 59.

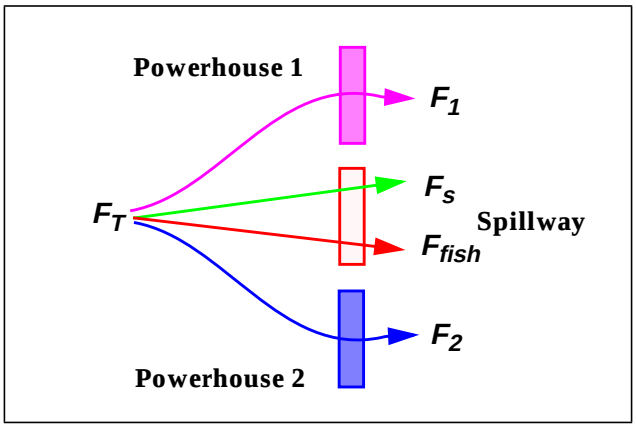

Fig. 59 Multiple powerhouse configuration showing allocation of spill and powerhouse flows.

In these cases, flow is allocated fractionally as follows:

- Flows are first allocated to planned spill in fish passage hours.
- Remaining flow is partitioned between the primary and secondary powerhouses and additional spill as follows:

The strategy is to:

- Operate highest priority powerhouse up to its hydraulic capacity.
- Spill water up to another level called the spill threshold.
- Above the threshold, use the second powerhouse.
- Over the second powerhouse hydraulic capacity, spill extra flow.

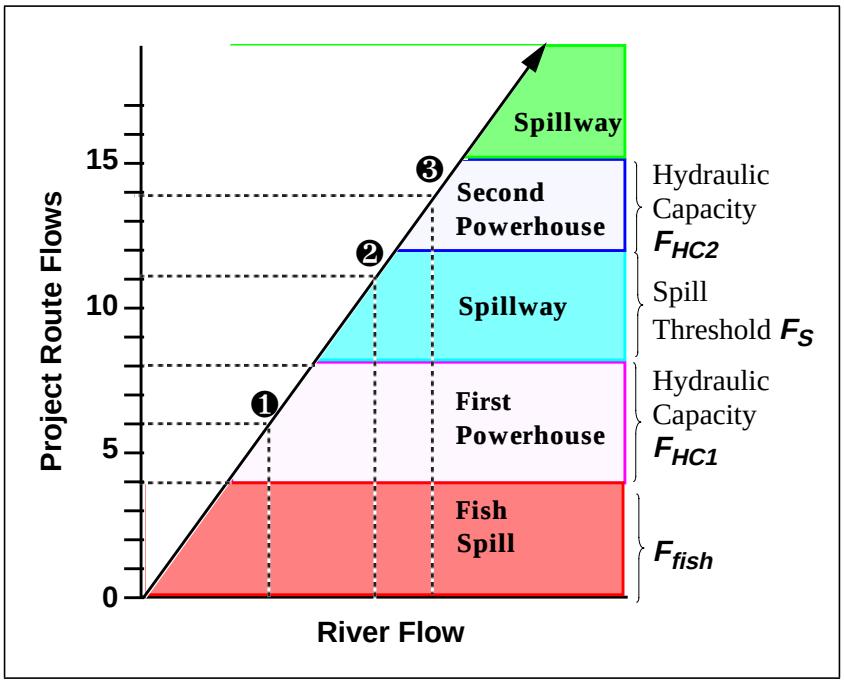

Fig. 60 Flow allocation through two powerhouse projects.

An example of flow allocations is described as follows (Fig. 60):

- At level ❶ 4 units of flow are put to Fish Spill and 2 units are put through the First Powerhouse.
- At level ❷ Fish Spill has four units of flow, the First Powerhouse is run at its hydraulic capacity, which is 4 flow units, and the spillway has 3 units of additional spill.
- At level ❸ the First Powerhouse is at hydraulic capacity, spill flow includes Fish Spill and additional spill up to the Spill Threshold and 2 units of flow pass the Second Powerhouse.

II.9.4 -Fish Passage Efficiency (FPE)

Fish passage efficiency is the percent of fish that pass a project by non-turbine routes (spill, bypass, and sluiceway passage). FPE considers that fish pass mostly during the night and spill generally occurs at night. The simple fish routing is illustrated below in Fig. 61. A fraction of the fish are first diverted in to spill water. What remains is diverted into the turbine intake and a fraction of this flux is diverted into the fish bypass system.

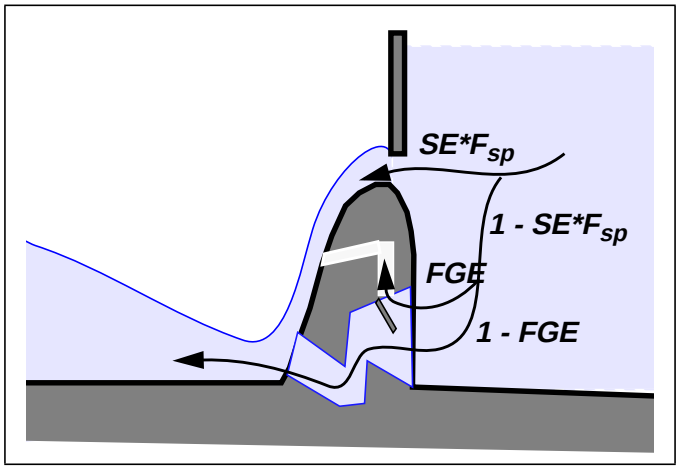

Fig. 61 Routing of fish for calculation of FPE

The formula expressing FPE considers these independent diversions and accounts for the fact that fish may be attracted to spill flow over flows into the turbine. The simplified formula for FPE which considers spill occurs at night and most of the fish pass at night can be expressed

$$\text{FPE} = \{D \cdot F_{sp} \cdot SE + D \cdot \text{FGE} \cdot (1 - F_{sp}SE) + (1 - D) \cdot \text{FGE}\} \cdot 100 \qquad (151)$$

where

- D = fraction of fish that pass dam during spill hours
- F_{sp} = fraction of daily flow that passes in spill
- SE = fraction of fish that pass in spill relative to the fraction of flow passing in spill
- FGE = fraction of fish passing into turbine intake that are bypassed

The spill flow, in percent of the total flow, required to generate a given FPE can be

expressed by arranging eq(151) to give

$$F_{sp} = \frac{\text{FPE} - \text{FGE}}{D \cdot SE \cdot (1 - \text{FGE})} \tag{152}$$

II.9.5 -Dam Passage Survival

Fish passing through the dams can take several routes (depicted in Fig. 47). Equations describing the number of fish that pass through each route in terms of the number that enter the dam from the forebay on a particular dam time slice are given below. In each case the mortality and passage efficiencies have deterministic and stochastic parts.

For mortalities and fge, the random elements are represented by additive deterministic and stochastic parts in

$$x = \bar{x} + x' \tag{153}$$

where

- $\bar{x}$ = deterministic part of the random parameter fixed for each species and dam
- x' = stochastic part of the parameter taken from a broken-stick distribution (see Stochastic Parameter Probability Density section on page II.146) over each dam time slice.

For spill efficiency, each equation contains a random term. A typical equation is

$$y = a + bx + e \tag{154}$$

where

- y = spill efficiency
- x = percent flow
- a and b = deterministic parameters
- e = stochastic parameter selected from a normal distribution.

Turbine Survival

The equation for turbine survival can be expressed

$$N_{tu} = N_{fo} \cdot p \cdot (1 - ySF) \cdot (1 - m_{fo}) \cdot (1 - m_{tu}) \cdot (1 - fge) \tag{155}$$

where

- N_{tu} = number of fish passing in a time increment (2 hrs)
- N_{fo} = number of fish in forebay ready to pass in the increment
- p = probability of passing during the increment from eq (136)
- m_{fo} = mortality in forebay (see eq (143))
- m_{tu} = mortality in turbine passage
- fge = fish guidance efficiency for a day or night period
- y = spill efficiency coefficient (see eq (146))

- S = fraction of total flow diverted to spill in the increment
- F = flow in increment.

Bypass Survival

The equation for bypass survival without spill is

$$N_{by} = N_{fo} \cdot p \cdot (1 - ySF) \cdot (1 - m_{fo}) \cdot (1 - m_{by}) \cdot fge \quad (156)$$

where

- m_{by} = mortality in the bypass.

Transport Survival

The equation for transport survival with fixed transport mortality is

$$N_{tr} = N_{fo} \cdot p \cdot (1 - ySF) \cdot (1 - m_{fo}) \cdot (1 - m_{by}) \cdot fge \cdot m_{tr} \quad (157)$$

where

- m_{tr} = mortality in the transport.

Users may also choose to relate transport mortality to river flow, via the surrogate of water particle travel time (WPTT). This model, proposed by modelers for the States and Tribes (ANCOOR 1994), relates transport survival to flow / travel time as follows:

- For flows equal to or greater than those in 1986, transport mortality is determined assuming a transport-benefit ratio (TBR) of 1.01 to 1 for fish released at Little Goose tailrace. This means that the ratio of returning adults from transported groups to non-transported groups will be 1.01 to 1.
- For flows equal to or lesser than those in 1977 (a very low-flow year), the TBR for Little Goose is assumed to be 3 to 1.
- For flows intermediate between 1977 and 1986 conditions, transport mortality is obtained by linear interpolation between those two end points.

The motivation for this model is that fish condition deteriorates with increasing residence time in the system, which could have a negative impact on survival through the presumably stressful process of being collected for transport. The results are illustrated as transport mortality as a function of system WPTT, remembering that as flows decrease, travel times increase. This is shown in Fig. 62 below.

The transport mortalities derived will depend on how the model in question calculates WPTT and also how it calculates the in-river survivals used to back-calculate

transport survivals from TBR data; the figure below uses CRiSP calibrated values.

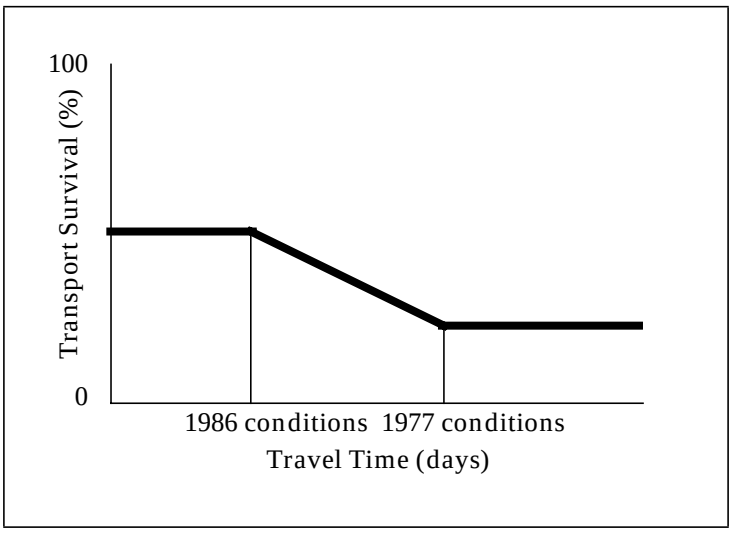

Fig. 62 Transport survival as a function of flow.

Spill Survival

The equation for spill survival is

$$N_{sp} = N_{fo} \cdot p \cdot (1 - m_{sp}) \cdot ySF \tag{158}$$

where m_{sp} = mortality in the spill passage.

Calibrating Passage Mortality

Turbine mortalities used in CRiSP.1.5 are generally 30% lower than values used in other salmon passage models including CRiSP.1 version 3. The lower values reflect the fact that CRiSP.1 accounts for additional delayed turbine passage mortality in the tailrace through an increased predation activity coefficient that reflects the vulnerability of fish immediately after dam passage.

Direct measure estimates are from

Oligher, R. C. and I. J. Donaldson. 1966
Weber, K. G. 1954.

Indirect measure estimates are from

Holmes, H. 1952.
Schoeneman, et al. 1961.
Long, C. W. 1968.
Long, C. W., F J. Ossiander, T. E. Ruehle and G. Mathews.
Raymond (1979)
Raymond and Sims (1980)
Ledgerwood, R.D. et al. 1990.

The recent measurements of turbine survival with inflated tags and PIT tags are given in Table 53.

Table 53 Recent turbine mortality estimates

Dam Species	Mortality estimate	Technique	Reference
Rocky Reach yearling fall chinook	5.6%	inflated tags	RMS Environmental Service, Inc. and J.R. Skalski. (1993)
Lower Granite spring yearling chinook	6.6%	inflated tags	RMS Environmental Service, Inc. and J.R. Skalski. (1994)
Lower Granite spring yearling chinook	17.3%	PIT tags	Iwamoto et al (1994)
Little Goose spring yearling chinook	8.0%	PIT tags	Iwamoto et al (1994)
Lower Monumental spring yearling chinook	13.5%	PIT tags	Muir et al (1995)
Lower Granite spring yearling chinook	7.3%	PIT tags	Muir et al (1996)
average	9.7%	-	-

Bypass and spill mortalities are based on the following studies. Full citations are given in the reference chapter.

Ceballos, J., S. Pettit, and J. McKern. 1991.
Ledgerwood, R. et al. 1990.
Ledgerwood, R. et al. 1991.
Muir et al (1996)

Passage mortalities used in calibration, including mean, low and high values, are given in Table 54. The mortalities are used for all species but most of the data was from studies involving spring chinook. The estimates are weighted towards the more recent studies. High estimates of dam passage mortality in 1972-1973 are used to represent documented problems in Snake River dam passage in these years. The high mortalities were assigned to both turbine and bypass routes.

Table 54 Percent mortality at dams: m = mean, l = low, h = high. These mortality estimates are applied to spring chinook in analysis up through 1995.

Dam	Spillway			Bypass			Turbine			Comments
	m	l	h	m	l	h	m	l	h	
All dams except where noted	2	0	7	2	0	8	7	1	10	-
Monumental[a] 1972	2	0	7	2	0	8	7 50	1	10	- slotted bulkheads

Table 54 Percent mortality at dams: m = mean, l = low, h = high. These mortality estimates are applied to spring chinook in analysis up through 1995.

Dam	Spillway			Bypass			Turbine			Comments
	m	l	h	m	l	h	m	l	h	
Little Goose[b] 1972 1973 1974	2	0	7	2 40 50 11	0	8	7 40 50 11	1	10	- slotted bulkheads bad fish condition -
Lower Granite 1979[c]	2	0	7	2 27	0	8	7 27	1	10	- trash problem

a. Raymond 1979
b. Raymond 1979
c. Raymond and Sims 1980

II.10 - Transportation Mortality

II.10.1 -Theory

Transportation survival from factors other than those observed in direct barge survival is estimated using in-river survival and the transport-benefit ratio (TBR) observed from differing stocks. The approach to estimating this transportation survival is through an analysis of data from a number of years and for different transport sites and species. The recent years of transportation studies produced more robust estimates of TBR (larger sample sizes, better controls) and are more representative of the current transportation operations. Transportation experiments from all years are considered elsewhere in this document (see Transportation validation section on page III.182).

The analysis of the transportation survival extends previous work of the Mundy Report (1994). Several deficiencies addressed in the analysis are dealt with in the present calibration, including

- partial transportation of control groups
- different arrival time to estuary of transport and control groups
- effects of spill
- updated estimates of in-river survival

The transportation survival of fall chinook transported from McNary Dam was estimated for the years 1986-1988 using the most current model parameters and data on the transport benefit ratios for those years. A similar analysis was performed for spring chinook in the same years, except that spring chinook tests were performed at McNary Dam during 1986-1988, and also at Little Goose Dam in 1986 and 1989; both sets of studies were included in the analysis. Finally, transportation studies in 1986 and 1989 using steelhead released at Little Goose Dam were also examined.

McNary Transportation

The analysis applies the scheme illustrated in Fig. 63. For Little Goose studies,

transport mortality at McNary was calculated and applied to the upper-river data because some of the "control" fish released into Little Goose tailrace in 1986 and 1989 were recaptured and transported from McNary Dam,

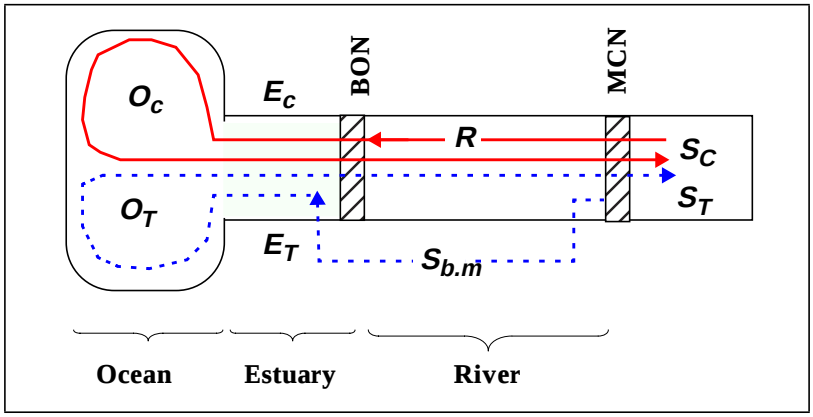

Fig. 63 Configuration for analysis of transport mortality. Paths and parameters for transported (- - - ▸) and in river migrants (⟶) are illustrated. See text for definition of variables.

The equation defining the transport benefit ratio (TBR) is

$$\text{TBR} = \frac{S_T}{S_C} = \frac{S_{b.m}}{R} \cdot \frac{E_T}{E_C} \cdot \frac{O_T}{O_C} \qquad (159)$$

where

- TBR = transport benefit ratio between transported and in river migrating juvenile fish
- S_T = survival of adult test fish with juvenile transport migration
- S_C = survival of adult control fish with juvenile in river migration
- $S_{b.m}$ = transport survival from observed mortalities in transport in barges and trucks from McNary dam
- R = in river juvenile survival past Bonneville Dam
- E_T = survival between Bonneville dam and the estuary for transport fish
- E_C = survival between Bonneville dam and the estuary for control fish
- O_T = survival of transported after ocean entry plus any delayed mortality not included in any upstream process
- O_C =survival of in-river control fish after ocean entry plus any delayed mortality not included in any upstream process

The total survival associated with transportation from McNary dam is

$$T_{\text{MCN}} = S_{b.m}\frac{O_T}{O_C} = \text{TBR} \cdot \frac{R \cdot E_C}{E_T} = \text{TBR} \cdot \frac{S_{\text{MCN}}}{S_{\text{BON}}} \qquad (160)$$

where

- T_{MCN} = total transport survival from McNary dam.
- S_{MCN} = model survival from McNary Dam tailrace to the estuary.
- S_{BON} = model survival from Bonneville Dam tailrace to the estuary.

The model transportation survival T_{MCN} is calculated by modeling S_{MCN} and S_{BON} and multiplying their ratio by the TBR as given in eq(160). For these model runs Bonneville tailrace releases were the same as McNary releases, except that they were delayed 2 days to account for transportation delays and holding of fish prior to transportation. Model runs used the active migration equation, with model parameters as described above (see Fish Migration section on page II.51).

Lower Granite Transportation

To model transportation of spring chinook from Lower Granite dam we account for the transportation of both control and transport fish (Fig. 64).

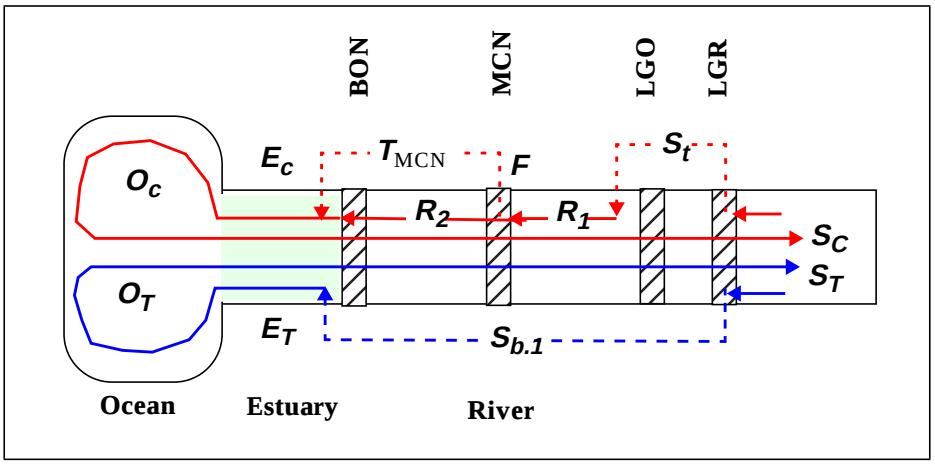

Fig. 64 Configuration of migration routes of fish in transportation experiments of spring chinook. Paths and parameters for transported (- - - ▸) and in river migrants (——▸) are illustrated.

The equation defining a transport benefit ratio from transport from Lower Granite dam (TBR) is

$$\mathrm{TBR} = \frac{S_T}{S_C} = \frac{S_{b.l}}{S_t R_1 (F T_{MCN} + (1-F) R_2)} \cdot \frac{E_T}{E_C} \cdot \frac{O_T}{O_C} \qquad (161)$$

Equation variables include:

- TBR = transport benefit ratio as computed from adult returning to Lower Granite Dam
- S_T = survival of returning adult fish from test group as determined from specified collection methods which may include ocean and in-river fisheries, counts at dams, hatcheries and spawning grounds.
- S_C = survival of returning adult fish from control group as determined from specified collection methods which may include ocean and in-river fisheries, counts at dams, hatcheries and spawning grounds.
- F = fraction of fish passing McNary Dam that are transported.
- S_t = transport survival from trucking fish in the control fish group. Includes mortality in collection, transport and release.
- $S_{b.l}$ = survival from barging fish at Lower Granite dam and include mortality in collection, transport release back in to the river.
- T_{MCN} = total transport survival from McNary Dams.

- E_T, E_C = test and control survival from Bonneville tailrace to estuary.
- O_T, O_C = survival of transported and control fish through the ocean and back up river. These parameters also contain any unidentified mortality factors not accounted for in the other processes.
- R_1 = survival of fish traveling in river from transport release in Little Goose trailrace through McNary Dam pool.
- R_2 = survival of fish traveling in river from McNary Dam forebay to Bonneville Dam tailrace.

The total transport mortality from Lower Granite dam can be expressed

$$T_{\mathrm{LGR}} = S_{\mathrm{b.l}} \cdot \frac{O_T}{O_C} = \mathrm{TBR} \cdot \frac{S_{\mathrm{LGR}}}{S_{\mathrm{BON}}} \tag{162}$$

where

- T_{LGR} = total transport survival from Lower Granite dam.
- S_{LGR} = model survival for fish transported from Lower Granite dam to Little Goose dam tailrace.
- S_{BON} = model survival from Bonneville Dam tailrace to estuary.

II.10.2 -Transport Survival Calibration

While there are differences in estimates of transport survival they are all relatively high (Table 55). Because the spring chinook estimates are similar for Lower Granite and McNary dams an average is used for all dams. The resulting average transport survivals from CRiSP1.5 are as follows:

- spring chinook transport survival = 89%
- fall chinook transport survival = 83%
- steelhead transport survival = 91%

Table 55 Transportation survival estimates and TBR data.

Year	Species	Dam	TBR	transport survival	mean survival
1986	spring chinook	MCN	0.75	47%	81.4%
1987			1.73	104.0%	
1988			1.54	93.3%	
1986	spring chinook	LGS	1.58	74.4%	99.7%
1989			2.46	125.0%	
1986	fall chinook	MCN	2.78	67.0%	82.8%
1987			3.55	91.1%	
1988			3.39	90.4%	
1986	steelhead	LGR	1.99	86.7%	90.6%
1989			2.19	94.5%	

That model calibration produces reasonably similar results across species. Data

from other years could also be used to produce estimates of transport survival, but in most years estimates are based on very small sample sizes and are of dubious value.

At first glance it may seem impossible to have transport survivals greater than 100%, but bear in mind this fraction represents the total difference in survival between transported and non-transported fish, a difference which may include differential post-transport survival. For example, if transport survival is 100% and in-river survival is 50%, but in-river fish also experience twice the mortality of transported fish in their first year at sea, the TBR will be 4:1, and if we only examine the in-river survival we would estimate transport survival of 200% (4 x 50%). High TBR values, therefore, probably reflect not only high transport survivals, but also improved early ocean survival as well.

Transportation schedule

The schedule of transporting fish from each transport dam depends on the flow, number of each species passing the dam, and the efficiency of separating fish for return back into the river. The schedules for transportation, compiled from FTOT annual reports, for the historical years are given in Table 56.

Table 56 Transport operations for historical data files, 1975-1994.

Year	Project	Start Date	Stop Date	Separation @ (kcfs)	Criterion
1975	L. Goose	4/10	6/15	none	transport all
1976	L. Granite	4/12	6/15	none	transport to 50% of run
	L. Goose	4/10	6/15	none	transport to 50% of run
1977	L. Granite	4/15	6/5	none	transport all
	L. Goose	4/29	6/16	none	transport all
1978	L. Granite	4/4	6/21	none	transport all
	L. Goose	4/10	6/21	none	transport all
1979	L. Granite	4/11	7/4	none	transport all
	L. Goose	4/17	7/4	none	transport all
	McNary	4/9	8/24	none	transport all
1980	L. Granite	4/3	7/7	none	transport all
	L. Goose	4/7	7/7	none	transport all
	McNary	4/3	9/22	none	transport all
1981	L. Granite	4/2	7/30	none	transport all
	L. Goose	4/7	7/24	none	transport all
	McNary	3/30	9/11	none	transport all
1982	L. Granite	4/8	7/29	85	full trans @ 80% yearlings
	L. Goose	4/10	7/22	85	full trans @ 80% yearlings
	McNary	3/30	9/24	220	full trans @ 80% yearlings

Table 56 Transport operations for historical data files, 1975-1994.

Year	Project	Start Date	Stop Date	Separation @ (kcfs)	Criterion
1983	L. Granite	4/3	7/30	85	full trans @ 80% yearlings
	L. Goose	4/5	7/8	85	full trans @ 80% yearlings
	McNary	5/30	9/22	220	full trans @ 80% yearlings
1984	L. Granite	4/1	7/26	none	transport all
	L. Goose	4/5	7/28	85	full trans @ 80% yearlings
	McNary	4/16	9/28	220	full trans @ 80% yearlings
1985	L. Granite	3/28	7/23	none	transport all
	L. Goose	3/30	7/23	85	full trans @ 80% yearlings
	McNary	4/6	9/26	220	full trans @ 80% yearlings
1986	L. Granite	3/27	7/24	none	transport all
	L. Goose	4/5	7/3	85	full trans @ 80% yearlings
	McNary	3/27	9/26	220	full trans @ 80% yearlings
1987	L. Granite	3/29	7/31	none	transport all
	L. Goose	4/6	7/4	100	full trans @ 80% yearlings
	McNary	3/28	10/29	220	full trans @ 80% yearlings
1988	L. Granite	3/28	7/26	none	transport all
	L. Goose	4/12	7/23	100	full trans @ 80% yearlings
	McNary	3/29	9/22	220	full trans @ 80% yearlings
1989	L. Granite	3/29	7/30	none	transport all
	L. Goose	4/8	7/11	100	full trans @ 80% yearlings
	McNary	3/27	9/20	220	full trans @ 80% yearlings
1990	L. Granite	3/27	7/26	none	transport all
	L. Goose	4/12	7/21	100	full trans @ 80% yearlings
	McNary	4/1	9/14	220	full trans @ 80% yearlings
1991	L. Granite	3/27	7/26	none	transport all
	L. Goose	4/12	7/20	100	full trans @ 80% yearlings
	McNary	4/1	9/14	220	full trans @ 80% yearlings
1992	L. Granite	4/27	10/31	none	transport all
	L. Goose	4/3	8/31	100	full trans @ 80% yearlings
	McNary	3/25	9/30	220	full trans @ 80% yearlings

Table 56 Transport operations for historical data files, 1975-1994.

Year	Project	Start Date	Stop Date	Separation @ (kcfs)	Criterion
1993	L. Granite	4/14	10/31	none	transport all
	L. Goose	4/15	10/31	none	transport all
	L. Mo.	5/3	10/31	none	transport all
	McNary	4/15	11/24	none	transport all
1994	L. Granite	4/5	10/31	none	transport all
	L. Goose	4/5	10/31	none	transport all
	L. Mo.	4/6	10/31	none	transport all
	McNary	4/8	11/28	none	transport all

Transportation Separation

The above table indicates conditions under which fish are ***separated*** and returned to the river. While it is assumed that transportation always benefits steelhead juveniles, many people believe that smaller migrants (chinook, coho, sockeye) benefit from transportation when flows are low, but are better off in the river when flows are higher and conditions are presumably better.

If a dam has a ***Separation Trigger***, when flows exceed that value, smaller fish are separated from the larger steelhead smolts and are returned to the river. This separation continues according to the ***Criterion*** given in the table. For example, if the criterion is “full transport at 80% yearlings”, this means that fish are separated under high flow conditions until it is estimated that 80% of yearlings have already passed the dam. After that point, all collected fish are transported regardless of flow condition.

There is great variability in separator efficiency: the idea is to retain steelhead for transport and return other fish to the river. As a rule of thumb, CRiSP uses the “80/20” criterion (Table 57), which means that 80% of steelhead are successfully retained, and 80% of smaller fish are successfully returned to the river, but 20% of steelhead also escape to the river, and 20% of smaller fish are retained for transport.

Table 57 Separation efficiencies at transport projects.

Stock	retained for transport	diverted to river
Steelhead	80%	20%
Yearling Chinook	20%	80%
Subyearling Chinook	20%	80%

Flow-based transport model calibration

The most recent versions of CRiSP include the capacity to vary transport survival as a function of water particle travel time (WPTT). This was put in place at the request

of members of the FLUSH modeling team to provide similar functionality found in the spring FLUSH model used by the State and Tribal Agencies (described in ANCOOR 1994). In their "transport model 3" they hypothesize that transportation mortality is related to flow such that:

- For flows equal to or greater than those in 1986, the TBR from Little Goose tailrace is 1.01 to 1,
- For flows equal to or less than those in 1977, the TBR from Little Goose tailrace is 3 to 1, and
- For flows between these conditions, transport survival is determined by linear interpolation between the two end points.

Note that this model is intended to apply only to yearling chinook stocks.

Determination of mortality levels for these conditions is exactly the same as described above and the reach defined for determining WPTT is Lower Granite Pool to below Bonneville Dam. The resulting parameters are given below in Table 58.

Table 58 Parameters used for flow-dependent transport mortality model.

Year	Assumed TBR	Transport Survival
1977	3:1	20.9%
1986	1.01:1	47.6%

II.11 - Stochastic Processes

CRiSP.1 provides the ability to vary parameters over a run. This allows a representation of random factors. The randomness is incorporated in different ways for flow, dam passage, reservoir mortality and travel time. The approach is to describe specific parameters as having a deterministic part and a stochastic part. A deterministic part may change with the independent variables that determine the parameter but the value obtained does not change from one model run to another if all factors are the same. The stochastic part changes each time it is calculated in CRiSP.1 or between model runs. The value of the stochastic part is obtained from a random number distribution function using a "broken-stick" distribution function. This is described along with deterministic and stochastic parts of the parameters.

II.11.1 -Stochastic Parameter Probability Density

Variation in many of the stochastic rate parameters is described by a *broken-stick* probability distribution function (pdf). This is a simple function based on a piecewise linear distribution. The probability density function and the cumulative density function are illustrated in Fig. 65. It is described using the 0, 50 and 100% cumulative

probability levels.

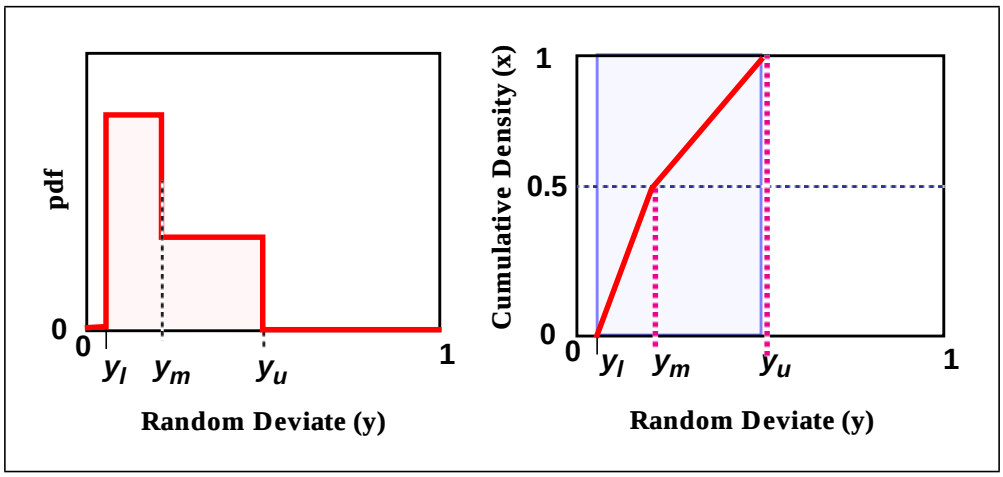

Fig. 65 Probability function (pdf) and cumulative function of the broken stick probability distribution

Random deviates for this broken stick density distribution are obtained from the following transformation formula

$$\begin{aligned} y &= y_l + 2x(y_m - y_l) && x \le x_m \\ y &= y_m + 2(x - 0.5)(y_u - y_m) && x \le x_m \end{aligned} \qquad (163)$$

where

- x = unit uniform random deviate range $0 < x < 1$
- y_l = lower limit of the distribution range
- y_m = distribution of the median value
- y_u = upper limit of the distribution range.

Although the distribution uses the median, the broken-stick input windows in CRiSP.1 use the mean value since most data reports include a mean in addition to the minimum and maximum values. The median is estimated from these three measures as

$$y_m = \frac{4\bar{y} - y_l - y_u}{2} \qquad (164)$$

assuming the mean of the distribution is equal to the average of the mean of the lowest 50% of the distribution and the highest 50%. These are simply the average of the minimum and median, and maximum and median, respectively.

Note that in a skewed distribution the mean and median are different. The result is that the mean specified by the user *must* fall in the middle two quartiles of the distribution, i.e. if the user specifies a minimum of 0 and a maximum of 100 for some distribution, the mean must lie between 25 and 75, inclusive. If the user specifies a distribution outside this range, CRiSP.1 will post a message to that effect in the message window and will direct the user to choose a mean that lies in the acceptable range.

II.11.2 -Stochastic Parameters

Predation

Variability in the predator activity coefficient used in eq (64) has deterministic and stochastic parts. The equation is

$$a_0 = \bar{a}_0 + a'_0 \tag{165}$$

where

- $\bar{a}_0$ = deterministic part set by sliders for each species where value of the activity is set by the mean value slider
- a'_0 = stochastic part whose range for a given species is set by the low and high value sliders.

For determining the stochastic part, a new sample is drawn for each release in each river segment. The parameter does not change over time steps but is different for each release and each river segment.

Supersaturation Mortality

Variability in nitrogen supersaturation mortality is incorporated by giving the gas mortality coefficient used in eq (103) deterministic and stochastic parts. The equation is

$$a = \bar{a} + a' \tag{166}$$

where

- $\bar{a}$ = gas mortality coefficient deterministic part and is set by mean value sliders for each species
- a' = stochastic part whose range for a given species is set by the low and high value sliders.

For determining the stochastic part, a new sample is drawn for each release in each river segment. The parameter does not change over time steps but is different for each release and each river segment.

Migration

Variability in the migration rate is determined by the equation

$$r_i(t) = r(t)V(i) \tag{167}$$

where

- $r(t)$ = determined from eq(52)
- $V(i)$ = variance factor which is different for each release i.

The term $V(i)$ is drawn from the broken-stick distribution. The mean value is set at 100%, representing the deterministic $r(t)$ and the upper and lower values are set with sliders under the migration rate variance item in the **BEHAVIOR** menu.

The variance factor assumes that variability in migration velocity relative to water velocity is associated with a particular stock of fish. Studies of travel time support this assumption since particular stocks exhibit their own unique relationship with flow.

Flow

Flow Variability is represented on a daily basis when running in the Monte Carlo mode. In this case, daily flow variation is expressed by an Ornstein-Uhlenbeck process. Details of this are described in the Spectral Analysis of Flow section on page II.25.

In the Scenario Mode, daily flow variations are described by a random process in headwater flow. Details of this process are described in the Headwater Modulation section on page II.37.

Dam Passage

Variability in dam passage parameters is applied on each dam time slice, (typically 2 hours). The variability is generated from the broken-stick distribution and is applied to the following variables:

- bypass mortality
- spill mortality
- turbine mortality
- transportation mortality
- day / night fge
- spill efficiency.

II.11.3 -Scales of Stochastic Variability

The scales over which stochastic variability are applied is given in the table below.

Table 59 Model probability density functions

Process	Equation	pdf	Scale
Predation mortality	eq (65)	broken-stick	river segment
N saturation mortality	eq (104)	broken-stick	river segment
Migration rate	eq (54)	broken-stick	release group
Flow in Monte Carlo	eq (6)	O-U using Normal	12 hrs, month, yr.
Flow in Scenario	eq (16)	Normal	12 hrs
FGE & dam mortality	eq (153)	broken-stick	2 hrs
Spill efficiency	eq (154)	Normal	2 hrs

III. Model Validation

III.1 - Overview

Model verification or validation accompanies model calibration. The purpose of the validation is to provide information by which a decision maker or model user can assess the probability of the model predicting a future event. An assessment of the uncertainty in the prediction can only be achieved in a qualitative sense because with any complex natural system, absolute predictive capability is impossible. We can not be assured if a model will predict future events. Orenske et al (1994) claimed that when we validate a model we can only determine if it is logically consistent and that such consistency says nothing about the model's predictive abilities. In an absolute sense they are correct but humans every day make judgements about the probability of future events occurring. Thus, the limited sense of validation taken by Orenske et al. needs to be considered in model validation.

Decision making has a strong psychological basis. The dynamics of such judgements have been studied in the contest of risk assessment (see Kahneman, Slovic and Tversky, 1982). This work identified heuristics by which judgements are made under uncertainty. An important assessment technique is designated *representativeness*. Simply stated, the level of uncertainty in a prediction is assessed in terms of how representative a model system is to the real system. Thus, validation needs to consider the model's representativeness in the sense defined by Kahneman et al. and a model's logical self-consistency as defined by Orenske et al (1994). Each of these aspects has several parts. Self consistency can be judged in terms of the mathematics and the calibration of the model. Representativeness can be judged in terms of intuitive, observational and mechanistic factors (Fig. 66).

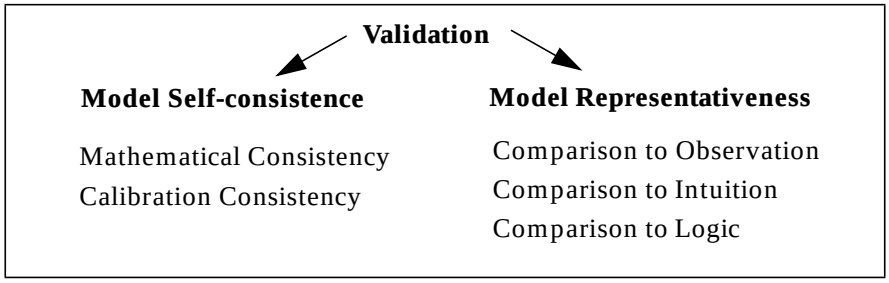

Fig. 66 Model validation involves determining if a model is self-consistent and representative of the real system. A self-consistent model is mathematically error free and has an acceptable measure of fit to the data. A model is representative of a real system if it intuitively and logically is consistent with the real system and its predictions fit independent data.

Self-consistency

A self-consistent model contains no errors in the mathematical expressions of the assumptions and the constructs relating the assumptions to the output or response. A model that is self consistent is one that follows logically from its assumptions. A test for self consistency does not address whether or not the assumptions themselves are valid; that is addressed in terms of the model's representativeness. Evaluation of self-consistency is in principle straightforward in terms of the model being mathematically correct. In practice validating mathematical consistency of a model can be difficult.

The first measure of self-constancy involves identifying (and eliminating) mathematical errors in formulating model assumptions mathematically and in solving the model equations. Mathematical consistency may also be measured in terms of the asymptotic characteristics of the model. That is, a model that generates physically impossible results as the parameters asymptotically approach limits is less likely to be valid than a model that does not generated unrealistic results. For example, a smolt passage model that predicts greater than 100% survivals at short travel times is less valid than a model that through the nature of its equations generates survival predictions between zero and 100%. Although asymptotically unrealistic models may fit observations within some restricted parameter range, if there are no underlying physical reasons for restricting the range, such models are of dubious utility.

The second measure of self-consistency involves quantifying how well the model fits the calibration data. In the calibration process model parameters are selected through a criterion of goodness-of-fit using a variety of statistical algorithms (Goodness-of-fit section on page II.18). These statistics are quantitative measures of a model's self-consistency.

Model representativeness

The second step in model validation is to determine the representativeness of a model for the real system. Here we must consider the psychological process by which people evaluate uncertainty. Although there is no fixed set of measures there are three general categories to assess the uncertainty in judgements: intuition, ecological theory, and ability to fit observations. A validity assessment will consider all three.

Intuitive validation

A person will make an intuitive evaluation of the validity of a model's predictions. There is no quantitative measure for intuitive validations and they are often influenced by simplified and qualitative anecdotal statements of assumed "truth". Such statements are often for public consumption, may be distorted and expressed as absolutes. In a public forum models are often used to backup the simple "truth" statements. Addressing these statements is difficult at best. One approach is to provide for people hands-on experience with the models so that they realize the simple public statements are inaccurate.

Mechanism validation

The second way to validate a model's representativeness is to consider how representative the model mechanisms or assumptions are of what is known about the system. That is, we can evaluate how closely a model describes the biological and physical elements of the system. At one extreme lie models based on empirical equations in which the parameters have little biological and physical interpretation. At the other extreme are models rich in complexity and biological realism. Models fall along a continuum between empirical and mechanistic formulations. In essence, a models is comprised of a number of submodels that have mechanistic foundations although the submodels themselves may be empirical.

For example, a number of survival models may be described along this continuum. At the empirical end, a model may express fish survival in terms of the rate of mortality, r, and exposure time, t. The equation would be

$$S(t) = \exp(-rt) \tag{168}$$

It is mechanistic in expressing mortality as a rate per unit time. It is empirical in that the mortality rate, *r*, must be derived from observations of survival over time. No other factors are required or relevant.

A more mechanistic model might express the rate of mortality in terms of another environmental variable such as temperature, θ. This new relationship might be empirical and derived strictly through observations of how predator feeding rate changes with temperature. This leads to a submodel describing how the mortality rate changes with temperature. For example we might have an exponentially increasing predation rate

$$r(\theta) = a \cdot \exp(b\theta) \tag{169}$$

where the coefficients *a* and *b* are empirical and have no biological meaning.

Additional mechanisms could be added by expressing exposure time in terms of factors that control fish travel time. Again the travel time submodel may be constructed by equations that are in part based on first principles and in part based on empirical fits to observations.

In moving from empirical to mechanistic models we gain validity by including more of the underlying processes that control a system. There is, however, a trade-off: as the model becomes more complex the number of model parameters that must be calibrated is larger and potential range of model responses become greater.

At what level of complexity is model validity greatest? No simple answer exists and it depends on the available data with which to test the model and the types of questions the model must address. In general, a model must contain mechanisms down to the level at which a system is managed and to the level at which data exists.

For example, a smolt passage model that does not explicitly formulate the impact of spill on fish survival is not mechanistically valid for addressing the impact of spill. Conversely, to validate the model's representativeness to observations it must be compared with data on the impacts of spill.

Observation validation

A third and most rigorous way to validation process is by comparing model or submodel predictions to data. Data in model validation is split into two parts; a *calibration part* with which a model parameter is fit and a *validation part* that is compared to a prediction. To compare a model to data we must choose a merit function that measures the agreement between the data and predictions. Merit functions involving a single measure may have a classical statistical basis such as the Student's t-test on prediction of observation means. Merit functions may also involve a number of measures or dimensions. In this case a model predicts a number of different but related measures of the system. For these multiple dimension tests there may be no clear method for how to weight the fit of each model dimension to the corresponding observations. This is particularly true when we have only limited observations for each measure.

Comparing validity assessment

Answering the question “how valid is a model?” is difficult and dependent on the context of how a model is used. Generally two approaches are possible: in a cardinal measure of validity we express the validity of a model in terms of some number, typically a goodness-of-fit merit function. Such measures can be based on self-consistency and representativeness of observations. They are of most use when model predictions explore the system within the parameter space of the calibrated model. Models also have the ability to make predictions beyond the observed states of the system, however, and in these cases validity established from observations is insufficient. Validity must then be established in terms of the representativeness of the model mechanisms to the real system. Such mechanism-based measures of validity are expressed in a ordinal scale confined to ranking the validity of a number of models.

Approach in CRiSP

The approach to validating CRiSP1 has applied the principles outlined in the section above. The following sections detail the validation.

The mathematical validity of CRiSP was addressed through a team approach. All mathematical formulations were developed and checked by at least three people. Theoretical aspects were usually developed by one researchers and checked by another. Submodels were coded by the programmers and the code was checked by the scientist who developed the theory. Submodel operation in CRiSP were checked by a third person.

An important aspect of a model validity is the response of the model outside the range in which it is calibrated. Most equations generate realistic results as model parameters are adjusted to high or low values. For example, the survival is confined within 0 and 100% under all ranges of model parameters. The temperature effect on the predation rate is the only parameter that is not confined by the form of the equation. In this case the input range of the temperature coefficient on predation is confined.

Model validity can be assessed in terms of how well the model fits the data used in the calibration. Calibrated submodels are referenced in (Table 60).

Table 60 Information for submodel calibration including page number in manual tales and figures referenced and merit function to estimate parameter values. (s) denotes spring chinook (f) indicates fall chinook and (st) denotes steelhead related information.

Submodel	Page	Tables and Figures	Merit Function	Years of data	Number of data
Flow-Velocity Calibration	II.48	Fig. 21 Fig. 22	least squares	1993	21
Monte Carlo Flow Modulator Validation	II.29	Fig. 13 and Fig. 14 Table 2	variance	1979-1989	multiple dams
Fish Migration	II.51	Fig. 30 to Fig. 33	least squares	1989-1994(s) 1988-1994(f) 1989-1994(st)	53 22 93
Calibration of Forebay Delay	II.112	Fig. 53 Fig. 54	Kendall's tau	1985 (s)	1
FGE Calibration	II.123	Table 43 Table 47 Table 49	mean	1989-1993(s) 1993 1989-1993(st)	5(s) 1(f) 5(st)
Spill Efficiency	II.119	Table 41	least-squares	varies w / dam	9 studies
Dam Passage Survival	II.135	Table 54	least-squares	11 studies	multiple dams
Nitrogen from Spill:	II.97	Table 36, Table 37 Fig. 46	chi-square	1994	daily average for 5 months
Mortality Rates	II.89	Table 30, Table 37 Fig. 40 Fig. 41	least squares	1976	30(f) 28 (st)
Fish Depth	II.96	Table 34	various reports	various years 1974 1989	10
Predator Density	II.67	Table 17	predator index	1990-1994	~ 4000
Activity Coefficient Estimation: Theory	II.75	Table 22 - Table 27	point estimates	1984-1986	~10,000 samples
Transportation Mortality	II.139	Table 55	means	1986-1989(s) 1986-1988(f) 1986, 1989(st)	5 3 2

One measure of validity is how accurate a model is in terms of its mathematical description of the underlying ecological processes. The CRiSP model defines mechanisms for fish migration and dam passage, which are detailed in the Theory manual. The important mechanisms involve the dam passage routes and associated mortalities, gas bubble disease mortality, mortality from predation, effects of temperature on mortality and gas generation, and effects of fish age, flow and date of

release on fish travel time. In CRiSP particular effort was given to developing a self-consistent smolt travel time model that applies a number of goodness-of-fit measures. The details of the model selection and fitting procedure are described in Zabel (1994). The work developed a series of nested models of increasing complexity and used three goodness-of-fit criteria to determine the balance between increasing model complexity and reliability of the predictions.

Potentially important mechanisms that are currently missing from smolt passage models including effects of fish vitality on mortality, effect of density dependence on fish growth, and effect of estuarine conditions on fish survival.

The validation of the CRiSP model to observations involves comparing the individual submodels and the total model to independent data. Submodel validations are contained in specific calibrations of the submodels developed previously in this chapter. Most submodel validations were assessed in terms goodness-of-fit used in the calibration. Total model validations are available by comparing model survivals to field studies in which survival was estimated through several reaches of the river and for several species.

III.2 - FGE validation

Fish guidance efficiencies estimated in CRiSP were validated against data independent of the data used for calibration. The calibration used PIT tag data collected between 1989 and 1995 (see Table 60). For validation the model-calibrated FGE's were compared to FGE measured in the PIT survival studies and FGE measured in fyke net studies. The results and discussion of the validation are given in FGE Calibration section on page II.123 and in Table 44 and Table 48. Specific comparisons made for CRiSP1.5 are given in Table 61.

Table 61 Comparison of observed and CRiSP predicted FGEs

Species	Location	Source of Obs	Date of Obs	Obs	CRiSP
spring chinook	LGR dam MCN dam	NMFS PIT tags NMFS fyke nets	1993 1992	45% 60%	49% 60%
fall chinook	LGR dam MCN dam	NMFS fyke nets	various years	35% 47%	35% 40%

III.3 - Travel time validation

III.3.1 -Snake River spring chinook

To validate the Snake River yearling chinook travel time submodel and calibration, model output was compared to an independent data set. The independent data were the PIT tagged hatchery yearling chinook used in the UW-NMFS survival study performed in 1993 and 1994. These fish were released in the Snake River upstream from Lower Granite Dam. The average travel times predicted by the model with the parameters listed in Table 11 were compared to observed average travel times in Table 62. The predicted and observed travel time are plotted together in Fig. 67.

Table 62 Average travel time (days) of model and observed PIT tagged yearling spring chinook. Parameters generating the modeled times are given in Table 11.

Observation point	travel time (days)	
	Observed	Modeled
1993 with T_{seasn} = 119.8		
Lower Granite dam	9.7	8.3
Little Goose dam	14.6	13.9
McNary dam	20.7	22.0
1994 with T_{seasn} = 119.8		
Lower Granite dam	9.1	6.8
Little Goose dam	14.5	12.8
McNary dam	23.0	21.7
1994 with T_{seasn} = 130		
Lower Granite dam	9.1	9.1
Little Goose dam	14.5	14.6
McNary dam	23.0	22.8

The correspondence between predicted and modeled average travel times was good for the 1993 data, with the largest deviation being 1.4 days. The correspondence was not as good for 1994 data. In particular, the model predicted fish arrive 2.3 days earlier at the first dam than was observed. This delay was propagated to lower dams. The predicted travel time between dams, however, was consistent with the data (Fig. 67).

A possible explanation for the observed deviation in 1994 is that the hatchery fish in this study were not as smolted compared to the Snake Trap run-of-the-river fish. In the active migration equation (eq (52)), the T_{seasn} parameter is a surrogate for smoltification. If this value is increased from 119.8 to 130.0 (in Julian date), the correspondence between model and data improves substantially, with the largest deviation between modeled and observed average travel times being 0.2 days (see Table 62).

For an alternative comparison of the migration model the travel time data from the 1993 and 1994 PIT tag studies was used to generate migration model parameters. A comparison of the observed PIT tag data and the model estimated travel times was excellent with an r^2 = 0.99 (Fig. 67). The resulting model parameters are compared to the base parameters in Table 63.

Table 63 Travel time calibration parameters for the Snake River spring chinook PIT tag survival studies

Variable	1993	1994	Base
β_{min}	2.35	2.67	1.34
β_{max}	13.98	17.87	20.2
β_{flow}	1.92	0.84	0.71
a	0.61	1.02	0.10
T_{seasn}	117.10	133.0	119.8
V_{var}	48.9	46.6	100.0
r^2	0.99	0.99	0.92

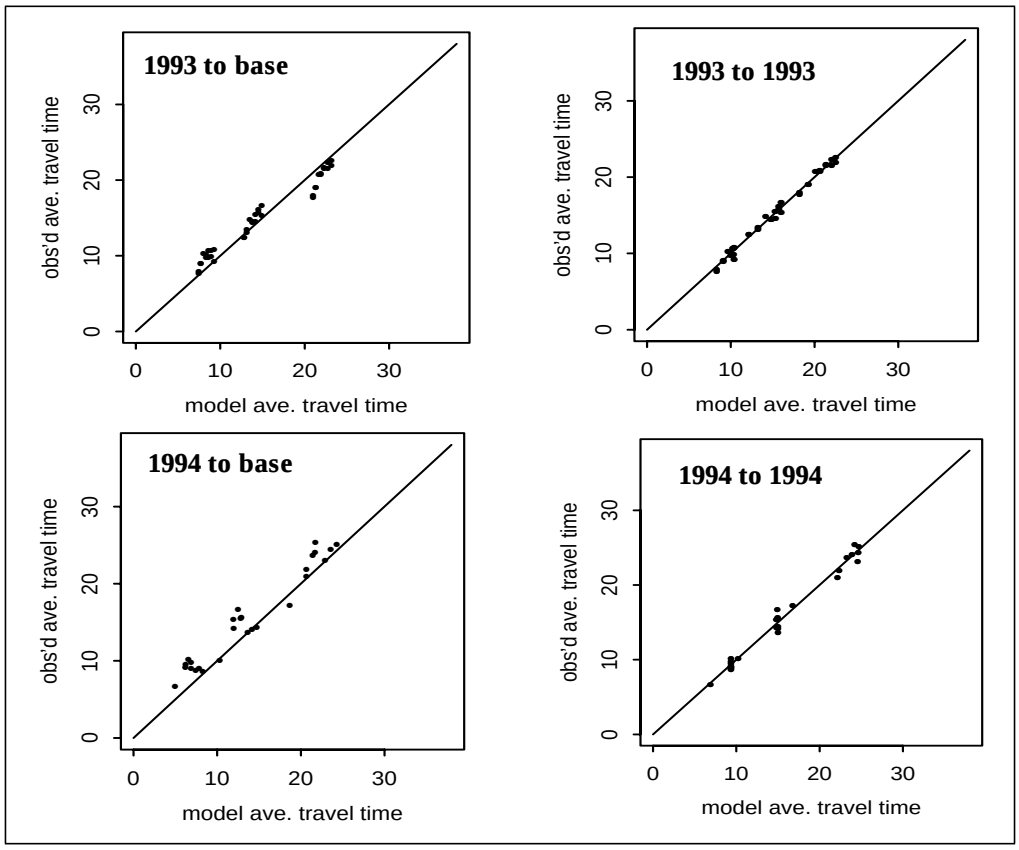

Fig. 67 NMFS PIT tag travel time data from 1993 and 1994 spring chinook survival experiments. Figures of year to base illustrate fit of model using calibration data from 1989 through 1993. Figures of year to year show fit of model to data used in calibration. Model parameters given in Table 63. Observed vs. modeled data includes travel time to L. Granite, L. Goose, and McNary dams.

III.3.2 -Snake River fall chinook

The model predictions were compared with the limited data available on the travel time of Snake River fall chinook. Since fish were tagged prior to smoltification, it is not possible to observe actual travel times. For this comparison, average passage dates at the observation sites (Lower Granite, Little Goose, McNary, and Lower Monumental in 1993 and 1994) are compared to model predicted dates. The smolt start/stop dates are those provided in Table 12. The migration rate parameters used are the ones calibrated from the Rock Island fall chinook (Table 11).

The sample sizes (provided in Table 66) are small in this data set, particularly at the downriver observation sites. Thus, the observed average passage dates to Lower Monumental and McNary dams are unreliable. In some cases, the average passage dates at Lower Monumental and McNary are earlier than at the upstream dams, Lower Granite and Little Goose. This could be due to decreasing survival as the season progresses; perhaps only early migrants survive to McNary, producing an extended arrival distribution that is truncated later in the season, but not at upstream dams.

Comparison results are contained in Table 64. For 1991, the difference between observed and predicted passage days is approximately 1 day. For 1993 and 1994, the differences are of 3-4 days. For 1992, the differences range from 8 - 10 days. These deviations are not unexpected given that the migration initiation dates are unknown.

Table 64 Mean Julian date of arrival observed from PIT tags and from CRiSP

Site	1991		1992		1993		1994	
	Obs	CRiSP	Obs	CRiSP	Obs	CRiSP	Obs	CRiSP
LGR	208.2	207.8	169.6	180.0	204.3	207.6	206.7	211.3
LGO	213.5	214.7	195.3	187.5	218.1	214.1	220.9	217.4
LMO	–	219.7	–	192.7	211.6	218.7	211.6	222.1
MCN	239.0	232.7	195.6	205.3	199.3	231.1	199.3	235.6
smolt start	194		166		196		199	
smolt stop	214		186		216		219	

For comparison purposes, we compare smolt start and stop dates to the distribution of lengths at tagging versus tag date in Fig. 68. In this plot, the horizontal line represents length = 85 mm, a commonly cited threshold length for migration initiation. Also included in the plot is the best fit linear relationship between length and tag date. The dashed vertical represent smolt start and stop dates as given in Table 64. For 1991, 1992, and 1993, smolt start date approximately corresponds to length = 90 mm, and smolt stop date approximately corresponds to length = 105 mm. In the future, we intend to relate fish length to migration initiation in the model.

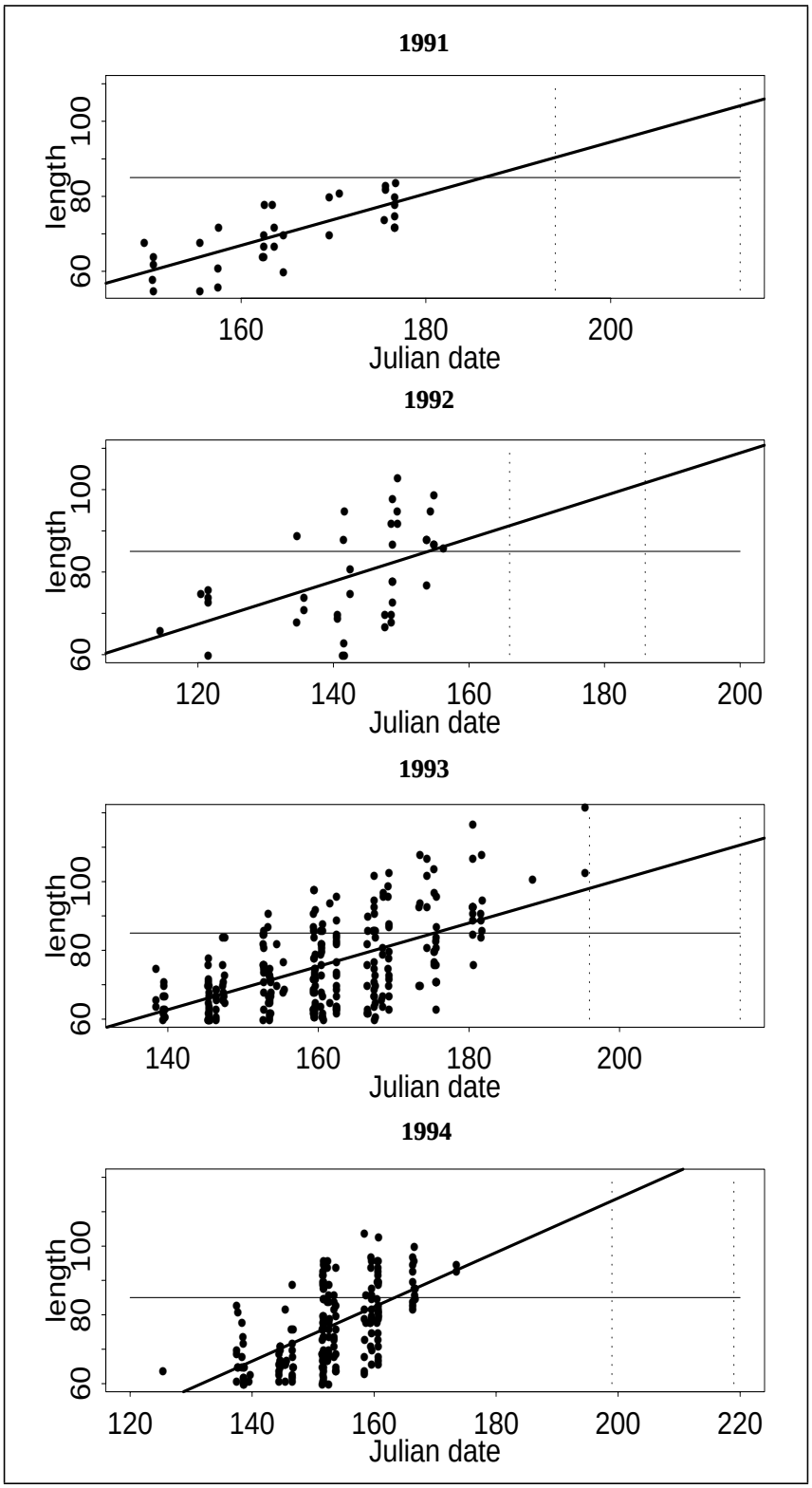

Fig. 68 Fish length (mm) versus tagging date for the Snake River fall chinook. The horizontal line is length = 85 mm. The dark line is the best fit linear relationship between length and tag date. The dashed vertical lines are smolt start and stop dates, as given in Table 64.

III.4 - Survival validations

The model predictions of fish survival through river reaches were validated against a variety of survival studies for fall and spring chinook and steelhead. The validations used data sets that provide estimates on either the number of fish collected at a downstream project or percent survivals. In cases when only numbers of fish were available, the survivals were estimated using the calibrated *FGE*. Model-estimated survivals depended on travel time parameters. In cases with PIT tag data, the migration rate was adjusted to fit exactly that data. Then the fit of predicted to observed survival was controlled by the reservoir mortality rate coefficients. Of these, the most important parameter was the predator activity coefficient, which scales the predator-induced mortality rate. The predator density index accounts for differences in predation between river reaches and the temperature parameter accounts for differences in predation associated with temperature.

A number of survival data sets are available throughout the river system (Fig. 69) and for different species. The predator activity coefficient was determined from predator consumption data in John Day reservoir. Validating to data above and below this mid-river point provides an evaluation of how representative the model calibration is of the entire river system, not simply a single portion of the river.

The validation topics below address fall chinook, spring chinook, and steelhead individually with a variety of data for each species.

The validation data sets cover the entire Columbia and Snake River system (Fig. 69). Specific data sets that the model was tested against are listed below and survival comparisons are given in Table 80. The circled numbers identify the location of data sets in Fig. 69. Results of the validation include:

- (1) Validation of spring and fall chinook FGE with studies based on fyke net and PIT tag collections.
- (2) Validation of fall chinook survival predictions using Priest Rapids adult return data as analyzed by Hilborn et al. (1994).
- (3) Validation of spring chinook reservoir survival using NMFS Snake River PIT tag survival estimates for 1993 and 1994. Validation of fall chinook migration and survival using PIT tag information from the Snake River.
- (4) Validation of mid-Columbia spring chinook survivals from Methow to Priest Rapids Dam fits observed values.
- (5) Validation of spring chinook and steelhead survivals with brand recapture survival studies (the Sims and Ossiander studies).
- (6) Validation of spring chinook survival from radio tag tracking of fish released below Bonneville Dam.

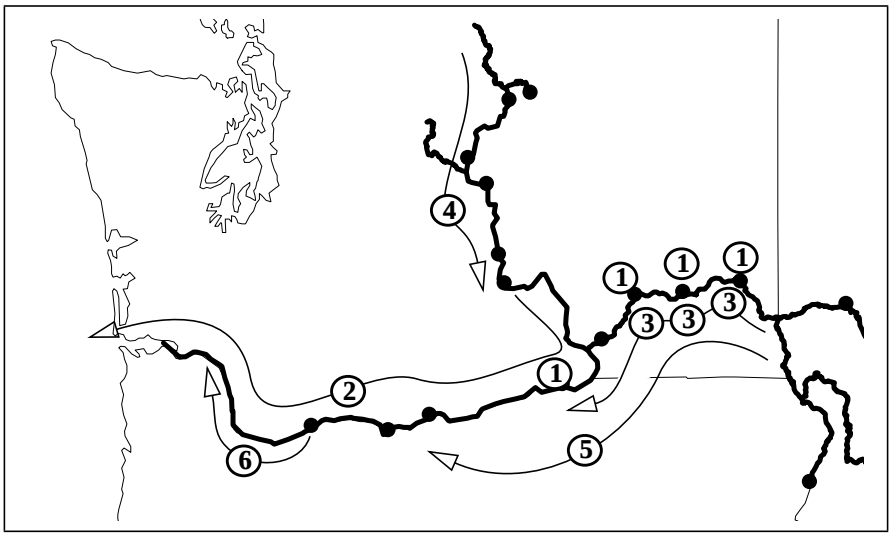

Fig. 69 Locations of survival studies for model validation.

III.4.1 -Fall Chinook survival

To verify the model predictions for fall chinook, collection and survival data from a number of field studies were compared to model predictions (Table 65) and (Fig. 70).

Table 65 Data sets used in the fall chinook validation

Data set	Type	Years
Snake River	PIT tag juveniles	1991-1994
Priest Rapids	CWT juveniles to adult return	1977-1987

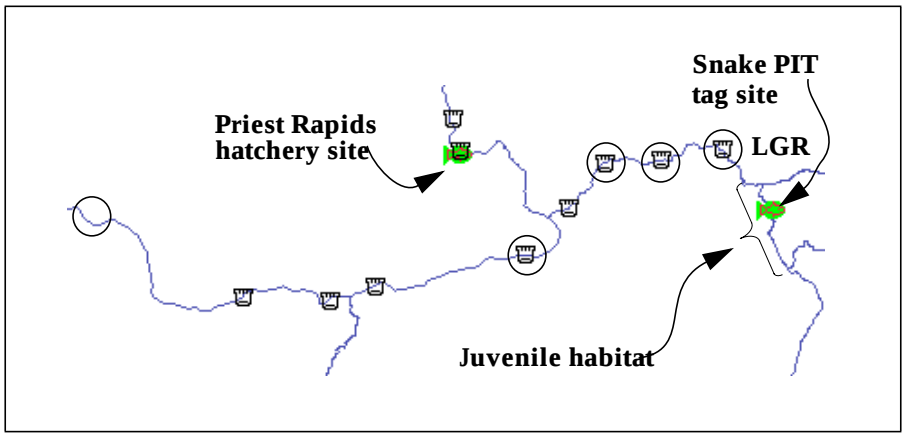

Fig. 70 Release ( ) and recovery sites (◯) of data for fall chinook validation. Juvenile habitat indicates where Snake River smolts were tagged prior to migration.

Snake River fall chinook

The evaluations of fall chinook survival predictions were made using PIT tag data from 1991-1994. Fish were collected in beach seines in their juvenile habitat in the Snake River reach above the confluence with the Clearwater (Fig. 70). Juvenile pre-smolt fish were tagged late May through mid-July in 1991, mid-April through mid-June in 1992, late April through mid-July in 1993, and mid-April through mid-June in 1994. The analysis used fish observed at Lower Granite, Little Goose, and McNary dams for 1991-1994, and at Lower Monumental in 1994 only.

Fitting the model to these data sets was problematic because of the variable nature of fall chinook behavior within a year and from year to year. In addition, fish were tagged prior to their active migration so they experienced an unknown amount of mortality prior to migration from the juvenile habitat. The variability in fish behavior between tagging and arrival at the first dam, Lower Granite, was considerable and using fixed model parameters provided poor fits to the arrival time and survival. In this situation strategy was to validate travel time and survival of fish (Table 66) once they had passed Lower Granite Dam. For this comparison smoltification onset (Table 64) and predator density (Table 66) in the juvenile habitat were adjusted so the model generated the observed arrival date and collection numbers at Lower Granite Dam. Since the collection numbers were determined with an assumed FGE as well as travel time and mortality rate the comparisons to observations is not a verification of survival parameters but of the overall predictions on fish collections numbers.

CRiSP predictions of are generally within a 2x factor of the observed collections for Snake River fall chinook (Table 66). For 1991, 1992 and 1994, the fit of model-predicted numbers to observed numbers is excellent. For 1993, the model consistently overpredicts the numbers of fish at each downstream site. This is partly due to a very high detection rate at Lower Granite as compared to the other three years but average detection rates (compared to the other three years) at the lower three dams.

Table 66 Comparisons of observed PIT tag and model-predicted detections at Snake River dams. Includes percent error of predicted relative to PIT numbers. The predicted detections at Lower Granite were set to observed values by adjusting predator densities in the juvenile habitat, so the validation is for the survival to the lower three dams.

	1991		1992		1993		1994	
	Obs	CRiSP	Obs	CRiSP	Obs	CRiSP	Obs	CRiSP
# tagged	805		1169		1687		2776	
pred. density	4200		8700		1800		412	
LGR	34	34	40	40	252	252	186	186
LGO	15	17	26	18	52	108	42	68
	-13%		-31%		+108%		+62%	
LMO	-	-	-	-	10	59	24	30
	-		-		+460%		+15%	
MCN	4	5	7	8	5	27	3	10
	+25%		0%		+420%		+200%	

Mid-Columbia fall chinook survival

Survival of Priest Rapids Hatchery fall chinook was evaluated for the outmigration years 1977 through 1987 by Hilborn et al. (1993). The study reported survival from hatchery release to entry into the ocean fishery. The CRiSP model predicts survival from hatchery release to the estuary so the difference in the observed and modeled survival is an estimate of the early ocean survival for each year.

To generate river survivals the Priest Rapids hatchery-derived travel time parameters were applied with the historical flows, spills, and temperatures, and estimates of predator activity derived from the John Day Pool study. Model release dates were set from Priest Rapids hatchery release information and were tracked to Jones Beach, near the site of the coded wire tag releases used by Hilborn et al. for comparison.

In the Hilborn et al. study recovery rates of coded wire tags (CWT) from Priest Rapids brand groups and branded fish from stocks below Bonneville Dam were used in a generalized linear model to estimate survival of the in-river and early ocean life stages.

CRiSP generates higher estimates of survival (23% average for CRiSP vs. 11% average for the Hilborn study) because the CRiSP model defines survival through the river and not to entry in to the ocean fishery. The difference in the Hilborn estimate is the inclusion of ocean mortality prior to entry into the fishery. The relationship between the two survivals is

$$S_{\text{hilborn}} = S_{\text{ocean}} \cdot S_{\text{crisp}} \tag{170}$$

The ocean survival can be estimated by a regression of $S_{\text{crisp.}}$ against S_{hilborn} in which the regression is constrained through zero (Fig. 71). The slope of the regression is $1/S_{\text{ocean}}$ where the ocean survival is the average survival over the years of observations. The survival depends on the early ocean mortality processes and any estuary mortality processes not accounted for in CRiSP. The regression in Fig. 71-A gave a slope of about 1.66 which implies an early ocean survival around 60%.

The Hilborn analysis produced a relationship between river flow and estimated survival. This flow relationship was not observed in CRiSP. The difference in the relationships could result from 1) CRiSP not correctly representing a fall chinook flow vs. in-river survival relationship, or 2) a flow-estuary survival relationship exists that is not captured by CRiSP.1.

The temperature predator activity relationship could account for the difference in survivals. If this were the case the fractional deviation between the two estimates could vary with temperature. This relationship is evident and can be illustrated by defining the fractional difference in the two survivals according to the equation

$$E = \frac{S_{\text{crisp}} - S_{\text{hilborn}}}{S_{\text{hilborn}}} \tag{171}$$

Fig. 71-B illustrates that *E* has a relationship with temperature during migration. This suggests that to improve the modeling of fall chinook better temperature modeling is required.

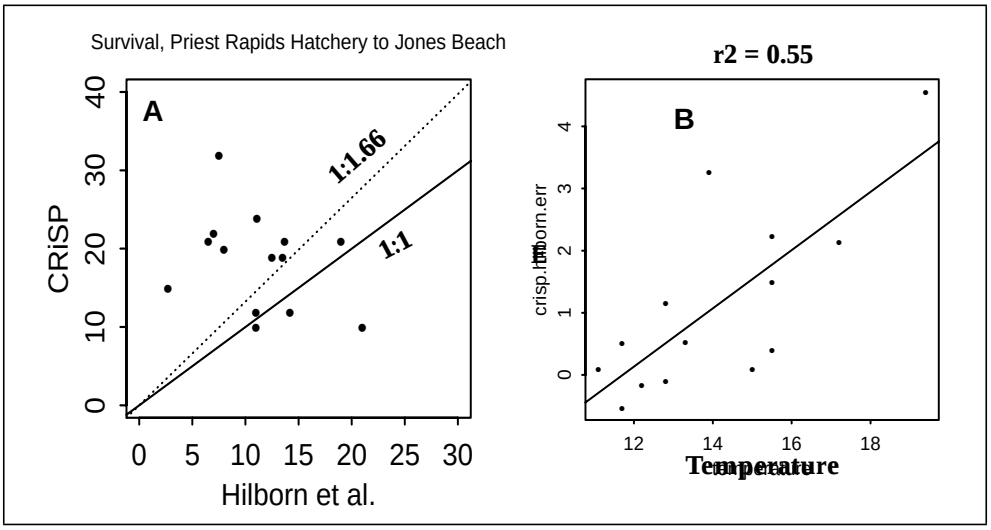

Fig. 71 -A. Priest Rapids Hatchery fall chinook survival. CRiSP-estimated survival to Jones Beach vs. Hilborn et al. (in revision) estimated survival to age 1 fishery. With forced zero intercept slope is 1.66. -B. Difference (E) between CRiSP and Hilborn et al. survival (eq(171)) as a function of temperature at release.

III.4.2 -Spring chinook survival

The validation of spring chinook used four studies that covered the Snake River, the mid-Columbia, and the lower Columbia below Bonneville dam. The validation applied standard model calibration parameters for flow, temperature, and dam operations. Release numbers and timing were defined by the data and travel time calibration parameters were derived by the validation data set. By fitting the travel time independently the exercise is a closer evaluation of the predator activity parameters independent of the migration rate parameters.

Data sets analyzed included PIT tag survival studies form the Snake River, brand release survival studies from the Snake to the lower Columbia (the Sims and Ossiander data), mid-Columbia brand release survival studies and radio tag survival studies below Bonneville Dam.

Snake River PIT tag survival studies

The Snake River PIT tag survival studies conducted by NMFS in 1993 and 1994 were used as validation date sets. The studies are described by Iwamoto et al. (1994) and Muir et al. (1995). Spring chinook were tagged with PIT tags and released at Nisqually John Landing 20 km upstream of Lower Granite Dam in 1993 and at the Snake / Clearwater confluence in 1994. Passage of individually tagged fish through Lower Granite, Little Goose and McNary Dams was monitored with PIT tag detectors in 1993. In 1994 Lower Monumental was added as a detector site (Fig. 72).

Two approaches were applied to compare the model predictions to the observed survivals. In both years of experiments the survival of fish from the release site to

Lower Granite Dam were high, approaching 100%. These high survivals are either an artifact of the experiments or they reflect an actual high survival in Lower Granite Reservoir. Since there is insufficient information to determine if the survival experiments are representative of typical fish survival through Lower Granite Reservoir the model was fit in two ways: (A) as the model is calibrated with Lower Granite Reservoir predator densities, and (B) adjusting the Lower Granite Reservoir density so the model predicted survival through Lower Granite tailrace fits the PIT tagged estimates (Table 67). In the case (A) predicted survivals to the lower collection point are less than the observed estimates of survival but the survivals may better represent actual survival conditions in the river assuming that some mortality occurs in Lower Granite Reservoir. The second validation approach, (Case B) gives survivals closer to the observed levels. This implies that the model accurately predicted chinook survival once smolts passed Lower Granite Dam.

Table 67 Observed and predicted survivals (%) for spring chinook from 1993 through 1995 PIT tag survival studies. Survivals are from Nisqually John Landing in 1993 and Silcott Island near the head of Lower Granite reservoir in 1994 and 1995. w indicates wild fish, h indicates hatchery fish. A series of CRiSP runs use the model as is, while the B series adjusts model survival at Lower Granite to equal observed.

River Reach	1993			1994			1995		
	CRiSP		OBS	CRiSP		OBS	CRiSP		OBS
	A	B		A	B		A	B	
Release to LGR tailrace	87	90	90.2	75	92	92.2 h 92.3 w	83	94	93.7
LGR tailrace to LGO tailrace	90	90	86.2	83	83	79.4 h 82.7 w	89	89	82.6
LGO tailrace to LMO tailrace	-	-	-	82	83	89.1 h 94.4 w	91	91	94.1
Release to LGS tailrace	78	81	78	62	76	73 h 76 w	74	84	77.4
Release to LMO tailrace	-	-	-	51	63	65.9 h 72.8 w	67	76	72.8
LGR predator density	388	200	-	388	240	-	388	260	-

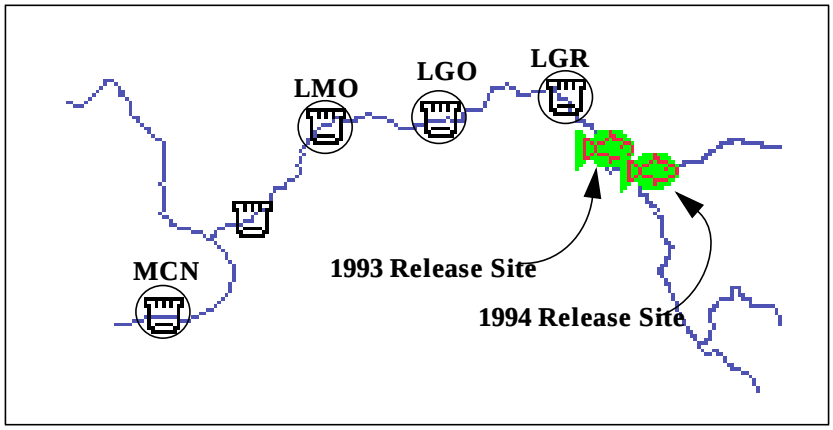

Fig. 72 Location of release and collection sites for the 1993 and 1994 survival studies. Collection sites are Lower Granite Dam (LGR), Little Goose Dam (LGO), Lower Monumental (LMO) and McNary Dam (MCN).

Spring chinook dam passage survival

The PIT tag study in 1993 provided estimates of total survival past two dams (Iwamoto et al. 1994). These were compared to the dam passage generated from CRiSP. The CRiSP predictions are within the standard error of the experimental estimates (Table 68).

Table 68 Dam survival comparison for 1993 PIT tag study.

Location	Estimate (Std. Err.)	CRiSP
Lower Granite	89 (2.6)	89
Little Goose[a]	97 (2.3)	95

a. Generated from unpublished results of the NMFS survival study 1994.

Mid-Columbia spring chinook survival

Mark-recapture experiments conducted in the mid-Columbia in the 1980s released fish in the Methow River and below Priest Rapids Dam (Fig. 73). Both releases were recaptured at McNary Dam and an estimate of survival between the two release sites was obtained. The data are given in smolt monitoring program annual reports (1986, 1987). The resulting survival estimates obtained using CRiSP are in very close agreement with those obtained in the study. Travel time observations suggest that the released fish “held up” for some time before initiating migration; when releases are delayed in CRiSP an excellent fit to travel time estimates is obtained (Table 69).

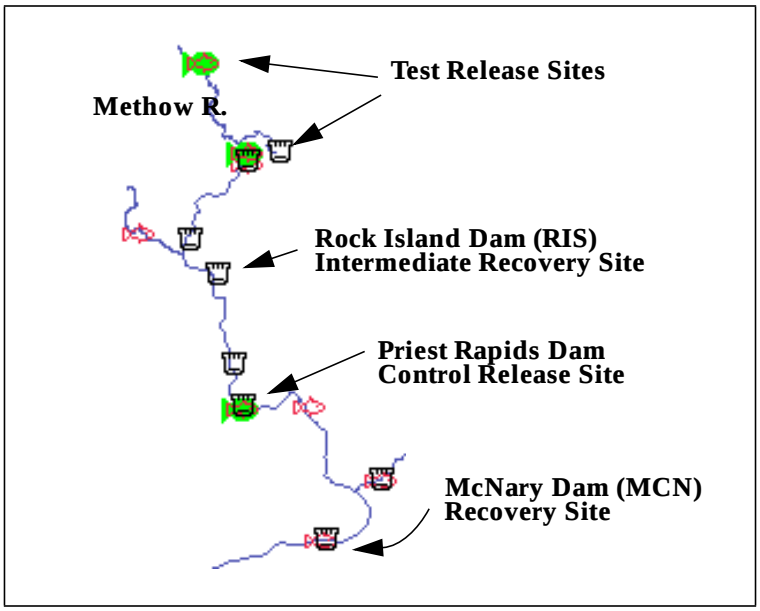

Fig. 73 Release and recovery sites for mid-Columbia spring chinook survival studies.

The estimated survival and travel time, and CRiSP estimates for the same parameters, for both years of experiments are given in Table 69.

Table 69 Survival and travel time data and model estimates for yearling chinook survival studies.

Year	1985		1986	
Release date	4/16-4/24		4/21-4/29	
Source	CRiSP	OBS	CRiSP	OBS
Median arrival date RIS	5/14	5/15	5/17	5/20
Median arrival date MCN	5/24	5/22	5/25	5/22
Survival to PRD	54.2%	45.1%	45.9%	46.8%

Snake River spring chinook survival 1966-1983

CRiSP was evaluated with survival estimates based on the brand release studies conducted between 1966 to 1983. These studies are informally knows as the Sims and Ossiander data after the report by Sims and Ossiander (1981) summarizing research between 1973 and 1979. The studies have been supplemented with information in Raymond (1979) and reports by the Coastal Zone and Estuaries Studies Division of the Northwest and Alaska Fisheries Center of NOAA for the years 1979 through 1983. These data cover a period prior to the construction of the Snake River dams above Ice Harbor Dam.

Because of the changes in the hydrosystem and differing research questions addressed over this period, release and recapture sites and the number of dams fish passed through changed from year to year. In the early years up through 1975 fish

were released at Whitebird or Riggins on the lower Salmon River. These are represented by a Whitebird release in the model (Fig. 74). Recovery sites included the upper dam in the Lower Snake River, a mid dam, which was typically Ice Harbor, and a downstream site which was either the Dalles Dam or John Day Dam on the lower Columbia River. In 1966 Ice Harbor dam was the only project on the lower Snake River (Table 70).

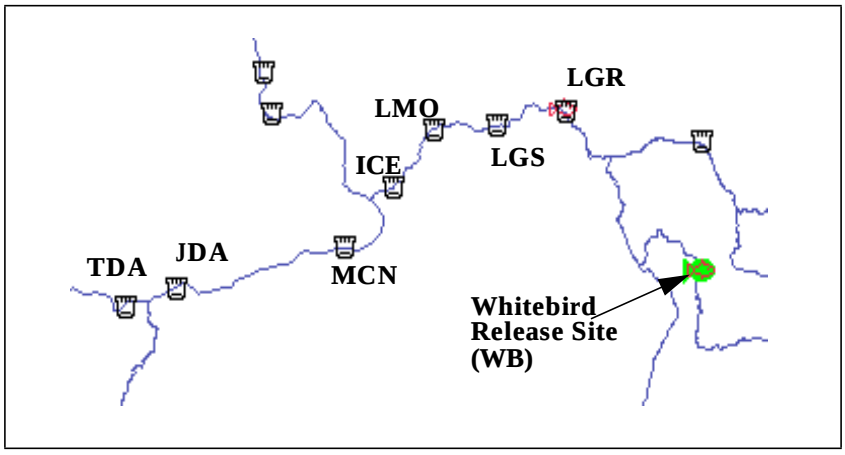

Fig. 74 Release and recapture sites of studies used to validate spring chinook survival from Snake River to lower Columbia.

Table 70 Dams in place during the survival studies.

Year	Upper dam	Dams between upper and lower dams	Lower dam
1966 - 1968	ICE	MCN	TDA
1969	LMO	ICE, MCN	TDA
1970	LGS	LMO, ICE, MCN	TDA
1971 - 1974	LGS	LMO, ICE, MCN, JDA	TDA
1975	LGR	LMO, ICE, MCN, JDA	TDA
1976 - 1983	LGR	LGS, LMO, ICE, MCN	JDA

A number of factors altered the mortality in passing through turbines and bypass systems. Debris accumulated in the forebay of the Snake River dams causing significant descaling and mortality. This trash was not removed on a regular basis until 1980 (Raymond and Sims 1980, Williams and Mathews 1995). Experimental slotted bulkheads were installed in Little Goose and Lower Monumental dams in 1972 to reduce gas levels. The action lowered gas levels but mortality through the bulkheads was high (Raymond 1979). In the model validation passage mortalities were adjusted for years where studies or estimates of survival were available (see Table 54).

Fish passage was also affected when new dams were brought on line (Raymond 1979) (Table 71). In the first year of operation at Lower Monumental and Little Goose dams the turbines were not in operation and the river was passed in spill. Because of the spill, Snake River supersaturations reached 120 to 140% and juvenile fish mortality

through gas bubble trauma was high (Raymond 1979).The survival studies covered 17 years and fish survivals were estimated in a variety of ways (Steward 1994). Between 1966 and 1979 survival was estimated from the number of fish passing Ice Harbor and the Dalles dams. Calculations were made from recoveries of juveniles that were marked and released in the Salmon River at hatcheries and in the forebays and tailraces of dams. In some years flow collection efficiency curves were used to estimate smolt passage at dams. In other years collection efficiency was estimated with forebay releases (Raymond 1979, Sims and Ossiander 1981). In years with transportation, accurate estimates of smolt survival were not possible because accurate estimates of the number transported were not available (Sims, Giorgi, Johnsen and Brege 1983).

Table 71 Hydraulic capacity of Snake and Columbia river projects (kcfs)

Year	BON	TDL	JDA	MCN	ICE	LMN	LGS	LGR	WEL	RRH	RIS	WAN	PRD
1966-68	136	239	NA	232	65	NA	NA	NA	220	220	220	178	187
1969	136	239	NA	232	65	0	NA	NA	220	220	220	178	187
1970	136	239	NA	232	65	65	0	NA	220	220	220	178	187
1971-72	136	239	322	232	65	65	65	NA	220	220	220	178	187
1973-74	136	375	322	232	65	65	65	NA	220	220	220	178	187
1975-77	136	375	322	232	106	65	65	65	220	220	220	178	187
1978	136	375	322	232	106	65	130	130	220	220	220	178	187
1979-82	136	375	322	232	106	130	130	130	220	220	220	178	187
1983-94	288	375	322	232	106	130	130	130	220	220	220	178	187
1995	288	375	322	232	66	130	130	130	220	220	220	178	187

To fit CRiSP to the survival estimates, the strategy was first to configure the model according to all relevant information on dam operations and passage conditions. Second, model dam passage parameters were adjusted to fit the reported dam passage information. Third, the model was fit to the survival information.

The river conditions, including daily river temperature and flows through the Snake and the Columbia, were set for all years. Hydrosystem operations for each year were also set; these included the number of dams, project hydraulic capacity (which reflected the number of turbines on line), reservoir elevation levels, spill on a daily basis, turbine and bypass mortalities reflecting projects, and the year with slotted bulkheads (Table 54).

Fish guidance efficiency estimates were obtained from a number of sources (see FGE Calibration section on page II.123). For transport dams the FGE was adjusted so the model predicted fraction of fish transported from the Snake River equaled the reported fraction (Table 72).

Table 72 Estimated and modeled Snake River transport results with adjusted FGE.[a]

Year	Snake River transport dams	Population size in millions		% transported from Snake River		FGE to fit transport %	
		Arrival at upper dam	Transport from Snake R.	Obs	Model	LGS	LGR
1971	LGS	4	0.109	3	3	9	0
1972	LGS	5	0.360	7	7	18	0
1973	LGS	5	0.247	5	7	7	0
1974	LGS	3.5	0	0	0	7	0
1975	LGS & LGR	4	0.414	10	10	12	7
1976	LGS & LGR	5	0.751	15	15	21	7
1977	LGS & LGR	2.3	1.365	59	59	47	47
1978	LGS & LGR	3.2	1.623	51	51	37	37
1979	LGS & LGR	4.3	2.10	51	51	33	33
1980	LGS & LGR	5.6	3.25	58	58	44	34
1981	LGS & LGR	3.2	1.55	46	46	29	29
1982	LGS & LGR	2.09	0.58	28	27	44	53
1983	LGS & LGR	3.9	1.0	26	26	44	46

a. 1971-1979 from Table 2 Smith Matthews Basham, Achord and McCabe 1980. For the years 1980 through 1983 results from Sims et al. 1981, 1982, 1983, 1984.

Spill was variable from year to year. During the construction of the Snake River dams spill was high because not all turbines were installed when the dams were completed. As a result, large spills were required in the early years of a dam's operation. The large spills generated high gas supersaturation. These were generally described by the model. The model-generated and reported ranges of supersaturation varied between 120% and 140% (Ebel Krcma and Raymond 1974; Ebel, Raymond, Monan, Farr and Tanonaka 1975; Raymond 1979). The effect of the gas depended on fish depth. The modal fish depth in the model was set at 12 ft. Observed chinook salmon depth varied between 5 and about 40 ft (Table 34 and Table 35).

Predator densities between the lower and upper dams were set by the predator densities studies (See Predator Density section on page II.67). For the years 1966 through 1968, prior to the construction of dams above Ice Harbor, predator density was set at 200 predators / sq km. Starting 1969 predator density above the upper most dam was set at the value observed for Lower Granite reservoir (440 predators / sq km).

References for validation of travel time and survival for the data from 1966 through 1983 is given in Table 73.

Table 73 References for survival and travel time studies

Ref #	Reference	Comment
0	Sims Bentely and Johnsen 1978	Table 2 and 3
1	Raymond 1979	
2	Sims and Raymond 1980	
3	Sims and Ossiander 1981	table 3 and page 9
4	Sims, Williams, Faurot, Johnsen and Brege 1981	Rapid River release RA IU
5	Sims, Johnsen and Brege 1982	
6	Sims, Giorgi, Johnsen & Brege 1983	Table 2 release RD IU 1 release RD SU 2
7	Sims, Giorgi, Johnsen & Brege 1984	Table 2

The observed median date of arrival of fish at dams and model fit are given in Table 74. For all years except 1973 and 1977, the two lowest flow years, a fit within a few days was obtained by adjusting the model parameter T_{seasn}. This parameter characterizes how quickly the flow dependent component of migration increases over season. A pattern emerged with T_{seasn}. Prior to hydrosystem development above Ice Harbor dam, 1966 through 1969, the T_{seasn} required to fit the migration data was early, Julian day 127 (May 7). In these years fish were predominately wild and their migration behavior was characteristically different from hatchery fish (Zabel 1994). Beginning in 1970, the hatchery contribution of fish migrating through the Snake River increased from less than 20% to over 40% (Raymond 1979) and the median arrival time at Whitebird trap was later by a week. This is coincident with a change in T_{seasn}: the model-fitted smoltification date was later, T_{seasn} = Julian day 160 days (June 9). From 1976 onward the median arrival data of the fish at the Whitebird trap was earlier by one to two weeks and the smoltification date again changed to T_{seasn} = Julian day 135 to 140 (May 15 to 20).

In 1973 and 1977 fish moved significantly slower than in all other years and the arrival time at dams could not be fit by adjusting T_{seasn} only. In both these years a good fit to the data was obtained by adjusting the maximum flow independent migration rate β_{max}. In contrast, for all years except 1973 and 1977 β_{max} = 20.2 miles / day. In 1973, to fit the observed arrival dates the parameter had to be reduced to 6 miles / day signifying a three fold decrease in the maximum flow independent component of migration. In 1977 β_{max} was set to β_{min}, which is the initial flow independent migration speed. In the model β_{min} = 1.34 miles / day which infers that the minimum initial migration speed, independent of any contribution of current, would be 1.34 miles / day. This suggests that migration rate was constant and very slow in 1977. The analysis indicates that travel time under these two low flow years was abnormal.

Several biological reasons for slow migrations are possible. Fish in poor condition in 1973 and 1977, due to descaling at dams and high water temperatures, may have been less likely to migrate. Also, a reduced spring freshet in these years may have affected migration speed. An adequate environmental signal required to initiate migration might not have occurred in these two years. As a result, the spring chinook could have drifted through the river system much like subyearling chinook.

Table 74 Spring chinook median Julian day of arrival at dams, observed and model plus the model parameters adjusted to obtain the fit. References (Ref) are given in Table 73

Year	Rls date	Upper dam		IHR		Lower dam		βmax	T_{seasn}	Release site[a] - Upper dam - Lower dam	Ref.
	Obs	Obs	Model	Obs	Model	Obs	Model				
1966	110	124	124					20.2	127	WB-IHR-TDL	1
1967	110	125	125					20.2	127	WB-IHR-TDL	1
1968	110	126	125					20.2	127	WB-IHR-TDL	1
1969	No data							20.2	127	WB-LMO-TDL	1
1970	96 105 110 126 135	127 131 133 139 146	117 123 127 139 145					20.2	160	WB-LGS-TDL	1
1971	88 96 105 111 120	121 123 122 125 131	108 112 119 124 132					20.2	160	WB-LGS-TDL	1
1972	76 96 111 121 126	114 116 130 133 140	99 112 124 133 136					20.2	160	WB-LGS-TDL	1
1973	115	134	132	141	142	156	156	6	140	WB-LGS-TDL	3
1974	115	121	121	126	126	133	135	20.2	160	WB-LGS-TDL	3
1975	117	137	133	141	141	149	149	20.2	160	WB-LGR-TDL	3
1976	99	111	112	118	119	128	127	20.2	135	WB-LGR-JDA	3
1977	108	129	129	146	153	168	168	1.34	130	WB-LGR-JDA	0,3
1978	104	119	118	125	125	132	133	20.2	135	WB-LGR-TDL	3
1979	108	124	124	131	131	139	139	20.2	140	WB-LGR-TDL	3
1980	105	119	119			132	133	20.2	135	RR.-LGR-JDA	4
1981	106	118[b]	121			134	133	20.2	135	WB-LGR-JDA	5
1982	106	119	120	128[c]	128	134	132	20.2	140	SC-LGR-JDA	6
1983	103	116	117	128[b]	127	130	131	20.2	135	SC-LGR-JDA	7

a. Release sites are Whitebird (WB), Rapid River(RR) and Salmon Creek (SC)
b. peak migration date
c. McNary Dam

A graphical comparison of observed and fitted arrival times is illustrated in Fig. 75. The points falling below the on-to-one line are arrival data from 1970, 1971, and 1972, which have some early fish release groups. It is likely that for these years fish released prior to Julian day 110 were not ready to migrate and consequently their

migration was delayed. For these years the release group in the middle of the migration season had predicted and observed arrival dates within 1 day (Table 74).

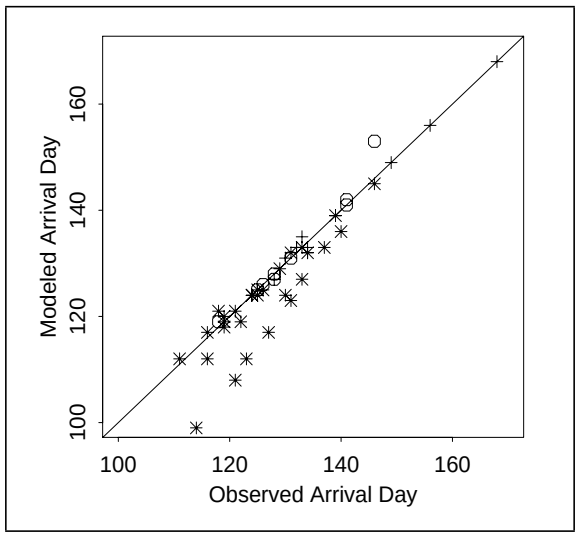

Fig. 75 Comparison of observed and model predicted median arrival days at upper dam (✻), Ice harbor dam (o) and lower dam (+) for years 1966-1982. (See Table 70 for specific dam)

Survivals were estimated from the CRiSP model once travel times were fit. Model survivals were computed as reported in the corresponding survival studies (Table 73). The equation was

$$S = \frac{\text{fish entering lower dam}}{\text{fish entering upper dam} - \text{fish transported between dams}} \qquad (172)$$

This equation does not correctly represent the effects of transportation on estimated survivals. Generally, the difference in total system survival would be upwards of 25% if transport were correctly estimated. For example, in 1982 between LGR and JDA dams an in-river survival of 41% using eq(172) becomes 50% when computed as the in-river survival without transportation. The difference is less when percent of fish transported is less. For comparing observed and model survivals eq(172) can be used as long as both observed and model survivals are reported using the same equation.

The resulting model survivals were close to the observed values (Table 75). For the years 1969 through 1983 no additional model parameters were altered other than; 1) fitting the travel time, 2) adjusting the model to the reported dam passage conditions discussed previously, 3) using the observed river temperature and flow. To fit survival between release site and the upper dam for 1966-1969 the predator density above Ice Harbor dam was set at 200 predator / sq km. This represents a density 50% lower than is estimated for the present levels in Lower Granite reservoir.

These survival estimates cover years with a wide variety of project operations and river conditions. Gas supersaturation levels in the 1970's reached 140% in the river and sometimes accounted for half of the fish mortality in passage (Raymond 1979). The model captures this effect.

Between 1966 and 1968 survival was high because the Snake River above Ice

Harbor was free-flowing. Between 1969 and 1974 survival was low because of dam construction on the Snake River and the need to spill at the new dams that did not have their full complement of turbines. The year 1973 did not have spill problems but mortality was high because fish migration was anomalously slow so fish experienced high exposure to predators.

Table 75 Survival observed and modeled from branded fish survival studies. Reference(Ref) are given in Table 73

Year	Release to Middle dam		Upper to Middle dam		Middle to Lower dam		Upper to Lower dam		Release.site[a]-Upper.dam-Middle.dam-Lower.dam	Ref
	Obs	Model	Obs	Model	Obs	Model	Obs	Model		
1966	85	86[b]					63	61	WB-IHR-IHR-TDL	1
1967	85	86[a]					64	61	WB-IHR-IHR-TDL	1
1968	95	84[a]					62	59	WB-IHR-IHR-TDL	1
1969			75	88	62	64	46	56	WB-LMO-IHR-TDL	1
1970	28	27	33	39	67	53	22	21	WB-LGS-IHR-TDL	1
1971	50	33	48	48					WB-LGS-IHR-TDL	1
1972	32	31	39	44	42	30	15	13	WB-LGS-ICE-TDL	1
1973	10	11	12	18	42	45	5	8	WB-LGS-ICE-TDL	1
1974	41	50	50	65	71	45	34	29	WB-LGS-ICE-TDL	1
1975	36	35	36	51	69	53	25	27	WB-LGR-ICE-TDL	1
1976			63	64	69	69	30	45	NA-LGR-ICE-JDA	0,3
1977	4	3.5	17	13	20	31	3	4	WB-LGR-ICE-JDA	0, 3
1978			69	65	64	75	44	48	NA-LGR-ICE-JDA	2, 3
1979		23	43	45	72	75	30	31	NA-LGR-ICE-JDA	2, 3
1980	46[c]	70	49	51	74	85	36	39	RR.-LGR-MCN-JDA	4
1981		30		53		86		32	NA.-LGR-MCN-JDA	
1982	- 56 43	- 56 41	34	54	68	88	23	41	NA-LGR-MCN-JDA CC to LGR SFS to LGR	6
1983			69	42	90	87	62	36	NA-LGR-MCN-JDA	7

a. Release sites: Whitebird (WB), Rapid River(RR), Clear Creek (CC) Salmon Creek (SC), South Fork Salmon (SFS)
b. Predator density = 200 above ICE which is 50% of densities after 1968. Using predator density of 442 makes Tributary to ICE survival of 75%.
c. Survival measured from Rapid River to LGR.

The relationship between modeled and observed survivals between release site and the lower dam is illustrated in Fig. 75. A linear regression of 43 data points allowing for an intercept has an $r^2 = 0.806$, a slope of 0.88 and an intercept of 6.4%. Confining the regression to a zero intercept the slope becomes 1.004 and the $r^2 = 0.957$.

These regressions suggests that the CRiSP model provides a good fit to survival data between the Salmon River and the lower Columbia. Of particular note are the low flow years 1973 and 1977. The observed and predicted survivals in these years were closely fit by adjusting the seasonal flow independent component of migration. This is an indication that the low survivals were a result of changes in fish migration behavior, which were independent of the flow itself. For example, in 1977 survival between Whitebird and John Day dam was 1.1%. If fish migratory behavior was not abnormally slow the survival would have been 7.3%. For comparison survival between Whitebird and John Day in 1983, a good flow year, was 25%. Thus in 1977, flow of its own accounts for a decrease in survival by a factor of 3 while fish behavior accounts for an additional decrease by a factor of 7.

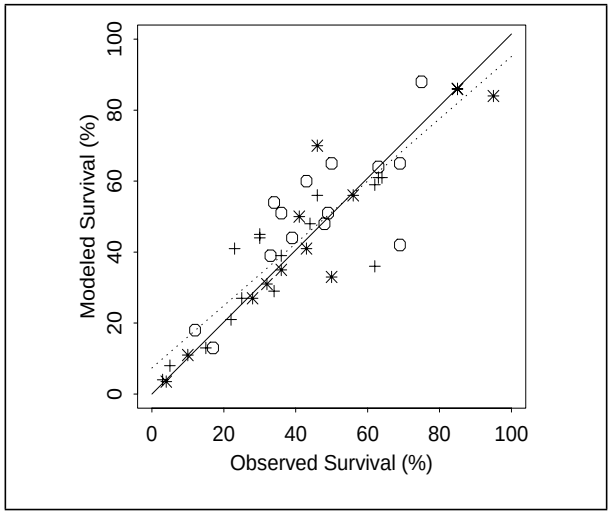

Fig. 76 Comparison of observed and model predicted survival from release site to Ice Harbor dam (✳), upper dam to middle dam (0), and upper dam to lower dam (+) for years 1966-1983. (See Table 70 for specific dams). The solid line is least squares regression with a forced zero intercept and the dotted line is a least squares regression allowing for an intercept.

Below Bonneville spring chinook survival

Data giving a minimum estimate of survival below Bonneville Dam was available to evaluate CRiSP in the lower river. Shreck et al. (1994) conducted a radio-tag study on spring chinook in this area in 1994. Fish were released at the Bonneville tailrace and were observed at a monitoring station 86 miles downstream (Fig. 77).

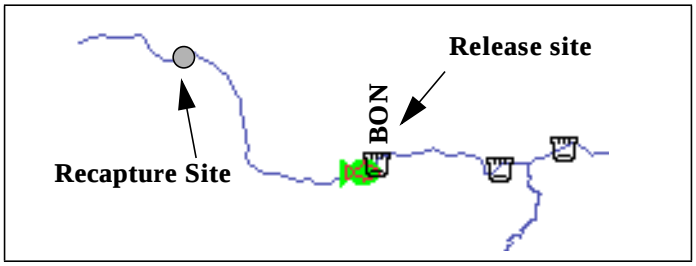

Fig. 77 Release and recapture locations for data used to validate lower river survival of spring chinook.

The survival estimates are “minimal” for several reasons. First, the fish were tagged at Lower Granite and then transported to the Bonneville tailrace. Upon release, some of the fish (2.5-10.0%) were never detected. It was not known whether this was due to tag failure, transportation mortality, or the inability to detect all the fish. Also, it is possible that some of the fish passed the downstream monitoring site without being detected. Also, travel time estimates may be biased downward because only larger fish (average fork length of 139 mm) were used in the study and the monitoring site was only operating for 4 days after release so some of the fish may have passed after monitoring concluded and would not be included as survivors.

The results and model comparison are given in Table 76. Model survivals are 12-18% higher than the “minimal” survivals, and model travel times were 1.2 days longer than reported by Schreck et al. (1994). These results are consistent with expectations, given the sources of bias indicated above.

Table 76 Comparison of CRiSP and radio tag based data from fish tracking studies conducted below Bonneville Dam[a]

	Obs May 11	CRiSP	Obs May 23	CRiSP
ave. TT	~2.5 days	3.7 days	~ 2.0 days	3.2 days
Survival	72.5	90.8	77.5	89.9

a. Schreck, C.B., L.E. Davis, D. Kelsey and P.W. Wood. 1994. Evaluation of facilities for collection, bypass and transportation of outmigrating chinook salmon. Draft annual report to U.S. Army Corps of Engineers by Oregon Coop. Fish. Res. Unit, Oregon State University, Corvallis

III.4.3 -Steelhead survival

Snake River steelhead survival

Survival predictions of steelhead in the Snake River were evaluated against survival estimated in the 1994 PIT tag study (Muir et al. 1995) (Fig. 78). The results of the validation are given in Table 77. Travel time parameters were set according to the calibration given in Table 11. Travel time was not adjusted to specifically fit the steelhead PIT tag data. In all reaches of the river the CRiSP predicted estimates of survival were lower than the PIT tag based survival estimates.

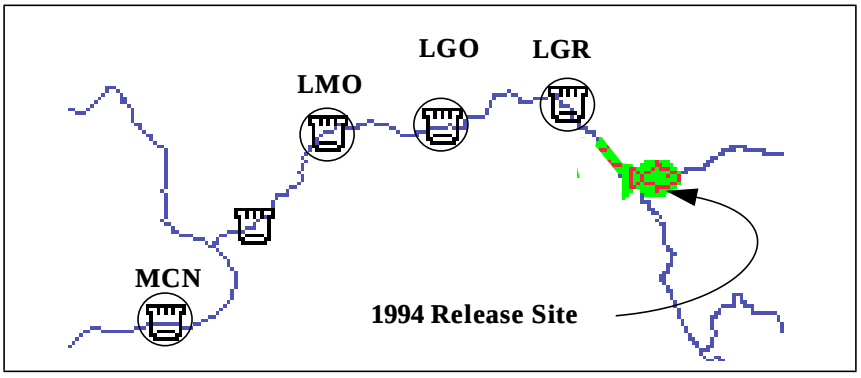

Fig. 78 Location of release and collection sites for steelhead in the 1994 survival studies. Collection sites are Lower Granite Dam (LGR), Little Goose Dam (LGO), Lower Monumental (LMO) and McNary Dam (MCN).

Table 77 Observed and predicted for steelhead survivals in Lower Granite reservoir from the 1994 PIT tag studies.

Reach	Survival (%)		Travel time (days)	
	CRiSP	OBS	CRiSP	OBS
Release to LGR tailrace	80	90.4	4.5	4.3
LGR tailrace to LGS tailrace	79	78.4	3.5	5.1
LGS tailrace to LMO tailrace	76	83.1	2.0	3.1
Release to LGS tailrace	63	71	8.0	9.4
Release to LMO tailrace	48	60	10.0	12.5

Sims and Ossiander steelhead study

Sims and Ossiander's (1981) compilation of yearly survival studies from the 1970's was used to compared CRiSP-estimated juvenile steelhead survivals (Table 78). In general, observed survivals vary considerably from year to year, but model estimates were less variable. Modeled and observed survivals agreed, although results for 1977 appear to be unusual. Note that the two low-flow years, 1973 and 1977, produce extremely high travel times which are not matched by the model, although CRiSP provides an excellent fit to travel time observations in other years. These characteristics were also observed in the spring chinook. Note that in 1973 and 1974 reports, actual numbers of fish collected are reported, but in 1975-1977, only estimated numbers of fish passing dams are reported.

Table 78 Observed and modeled survivals for Dworshak Hatchery steelhead.

Year	Site	Arrival Date		Counts	
		Obs	Model	Obs	Model
1973	LGS	--	--	17565	24999
	IHR	5/24	5/15	1293	1628
	TDA	--	5/24	592	978
1974	IHR	5/12	6/4	893	1205
	MCN	--	5/12	319	872
	TDA	5/21	5/16	35	53
1975	IHR	5/23	5/20	1700000 (est)	1632956
	TDA	5/31	5/23	1100000 (est.)	836004
1976	IHR	5/6	5/29	1800000 (est.)	1664916
	JDA	5/15	5/5	900000 (est.)	1102973
1977	IHR	--	5/13	100000 (est.)	217528
	TDA	6/18	5/21	10000 (est.)	33576

Mid-Columbia steelhead survival

Steelhead survivals estimates in the mid-Columbia were available from mark-recapture experiments conducted in the 1980s. Steelhead smolts released in the Methow River and below Priest Rapids Dam were recaptured at McNary Dam (Fig. 79). This gave survival estimates from the Methow River to below Priest Rapids Dam. The data are given in McConnaha and Basham (1985) and Fish Passage Center (1986, 1987). CRiSP as calibrated provided a good fit to observed travel times, but underestimated survival by 30 to 40%. It is worth noting, however, that survival estimates depend critically on the assumption of "equal risk" for test and control releases; in the same study, similar test/control experiments were performed for steelhead in the lower Snake River, and recoveries were such that survival for the test group was estimated to be over 100% for two years running. Obviously, survival estimates using this protocol were variable. In 1986, fish were also collected at John Day Dam, providing a second estimate of survival (39%), and this estimate differs considerably from that obtained at McNary Dam (73%). Considering that the CRiSP-derived estimate falls between these two estimates (43.4%), we believe that while steelhead survival demands further investigation. In 1985 and 1986, observations were made at Rock Island Dam as well; Table 79 gives CRiSP fits to those data also.

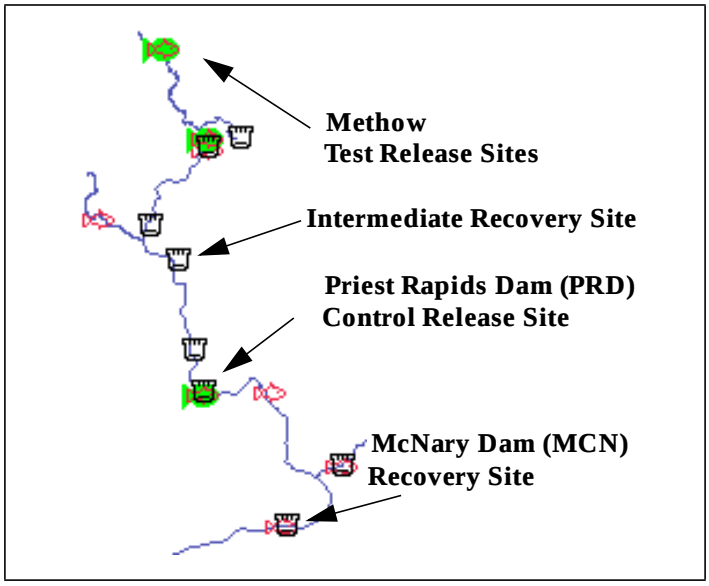

Fig. 79 Mid-Columbia release and recovery sites for steelhead survival studies

Table 79 Data for steelhead survival studies from mid-Columbia.

	1984		1985		1986	
Release date	4/23		5/6-5/14		5/1-5/9	
	Obs	CRiSP	Obs	CRiSP	Obs	CRiSP
Median arrival date RIS	NA	-	5/18	5/17	5/15	5/13
Median arrival date MCN	5/11	5/13	5/25	5/23	5/21	5/18
Survival to PRD	51.8%	40.7%	73.0%	52.1%	72.2%	49.5%

III.4.4 -Summary of validation with survival studies

Spring chinook

Yearling chinook provide the largest number of studies for comparison, as well as broad geographic coverage. In general, model predictions of survival are in excellent agreement with the survival observations in three regions of the river system: the Snake River, mid-Columbia, and below Bonneville. All of the model-estimated survivals are plotted against observed survivals in Fig. 80; the fit appears excellent, and the regression, though not forced through the origin, is highly significant and close to a one-to-one line (modeled survival (%) = 5.05 + 0.94*(observed survival), $r^2 = 0.86$).

The validation of the model with the survival studies from brand releases of fish between 1966 and 1983 for the Snake River and 1984 through 1986 in the Upper Columbia indicates that for this species the model fits the survival pattern in the years that the hydrosystem was being completed.

It appears that in many of the PIT tag studies that fish, following tagging, were sedentary for a time, ranging from a few days to a few weeks, during which they were presumably acclimating to the presence of a PIT tag. Observations suggest that tagged fish took a longer time to arrive at the first collection point but afterwards their migration rate increased. We found that delaying movement of yearling chinook for a time after actual release produced model predictions that were close to observations.

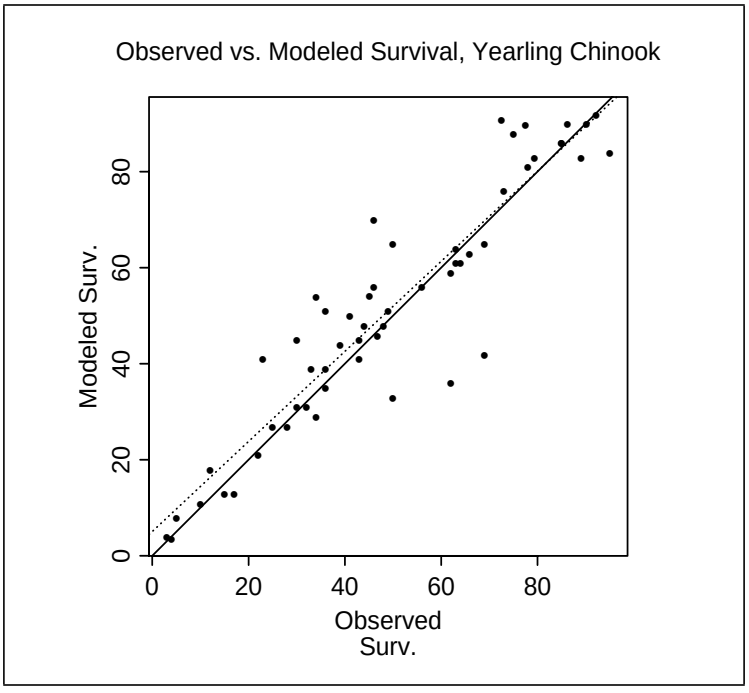

Fig. 80 Graph of all yearling chinook survival validation efforts. Solid line is a one-to-one relationship, the dotted line is a linear regression.

Fall chinook

Data to evaluate the ability of the model to predict fall chinook survival was limited, reliant on assumptions and constrained by uncertainties in the analysis. Even so, the model does provide a consistent representation of Snake River and mid-Columbia fall chinook during their in-river migration. The analysis also suggests that temperature is an important factor in fall chinook survival. Some of the inconsistencies between the modeled and observed survival may be resolved with better temperature modeling. Modeled and observed survivals are plotted in Fig. 81; the fit is not particularly good, and the regression line suggests a bias toward overestimating survival at the low end and underestimating at the high end {modeled survival (%) = 13.71 + 0.64*(observed survival), $r^2 = 0.67$}. We suspect that making model parameters more stock-specific (i.e. distinguishing the different travel time properties of Snake and mid-Columbia stocks) will improve the fit.

The CRiSP model was not able to predict fall chinook survival between the time they were tagged in their juvenile habitat and arrived at Lower Granite dam. Preliminary work does suggest that the timing of arrival can be predicted from accumulative temperature but survival predictions remain problematic.

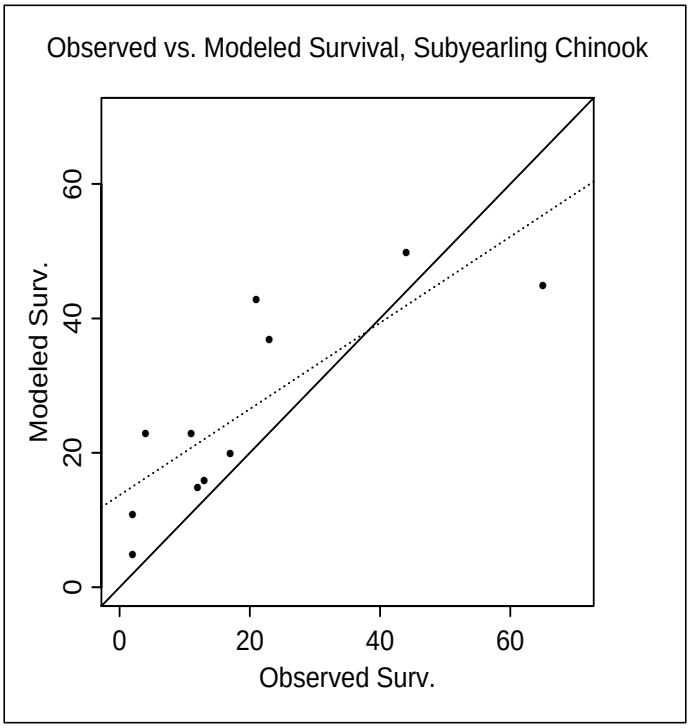

Fig. 81 Graph of all subyearling chinook survival validation efforts. Solid line is a one-to-one relationship, the dotted line is a linear regression.

Steelhead

Data for steelhead comparisons are neither as abundant as for yearling chinook, nor as sparse as for subyearling chinook. CRiSP comparisons, to 1994 PIT tagged fish from the NMFS survival study and mid-Columbia brand releases from 1984-1986,

produce consistently good fits with regard to travel time, but equally consistently underestimate survival. Because travel time fits are adequate, it appears that the current calibration overestimates the rate of mortality suffered by steelhead as they travel through reaches (but we note that the 1994 NMFS survival study provides estimates of lower survival for steelhead than for yearling chinook, contrary to expectations; Muir et al. 1995). At the same time, fits to survival data from the 1970's in the Snake River provide excellent agreement to travel times and good fits to survivals. Future calibration work will take this into account, and model estimates of survival will be adjusted to provide agreement to all available data. Modeled and observed survivals for steelhead are plotted in Fig. 82; the tendency for slight overestimation of survival at the low end produces a moderately large intercept in the regression {modeled survival (%) = 4.74 + 0.80*(observed survival), $r^2 = 0.94$}, but the attenuation of the data provide an excellent overall fit. Here, as with subyearling chinook, our analysis will benefit from distinguishing behavioral components that differ among the various steelhead stocks in the river system.

Steelhead, due to their size, are also more vulnerable to gas bubble-based mortality than are chinook salmon. This may be a source of overestimation of mortality, and will also be examined.

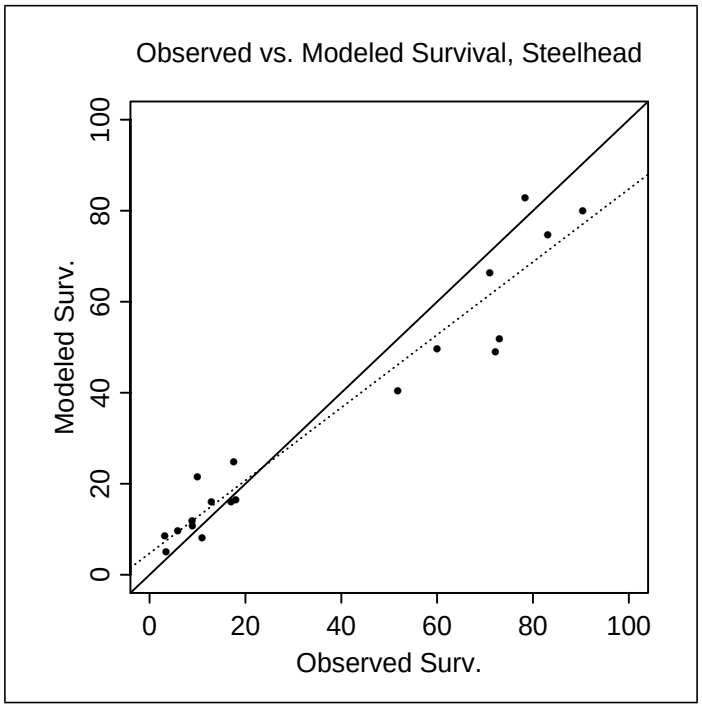

Fig. 82 Graph of all steelhead survival validation efforts. Solid line is a one-to-one relationship, the dotted line is a linear regression.

Summary of fits to survival estimates

The difference between the predicted and observed survival can be expressed in terms of a generalized fitting measure: the percent difference between the two survival estimates relative to the observed survival estimate. This is expressed as the FIT measure and is defined

$$FIT = 100\left(1 - \frac{S_{CRiSP}}{S_{Obs}}\right) \quad (173)$$

Values of FIT greater than zero imply that observed survivals exceed model predicted survivals, while negative values imply the model predicted survivals higher than observed. The mean and standard deviation of the FIT measure is illustrated in Table 80.

Table 80 Comparison of observed and CRiSP predicted survivals

Species	Location	Source of Obs	Date of Obs.	FIT mean (FIT std)
fall chinook	Priest Rapids Hatchery to entry in fishery	Hilborn (1993)	1977 -1987	- 64% (113%)
	Snake River	PIT tag data base	1991 -1994	95% (150%)
spring chinook	Methow River to Priest Rapids Dam	FPC (1988)	1985 - 1987	-10% (2%)
	Snake River to Little Goose Dam Lower Monumental	Iwamoto et al (1994) Muir et al. (1995)	1993 - 1994	3% (9%)
	Salmon River to Lower Columbia River dams	Raymond (1979) Sims and Ossiander (1981) Sims et al 1981-82, 83, 84	1966 - 1983	2% (25%)
	Below Bonneville Dam	Schreck et al. (1994)	1978	- 22% (7%)
steelhead	Snake to Lower Monumental Dam	Muir et al. (1995)	1994	10% (8%)
	Methow River to Priest Rapids Dam	Smolt Monitoring Reports	1984 -1986	33% (8%)

III.5 - Transportation validation

A validation of transportation calibration was initiated by comparing model predicted measures of TBR to observed TBR values from transportation experiments conducted between 1968 and 1987. The analysis is preliminary at this time. Information was obtained by Fisher (1993).

Table 81 Estimated and Observed transport benefits ratios (TBR) for experiments conducted in the Snake River (Fisher 1993).

Year	Species	$TBR_{estimated}$	$TBR_{observed}$
1968	spring	1.50	1.57
1969	spring	1.77	0.96
1969	steelhead	1.93	2.75
1972	spring	8.95	1.10
1973	spring	8.23	16.08
1975	spring	3.15	2.02
1975	steelhead	3.21	3.61
1976	spring	4.92	1.17
1976	steelhead	3.21	2.66
1977	spring	31.74	NA
1977	steelhead	7.04	NA
1978	fall	2.57	5.16
1978	spring	2.10	3.68
1978	steelhead	2.89	4.83
1979	fall	3.18	6.29
1979	spring(lgs)	1.72	3.42
1979	spring(mcn)	1.76	0.64
1979	steel(lgr)	1.59	1.78
1979	steel(mcn)	1.96	NA
1980	fall	2.73	3.63
1980	spring(mcn)	1.48	3.33
1980	steel(mcn)	1.41	NA
1980	spring(lgs)	1.88	NA
1980	steel(lgs)	2.38	1.71
1981	fall	2.24	3.63
1982	fall	2.84	0.99
1982	fall	2.54	4.88
1982	fall	2.25	1.30
1983	fall	2.53	2.10
1983	fall	2.94	2.60

Table 81 Estimated and Observed transport benefits ratios (TBR) for experiments conducted in the Snake River (Fisher 1993).

Year	Species	$TBR_{estimated}$	$TBR_{observed}$
1983	fall	3.07	5.95
1984	fall	2.81	NA
1984	fall	3.02	NA
1984	fall	2.98	NA
1985	fall	3.49	NA
1985	fall	3.13	NA
1985	fall	2.93	NA
1986	steelhead	2.09	1.99
1986	fall	3.45	2.05
1986	spring(mcn)	1.42	0.73
1986	spring(lgs)	1.86	1.58
1987	spring(mcn)	1.48	1.73
1987	fall	3.23	3.68
1988	spring(mcn)	1.47	NA
1988	fall	3.11	NA
1989	spring	1.75	2.46
1988	steelhead	2.03	2.19

For the comparison a measure of river passage effects on transportation was computed using the equation

$$TBR_{estimated} = T \cdot \frac{S_{BON}}{S_{\text{from tansport dam}}} \tag{174}$$

where

- T = total transport survival from transport dam. In this analysis T was set to 1 so the TBR measure does not include transportation effects
- $S_{\text{from transport dam}}$ = model in river survival for fish from tailrace of transported to the estuary
- S_{BON} = model survival from Bonneville Dam tailrace to estuary.

The resulting correlation for all species and years between the observed TBR and the estimated TBR measure is illustrated in Fig. 83. A linear regression gives the relationship

$$TBR_{estimated} = 1.90 + 0.29 \cdot TBR_{observed} \tag{175}$$

Notice that the regression indicated that the estimated TBR underestimates observed TBR. Since the estimated TBR assumes a 100% transport survival factor the regression would suggest that actual fish survive better than predicted by the model. At the same time, note that the regression is very strongly affected by the outlier of 1973, where the observed TBR was over 16.

If we examine only the TBR below the mean of the estimated and observed TBR, both values are equal at 2.2. This additional information could be interpreted in one of several ways. The model could overestimate in-river survival in years with large TBRs or in years with large TBR the handling of the fish in the control groups produced additional mortality that was not represented in the model. In either scenario the fish transportation from model analysis and observations seems to produce survivals greater than could be obtained for in-river migration. Large TBR values are generally based on very small sample sizes and are therefore cannot be considered very robust. Fits for years with substantial recoveries are considerably better. Results of this analysis are preliminary and additional work will be conducted at a later date.

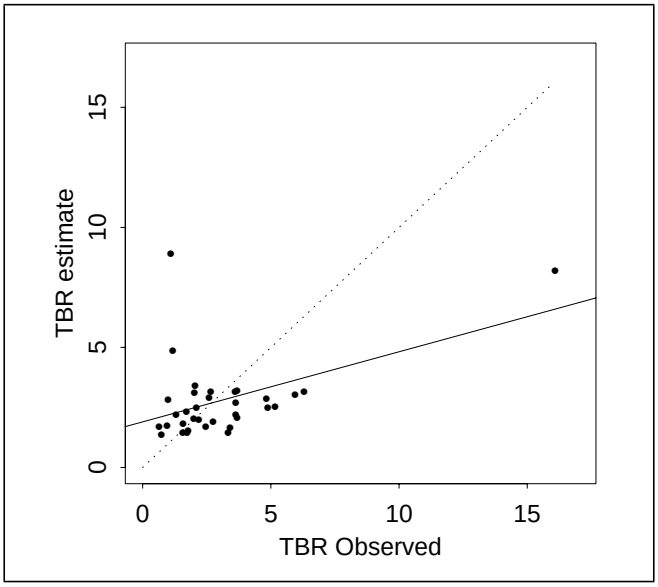

Fig. 83 Comparison of estimated and observed TBR for all species (chinook subyearling and yearling and steelhead) for years 1968 - 1987.

IV. Sensitivity Analysis

IV.1 - Description

CRiSP.1 version 5 (CRiSP.1.5) is a complex model, with hundreds of parameters. It is impossible to examine the potential interactions of all of these parameters. Consequently, sensitivity of fish survival for a number of single parameters is evaluated independently, as well as for several potentially interesting pairs of parameters.

In general, sensitivity is determined by first obtaining some baseline output - the survival of some arbitrary species under arbitrary model conditions. Individual parameters are then changed to some reasonable limit values, while all other parameters are held constant, and the resulting impact on model output is recorded. For pairs of parameters, several values for each parameter are chosen and the output for all possible combinations is recorded.

Analysis of the individual parameters are presented as graphs of survival as a function of the parameter, and pairs of parameters are shown as similar response surfaces in three-dimensional space.

Time-dependent and time-independent parameters

The parameters in CRiSP.1 fall into two categories: those that vary over the season of migration (e.g. flow, temperature, migration characteristics) and those that do not vary over the season (e.g. dam mortality components, predator density). Some of the parameters will not produce any change in model output. For example, if flow and temperature are held constant; it makes no difference when fish are released if there is no seasonal variation.

Most parameters were analyzed under constant conditions, that is, without seasonal variation. Variation was added when considering variables that would be meaningless without it.

Analysis of single parameters

The model was initiated and run using 1993 parameter values, except for dam survival-related parameters (turbine, bypass, spillway, and transport mortality) and *FGE* values, both of which were assigned based on calibrated values (see FGE Calibration section on page II.123 and Dam Passage Survival section on page II.135). A single release of yearling (spring) chinook was input into the model at the head of Lower Granite Pool, and survival to Bonneville Dam, or to the estuary, was recorded. The effects of variation in:

- reach predator density
- forebay predator density
- tailrace predator density
- predator activity exponent
- Velocity variance (Vvar)
- Migration rate parameters

- Turbine mortality
- Bypass mortality
- Spillway mortality
- Transport mortality
- Fish Guidance Efficiency
- Total Flow (no seasonal variation)
- Temperature (no seasonal variation)
- Spill (same fraction at all dams)

have been examined. Note that because predation is determined by a multiplicative combination of predator density and predator activity coefficient, varying one of these two parameters gives identical results to varying the other; here predator density was varied rather than the activity coefficient.

IV.2 - Results

Results for the single-factor sensitivity analysis are shown in Fig. 84 through Fig. 88, and the three two-way interactions examined are shown in Fig. 93 through Fig. 95.

Flow and temperature

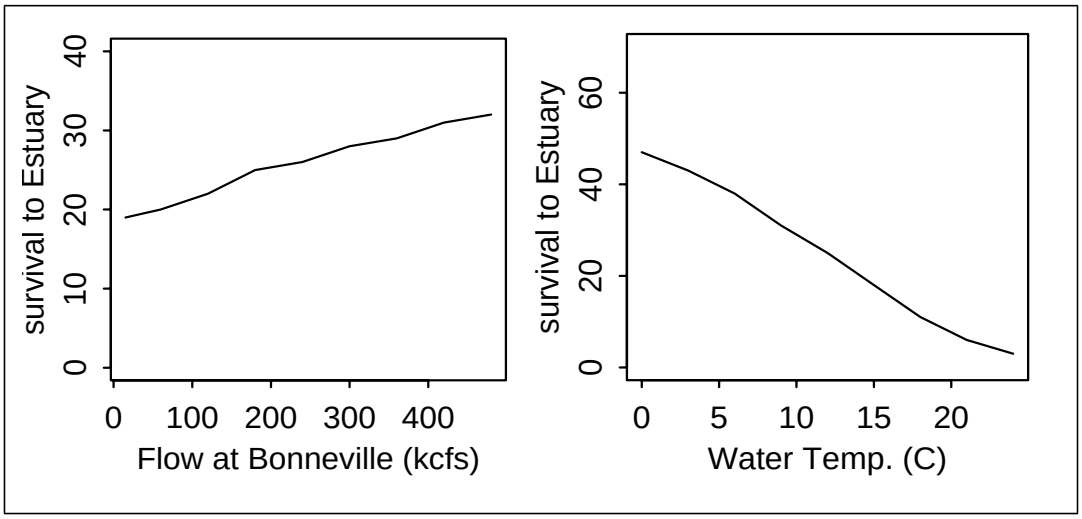

Fig. 84 Survival as a function of total system flow and water temperature

Fish guidance efficiency

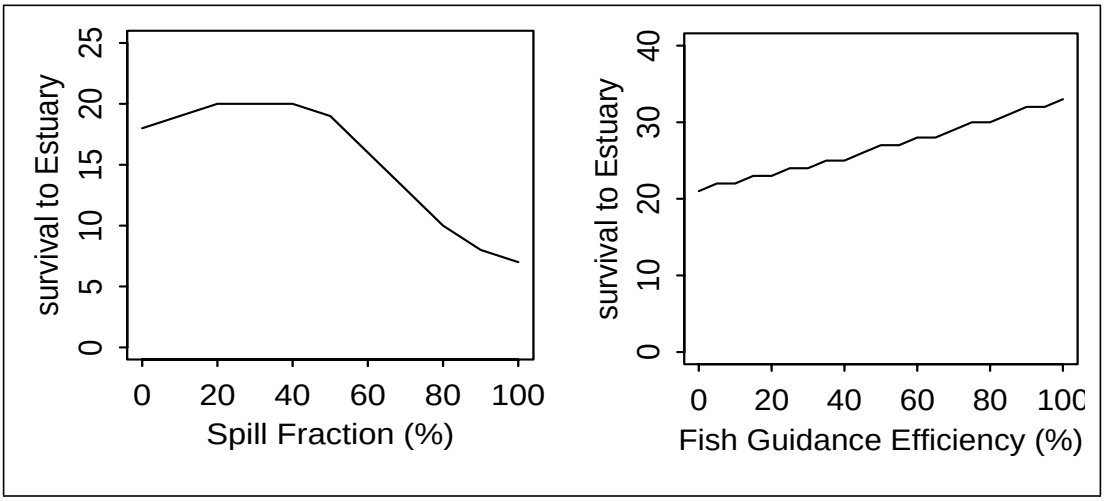

Fig. 85 Survival as a function of spill fraction, and fish guidance efficiency held constant at all dams at once

Predator density

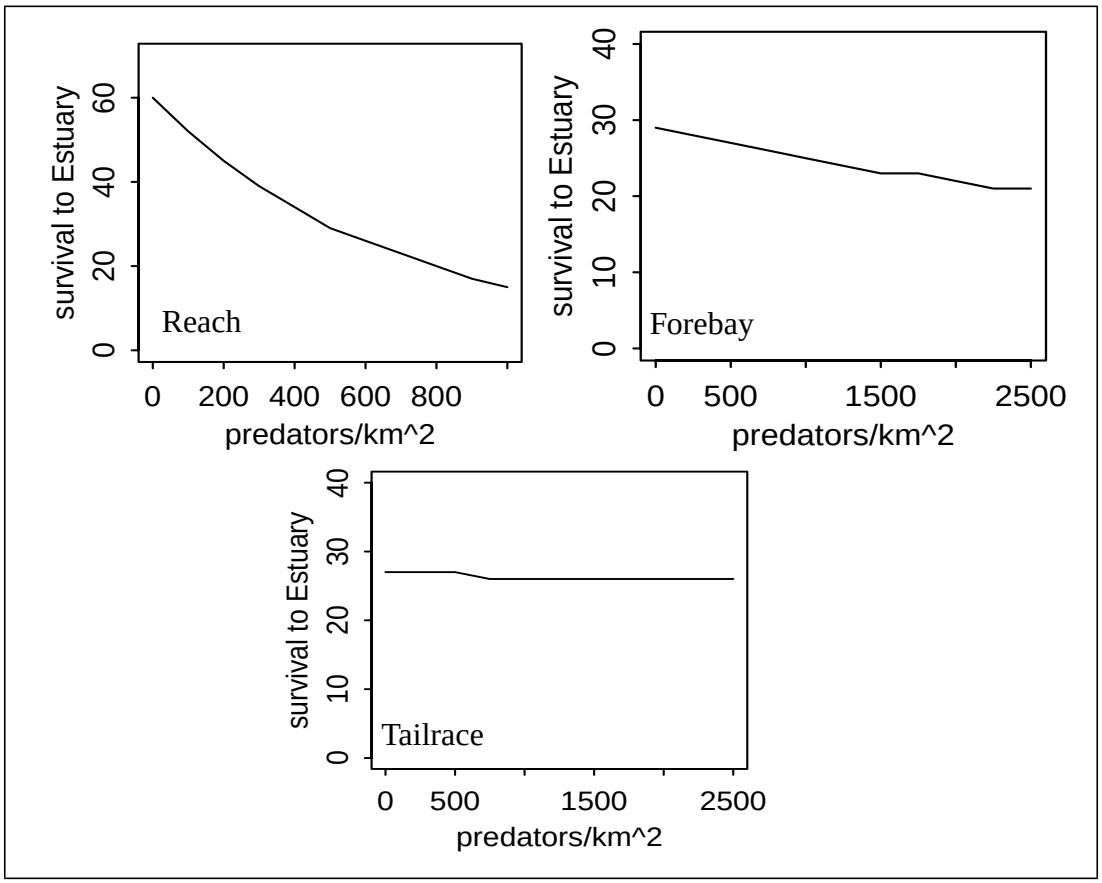

Fig. 86 Survival as a function of predator density in river reach, dam forebay, and tailrace

Predator activity and velocity variance

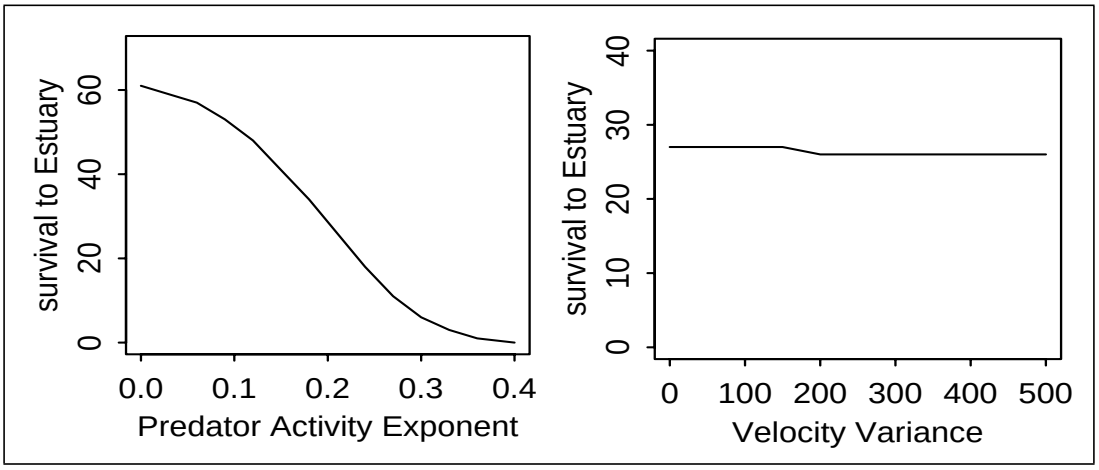

Fig. 87 Survival as a function of predator activity exponent and velocity variance

Dam passage mortalities

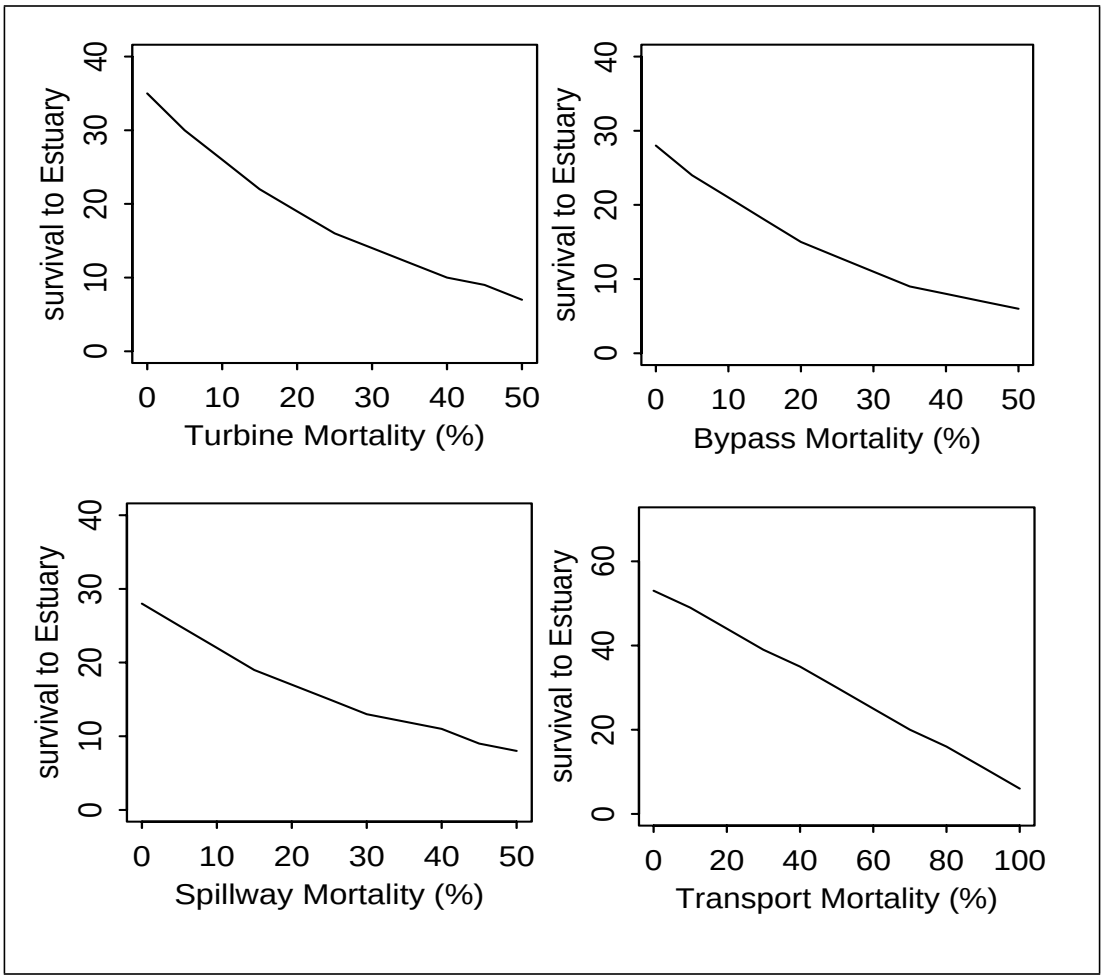

Fig. 88 Survival as a function of dam passage mortalities.

Analysis of Migration Equation parameters

Much of the behavior of the model depends on the parameters used to describe fish movement within the system, and many different stock behaviors can be produced by varying one or several of these parameters. We have examined the impact of changing four parameters in particular:

- β_{min} = the initial downstream velocity of smolts
- β_{max} = the final downstream velocity of smolts
- T_{seasn} = date of the inflection point in the flow related term of the migration rate equation
- Smolt Start / Stop Date = the date at which fish begin migration down the hydrosystem.

For the purposes of this analysis, fish were released at the head of Lower Granite Pool, using the standard set of travel time parameters (see Table 11), on Julian day 100 (April 10), using 1993 conditions, with the exception that no transportation was allowed. Both survival and travel time to the Estuary were recorded.

Results of this analysis are presented graphically in Fig. 89 through Fig. 92.

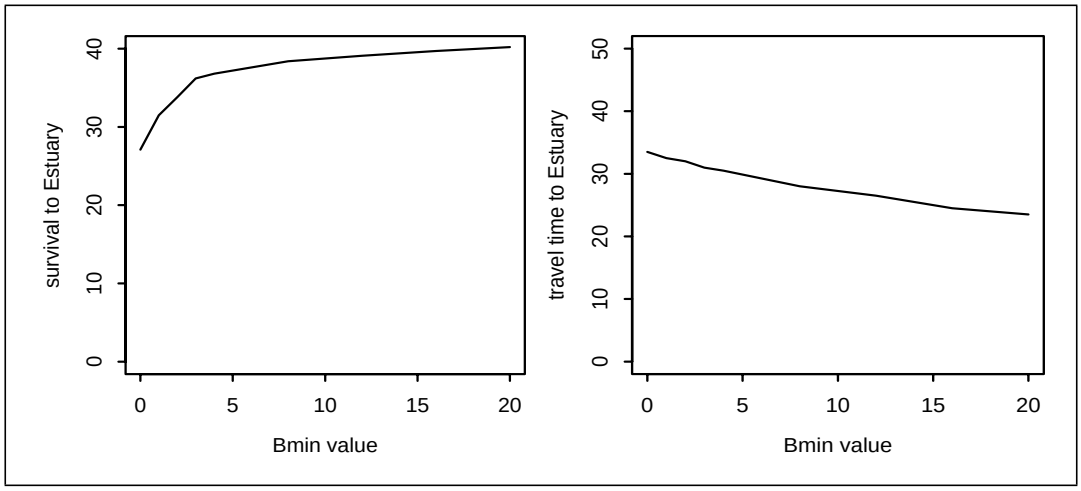

Fig. 89 Change in survival and travel time as a function of changing β_{min}.

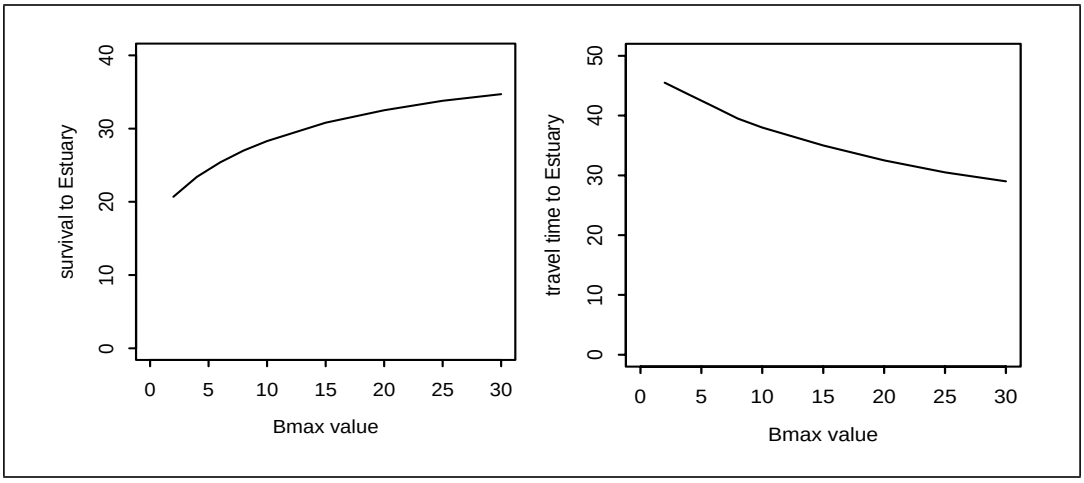

Fig. 90 Change in survival and travel time as a function of changing β_{max}.

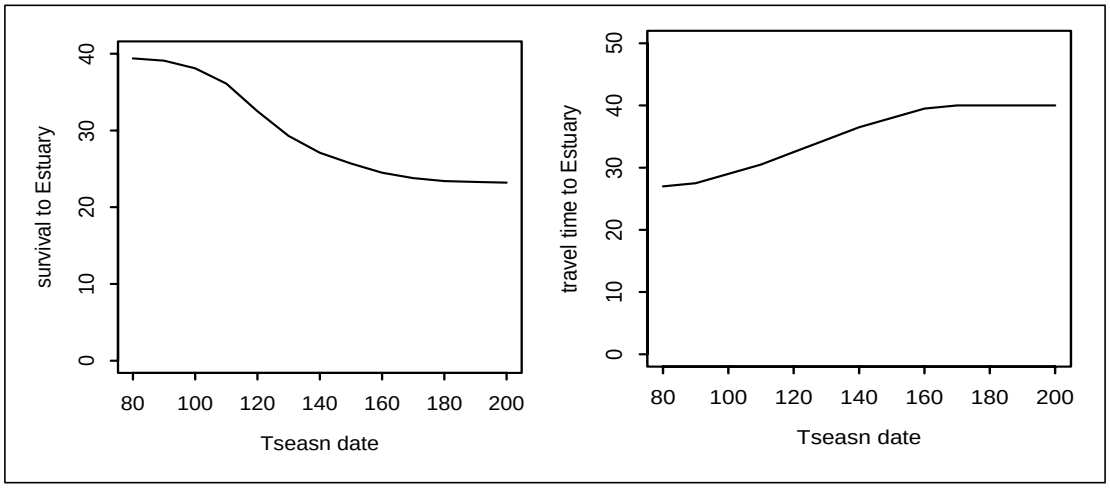

Fig. 91 Change in survival and travel time as a function of changing T_{seasn}.

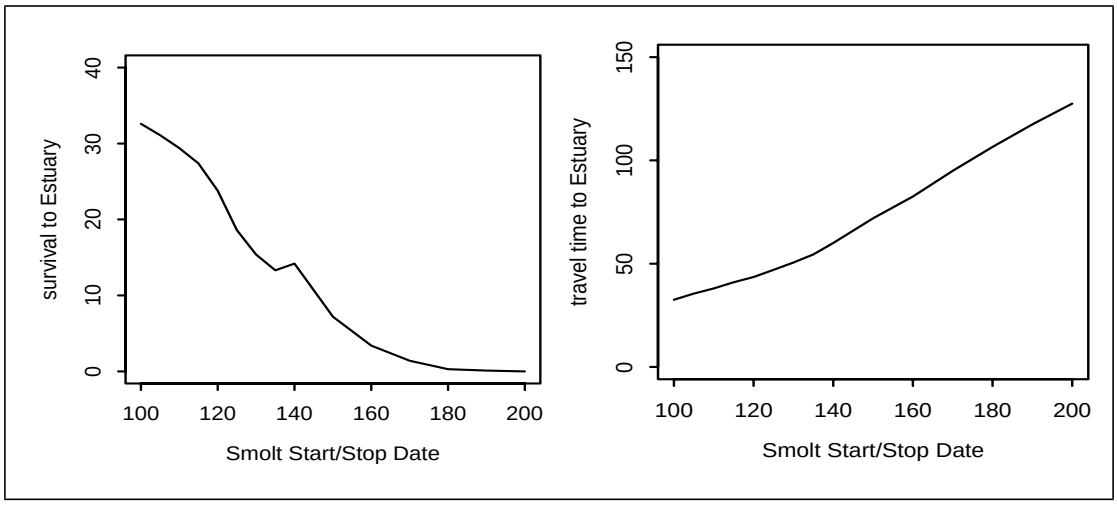

Fig. 92 Change in survival and travel time as a function of changing smolt start and stop date together.

Note that almost without exception, the results are exactly as one would expect: increasing either β_{min} or β_{max} produces increased net velocity, decreased net travel time, and increasing survival. Similarly, moving T_{seasn} closer to the release date (or even before the release date) forces the fish to reach β_{max} more quickly, producing a more rapid migration and higher survival.

The only exception to this rule is change in smolt date, where we might expect a smooth decline in survival as fish are delayed before migration, but in fact there is a small rise around day 140. This corresponds to the peak flow date of 1993, and fish that are delayed until peak flows can "surf" out to the estuary on the spring freshet. Consequently, they spend more time near the release site, suffering mortality, but move more rapidly through the mainstem proper, where predator densities are higher, and thus have a slightly higher survival than fish departing either before or after the freshet.

Two-way interactions

Two-way interactions are of particular interest. Obviously, there are a number of such interactions that could be examined, but three are of particular importance.

First, the interaction between *FGE* and turbine mortality was studied. This interaction turns out not to be as simple as might be expected. Second, the interactions between *FGE* and transport mortality were examined. Note that transport must be enabled at some dams for this comparison to have any meaning; for this segment of analysis, 1993 conditions including transport operations were used. The results for both analyses are shown below (Fig. 93 and Fig. 94) as response surfaces in three dimensions.

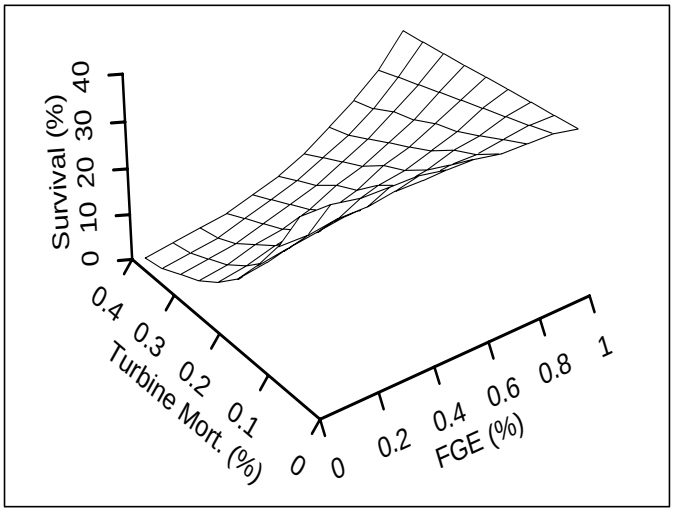

Fig. 93 Survival as a function of turbine mortality rate and fish guidance efficiency as they covary.

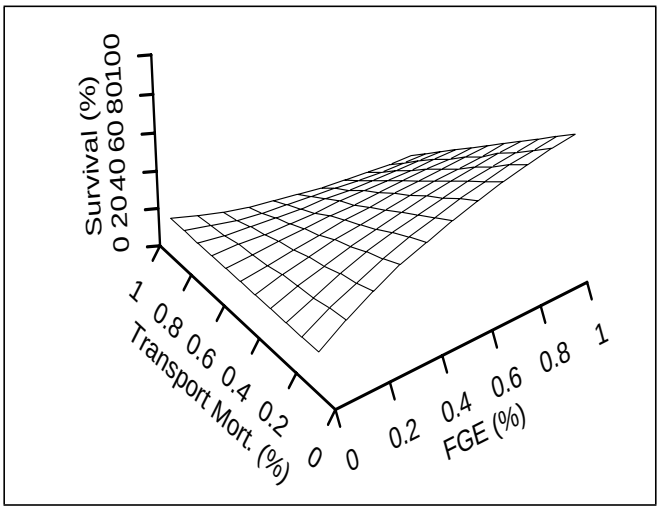

Fig. 94 Survival as a function of *FGE* and transport mortality as they covary.

The final two-way analysis conducted examined the interaction between spill fraction (equal at all dams) and the modal depth at which fish swim. CRiSP.1.5 models mortality due to gas saturation as a function not only of the saturation but also of the depth distribution of fish: the deeper fish swim, the less affected by gas bubble trauma they are. The results of this analysis are shown below in Fig. 95.

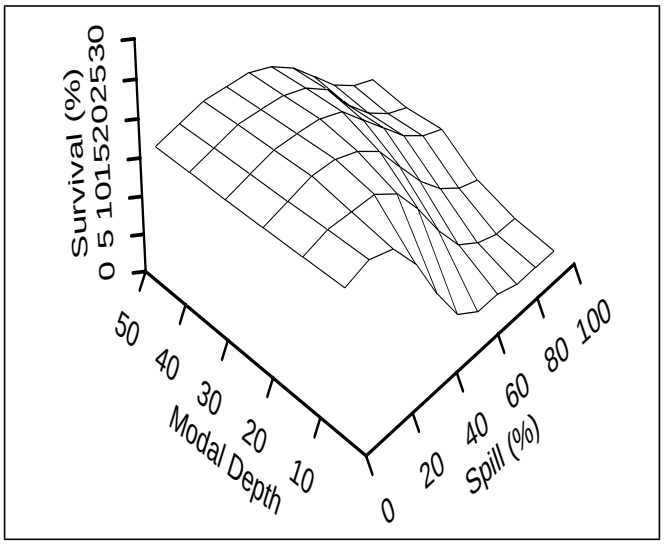

Fig. 95 Survival as a function of spill fraction and modal fish depth as they covary.

IV.3 - Discussion

While all the parameters examined have some influence on the outcome of model runs, it is clear that some are substantially more important than others. Total flow, water temperature, predator activity exponent, *FGE*, turbine and bypass mortality, and spill fraction all produce significant change in salmonid survival, while Vvar, forebay and tailrace predation components have little influence over the range of values investigated.

There are substantial nonlinearities in some responses. This is due to the underlying theory of the model in these cases, which is itself nonlinear. The relationship between flow and survival, however, is a result of several interacting submodels: because increased flow increases fish velocity, it reduces the mortality suffered due to predation, and thus increasing flow produces increasing survival. As flows increase, however, water is forced into the spillway, which produces elevated dissolved gas levels (Nsat). This causes mortality via gas bubble disease; as spill increases, this mortality increases (e.g. Fig. 85).

CRiSP.1 incorporates tailrace and forebay predation explicitly as a different process from general reach predation. It appears that the impact of predation in these two locations on total mortality incurred is trivial by comparison with that inflicted by predators in the reach proper or in dam passage (Fig. 86).

The interaction between *FGE* and turbine mortality (Fig. 93) is decidedly nonlinear; the rate of gain in survival with improving *FGE* is substantially larger with increasing turbine mortality. When turbine mortality is lower than bypass mortality, however, increasing *FGE* results in decreasing survival, as fish are guided away from turbines and into bypass facilities with a higher level of associated mortality. Despite these somewhat surprising patterns, it is not difficult to interpret the results of this analysis.

Similarly, the interaction between transport mortality and *FGE* (Fig. 94) is fairly

straightforward: under very high transport mortality (80-100%), increasing *FGE* produces decreasing system survival, while under low transport mortality (0-60%), increasing *FGE* leads to increasing survival. Around 70% transport mortality seems to be a break-even point: average system survival is about equal to 30%, so transport is neither beneficial nor deleterious.

Finally, even when fish are designated as swimming quite deep in the water column, they are still affected by nitrogen bubble trauma produced by high levels of spill (Fig. 95), although the drop in survival begins at around 50-60% spill, and survival declines from about 20% to about 8% at the worst. Conversely, if fish are swimming at shallow depths, for example a modal depth of 10 feet, the decrease in survival begins at about 40-50% spill and drops from 20% to 1% as spill approaches 100%. There is only a small benefit system-wide to moderate levels of spill, raising survival from 18% with no spill to about 20% for spills from 20-30%; this is, however, in-river survival only, and does not reflect the cost paid in decreased transport efficiency as spill levels rise.

Analyzed Range and Observed Range

In performing a sensitivity analysis, the range examined for each parameter is to some extent arbitrary. For some parameters, obvious extremes are suggested: for spill fraction, for example, the range from 0% spill to 100% spill is a natural choice to examine. At the same time, managers are interested in the real range of these parameters and how the model responds within reasonable system operations.

In general, for each parameter examined, we have forced the model to produce output over a much broader range than would ever be observed in reality. For those parameters to which the model is relatively insensitive, this indicates that the real system may be even more insensitive to changes in the modeled process, and that therefore mitigation measures that focus on those areas will be unlikely to produce significant benefit. At the same time, even those parameters which produce moderate to large impacts on survival may in reality be confined to a much narrower band in the actual hydrosystem. For example, a system-wide change in turbine mortality from 50% mortality to 0% produces a very large response in the model -- but turbine mortality in the system probably already lies between 5% and 10%, and so the potential benefits from further reductions in turbine mortality, while real, are likely to be quite small. Similarly, although survival is increased as water temperature decreases, little can be done to alter system water temperatures by more than a fraction of a degree, which (in the model) produces a negligible effect.

There has been considerable pressure to make improvements in the hydrosystem that lead to improved juvenile salmonid survival; in that sense, the current configuration is, within its constraints, close to optimized for fish survival. The small changes that are allowed within system operation guidelines are unlikely to produce other than equally small changes in fish survival. This is a property of the real world system that is reflected accurately in CRiSP.

V. Parameter Definitions

Equation parameters and their descriptions are given in Table 82. Dam and reservoir activities are assumed to be identical for all dams and reservoirs. Exceptions are treated individually so there is no index for the specific dam or reservoir. Within CRiSP.1, parameters for each dam and reservoir are unique.

Table 82 Parameters used in the Theory chapter

parameter	Description	page(s)
α	0.0295	103
a	0.0466 mm^{-1}, length coefficient for nitrogen mortality rate with an r^2 of 0.95.	94
a	a rate coefficient with units of N^{-1} d^{-1} species and length specific gas mortality coefficient which may have additive deterministic (a) and stochastic parts (*a*'), thus	84
a	a species specific gas mortality rate (low slope)	95
α	density of water (0.0295 atm / ft)	99
a	gas mortality coefficient deterministic part and is set by mean value sliders for each species	148
a	predation activity coefficient	66, 116, 117, 78
α	slope parameter in migration rate equation	55, 58
a	spill efficiency coefficient	119
A	surface area of the segment	101
a and *b*	deterministic parameters	135
a and *b*	regression coefficients	119
a, *b* and *h*	coefficients specific to each dam and can be derived from nitrogen rating curves available from the Corps of Engineers.	98, 102
a, *b* and *k*	coefficients specific to each dam derived from nitrogen rating curves provided by the Corps of Engineers.	98
a, *b*, and *c*	coefficients calculated from multiple linear regression of data in Table 28.	103
a, *b*, and *c*	dam dependent empirical coefficients.	100
a'	stochastic part whose range for a given species is set by the low and high value sliders.	148
a'_0	stochastic part whose range for a given species is set by the low and high value sliders.	148
a_0	deterministic part set by sliders for each species where value of the activity is set by the mean value slider	148
α_0	specific gravity of the roller at the base of the spill	99
a_k, b_k	Fourier coefficients estimated for each river	37
A_m	area of zone in as given in Table 45.	81

parameter	Description	page(s)
a_n, b_n	Fourier coefficients	26
A_{name}	area of each zone [tailrace (tr) reservoir (re) and forebay (fb)] (From Table 45)	68
b	a rate coefficient with units of N^{-1} d^{-1} species and length specific gas mortality coefficient which may have additive deterministic (b) and stochastic parts (b'), thus	84
b	a species specific gas mortality rate (high slope)	95
$B(I(t))$	behavioral factor dependent on the illumination.	110
$b(t)$	diurnal mortality rate factor $0 \pounds b \pounds 1$ assumed to be constant over a dam time slice.	116, 117
b's	regression coefficients	55, 58
b_i	rate at which smolts exit the region.	76
βmax	the maximum flow independent downstream velocity of smolts	55, 58,190
βmin	the minimum flow independent downstream velocity of smolts	190
c	1983.5 is a conversion factor	38
$C_{i, m}$	salmonid consumption rate for zone i in month m as given in Table 45	81
Cf	forebay concentration	103
c_{name}	average salmonid consumption rate of walleye (w), smallmouth bass (b) or squawfish (s) in zones (From Table 46)	68
$CPUE_{name}$	catch per unit effort in the tailrace (tr) or the combined regions of the forebay and reservoir (pool).	68
D	depth of the segment	101
Δ	differential pressure factor defined	99
D	fraction of fish that pass dam during spill hours	134
δ	offset for day of week alignment.	26
D	screen depth relative to full pool forebay elevation	121
d	stilling basin depth in feet	104
D	water depth at the end of the stilling basin	99
Δt	one day increment	38
$D(T)$	day length is a function Julian day, T,	111
D_c	fge calibration parameter	121
D_m	molecular diffusion coefficient of nitrogen	101
$\Delta P\ (t_j \mid t_i)$	probability that a fish entering on day t_i survives to exit on day t_j.	66
dS_i / dt	rate of change of smolts in region i	76
Δt	duration of a dam time slice, typically 2 hours	109, 110
ΔT	hours in a reservoir time slice, typically set for 12 hours	109
Δt	increment of time over which fge changes	122

parameter	Description	page(s)
Δt	reservoir computational time increment.	65
δt	residence time of fish in the tailrace	117
δt	time in hours before or after local noon	111
dt	time increment, typically 1 day	38
$\delta t_{\text{tailrace}}$	measure of water residence time in the tailrace	117
dV	change in reservoir volume in acre-ft	38
dX/dt	velocity of fish in migration	51
E	amount the pool is lowered below full pool elevation / Elevation drop	43, 48, 121, 67
E	energy loss rate	103
E	energy loss rate expressed as total headloss divided by residence time of water in the stilling basin	100
e	error term (var) selected from random distribution.	119
e	stochastic parameter selected from a normal distribution.	135
$E(t)$	elevation drop.	122
e_0		37
E_C	survival between Bonneville dam and the estuary for control fish	140
e_t	stochastic error term	37
E_T, E_C	test and control survival from Bonneville tailrace to estuary.	140, 142
exp ($u\theta$)	temperature effect on predation	66
Φ	cumulative distribution of the standard normal distribution	53
f	exploitation rate from the predator removal program	73
F	flow	43, 47, 48, 98, 100, 109, 117, 136
Φ	flux of nitrogen across the air water interface	101
$F_{D(r)}$	flow output at dam immediately below reach r	31, 34, 35
F_i	flow in kcfs in segment i	100
$F_{\text{loss (i)}}$	loss modulated flow in river segment upstream of dam i	32, 36
$F(T)$	river flow in kcfs which depends on the reservoir time slice	110
$F(t)_{\text{arch (i)}}$	archive flow at dam i	36
$F(t)_{\text{day (i)}}$	daily modulated flow in regulated headwater j	36
$F(t)_{\text{week (i)}}$	weekly modulated flow in regulated headwater j	36
$F(t)_i$	modulated flow at dam i	36
$F(t)_{\text{week (j)}}$	weekly variation in flow for headwater dam j	26
$F_{D(r)}$	flow output at dam r	34

parameter	Description	page(s)
F_{day}	daily variation in flow in kcfs at headwater dam	27
fge	fish guidance efficiency	121, 135
FGE	fraction of fish passing into turbine intake that are bypassed	134
fge_0	fge at onset of smoltification	121
F_i (t)	flow regulation point *i* at reservoir time increment *t*	35
F_i	flux of smolts into the region	76
$F_i(t)$	flow from headwater *i* through the river segment in question on day *t*	50
F_{i+1}	flux of smolts out of the region	76
F_j (t)	flow at regulation point *j* immediately upstream at reservoir time increment *t*.	35
$F_{L(i)}$	flow loss at reach *i*	35
$F_{L(r)}$	new flow loss at reach *r*, as adjusted for mass imbalance	31, 35
$F_{M(i)}$	flow maximum at reach *i*	31
$F_{M(r)}$	flow maximum at reach *r*	31
$F_{M(r)}$	flow maximum at reach *r or i*	35
F_{max}	hydraulic capacity of a project in kcfs	110
$F_{min(i)}$	minimum allowable flow at dam *i*	36
F_R	outflow from reservoir according to the constraints	39
F_R	regulated flow out of the reservoir, which is controlled by the user under volume constraints in kcfs	38
$F_{R(j)}$	flow at regulation point *j*	31, 31, 35
$F_{request}$	requested outflow from reservoir	39
F_s	spill flow in kcfs	98, 98, 100, 102
F_{sp}	fraction of daily flow that passes in spill	134
F_t	Fourier term	37
$F_{TU(r)}$	total unregulated flow input to dam *r*	34
$F_{U(i)}$	flow at unregulated headwater *i*	35
F_U	unregulated natural flow into the reservoir in kcfs	38, 39
F_U and F_R	unregulated and regulated flows in kcfs	38
$F_{U\ max\ (i)}$	maximum flow at unregulated headwater *i or j*	34
G	32.2 (gravitational constant)	104
G	flow scaling factor in kcf.s	26
g	intrinsic predator population growth rate: the difference between growth mortality rate elements independent of population size	73

parameter	Description	page(s)
G_m	fraction of salmon in the salmonids samples for month *m* as given in Table 47	81
$h(0)$	forebay or tailrace depth at full pool conditions	67
$h(E)$	forebay or tailrace depth at elevation *E*	67
h	forebay (tailrace) depth at a lowered pool	115
H	forebay (tailrace) depth at full pool	115
H	hydraulic head expressing the forebay elevation minus the elevation of the spilling basin floor (*H* is in ft and gravity constant, g, is 32 ft s^{-2})	99, 104
H()	Heaviside function, also known as the unit step function; equal to zero when its argument is negative, and equal to one when its argument is positive.	85
H_d	full pool depth at the downstream end of the segment	43, 67
$H_{forebay}$	depth of forebay	110
H_u	depth of the tailrace, the upper depth of a reservoir at full pool	43, 48, 117, 67
I	illumination which depends on season and time of day	110
I	number of dams upstream of dam *i*, including dam *i*	36
I_i	Northern squawfish density index in segment *i*. The predator density index is calculated according to Ward and Peterson Table 5 (in press) as the Index value 1 divided by the square root of the proportion of the zero catch electrofishing runs.	70
$I_{threshold}$	light threshold at which fish behavior switches.	111
φ	combined mortality rate	64, 65
J	number of regulated headwaters upstream of dam *i*	36
$J(t)$	input to forebay from the reservoir	109
$J(t)$	number of fish entering the forebay on dam slice increment *t*	109
K	carrying capacity of predators in a reservoir. This is taken as the predator index-based value prior to predator removal.	73
k	dimensionless constant describing the propensity of the fish to move with the flow which is species dependent	110
k	dissipation coefficient defined by eq (90)	87, 102
k		39
K_i	flow coefficient at unregulated headwater *i*	34
$K20$	entrainment coefficient	99, 103
K_d	transfer coefficient defined	101
K_e	bubble entrainment coefficient with units of ft $s^{-1}atm^{-1/3}$ and is defined	99
L	fish length	94

parameter	Description	page(s)
L	length of pool	43, 102, 87
L	length of the stilling basin in feet	99, 117, 104
L	segment length	47, 53, 89
L	tailrace length	117
L_{day}	forebay horizontal length scale associated with fish in full daylight	110
L_{e}	length of fish in nitrogen mortality experiments	94
L_{night}	forebay horizontal length scale associated with fish in the night. Note: $L_{\text{day}} > L_{\text{night}}$	110
local noon	typically 1300 hr with daylight savings time	111
m	mean annual flow computed over a 10 year period	37
m	number of unregulated headwaters above **r** (m = 3 in Fig. 14)	35
m_0	slope of distribution function above mode	88
m_1	slope of distribution function below mode	88
m_{by}	mortality in the bypass system	136
m_{fo}	mortality in forebay see eq (103)	135
$\overline{M}$	the mortality rate due to gas bubble disease averaged throughout the length and depth of the pool.	89
M_{n}	mortality rate from nitrogen supersaturation	65, 90
$M_{\text{n}}(L)$	nitrogen mortality rate as a function of fish length	94
M_{p}	mortality rate from predation with units of time^{-1}	65
m_{sp}	mortality in the spill passage.	137
m_{tr}	mortality in the transport.	136
m_{tu}	mortality in the turbine	135
$N\,(t_{\text{i}})$	number of fish that enter the river segment on day t_{i}	66
N	nitrogen supersaturation concentration in the segment	101
n	number of regulated points upstream	31, 35
N	percent nitrogen saturation *above* 100%	95
N	tailrace concentration	102
N	tailwater nitrogen supersaturation (in percent)	100
N_{crit}	critical supersaturation level	95
N_{i}	nitrogen in percent supersaturation in segment i of the confluences.	100
N_0	is percent supersaturation above 100% at the upstream end of a river segment, which may be a tailrace	87

parameter	Description	page(s)
N_c	threshold above supersaturation at which the gas bubble disease mortality rate is observed to change. This function depends on depth.	84
N_{eq}	nitrogen equilibrium concentration	98, 101, 101
N_{fb}	forebay nitrogen supersaturation (in percent)	98, 100
N_{fo}	number of fish in forebay ready to pass in the increment	135
N_s	nitrogen concentration in tailrace in mg./l	98
N_s	percent nitrogen saturation *above* 100% measured at the surface.	84
N_s	percent supersaturation above 100%	100, 98, 102
Nsw	back-calculated spillway gas saturation	104
N_{tu}	number of fish passing in a time increment (2 hrs)	135
O_C	survival of in-river control fish after ocean entry plus any delayed mortality not included in any upstream process	140
O_T	survival of transported after ocean entry plus any delayed mortality not included in any upstream process	140
O_T, O_C	survival of transported and control fish through the ocean and back up river. These parameters also contain any unidentified mortality factors not accounted for in the other processes.	142
P (E)	average predator density in a segment (fish km^{-2}), specific to the type of river section.	66
p (F, t)	forebay rate coefficient. This depends on the flow F, and an illumination dependent time t as is developed below.	110
P	average hydrostatic pressure in the main flow of the stilling basin in atmospheres	99
P	forebay percent saturation	100
p	fraction of mean annual	37
p	number of reaches between dam r and all regulation point	31, 35
p	number of regulated flows in region	34
P	predator density	115, 67, 73, 84
p	probability of passing during the increment	135
$P(0)$	predator density in a river segment per unit area at full pool (predators km^{-2}).	67
$P(E)$	Predator Density / Reservoir Volume Coefficient (a function of the elevation of the river segment below full pool)	66
$p(F,t)$	rate at which fish pass from the forebay into the dam	109
$P(h)_{fb}$	predator density in the forebay as a function of forebay depth h (predators km^{-2}) defined by eq (101)	116

parameter	Description	page(s)
$P(h)_{tr}$	predator density in the tailrace as a function of tailrace depth h (predators km^{-2}). This is defined by eq (101)	117
$P(t + \Delta t)$	predator population density at time $t + \Delta t$	73
$P(t)$	predator population density at time t	73
P_0	barometric pressure in atmospheres (assume P_0 is 1)	99
P_i	squawfish density (predators km^{-2}) in a given segment i	70
P_{name}	total density of walleye (w), smallmouth bass (b) or squawfish (s) (From Table 36)	68
P_{re}	equivalent density of predators in the reservoir zone including smallmouth bass, walleye and squawfish	68
P_{ref}	reference average squawfish density = 472 (predators km^{-2})	70
θ	average slope of the pool side	43
q	number of adjacent unregulated headwaters in region	34
θ	temperature in degree centigrade	66, 116, 117, 78
$\theta(t)$	temperature for selected river segment on day t	50
$\theta_i(t)$	temperature from headwater i on day t	50
r	average migration velocity through the segment	51, 53
r	deterministic rate of change of flow per unit of flow	16, 94
R	in river juvenile survival past Bonneville Dam	137
r	predation rate.	135
$r(t)$	determined from (48)	38, 72
r(t)	migration rate (miles / day)	37, 89
R_1	survival of fish traveling in river from transport release in Little Goose trailrace through McNary Dam pool.	138
R_2	survival of fish traveling in river from McNary Dam forebay to Bonneville Dam tailrace.	138
r_i	consumption rate coefficient.	127
R_i	consumption rate of smolts by predators in the region.	127
r_t	randomly generated variable from a normal distribution centered on 0 with variance appropriate for dry and wet years as described above. The switch from dry year to wet year variance parameters occurs at p =0.4.	24
$S(t_j \mid t_i)$	actual number of fish that enter the segment on day t_i and leave on day t_j.	41, 55
S	cumulative survival	111
S	fraction of total flow diverted to spill in the increment	68, 98
σ	intensity on the random variations in flow	16
S	measure of smolt density in the river segment and can be taken as the total number in the segment	40

parameter	Description	page(s)
S	number of smolts leaving reservoir per day (smolts reservoir $^{-1}$)	41
S	spill in kcfs	108
σ	spread parameter setting variability in the fish velocity	33
S and P	average numbers of smolts and predators in the region which could also be expressed on a unit area basis	127
S_i^*	steady state average smolt density in region i	129
$S(*)$	smolt density	135
$S_0\,(t_j \mid t_i)$	potential number of fish that enter the segment on day t_i and survive to leave the segment on day t_j	41
$S_{b.l}$	survival from barging fish at Lower Granite dam and include mortality in collection, transport release back in to the river.	138
$S_{b.m}$	transport survival from observed mortalities in transport in barges and trucks from McNary dam	137
S_{BON}	model survival from Bonneville Dam tailrace to the estuary.	137, 139, 178
S_C	survival of adult control fish with juvenile in river migration	137
S_C	survival of returning adult fish from control group as determined from specified collection methods which may include ocean and in-river fisheries, counts at dams, hatcheries and spawning grounds.	138
SE	fraction of fish that pass in spill relative to the fraction of flow passing in spill	67
$S_{\text{from transport dam}}$	model in river survival for fish from tailrace of transported to the estuary	178
sgr	specific gravity of roller (usually 1)	108
σ_i	the standard deviation of the difference in flows (kcfs) at dam i and i +1 as computed by daily observed flows at all dams over the years 1979-1981.	18
S_{LGR}	model survival for fish transported from Lower Granite dam to Little Goose dam tailrace.	139
S_{MCN}	model survival from McNary Dam tailrace to the estuary.	137
Smolt Start / Stop Date	the date at which fish begin migration down the hydrosystem.	184
S_T	survival of adult test fish with juvenile transport migration	137
S_T	survival of returning adult fish from test group as determined from specified collection methods which may include ocean and in-river fisheries, counts at dams, hatcheries and spawning grounds.	138
S_t	transport survival from trucking fish in the control fish group. Includes mortality in collection, transport and release.	138

parameter	Description	page(s)
t	day of the year	15
t	fish age since the onset of smoltification, see eq (51)	64
t	hour of day	57
t	Julian date	24, 37, 89
T	residence time in this calculation is in kilo seconds or ks.	30, 85
T	temperature in degrees C	49, 108
t	time	44, 51, 55, 135
T	total transport survival from transport dam. In this analysis T was set to 1 so the TBR measure does not include transportation effects	178
t_0	onset of change in fge relative to the onset of smoltification set in the release window	64
TBR	transport benefit ratio as computed from adult returning to Lower Granite Dam	138
TBR	transport benefit ratio between transported and in river migrating juvenile fish	137
T_{LGR}	total transport survival from Lower Granite dam.	139
T_{MCN}	total transport survival from McNary dam.	137, 138
$\mathrm{T_{RLS}}$	release date (in Julian Days) of a group of fish.	37, 89
$\mathrm{T_{SEASN}}$	seasonal inflection point (in Julian Days) for flow-related term of the migration rate equation	37, 89
U	velocity	31, 50
u	predator activity exponent independent of prey species	59, 60
u	Predator Activity Temperature Exponent.	42
u	temperature coefficient	118, 129
U_{free}	velocity of free flowing river.	26, 30, 31, 44, 85
$\overline{V}_t$	average river velocity during the average migration period	37
$V(E)$	river segment volume when the elevation is lowered by an amount E	118
$V(0)$	river segment volume at full pool conditions	43, 84, 118
$V(E)$	pool volume (ft^3) as a function of elevation drop E in feet	30, 43, 85
$V(\mathrm{i})$	reservoir volume in reservoir time step i	25, 26, 38
$V(i)$	variance factor that varies *between* releases only.	38, 72, 94
V_1 and V_2	volume elements defined by eq (34)	31
$\mathrm{V_f}$	average river velocity during the average migration period	89

parameter	Description	page(s)
$V_{forebay}(t)$	effective forebay volume containing fish and depends on illumination I as a function of time.	56
V_{max}	maximum reservoir volume	26
V_{min}	minimum reservoir volume	26
Volume	pool volume at a specific elevation	51
$V_{request}$	requested outflow from reservoir	26
ω	$2\pi/365$	24, 80
W	pool width / average pool width / reservoir width	26, 51, 60, 84
W	spillway width	48, 108
w	squawfish distribution factor	119, 120
W	tailrace width	94
$W(t)$	Gaussian white noise process	33
$w(t)$	Gaussian white noise process describing the temporal aspects of the flow variation.	16
x	deterministic part of the random parameter fixed for each species and dam	68
x	distance downstream	45
X	fraction of water spilled	62
x	percent flow	68
x	pool length at lowered pool	26, 30
X	position of a fish down the axis of the river	33
X	smolt density in the forebay	59
x	unit uniform random deviate range $0 < x < 1$	70
$X(t)$	number of fish exiting the tailrace within dam time step t	60
x'	stochastic part of the random parameter taken from a broken-stick distribution (see Reservoir Mortality section on page III.118) over each dam time slice.	68
$X_0(t)$	number of fish entering the tailrace at dam time step t	60
y	fish in forebay	55
Y	fraction of total fish passed in spill	62
y	spill efficiency	68
y_0		108
Y_0	thickness of the spill at the stilling basin entrance	48
y_l	lower limit of the distribution range	70
y_m	distribution of the median value	71
Y_t	estimated daily flow	24
Y_t	number of fish in the forebay in the dam time slice t	56

parameter	Description	page(s)
y_u	upper limit of the distribution range.	71
z	median depth of fish in the forebay at a distance from the dam where fish are susceptible to being drawn into the intake.	64
z	the fix depth is with range where D_{ave} is the average depth of the reservoir.	44
z_0	initial mean fish depth (at age t equals 0) in the forebay	64
z_1	final mean fish depth (at age t equals $t_0 + \Delta t$) in the forebay	64
z_b	maximum depth of fish distribution	46
z_D	depth of the reservoir	46
z_m	mode of fish distribution	46

VI. References

Bypass Survival

Ceballos, J., S. Pettit, and J. McKern. 1991. *Fish transportation and oversight team annual report - FY 1990.* NMFS.

Ledgerwood, R. et al. 1990. *Relative survival of subyearling chinook salmon which have passed Bonneville Dam via the spillway or the second powerhouse turbines or bypass system in 1989, with comparisons to 1987 and 1988.* Research report to USACOE, NMFS.

Ledgerwood, R. et al. 1991. *Relative survival of subyearling chinook salmon which have passed through the turbines or bypass system of Bonneville Dam second powerhouse, 1990.* Research report to USACOE, NMFS.

Fish Depth

Brege, D.A., Gabowshi, S.J., Muir, W.D., Hirzel, S.R., Mazur, S.J., and Sandford, B.P. 1992. Studies to determine the effectiveness of extended traveling screens and extended bar screens at McNary Dam, 1991.

Columbia River Biological Service, NBS. 1994. Preliminary Lower Granite Reservoir juvenile salmon distribution and behavior.

Dauble, D.D., T.L. Page, and Hanf, R.W. 1989. Spatial distribution of juvenile salmon in the Hanford Reach, Columbia River. Fishery Bulletin 87: 775-790.

Erho, M. 1964. Vertical distribution of coho smolts in the forebay of Merwin Dam in 1964. Prepared for Puget Power and Light Co.

Johnson, L., Murphy, A., and Rawlinson, C. 1985. Hydroacoustic Assessment of Downstream Migrating Salmonids at Lower Monumental Dan in Spring 1985. Prepared for Bonneville Power Administration, contract number DE-A C79-85 BP23174.

Krcma, R.F. Brege, D.A., and Legerwood, R.D. 1986. Evaluation of the rehabilitated juvenile salmonid collection and passage system at John Day Dam, 1985. Prepared for US Army Corps of Engineers, contract number DACW57-85-H- 0001.

Legerwood, R.D., Swam, G.A., and Krcma, R.F. 1987. Fish guiding efficiency of submersible traveling screens at Lower Monumental Dam, 1986. Prepared for National Marine Fisheries Service, Seattle, WA and US Army Corps of Engineers, contract number DACW68-84-4-0034.

McComas, R.L., Sandford, B.P., and Dey, D.B. 1994. Studies to evaluate the effectiveness of extended-length screens at McNary Dam, 1993. Prepared for National Marine Fisheries Service, Seattle, WA and US Army Corps of Engineers, contract number E86910060.

Raemhild, G.A., Kuehl, S., and Murphy, A. 1984. Hydroacoustic assessment of downstream migrating juvenile salmonids at Priest Rapids Dam in summer 1983. Prepared for Grant County Public Utility District No.2, and Bonneville Power Administration, Portland, Oregon.

Smith, J.R. 1974. Distribution of seaward-migrating chinook salmon and steelhead trout n the Snake River above Lower Monumental Dam. Marine Fisheries Review 36: 42-45.

Wright, R.J., Johnson, L., and Schadt, T.H. 1986. Hydroacoustic evaluation of juvenile fish passage at Lower Monumental Dam in Spring 1986.

Zabel, R.W. 1994. Spatial and temporal models of migrating juvenile salmon with applications. Doctoral dissertation. University of Washington, Seattle.

FGE

Bonneville Dam

Gessel, M.H., D.A. Brege, B.H. Monk and J.G. Williams. April 1990. *Continued studies to evaluate the juvenile bypass systems at Bonneville Dam-1989.* U.S. Army Corps of Engineers, and Coastal Zone and Estuarine Studies report.

Muir, W.D., A.E. Giorgi, W.S. Zaugg, and B.R. Beckman. May 1989. *An assessment of the relationship between smolt development and fish guidance efficiency at Bonneville Dam.* NMFS / Coastal Zone Report.

Gessel, M.H., B.H. Monk, D.A. Brege, and J.G. Williams. January 1989. *Fish guidance efficiency studies at Bonneville Dam first and second powerhouses-1988.* NMFS / Coastal Zone Report.

Gessel, M.H., B.H. Monk, and J.G. Williams. August 1988. *Evaluation of the juvenile fish collection and bypass systems at Bonneville Dam-1987.* NMFS / Coastal Zone Report.

Gessel, M.H., L.G. Gilbreath, W.D. Muir, B.H. Monk and R.F. Krcma. May 1987. *Evaluation of the juvenile salmonid collection and bypass systems at Bonneville Dam-1986.* NMFS / Coastal Zone Report.

Gessel, M.H., L.G. Gilbreath, W.D. Muir and R.F. Krcma. June 1986. *Evaluation of the juvenile collection and bypass systems at Bonneville Dam-1985.* NMFS / Coastal Zone Report.

Gessel, M.H., R.F. Krcma, W.D. Muir, C.S. McCutcheon, L.G. Gilbreath and B.H. Monk. May 1985. *Evaluation of the juvenile collection and bypass systems at Bonneville Dam-1984.* NMFS / Coastal Zone Report.

Krcma, R.F., M.H. Gessel, W.D. Muir, C.S. McCutcheon, L.G. Gilbreath and B.H. Monk. May 1984. *Evaluation of the juvenile collection and bypass system at Bonneville Dam-1983.* NMFS / Coastal Zone Report.

Krcma, R.F., D. DeHart, M. Gessel, C. Long, and C.W. Sims. May 1982. *Evaluation of submersible traveling screens, passage of juvenile salmonids through the ice-trash sluiceway, and cycling of gatewell-orifice operations at the Bonneville first powerhouse, 1981.* NMFS / Coastal Zone Report.

Krcma, R.F., W.E. Farr, and C.W. Long. April 1980. *Research to develop bar screens for guiding juvenile salmonids out of turbine intakes at low head dams on the Columbia and Snake Rivers, 1977-79.* NMFS / Coastal Zone Report.

Krcma, R.F., C.W. Long, C.S. Thompson, W.E. Farr, T.W. Newcomb, and M.H. Gessel. April 1979. *The development of an improved fingerling protection system for low-head dams, 1978.* NMFS / Coastal Zone Report.

The Dalles Dam

Monk, B.H., W.D. Muir, and M.H. Gessel. May 1987. *Studies to evaluate alternative methods of bypassing juvenile fish at The Dalles Dam--1986.* NMFS / Coastal Zone Report.

Monk, B.H., W.D. Muir and R.F. Krcma. June, 1986. *Studies to evaluate alternative methods of bypassing juvenile fish at The Dalles Dam--1985.* NMFS / Coastal Zone Report.

John Day Dam

Brege, D.A., D.R. Miller, and R.D. Ledgerwood. May 1987. *Evaluation of the rehabilitated juvenile salmonid collection and passage system at John Day Dam--1986.* NMFS / Coastal Zone Report.

Krcma, R.F., D.A. Brege, and R.D. Ledgerwood. 1986. *Evaluation of the rehabilitated juvenile salmonid collection and passage system at John Day Dam--1985.* NMFS / Coastal Zone Report.

Krcma, R.F., M.H. Gessel and F.J. Ossiander. 1983. *Research at McNary Dam to develop*

and implement a fingerling protection system for John Day Dam. NMFS / Coastal Zone Report.

Swan, G.A., R.F. Krcma and C.W. Long. 1982. *Research to develop an improved fingerling-protection system for John Day Dam, 1981.* NMFS / Coastal Zone Report.

McNary Dam

Brege, D.A., W.T. Norman, G.A. Swan and J.G. Williams. 1988. *Research at McNary Dam to improve fish guiding efficiency of yearling and subyearling chinook salmon, 1987.* NMFS / Coastal Zone Report.

Cramer, S.P., C. F. Willis and K.L. Witty. 1995. Assessment of negative impacts from spill on survival of anadromous salmonids in the Columbia Basin. Submitted to Direct Service Industries, Inc.

Krcma, R.F., G.A. Swan and F.J. Ossiander. 1985. *Fish guiding and orifice passage efficiency tests with subyearling chinook salmon, McNary Dam, 1984.* NMFS / Coastal Zone Report.

Krcma, R.F., M.H. Gessel and F.J. Ossiander. 1983. *Research at McNary Dam to develop and implement a fingerling protection system for John Day Dam*. NMFS / Coastal Zone Report.

Krcma, R.F., W.E. Farr, and C.W. Long. 1980. *Research to develop bar screens for guiding juvenile salmonids out of turbine intakes at low head dams on the Columbia and Snake Rivers, 1977-79.* NMFS / Coastal Zone Report.

Krcma, R.F., C.W. Long, C.S. Thompson, W.E. Farr, T.W. Newcomb, and M.H. Gessel. 1979. *The development of an improved fingerling protection system for low-head dams, 1978.* NMFS / Coastal Zone Report.

McCabe, G.T., Jr., and R.F. Krcma. 1983. *Effects of the intermittent operation of submersible traveling screens on juvenile salmonids, 1982.* NMFS / Coastal Zone Report.

Swan, G.A. and W.T. Norman. 1987. *Research to improve subyearling chinook salmon fish guiding efficiency at McNary Dam--1986.* NMFS / Coastal Zone Report.

Stuehrenberg, L. and O.W. Johnson. 1990. *Evaluation of factors affecting collection efficiency estimates of chinook salmon and steelhead smolts at McNary Dam.* NMFS / Coastal Zone Report.

Upper Columbia Projects

No fge estimates are available for dams above McNary on the Columbia (Priest Rapids, Wanapum, Rocky Reach, Rock Island, and Wells), despite the fact that at least some of these dams have bypass systems installed (e.g. Rock Island).

Lower Snake Projects

Limited fge estimates are available for some stocks at each of Ice Harbor, Lower Monumental, Little Goose, and Lower Granite Dams.

Ice Harbor Dam

Brege, D.A., G.A. Swan, and J.G. Williams. 1988. *Fish guiding efficiency studies at Ice Harbor Dam, 1987.* NMFS / Coastal Zone Report.

Lower Monumental Dam

Ledgerwood, R.D., G.A. Swan and R.F. Krcma. 1987. *Fish guiding efficiency of submersible traveling screens at Lower Monumental Dam--1986.* NMFS.

Little Goose Dam

Swan, G.A., A.E. Giorgi, T.Coley and W.T. Norman. 1987. *Testing fish guiding efficiency*

of submersible traveling screens at Little Goose Dam; is it affected by smoltification levels in yearling chinook salmon? NMFS / Coastal Zone Report.

Lower Granite Dam

Swan, G.A., B.H. Monk, J.G. Williams and B.P. Sandford. 1990. *Fish guidance efficiency of submersible traveling screens at Lower Granite Dam--1989.* NMFS / Coastal Zone Report.

Ledgerwood, R.D., W.T. Norman, G.A. Swan, and J.G. Williams. 1988. *Fish guiding efficiency of submersible traveling screens at Lower Granite and Little Goose Dams--1987.* NMFS / Coastal Zone Report.

Muir, W.D., A.E. Giorgi, W.S. Zaugg, W.W. Dickhoff, and B.R. Beckman. 1988. *Behavior and physiology studies in relation to yearling chinook salmon guidance at Lower Granite and Little Goose Dams, 1987.* NMFS.

Swan, G.A., R.F. Krcma and F.J. Ossiander. 1986. *Continuing studies to improve and evaluate juvenile salmonid collection at Lower Granite Dam--1985.* NMFS / Coastal Zone Report.

Kiehl, S. 1986. *Hydroacoustic evaluation of fish collection efficiency at Lower Granite Dam in Spring 1985.* NMFS / Coastal Zone Report.

Swan, G.A., R.F. Krcma and F.J. Ossiander. 1985. *Development of an improved fingerling protection system for Lower Granite Dam 1984.* NMFS / Coastal Zone Report.

Swan, G.A., R.F. Krcma and F.J. Ossiander. 1984. *Research to develop an improved fingerling protection system for Lower Granite Dam.* NMFS / Coastal Zone Report.

Swan, G.F., R.F. Krcma and F. Ossiander. 1983. *Studies to improve fish guiding efficiency of traveling screens at Lower Granite Dam.* NMFS / Coastal Zone Report.

McCabe, G.T. Jr., and R.F. Krcma. 1983. *Effects of the intermittent operation of submersible traveling screens on juvenile salmonids, 1982.* NMFS / Coastal Zone Report.

Iwamoto, R.N. W.D. Muir, B.P. Sandford, K.W.McIntyre, D.A. Frost, J.D. Williams, S.G. Smith, and J.D. Skalski 1994. Survival estimates for the passage of juvenile chinook salmon through Snake River dams and reservoirs. Annual Report 1993. Bonneville Power Administration, Project No. 93-29 Contract No. DE-AI79-93BP10891.

Gas Bubble Disease

Bentley, Wallace W. and Earl M. Dawley, NMFS. 1981. *Effects of Supersaturated Dissolved Gases on Northern Squawfish,* Ptychocheilus orogenesis. Northwest Science, Vol. 55, No. 1.

Dawley, Earl M. and Wesley J. Ebel, NMFS. 1975. Effects of Various Concentrations of Dissolved Atmospheric Gas on Juvenile Chinook Salmon and Steelhead Trout. Fishery Bulletin: Vol. 73, No. 4.

Dawley, Earl, Bruce Monk, Michael Schiewe, Frank Ossiander, and Wesley Ebel, NMFS. 1976. Salmonid Bioassay of Supersaturated Dissolved Air in Water. EPA Ecological Research Series, Report #EPA-600 / 3-76-056, July 1976.

Ebel, Wesley J., Earl M. Dawley, and Bruce H. Monk, NMFS. 1971. Thermal Tolerance of Juvenile Pacific Salmon and Steelhead Trout in Relation to Supersaturation of Nitrogen Gas. Fishery Bulletin: Vol. 69, No. 4.

Ebel, Wesley J., Richard F. Krcma, and Howard L. Raymond. 1973. Evaluation of fish protection facilities at Little Goose Dam and review of other studies relating to protection of other salmonids in the Columbia and Snake Rivers, NOAA, NMFS NWFC, Seattle Washington Progress Report to U.S. Army Corps of Engineers, Contract DACW68-71-0093. 62 p (Processed.)

Ebel, Wesley J. and Howard L. Raymond, NMFS. 1976. Effect of Atmospheric Gas Supersaturation on Salmon and Steelhead Trout of the Snake and Columbia Rivers. - MFR Paper 1191. Marine Fisheries Review, Vol. 39, N0.7, July 1976

Fidler, L.E. and S.B. Miller. 1994. British Columbia Water Quality Guidelines for

Dissolved Gas Supersaturation. Draft report to B.C. Ministry of Environment, February 1994. 93 pp. + appendices.

Scully, Richard, Edwin. Buettner and Clay Cummins 1983. Smolt condition and timing of arrival at Lower Granite Reservoir. Bonneville Power Administration Project No. 83-323B. Annual Report 1983

Smith, Jim Ross, NMFS. 1974. Distribution of Seaward-Migrating Chinook Salmon and Steelhead Trout in the Snake River above Lower Monumental Dam. - MFR Paper 1081. Marine Fisheries Review, Vol. 36, No. 8, August 1974.

U.S. Army Corps of Engineers, 1994. Dissolved Gas Abatement Interim Letter Report. COE Portland and Walla Walla District, December 1994.

White, P.G. et al. 1991. Effects of supersaturation of dissolved gases on the fishery of the Bighorn River downstream of the Yellowtail afterbay Dam. Prepared for the U.S. Department of the Interior Bureau of Reclamation Missouri Basin Region 6.

Hatchery Release Sites

Chaney, Ed et al. 1988. *Umatilla Subbasin*. Columbia Basin System Planning Drafts. Northwest Power Planning Council and the agencies and tribes of the Columbia Basin Fish and Wildlife Authority.

Columbia Basin Inter-agency Committee. 1962-1966. *River Mile Indices*. Hydrology Subcommittee.

Feist, Blake. 1991. *Hatchery Listing*. Fisheries Research Institute, School of Fisheries, University of Washington.

Fish Passage Center. 1991. *Hatchery Release Site Locations*. Fish Passage Data System file containing hatchery releases for the Columbia Basin from 9/01/90 to 9/11/91.

Jonasson, Brian et al. 1988. *Deschutes Subbasin*. Columbia Basin System Planning Drafts. Northwest Power Planning Council and the agencies and tribes of the Columbia Basin Fish and Wildlife Authority.

Parker, Steve et al. 1988. *Klikitat Subbasin*. Columbia Basin System Planning Drafts. Northwest Power Planning Council and the agencies and tribes of the Columbia Basin Fish and Wildlife Authority.

Seidel, Paul et al. 1988. *Snake Subbasin*. Columbia Basin System Planning Drafts. Northwest Power Planning Council and the agencies and tribes of the Columbia Basin Fish and Wildlife Authority.

Seidel, Paul et al. 1987. *Lower Snake River Compensation Plan, Lyons Ferry Evaluation Program, Annual Report*. WA Dept. of Fisheries report to the Lower Snake River Compensation Plan office in Boise, ID.

Water Budget Center. 1991. *Site Definitions Listing.* Supplied by D. Anderson of the BPA to CRiSP staff.

Hydraulic Capacities at Dams

Corps of Engineers. 1989. *Columbia River and Tributaries Review Study: Project Data and Operating Limits. CRT 49 (Revised), Book No. 1.* US Army Corps of Engineers, North Pacific Division, Power Section.

Corps of Engineers. 1989. *Columbia River and Tributaries Review Study: Project Data and Operating Limits. CRT 69, Book No. 2.* US Army Corps of Engineers, North Pacific Division, Power Section.

Modulators

Chatfield, C. 1989. *The Analysis of Time Series - An Introduction*. 4th Edition. Chapman and Hall.

Goel, Narendra S. and Nira Richter-Dyn. 1974. *Stochastic Models in Biology.* Academic Press.

S-PLUS Manual, Statistical Sciences, Inc., 1990.

Nitrogen Supersaturation

Boyer, Peter B. 1974. *Lower Columbia and Lower Snake Rivers Nitrogen (Gas) Supersaturation and Related Data Analysis and Interpretation*. NMFS/Coastal Zone Report

Corps of Engineers. 1989. *Project Data and Operating Limits, CRT Report #49, Book 1*. US Army Corps of Engineers, North Pacific Division, Power Section.

Corps of Engineers. 1986. Gasspill: *A System Spill Allocation Model for the Control of Dissolved Gas Saturation in the Columbia River Basin*. Corps of Engineers, North Pacific Division, Water Quality Section, Water Management Branch, Engineering Division.

Corps of Engineers. 1978. *Report on Modeling of Dissolved Nitrogen Gas Data for the Lower Columbia and Lower Snake Rivers, Appendix A*. US Army Corps of Engineers, North Pacific Division, Water Management Branch, Water Quality Section.

Ebel, Wesley J. H., G. E. Monan, W. E. Farr and G. K. Tanonaka. 1975. Effect of Atmospheric Gas Supersaturation Caused by Dams on Salmon and Steelhead Trout of the Snake and Columbia Rivers. Northwest Fisheries Center Processed Report.

Roesner, L.A. and W.R. Norton. 1971. *A Nitrogen Gas Model for the Lower Columbia River, Final Report*. Water Resources Engineers, Inc.

Weast, Robert C. and Samuel M. Selby. 1967. *Handbook of Chemistry and Physics.* The Chemical Rubber Co.

Predation Mortality

Beamesderfer, R.C. and B.E. Rieman. 1988. Predation by Resident Fish on Juvenile Salmon in a Mainstem Columbia Reservoir: Part III. Abundance and Distribution of Northern Squawfish, Walleye, and Smallmouth Bass. In Predation by Resident Fish on Juvenile Salmonids in John Day Reservoir. Volume I- Final Report of Research. Final Report 1983-1986. Bonneville Power Administration Report Project No. 82-3 and 82-12. July 1988.

Beamesderfer R.C. and B.E. Rieman 1991. Abundance and distribution of northern squawfish, walleye and smallmouth bass in John Day Reservoir, Columbia River. *Trans. Am. Fish. Soc.* 120:439-447.

Burley, C. C. A.C. Klaybor, G. W. Short and G.J.Hueckel 1991. Report E. Evaluation of the North Squawfish Sport-Reward Fishery in the Columbia and Snake Rivers. Washington Department of Wildlife 600 Capitol Way N.E. Olympia WAS 98501-1091. December 3 1991.

Fish Passage Center, 1986. Smolt Monitoring Program Annual Report 1985. Part I: Estimation of survival for the Columbia Basin Fish and Wildlife Agencies and Tribes, under contract to the Bonneville Power Administration, Contract No. DE-A179-83BP11797, Project No. 80-1.

Fish Passage Center, 1987. Smolt Monitoring Program Annual Report 1986. Volume I: Migrational Characteristics of Columbia Basin Salmon and Steelhead Trout, 1986. For the Columbia Basin Fish and Wildlife Agencies and Tribes, under contract to the Bonneville Power Administration, Contract No. DE-AI79-86BP61747, Project No. 86-60.

Giorgi, A. E., D. M. Miller and B. Sandford. 1990b. Migratory behavior and adult contribution of summer out-migrating subyearling chinook salmon in John Day Reservoir 1981-1983. Annual Report of Research Financed by Bonneville Power Administration (Agreement DE-A179-88BP50301) and Coastal Zone and Estuarine Studies Division. Northwest Alaska Fisheries Center, National Marine Fisheries Center, National Oceanic and Atmospheric Administration.

Loch, J. L., Ballinger, D. Christofferson, G. J.A. Ross, M. Hack, C. Foster, D. Snyder and

D. Schultz. 1994 (DRAFT May 1994). Significance of Predation in the Columbia River from Priest Rapids Dam to Chief Joseph Dam: Abundance and Predation Indexing. Report B. In Significance of Predation in the Columbia River from Priest Rapids Dam to Chief Joseph Dam, Editors C. C. Burley and T.P. Poe. Contract 430-486. Prepared for Chelan County Utility district No. 1 P.O. box 1231. Wenatchee, Washington 98807, and Douglas County and Grant County Public Utilities. Draft January 1994.

McConnaha, W.E. and L.R. Basham. 1985. Survival of Wells Hatchery Steelhead in the Mid-Columbia River. Part 1: Smolt Monitoring Program, Annual Report, 1985.

Oregon Dept. of Fish and Wildlife (1988). "Predation by resident fish on juvenile salmonids in John Day Reservoir 1983-1986", Vol.1 U.S. Department of Energy Bonneville Power Administration Division of Fish and Wildlife, U.S. Fish and Wildlife Service Nat. Fishery Research Center, Ore. Dept. of Fish and Wildlife. July 1988. (Referred to as "ODF&W (1988)").

Parker, R. M. Zimmerman, and D. Ward 1994. Report G. Development of a system wide program: Indexing and Fisheries Evaluation. In: Development of a System wide program: Stepwise Implementation of a Predation Index,. Predator Control Fisheries, and Evaluation Plan in the Columbia River Basin, Volume II. Annual Report 1992. Bonneville Power Administration Report project No. 90-077. June 1994

Petersen, J.H., D.M. Gadomski, T.P. Poe. 1994. Differential predation by northern squawfish (Pthchocheikys Oregonensis) on live and dead juvenile salmonids in the Bonneville Dam tailrace (Columbia River). Canadian Journal of Fisheries and Aquatic Science. 51(5):1197:

Poe, T. P. and B. Rieman. 1988. Predation by Resident Fish on Juvenile Salmonids in John Day Reservoir. Volume I- Final Report of Research. Final Report 1983-1986. Bonneville Power Administration Report Project No. 82-3 and 82-12. July 1988.

Rieman. B.E., R.C. Beamesderfer, S. Vigg, and T.P. Poe. 1991. Estimated loss of juvenile salmonids to predation by northern squawfish, walleyes and small mouth bass in John Day Reservoir, Columbia River. Trans. Am. Fish Soc. 120:448-458.

Rieman.B.E., and R.C. Beamesderfer. 1990. Dynamics of a Northern Squawfish population and the potential to reduce predation on juvenile salmonids in a Columbia River reservoir. North American Journal of Fisheries Management 10:228-241.

Stevenson, J. and D. Olsen. 1991. Yearling chinook travel time and flow regime relationships in the John Day Pool, 1989 and 1990. Pacific Northwest Utilities Conference Committee, Portland OR. Internal report.

Vigg and Burley. 1991. *Temperature dependent maximum daily consumption of juvenile salmonids by norther squawfish (Ptychocheilus orogenesis) from the Columbia River.* Canadian Journal of Fisheries and Aquatic Resources, Vol. 48, pp 2491-2498.

Vigg, S., C. Burley, D. Ward, C Mallette, S. Smith, and M. Zimmerman 1990. Development of a system-wide predator control program: Stepwise implementation of a Predation index, predator control fisheries, and evaluation plan in the Columbia River Basin. Annual report 1990. Bonneville Power Administration Report. Project 90-77.

Vigg S., T.P. Poe, L.A. Pendergast and H.C. Hansel. 1991. Rates of consumption of juvenile salmonids and alternative prey fishes by northern squawfish, walleyes, smallmouth bass and channel catfish in John Day Reservoir, Columbia River. *Trans. Am. Fish. Soc.* 120:421-438

Ward, D.L. M.P. Zimmerman, R. M. Parker and S. S. Smith. 1994. Report G. Development of a system-wide predator control program: Indexing, fisheries evaluations and harvesting technology development. In: Development of a Systemwide program: Stepwise Implementation of a Predation Index,. Predator Control Fisheries, and Evaluation Plan in the Columbia River Basin, Annual Report 1991. Bonneville Power Administration Report project No. 90-077.

February 1993

Ward, D.L. and J. H. Peterson (in press) Index of Predation of Juvenile Salmonids by Northern Squawfish in the Lower Columbia and Snake Rivers. Transactions of the American Fisheries Society.

Reservoir Survival

Hilborn, R. R. Donnelly, M. Pascual, C. Coronado-Heranadez. 1993. Draft the relationship between river flow and survival for Columbia River chinook salmon. Draft report to BPA by University of Washington. Project manager Pat Poe.

Iwamoto, R. E., W.D. Muir, B.P. Sandford, K.W. McIntyre, D.A. Frost, J.G. Williams, S.G. Smith and J. R. Skalski. (1994) Survival estimates for the passage of juvenile chinook salmon through Snake river dams and reservoirs, 1993. US. Dept. of Energy Bonneville Power Administration Division of Fish & Wildlife. October 1993.

Muir, W.D., S. G. Smith, Iwamoto, R. E., D. J. Kamikawa, K.W. McIntyre, E.E. Hockersmith, B.P. Sandford, P.A. Ocker, T.E. Ruehle and J. R. Skalski. (1995) Survival estimates for the passage of juvenile chinook salmon through Snake river dams and reservoirs, 1994. US. Dept. of Energy Bonneville Power Administration Division of Fish & Wildlife. October 1995.

Muir, W.D., S.G. Smith, E.E. Hockersmith, S.Achord, R.F. Absolon, P.A. Ocker, B. Eppard, T.E. Ruehle, J.G. Wiliams, R.N. Iwamoto and J.R. Skalski. (1996) Survival estimates for the passage of yearling chinook salmon and steelhead through Snake River dams and reservoirs, 1995. US. Dept. of Energy, Bonneville Power Administration, Division of Fish and Wildlife. January 1996.

Raymond, H. L. 1979. Effects of dams and impoundments on migrations of juvenile chinook salmon and steelhead from the Snake river, 1966 to 1975. Transactions American Fisheries Society 108(6): 505-529.

Raymond, H. L. and C.W. Sims. 1980. Assessment of smolt migration and passage enhancement studies for 1979. National Marine Fisheries Service, Northwest and Alaska Fisheries Center, Coastal Zone and Estuarine Studies Division.

Schreck, C.B., L.E. Davis, D. Klsey and P.W. Wood. 1994. Evaluation of facilities for collection, bypass and transportation of outmigrating chinook salmon. Draft annual report to U.S. Army Corps of Engineers by Oregon Coop. fish. Res. Unit, Oregon State University, Corvallis

Sims, C. W, R.C. Johnsen, W. W. Bentley. 1976. Effects of power peaking operations on juvenile salmon and steelhead trout migrations, 1975. National Marine Fisheries Service, Northwest and Alaska Fisheries Center, Coastal Zone and Estuarine Studies Division.

Sims, C. W, W. W. Bentley, R.C. Johnsen, 1978. Effects of power peaking operations on juvenile salmon and steelhead trout migrations - Progress 1977, National Marine Fisheries Service, Northwest and Alaska Fisheries Center, Coastal Zone and Estuarine Studies Division.

Sims, C. W. W. W. Bentley, and R. C. Johnsen. 1978 Effects of power peaking operations on juvenile salmon and steelhead trout migrations: progress 1977. National Marine Fisheries Service, Northwest and Alaska Fisheries Center, Coastal Zone and Estuarine Studies Division.

Sims, C. W., A. E. Giorgi, R. C. Johnsen, and D. A. Brege. 1983. Migrational characteristics of juvenile salmon and steelhead trout in the Columbia River Basin-1982. National Marine Fisheries Service, Northwest and Alaska Fisheries Center, Coastal Zone and Estuarine Studies Division.

Sims, C. W., A. E. Giorgi, R. C. Johnsen, and D. A. Brege. 1984. Migrational characteristics of juvenile salmon and steelhead trout in the Columbia River Basin-1983. National Marine Fisheries Service, Northwest and Alaska Fisheries Center, Coastal Zone and Estuarine Studies Division.

Sims, C. W., J. G. Williams, D. A. Faurot, R. C. Johnsen, and D. A. Brege. 1981. Migrational characteristics of juvenile salmon and steelhead trout in the Columbia River Basin and related passage research at John Day Dam. Volumes I & II. National Marine Fisheries Service, Northwest and Alaska Fisheries Center, Coastal Zone and Estuarine Studies Division.

Sims, C. W. and F. J. Ossiander. 1981 Migrations of juvenile chinook salmon and steelhead in the Snake River, from 1973 to 1979: a research summary. National Marine Fisheries Service, Northwest and Alaska Fisheries Center, Coastal Zone and Estuarine Studies Division.

Steward, C.R. 1994. Assessment of the flow-survival relationship obtained by Sims and Ossiander (1981) for Snake River spring/summer chinook salmon smolts. US. Dept. of Energy, Bonneville Power Administration Division of Fish & Wildlife. April 1994.

Williams, J.G. and G.M. Matthews. 1995. A review of flow and survival relationships for spring and summer chinook salmon, *Oncorhynchus tshawytscha*, from the Snake River Basin. Fish. Bull. 93: 732-740.

Spill Efficiency

Dawson, J., A. Murphy, P. Nealson, P. Tappa, and C. Van Zee. 1983. *Hydroacoustic assessment of downstream migrating salmon and steelhead at Wanapum and Priest Rapids Dams in 1983*. Report to Grant Co. PUD No. 2 (BioSonics, Inc.).

Erho, M.W., G.E. Johnson, and C.M. Sullivan. 1988. *The salmonid smolt bypass system at Wells Dam on the Columbia River*. Proceedings: Fish Protection at Steam and Hydroelectric Power Plants (EPRI): I-55 - I-69.

Johnson, L., A. Murphy, and C. Rawlinson. 1985. *Hydroacoustic assessment of downstream migrating salmonids at Lower Monumental Dam in Spring 1985*. BPA report, Contract DE-A C79-85 BP23174, Project Number 84-15 (BioSonics, Inc.).

Kudera, E.A., C.M. Sullivan, G.E. Johnson, and A.G. Birmingham. 1991. *Evaluation of the smolt bypass system at Wells Dam in 1991*. Draft report; Douglas Co. PUD. (BioSonics, Inc.)

Raemhild, G., T. Steig, R.Riley, and S. Johnston. 1984. *Hydroacoustic assessment of downstream migrating salmon and steelhead at Rocky Reach Dam in 1983*. Report to Chelan Co. PUD No. 1 (BioSonics, Inc.).

Ransom, B.H., G.A. Raemhild, and T.W. Steig. 1988. *Hydroacoustic evaluation of deep and shallow spill as a bypass mechanism of downstream migrating salmon and steelhead at Rock Island Dam*. Proceedings: Fish Protection at Steam and Hydroelectric Power Plants (EPRI): I-70 - I-84.

Ransom, B.H., and A.E. Sullivan. 1989. *Hydroacoustic evaluation of juvenile fish passage at Lower Monumental Dam in 1989*. Final Report (to Army Corps; BioSonics, Inc.).

Parametrix 1987. Hydroacoustic evaluation of the spill program for fish passage at the Dalles Dam in 1986, final Report. March 1987, Parametrix, Inc. for Portland District COE contract no. DACW57-86-0062.

Transportation

Fisher, T.R. 1993. Modeling effects of transportation assumptions on the population trends of Snake River chinook salmon: A risk analysis. Bonneville Power Administration manuscript July 1993.

ANCOOR (Analytical Coordination working Group) 1994. A Preliminary Analysis of the Reasons for Differences Among Models in the 1994 Biological Opinion Prepared by the National Marine Fisheries Service. Final draft report. Prepared by ANCOOR for the National Marine Fisheries Service. 87. pp.

Travel Time

Dawley, E. M., L.G. Gilbreath, R.D. Ledgerwood, P.J. Bentley, B.P. Sanford, and M.H. Schiewe. 1989. Survival of subyearling chinook salmon which have passed through the turbines, bypass system, and tailrace basin of Bonneville Dam Second Powerhouse, 1988. NOAA, NWFSC, NMFS, Seattle, WA.

Giorgi, A.E., Stuehrenberg, L.C., Miller, D.R., and Sims, C.W. 1986. *Smolt Passage Behavior and Flow-Net Relationship in the Forebay of John Day Dam*. Bonneville Power Administration, Contract No. DE-A179-84BP39644.

Giorgi, A. E., D. M. Miller and B. Sandford. 1990b. Migratory behavior and adult contribution of summer out-migrating subyearlings chinook salmon in John Day Reservoir 1981-1983. Annual Report of Research Financed by Bonneville Power Administration (Agreement DE-A179-88BP50301) and Coastal Zone and Estuarine Studies Division. Northwest Alaska Fisheries Center, National Marine Fisheries Center, National Oceanic and Atmospheric Administration.

Stuehrenberg, L.C., Giorgi, A.E., Sims, C.W., Ramonda-Powell, J., and Wilson J. 1986. Bonneville Power Administration, Project No. 85-35.

Stevenson, J. and D. Olsen. Yearling chinook salmon travel time and flow regime relationships in the John Day Pool, 1989 and 1990. Report to the Pacific Northwest Utilities Conference Committee, Portland, Oregon.

Fish Passage Managers. 1989. Annual Report. Fish Passage Center, Portland, Oregon.

Fish Passage Managers. 1990. Annual Report. Fish Passage Center, Portland, Oregon.

Fish Passage Managers. 1991. Annual Report. Fish Passage Center, Portland, Oregon.

Ledgerwood, R.D., E.M. Dawley, L.G. Gilbreath, P.J. Bentley, B.P. Sanford, and M.H. Schiewe. 1990. Relative survival of subyearling chinook salmon which have passed Bonneville Dam via the spillway or the second powerhouse turbines or bypass system in 1989, with comparisons to 1987 and 1988. NOAA, NWFSC, NMFS, Seattle, WA.

Ledgerwood, R.D., E.M. Dawley, L.G. Gilbreath, P.J. Bentley, B.P. Sanford, and M.H. Schiewe. 1991. Relative survival of subyearling chinook salmon that have passed through the turbines or bypass system of Bonneville Dam second powerhouse. NOAA, NWFSC, NMFS, Seattle, WA.

Smolt Monitoring Program Annual Report. 1985. Brand Release Data. Fish Passage Center, Portland, Oregon.

Smolt Monitoring Program Annual Report. 1986. Brand Release Data. Fish Passage Center, Portland, Oregon.

Smolt Monitoring Program Annual Report. 1987. Brand Release Data. Fish Passage Center, Portland, Oregon.

Smolt Monitoring Program Annual Report. 1988. Brand Release Data. Fish Passage Center, Portland, Oregon.

Smolt Monitoring Program Annual Report. 1989. Brand Release Data. Fish Passage Center, Portland, Oregon.

Smolt Monitoring Program Annual Report. 1990. Brand Release Data. Fish Passage Center, Portland, Oregon.

Stevenson, J. and D. Olsen. 1991. Yearling chinook travel time and flow regime relationships in the John Day Pool, 1989 and 1990. Pacific Northwest Utilities Conference Committee, Portland OR.

Zabel. R.W. (1994) Spatial and temporal models of migrating juvenile salmon with applications. University of Washington Ph.D dissertation. 223 pp.

Supporting Evidence

Brawn, V.M. 1982. *Behavior of Atlantic Salmon (*Salmo salar*) during suspended migration in an estuary, Sheet Harbour, Nova Scotia, observed visually and by ultrasonic tracking*.

Can. J. Fish. Aquat. Sci. 39: 248-256.

Hiramatsu, K.; Ishida, Y. 1989. *Random movement and orientation in pink salmon (*Oncorhynchus gorbuscha*) migrations.* Can. J. Fish. Aquat. Sci. 46:1062-1066.

Holm, Marianne, Ingvar Huse, Erlend Waatevik, Kjell B. Doving and Jan Aure. 1982. *Behavior of Atlantic salmon smolts during seaward migration. I: Preliminary report on ultrasonic tracking in a Norwegian fjord system.*

Saila, S. B, and Shappy, R.A. 1963. *Random movement and orientation in salmon migration*. J. Cons. Int. Explor. Mer. 128: 153-166.

Stasko, A.B. 1975. *Progress of migrating Atlantic salmon (*Salmo salar*) along an estuary, observed by radio-tracking.* J. Fish Biol. 7:329-338.

Tyler, P., J. E. Thorpe, and W. M. Shearer. 1978. *Ultrasonic tracking of the movements of atlantic salmon smolts (*Salmo salar L*) in the estuaries of two Scottish rivers*. J. Fish Biol. 12: 575-586.

Turbine Survival/Mortality

Direct Measure Estimates

Oligher, Raymond C. and Ivan J. Donaldson. 1966. *Fish passage through turbines tests at Big Cliff hydroelectric plant.* Progress Report #6, USACOE.

Weber, Kinsley G. 1954. *Testing the effect of a Bonneville draft tube on fingerling salmon*. Unpublished research report. Bureau of Commercial Fisheries (now NMFS), Seattle.

RMS Environmental Service, Inc. and J.R. Skalski. (1994). Survival of yearling fall chinook salmon smolts (Oncorhynchus tshawaytscha) in passage through a Kaplan turbine at the Rocky Reach hydroelectric dam, Washington. Prepared for Public Utility district No. 1 of Chelan county. October 1993.

RMS Environmental Service, Inc. and J.R. Skalski. (1993). Turbine passage survival of spring migrant chinook smolts (Oncorhynchus tshawaytscha) at Lower Granite Dam, Snake river, Washington. Prepared for Department of the Army. July 1994.

Indirect Measure Estimates

Holmes, Harlan. 1952. *Loss of fingerlings in passing Bonneville Dam as determined by marking experiments.* USF&W unpublished manuscript.

Schoeneman, Dale E., Richard T. Pressey, and Charles O. Junge. 1961. *Mortalities of downstream migrant salmon at McNary Dam.* Transactions of the American Fisheries Society, Vol. 90 (1), pp. 58-72.

Long, Clifford W. 1968. *Research on fingerling mortality in Kaplan turbines.* Unpublished research report, Bureau of Commercial Fisheries (now NMFS), Seattle.

Long, Clifford W., Frank J. Ossiander, Thomas E. Ruehle and Gene Mathews. 1975. *Survival of coho salmon fingerlings passing operating turbines.* Unpublished research report, NMFS, Seattle.

Ledgerwood, R.D. et al. 1990. *Relative survival of subyearling chinook salmon which have passed Bonneville Dam via the spillway or the second powerhouse turbine or bypass system in 1989, with comparisons to 1987 and 1988.* Unpublished research report, NMFS, Seattle.

Iwamoto, R. E., W.D. Muir, B.P. Sandford, K.W. McIntyre, D.A. Frost, J.G. Williams, S.G. Smith and J. R. Skalski. (1994) Survival estimates for the passage of juvenile chinook salmon through Snake river dams and reservoirs, 1993. US. Dept. of Energy Bonneville Power Administration Division of Fish & Wildlife. October 1993.

Muir, W.D., S. G. Smith, Iwamoto, R. E., D. J. Kamikawa, K.W. McIntyre, E.E. Hockersmith, B.P. Sandford, P.A. Ocker, T.E. Ruehle and J. R. Skalski. (1995) Survival estimates for the passage of juvenile chinook salmon through Snake river

dams and reservoirs, 1994. US. Dept. of Energy Bonneville Power Administration Division of Fish & Wildlife. October 1995.

Muir, W.D. S.G. Smith, E. E. Hockersmith, S. F. Achord, R. F. Absolon, P. A. Ocker, T. E. Ruehle, J. G. Williams, R. N. Iwamoto, and J. R. Skalski. Survival estimates for the passage of yearling chinook salmon and steelhead through the Snake River dams and reservoirs, 1995. US. Dept. of Energy Bonneville Power Administration Division of Fish & Wildlife. January 1996.

River Geometry and Velocity

Nigro, Anthony A. 1989. *Developing a Predation Index and Evaluating Ways to Reduce Salmonid Losses to Predation in the Columbia River Basin*, Table A-2. US Dept. of Energy, Bonneville Power Administration, Division of Fish & Wildlife and Oregon Dept. of Fish and Wildlife, Report #DOE / BP-92122-1.

US Geological Survey provided data from individual field stations using either USGS Form # 9-207 or "Summary of Discharge Measurement Data" forms.

Project Data and Operating Limits: Columbia River Tributaries Review Study. US Army Corps of Engineers North Pacific Division. CRT 49 Book No. 1 1989.

Project Data and Operating Limits: Columbia River Tributaries Review Study. US Army Corps of Engineers North Pacific Division. CRT 69 Book No. 2 1989.

Lower Granite & Little Goose Projects Draft. US Army Corps of Engineers Walla District, October 1992.

Miscellaneous

Beamesderfer, R.C. B.E. Rieman, L.J. Bledsoe and S.Vigg. 1990. Management implication of a model of predation by a resident fish on juvenile salmonids migrating through a Columbia River reservoir. North American Journal of fisheries Management 10:290-304.

Ebel, W.J., R. W. Krcma and H.L. Raymond. 1974. Evaluation of fish protection facilities at Little Goose Dam and Review of other studies relating to protection of juvenile salmonids in the Columbia and Snake Rivers, 1973. National Marine Fisheries Service, Northwest and Alaska Fisheries Center, Coastal Zone and Estuarine Studies Division.

Hinrichsen, R. T. Frever, J. Anderson, G. Swartzman and B. Sherer 1991. Columbia River Salmon Passage (CRiSP) Model. Documentation for CRiSP.0. University of Washington, unpublished report. May 1991.

Henderson, F.M. 1966. Open Channel Flow. Macmillian Publishing Co. New York. Macmillian Series in Civil Engineering-Gene Norby, Editor. 522 p

Oreskes, N, K. Shrader-Frechette and K. Belitz. 1994. Verification, validation and confirmation of numerical models in the earth sciences. Science vol 263 4 February 1994. p 641-646.

Matthews, G. V. T. 1966. *Book Reviews,* Animal Behavior, 14:593-4.

Press, W. H., B. P. Flannery, S. A. Teukolsky and W. T. Vetterling. 1988. *Numerical Recipes in C*. Cambridge University Press, Cambridge. 735

Norman, W.T. (1992). Factors controlling variations of naturally spawning fall chinook salmon in the Upper Columbia River. Masters Thesis University of Washington 239 pp.

Rieman. B.E., R.C. Beamesderfer, S. Vigg, and T.P. Poe. 1991. Estimated loss of juvenile salmonids to predation by northern squawfish, walleyes and small mouth bass in John Day Reservoir, Columbia River. Trans. Am. Fish Soc. 120:448-458.I

Richards, F.A. 1965. Dissolved Gases Other than carbon dioxide. Chapter 6 (p 211) in Chemical Oceanography Eds. J.P. Riley and G. Skirrow. Volume 1. Academic Press London.

Smith, J.R., G.M. Matthews, R. Basham, S. Achord, and G. T. McCabe. 1980. Transportation operations on the Snake and Columbia rivers 1979. National Marine Fisheries Service, Northwest and Alaska Fisheries Center, Coastal Zone and Estuarine Studies Division.

Skalski, J.R., A. Hoffman and S. G. Smith. 1993. Development of survival relationships using concomitant variables measured from individual smolt implanted with PIT-tags. Annual Report 1990-1991. US. Dept. of Energy Bonneville Power Administration Division of Fish & Wildlife. October 1993.

Spain, G. (1994) Federal mismanagement at heart of salmon decline. Seattle Times 7.14.94. Glen Spain is the Northwest Regional director of the Pacific Coast Federation of Fishermen's Associations (PCFFA), an organization of commercial fisherman on the West Coast.

Ward, D.L. J.H. Peterson, T.P. Poe (1993). Index of predation on juvenile salmonids by northern squawfish in the lower Columbia and Snake Rivers. Report US. Dept. of Energy Bonneville Power Administration Division of Fish & Wildlife. October 1993